Master Thesis in Reservoir Chemistry

Low Salinity Waterflooding in Combination with Surfactant/Polymer

A Field Scale Simulation Study of Hybrid EOR

Vilde Loug Pedersen

Centre for Integrated Petroleum Research

Department of Chemistry

University of Bergen

June 2018

Abstract

It is projected that 77% of energy consumption will originate from fossil fuels in 2040, indicating a continuous demand for crude oil [1]. Nevertheless, more than half of the hydrocarbons produced at present originate from mature fields, where the worldwide oil recovery factor averages at 20-40% of OOIP [2, 3]. Most of the sedimentary basins have already been explored, and it is becoming increasingly demanding to discover new giant fields. Consequently, there is a growing interest within the petroleum society for maximising the oil recovery from fields already discovered.

Waterflooding is the most widely practiced recovery technique for pressure support and enhanced sweep efficiency purposes, and has been deployed for over a century. However, little consideration has been bestowed upon the injection-water chemistry and its effect on crude oil/brine/rock (COBR) - systems. Low salinity waterflooding is a relatively recent developed EOR-process that improves the sweep efficiency by modifying reservoir wettability and destabilize oil layers [2]. Previous studies demonstrate that the low salinity brine can be successfully combined with surfactant flooding and polymer flooding in a hybrid tertiary process. The low salinity environment is beneficial for both surfactants and polymers with regards to their physiochemical properties, as their functions are optimized in diluted water [4, 5]. Research notifies that the composite effect of the tertiary fluids may even be higher than the individual effects [6].

This thesis concerns a field scale simulation study of low salinity waterflooding in combination with surfactants and polymers in a 3-dimensional reservoir model supplied by Lundin Norway AS. The compositional reservoir simulator STARS was applied to perform the simulations. During the numerical simulations, the reservoir response towards the different tertiary fluids was examined, both when injected individually and together in a composite experiment.

Compared to the reference case of continuous high salinity waterflooding, the model responded well to low salinity waterflooding in a secondary mode. Low salinity waterflooding was also successful in enhancing oil recovery in a tertiary mode, where a sensitivity study confirmed that more oil was produced for a short secondary phase and a prolonged tertiary phase. Simulation studies revealed that the surfactants were able to effectively enhance the microscopic sweep in contacted zones, but were more competent in reducing residual oil in a pre-established low salinity environment. The polymers were also effective in rising oil production beyond the capability of high salinity waterflooding.

Composite low salinity surfactant/polymer –flooding simulations were conducted, where the influence of chemical adsorption and slug size on oil recovery were examined. The combination of the tertiary fluids was successful, and the process generated a higher oil recovery than the low salinity water, surfactants and polymers individually. The inevitable adsorption of surfactants and polymers onto the reservoir rock reduced the oil recovery. Nevertheless, the loss of chemicals due to adsorption did not break down the injected slug size.

A sensitivity study on surfactant and polymer slug sizes revealed that the reduction from 1/3 PV to 1/6 PV only diminished the oil recovery by 1.27%. With regards to project economy, the additional oil produced by the 1/3 slug sizes is not likely to counteract the expenses of the prolonged chemical injection.

Table of Contents

Acknowledgements

First and foremost, I would like to express my sincere gratitude towards my supervisor Professor Arne Skauge for his guidance and support during the work of this thesis. This thesis would not have been possible without him and his cheerful attitude.

Special thanks to Lundin Norway AS for contributing with an interesting research topic, and corresponding data.

Furthermore, a sincere appreciation goes to Principal Researcher Øystein Pettersen for helping me translate data files from Eclipse syntax to STARS syntax, and for all technical support and assistance during my simulation work. Additionally, I would like to express my thankfulness towards Dr. Iselin Salmo for always being available for discussions and counselling.

I am beyond thankful for my incredible fellow students, and for all the social and academic activities throughout the past five years. In particular "PTEK-jentene" for always brightening up my day, and of course my "office buddies" Helene Irgens Sjo, Diderik Olav Jarlsby, Trude Sætnan Sæther, Sivert Mordal Nærbøvik and Henning Kvaløy. Thank you for all the laughs, coffee and discussions on and off topic, and for helping me maintain my sanity throughout the most stressful times.

Finally, I would like to thank my family and friends for their support and encouragement during my studies, and for always being there for me. I am especially thankful for my parents, Jarle Pedersen and Vibeke Loug, for constantly cheering on me and helping me with anything needed.

Vilde Loug Pedersen

Bergen, June 2018

Nomenclature

Variables

A	Area	$[m^2]$
B_{oi}	Initial oil volume factor	$[Rm^3/Sm^3]$
c	Concentration	$[mol/L]$
dP	Differential pressure	$[kPa]$
dv/dy	Shear rate	$[s^{-1}]$
E_A	Area sweep efficiency	dimensionless
E_D	Microscopic displacement efficiency	dimensionless
E_R	Recovery factor	dimensionless
E_V	Vertical sweep efficiency	dimensionless
E_{vol}	Volumetric displacement efficiency	dimensionless
F	Force	$[kg \cdot ms^{-2}]$
f_w	Fractional flow of water	dimensionless
I_{AH}	Amott-Harvey index	dimensionless
I_{USBM}	USBM index	dimensionless
h	Height	$[m]$
I	Ionic strength	$[mol/L]$
K	Absolute permeability	$[mD]$ $(1\ D = 0.98692 \cdot 10^{-12} m^2)$
$K_{e,i}$	Effective permeability of phase i	$[mD]$ $(1\ D = 0.98692 \cdot 10^{-12} m^2)$
$K_{rel,i}$	Relative permeability of phase i	dimensionless
L	Length	$[m]$
M	Mobility ratio	dimensionless
m	Mass	$[kg]$
N	Total oil reserves originally in place	$[m^3]$
n	Sum	dimensionless
N_p	Produced oil reserves	$[m^3]$
N_c	Capillary number	dimensionless
$OOIP$	Oil originally in place	$[m^3]$
P	Pressure	$[kPa]$
PV	Pore volume	dimensionless
Q	Flow rate	$[m^3 \cdot s^{-1}]$
R, r	Radius	$[m]$
R_z	Radius of gyration	$[m]$
S	Saturation	dimensionless
T	Temperature	$[^oC]$ $(0^oC = 273.15\ K)$
t	Time	$[days]$
V	Volume	$[m^3]$
v	Velocity	$[ms^{-1}]$
z	Charge	

Δ	Difference	dimensionless
γ	Shear rate	$[s^{-1}]$
η	Viscosity (dependent on shear rate)	$[Pa \cdot s]$ ($1\ Pa \cdot s = 10^3\ Cp$)
θ	Contact angle	[°]
λ	Mobility	$[m^2/Pa \cdot s]$
λ_0	End point mobility	$[m^2/Pa \cdot s]$
φ	Porosity	dimensionless
σ	Interfacial tension	$[N \cdot m^2]$
μ	Viscosity	$[Pa \cdot s]$ ($1\ Pa \cdot s = 10^3\ Cp$)
ρ	Density	$[kg \cdot m^{-3}]$
τ	Shear stress	$[Pa]$

Subscripts

A	area
abs	absolute
b	bulk
c	capillary
$crit$	critical
D	microscopic
$diff$	differential
eff	effective
$ineff$	ineffective
g	gas
i	component (phase)
i	initial
i	irreducible
inj	injected
max	maximum
min	minimum
nw	non-wetting phase
o	oil
pol	polymer
p	pore
p	produced
r	relative
r	residual
R	recovery
rel	relative
s	solid
tot	total
V	vertical
vol	volumetric
w	water
w	wetting phase

Abbreviations

CDC	Capillary desaturation curve
CFC	Critical flocculation concentration
CMC	Critical micelle concentration
CMG	Computer Modelling Group
COBR	Crude oil/brine/rock
Ca^{2+}	Calcium ion
CO_2	Carbon dioxide
CO_3^{2-}	Carbonate ion
$CaCO_3$	Calsium carbonate
CIPR	Centre for Integrated Petroleum Research
DLVO	Deryaguin, Landau, Verwey and Overbeek
EIA	Energy Information Administration
EOR	Enhanced oil recovery
FW	Fractionally wet
IFT	Interfacial tension
IOR	Improved oil recovery
IPV	Inaccessible pore volume
HPAM	Hydrolyzed polyacrylamide
HS	High salinity
H^+	Hydrogen ion
H_2O	Water
H_3O^+	Hydronium ion
HCO_3^-	Bicarbonate ion
K^+	Potassium ion
LSP	Low salinity polymer
LSS	Low salinity surfactant
LSSP	Low salinity surfactant polymer
LSW	Low salinity water
MIE	Multicomponent ionic exchange
Mg^{2+}	Magnesium ion
MWL	Mixed wet large
MWS	Mixed wet small
Na^+	Sodium ion
NCS	Norwegian Continental Shelf
OOIP	Oil originally in place
OH^-	Hydroxide ion
PAM	Polyacrylamide
ppm	Parts per million
Sal	Salinity
STARS	Steam, Thermal and Advanced Processes Reservoir Simulator
U.S	United States

STARS Keywords

ADMAXT	Maximum adsorption capacity	$[gmol \cdot cm^{-3}]$
ADRT	Residual adsorption level	$[gmol \cdot cm^{-3}]$
ADSCOMP	Component adsorption function will apply	Dimensionless
ADSTABLE	Adsorption table (component concentration and corresponding adsorption)	Mole Fraction and $[gmol \cdot cm^{-3}]$
COMP	Interpolation component name and phase	Dimensionless
DTRAPW	Value of wetting phase interpolation parameter	Dimensionless
INFTABLE	Interfacial tension table (surfactant concentration and corresponding interfacial tension)	Mole Fraction and $[dyne/cm]$
INTCOMP	Interpolation component	Dimensionless
KRINTRP	Interpolation set number	Dimensionless
LOWER_BOUND	Lower bound of interpolation parameter	Dimensionless
RPT	Rock type number	Dimensionless
RPT_INTRP	Specifies interpolation between two rock types	Dimensionless
SMOOTHEND QUAD	Quadratic interpolation for the relative permeability tables	Dimensionless
SLT	Liquid-gas relative permeability table	Dimensionless
SWT	Water-oil relative permeability table	Dimensionless
UPPER_BOUND	Upper bound of interpolation parameter	Dimensionless
VSMIXCOMP	Component using nonlinear viscosity mixing	Dimensionless
VSMIXENDP	Abscissas for the first and last table entries	Dimensionless
VSMIXFUNC	Table entries describing non-linear mixing	Dimensionless

List of Figures

List of Tables

Chapter 1

Introduction

1.1 Introduction

Despite the predicted growth of renewable energy in the upcoming years, crude oil is still presumed to play a crucial role in the international energy market for a long time [1]. The expected population growth and development of Third World Countries will accelerate future energy consumption, and with many hydrocarbon reservoirs approaching an residual oil saturation, the petroleum industry is challenged to develop new effective and creative techniques to further stimulate oil recovery.

According to the U.S. Energy Information Administration, the North Sea Brent crude oil average monthly price has increased for seven consecutive months, and in January 2018, spot prices moved higher than $70/b for the first time since December 2014 – giving rise to a wave of overt oil optimism. Furthermore, the total world consumption is assumed to escalate. EIA estimates that global petroleum and other liquid fuels inventories will grow by approximately 0.2 million b/d in both 2018 and 2019 [7]. As much as 77% of energy usage is assumed to originate from fossil fuels in year 2040 [1].

Figure 1.1 portrays the projected future worldwide energy consumption, where the anticipated growth in energy expenditure by non-OECD countries is in particular increasing.

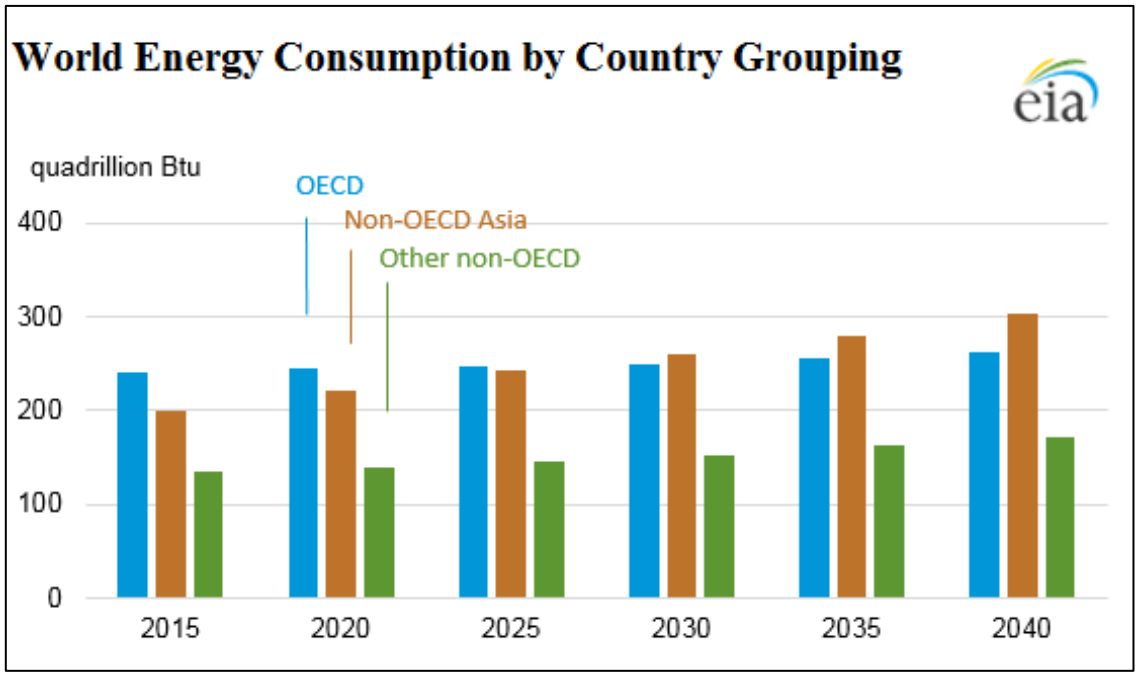

Figure 1.1: Historic and projected worldwide energy consumption given in British thermal units (Btu) [1].

The oil industry is entering a challenging era in terms of matching the demanded future oil consumption. The vast majority of the potential oil-bearing sedimentary basins have already been explored, and it is becoming increasingly strenuous to discover new giant fields. The unexplored basins often obtain a remote and environmental sensitive location, which present considerable technical and political complications [2]. Moreover, more than half of the hydrocarbons produced today stem from mature fields, many of them approaching an irreducible oil saturation [3]. Hence, there is a growing focus on optimizing the recovery from the hydrocarbon fields already discovered.

Considering the importance of hydrocarbons as a global energy source, several techniques exist to extract the valuable fluids trapped several kilometres below the surface. Originally, hydrocarbons were produced by the usage of the natural energy within the reservoir, exemplified by pressure depletion, pore compaction, aquifer drive and gas drive. Although several reservoirs are still drained by these primary recovery methods, most reservoirs are now producing by secondary recovery techniques. At present, the prevailing recovery technique is the injection of seawater or gas re-injection for pressure support and sweep efficiency purposes [8].

Even though secondary recovery techniques are employed to escalate oil production, an estimated 55% of the hydrocarbons originally in place on the Norwegian Continental Shelf are left behind due to physiochemical forces keeping them trapped [9]. The observed production decline from multiple hydrocarbon reservoirs drained with conventional techniques inspires researchers to develop new methods to extract the trapped hydrocarbons. The remaining hydrocarbon reserves may represent great value to an oil company, which generates a growing interest in studying chemicals and added forms of energy to overcome the forces keeping the hydrocarbons in place, and mobilize residual oil.

Enhanced oil recovery, EOR, is a term describing unconventional techniques implemented to increase oil production in reservoirs with large volumes of oil unrecoverable by conventional techniques. These tertiary recovery methods include thermal injection and the introduction of chemicals and gases not naturally present in a reservoir, dissimilar to regular seawater and hydrocarbon gas used under secondary recovery [8]. EOR is often interchanged with IOR (improved oil recovery), but is only a subpart of IOR, which includes a much broader spectre such as management improvements, more complex geological models, and futuristic engineering [2]. EOR solely involves the addition of energy to a reservoir for incremental recovery purposes [8].

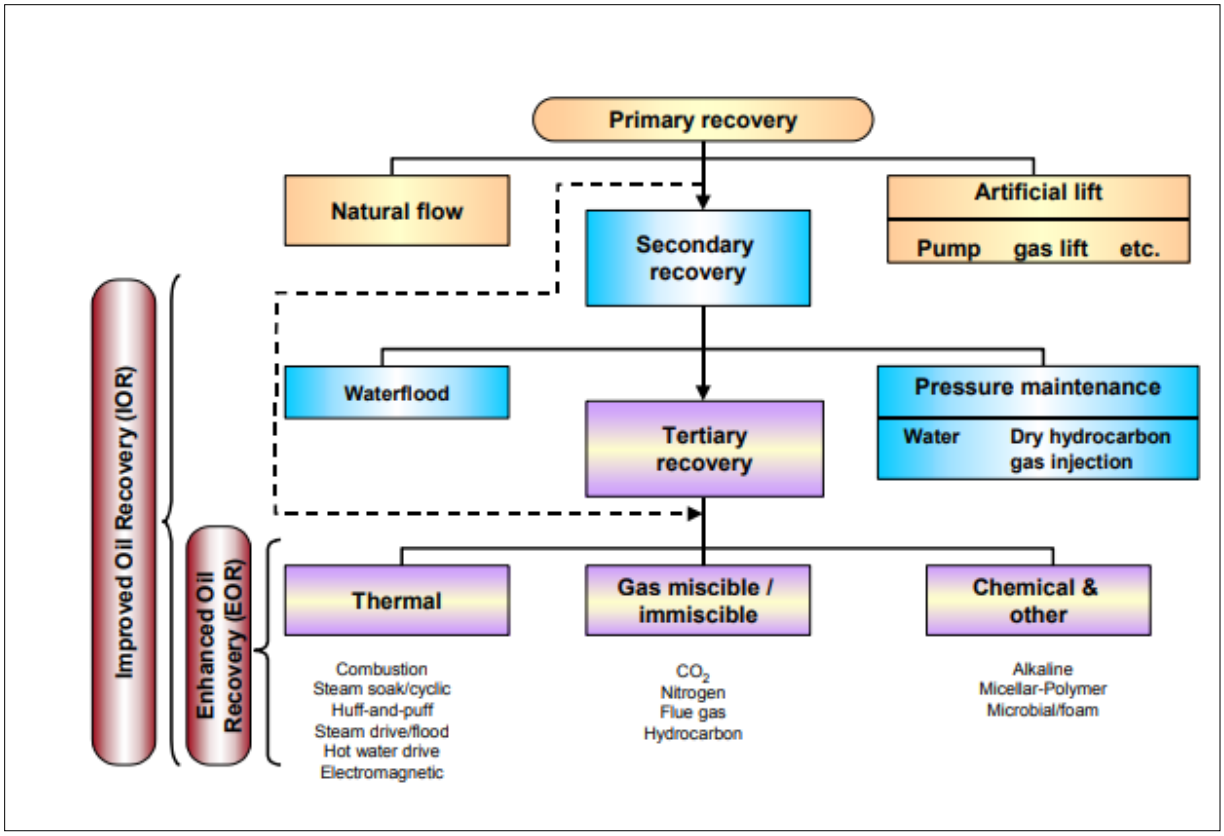

Figure 1.2: EOR is a subpart of IOR, which encompasses a broad spectre of methods to increase oil recovery [8].

In contempt of the position of waterflooding as the leading recovery mechanism, little attention has been allotted to the chemistry of the brine, and how a change in its ionic composition may affect interactions between crude oil, water and rock. Low salinity waterflooding is a relatively recent promising EOR-method proved to significantly increase oil recovery by modifying the reservoir wettability [10]. Connate water salinity is considerably variable, and is typically in the range of 10 000 – 250 000 ppm [11]. By reducing the brine salt content in injection water to a value below 6000 ppm, the injection water will meet the requirements of being called low salinity water [12]. When diluted water is injected into a reservoir initially filled with high salinity connate water, it will disturb the chemical equilibrium existing within the reservoir [11]. Low salinity waterflooding gives rise to several mechanisms that release trapped oil; including multicomponent ionic exchange, double layer expansion, fine migration and an elevated pH [13].

Studies also reveal that the effects of the diluted brine injection may benefit from being combined with surfactants and polymers for incremental oil recovery in a hybrid EOR-process [6]. Surfactant molecules are acknowledged for their interfacial-tension-lowering abilities, and their function is optimized under low saline conditions [4, 14]. This case also yields for the water-viscosifying and mobility-ratio-reducing polymer molecules [5].

1.2 Scope of Work

Before commencing practical work on this thesis, literature studies of relevant research topics were accomplished. It is of great importance to obtain a vast depth of knowledge regarding the individual processes of low salinity waterflooding, surfactant flooding and polymer flooding, and how they all interact and contribute to incremental oil recovery. The insight into the theoretical aspects provides the foundation required to properly analyze and interpret simulation results.

Thenceforward, the numerical simulation background for STARS was acquired, with a focus on how the simulator treats the physiochemical phenomena following low salinity water-, surfactant- and polymer flooding. A base file with a STARS syntax was created based on the Eclipse files supplied by Lundin Norway AS. The water and oil relative permeabilities for the high salinity waterflood were equal to the values initially provided, and the relative permeabilities for the low salinity waterflood were constructed based on unpublished work. Water and oil relative permeabilities for surfactants were calculated based the assumption of an "extreme process" with straight curves and a residual oil saturation of zero.

In the practical part, a base case with high salinity waterflooding was simulated for reference purposes. Additionally, low salinity waterflooding was studied in a secondary mode under the same conditions as for the base case to observe the full potential of the EOR-method when not limited by project economy. Since economy obtains a crucial role when planning recovery techniques, and the injection of low salinity water presents considerable expenses, low salinity water injection was tested in a tertiary mode. Different interval sizes of the secondary phase (high salinity waterflooding) and tertiary phase (low salinity waterflooding) were examined to see the effect that the onset of low salinity water injection has on oil recovery.

Furthermore, the full oil recovery potential of surfactants by injecting them continuously for a long period was tested. The same study was also conducted for polymers. Moreover, the potential of surfactants to reduce the residual oil saturation after a production plateau for the low salinity waterflood had been established was examined. Ultimately, hybrid EOR-simulations of combined low salinity waterflooding, surfactant flooding and polymer flooding were conducted. The role of chemical adsorption was researched, in addition to a sensitivity study of slug-sizes.

During the numerical simulation studies, an emphasis was put on cumulative oil recovery, but water cut, oil production rate and reservoir pressure were also among the factors of interest.

Chapter 2

Fundamental Definitions for Reservoir Engineering

In order to enable investigation of fluid flow and interactions in a hydrocarbon reservoir, certain fundamental properties regarding the porous media and its saturating fluids must be understood. This chapter covers basic rock characteristics, liquid properties and oil recovery definitions that provide the common denominator of how to make accurate reservoir behaviour predictions.

2.1 Petrophysical Properties

Numerous studies have been designated to reservoir rocks and their importance for hydrocarbon recovery. The requirements for being named a reservoir rock concern the existence of pore space inhabitable by fluids and channels connecting these voids such that fluid flow may be enabled. The professional terminology describing these demands is *porosity* and *permeability*, respectively. Furthermore, the study of reservoir fluid properties and their interactions with the reservoir rock constitutes important subjects within the petrophysical field [15].

2.1.1 Porosity

Porosity is the measure of void space between mineral grains within a rock, and is of great importance in the petroleum industry as these pores may contain hydrocarbons [16]. Porosity is a normal phenomenon in sedimentary rocks, and is usually evoked by sediments not being compacted together completely under the diagenesis process, referred to as primary porosity [17]. Post-depositional processes may also increase the porosity further. Secondary porosity is created by dissolution of detrital particles, and intergranular calcite and dolomite cement by formation water. Porosity enhancement may also be a result of tectonic stress, causing the development of fractures [18].

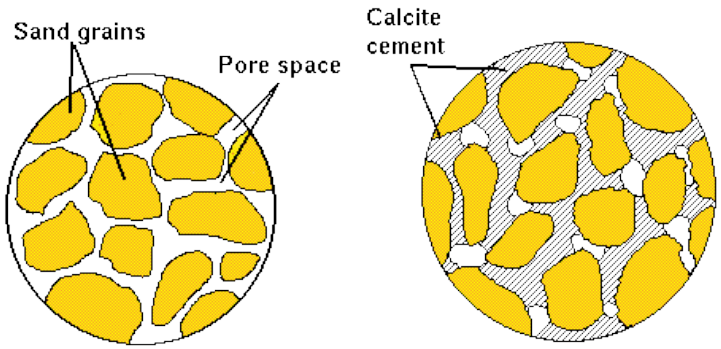

Figure 2.1: Mineral grains (yellow) and pore space (blank) within a rock.
Calcite cement (striped) may reduce porosity significantly [19].

The transportation- and depositional history of sediments is crucial for pore volume. As a rule of thumb, the preferred homogenous rocks that are interlinked with higher porosities are found in areas where the sediments have been well rounded and sorted, in addition to an overall equal size distribution. This favoured matrix texture – referred to as sediment maturity - is improved along the path of transport from source area to basin where the maturity is proportional to the distance of transport [20].

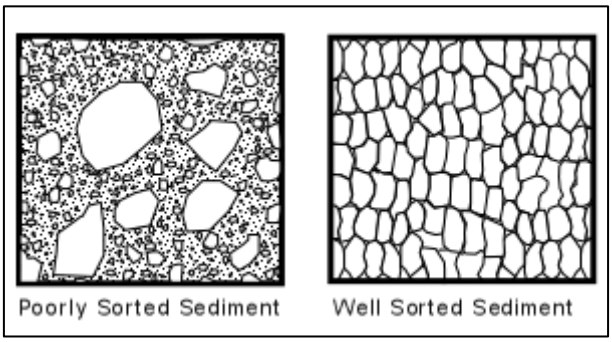

Figure 2.2: The sorting of sediments are of importance for the pore volume [20].

When estimating the porosity of a rock, all pores may not be of interest. The total porosity is a measure of all pore space within it, but it is the effective porosity of the rock that receives the most interest as these voids are interconnected and can contribute to fluid flow [15].

The porosity, φ, within a rock is described by the following dimensionless parameter:

$$\varphi = \frac{V_p}{V_b} \tag{2.1}$$

Where V_p and V_b represents the pore volume and bulk volume, respectively.

The total porosity is the sum of the effective porosity, φ_{eff} and ineffective porosity, φ_{ineff}:

$$\varphi_{tot} = \varphi_{eff} + \varphi_{ineff} \tag{2.2}$$

Most log tools only possess the capacity of examining the total void space. The effective porosity is usually calculated based on empirical data from nearby formations or core plugs of similar geological properties [15].

2.1.2 Absolute Permeability

Another significant rock parameter in petroleum reservoir engineering is permeability. Permeability is the study of the ability of a rock to maintain a fluid flow in a porous media, and the factors that may affect the motion of fluids. The permeability of a rock requires porous volume, but a high porosity is not necessarily linked to a high permeability. For a rock to be permeable, it necessitates interlinked pores such that a continuous flow of fluids can be transmitted through [17].

Permeability is a rock property and is affected by the sorting of the rock and the structure and size of the grains, as exemplified in figure 2.3. A homogenous rock constituting of well-rounded and spherical grains of similar size will usually yield a higher permeability. However, the permeability is not only dependent on the initial sorting. Fractures caused by tectonic stress can enhance the permeability significantly [21].

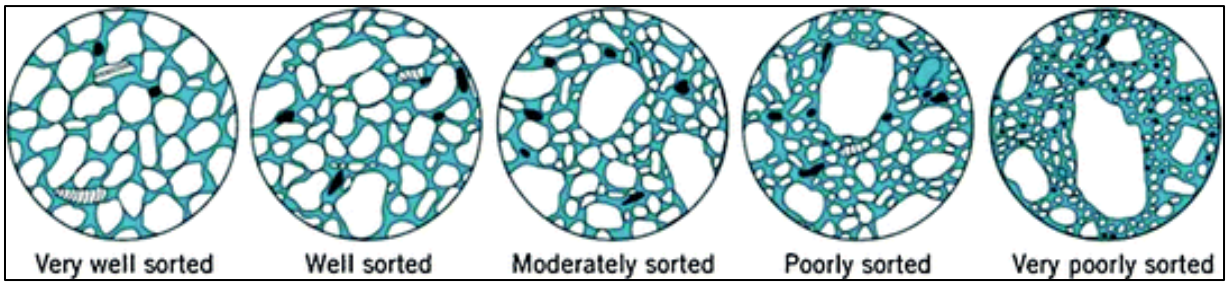

Figure 2.3: A high permeability is often a product of the heterogeneity of the reservoir [21].

Absolute permeability considers the flow of a single incompressible fluid through a porous media that is 100% saturated with the fluid [16]. For liquids, Darcy´s law may be applied for permeability calculations:

$$K = \frac{Q\mu L}{A\Delta P} \tag{2.3}$$

Where:

- K = Absolute permeability (Darcy)
- Q = Flow rate (cm^3/s)
- μ = Viscosity (cP)
- L = Length of core sample (cm)
- A = Cross sectional area (cm^2)
- ΔP = Pressure difference across core sample

The above equation is valid under the assumptions of no chemical reactions between fluid and core, a steady-state laminar viscous flow, and a horizontal flow such that gravity may be neglected.

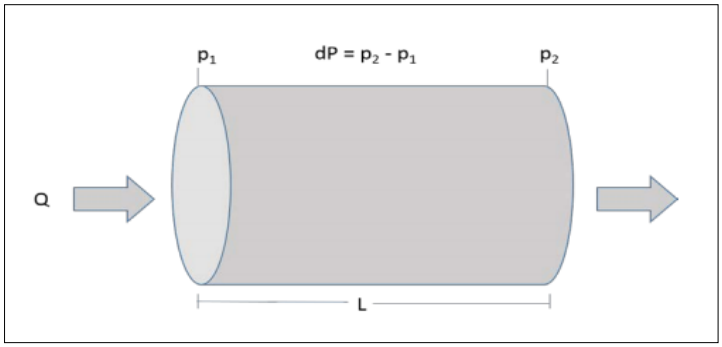

Figure 2.4: Permeability is a measure of fluid flow in porous media.

2.1.3 Fluid Saturation

In a hydrocarbon reservoir rock, the fluids that may be present are water, oil and gas. The hydrocarbons existing in petroleum reservoirs today have not always been there. The petroleum fluids are originally formed in source rocks and have posterior to their formation migrated into a surrounding reservoir rock due to buoyancy effects. Being less dense than water, the hydrocarbons will migrate upwards until trapped by geological structures. Hence, the gas will be distributed on the top of the reservoir, followed by oil in the middle and water at the bottom [15].

The total saturation of a reservoir rock is given by:

$$S_w + S_o + S_g = 1 \tag{2.4}$$

Where:

- S_w= Water saturation
- S_o = Oil saturation
- S_g = Gas saturation

The saturation of each fluid is given by:

$$S_w = \frac{V_w}{V_p} \qquad S_o = \frac{V_o}{V_p} \qquad S_g = \frac{V_g}{V_p} \tag{2.5 a,b,c}$$

Where:

- V_w= Volume of water
- V_o = Volume of oil
- V_g = Volume of gas
- V_p = Pore volume

2.1.4 Effective and Relative Permeability

In general, there are two or three fluids contained within a reservoir simultaneously. In order to evaluate the flow of such multiphase systems, effective and relative permeability may be defined. When two or more fluids are accompanied in a reservoir, the effective permeability is a measure of the ability of a specific fluid to be transmitted through when surrounded by other immiscible fluids [16].

The effective permeability of a fluid, *i*, is given by:

$$K_{eff,i} = \frac{Q_i \mu_i L}{A \Delta P} \tag{2.6}$$

Where:

- i = Specific fluid (water, oil or gas)
- Q = Flow rate
- μ = Viscosity
- L = Length
- A = Cross sectional area
- ΔP = Pressure difference

The relative permeability is a dimensionless saturation dependent measure of the ability of a specific fluid to flow through a porous rock in the presence of other immiscible fluids [16]. The relative permeability is given as a number between 0 and 1. When the effective permeability is known, the relative permeability may be found by the following correlation:

$$K_{r,i} = \frac{K_{eff,i}}{K} \tag{2.7}$$

Where:

- i = Specific fluid (water, oil or gas)
- $K_{eff,i}$ = Effective permeability of specific fluid
- K = Total permeability

The relative permeability is often visualized in a plot called the relative permeability curve. The relative permeability of the phases present in the reservoir is plotted against the water saturation. Figure 2.5 illustrates typical relative permeability behavior for a two-phase water-oil system under strongly water-wet and strongly oil-wet conditions.

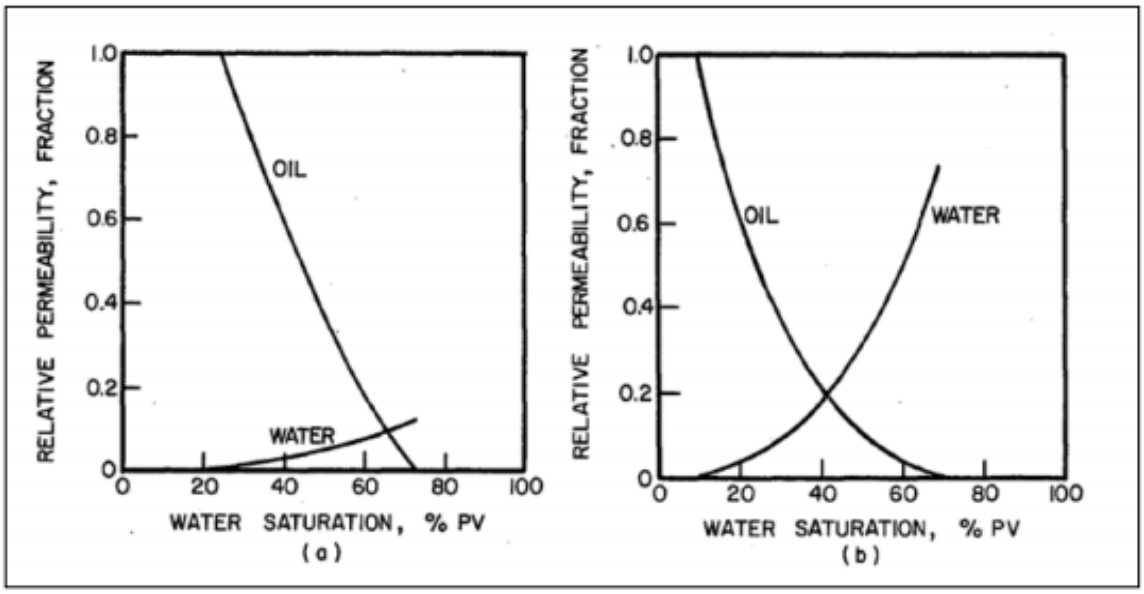

Figure 2.5: Relative permeability curves for a water-wet system (a) and an oil-wet system (b), respectively [22].

From the relative permeability figures above, it may be deducted that the flow properties of oil and water are highly dependent on the wettability of the system and the saturation of the individual phases. In general, the water relative permeability will naturally increase proportional to the water saturation, whereas the oil relative permeability will decrease. The non-wetting phase yields a straighter relative permeability curve as it flows more smoothly considering its position in the middle of the pores avoiding wall friction. Figure 2.5b reveals that the end-point relative permeability for water is significantly higher in oil-wet systems. This phenomenon may be explained by the distribution of fluids under different wetting regimes, and that water flows more rapidly throughout a porous media when it flows in the middle of the largest pores, refraining friction with the wall. In addition, the water can obtain a relatively straight path in oil-wet systems. In water-wet systems, the capillary trapped residual oil remains as globules distributed in the pore centers. These oil globules may portray an obstacle for the free movement of water [22].

Other observations from figure 2.5 is that the initial water saturation, S_{iw}, is higher in the water-wet system, explained by the wetting preference of the rock. Moreover, the relative permeability curves cross after S_w = 0.5 in the water-wet system, and before S_w = 0.5, in the oil-wet system [22]. Some of the rules for determining wettability based on the relative permeability curves are presented in table 2.1:

Table 2.1: Relative permeability behavior dependence on wettability [22].

	Water-Wet	**Oil-Wet**
S_{iw}	>0.2-0.25	<0.15 – 0.1
Intersection of curves at S_w	>0.5	<0.5
$K_{rw,or}$	<0.3	>0.5 - 1

2.1.5 Mobility

Mobility is a measure of the ability of a fluid to flow, and depends on the relative permeability, $K_{r,i}$, and viscosity, μ_i, of the specific fluid [15]:

$$M = \frac{K_{r,i}}{\mu_i} \tag{2.8}$$

The subscript i denotes the fluid phase, which can be water, oil or gas.

For stability predictions of a waterflood and production behavior, the mobility ratio is an important measure. The mobility ratio is defined as the ratio between the mobility of the displacing phase and the mobility of the displaced phase [15]. In an oil recovery scenario, the displacing fluid is water, and the displaced phase is oil:

$$M_{wo} = \frac{M_{displacing\ phase}}{M_{displaced\ phase}} = \frac{k_{rw}}{k_{ro}} \frac{\mu_o}{\mu_w} \tag{2.9}$$

The most ideal scenario for oil recovery is that the mobility ratio, $M_{wo} \leq 1$ [15].

2.2 Fluid Properties

2.2.1 Surface and Interfacial Tension

The surface tension of liquids is in relation with intermolecular forces, and can cause the formation of droplets. Molecules are surrounded by attractive and repulsive forces in varying strength. A molecule placed in a liquid bulk phase will experience equal attractive forces from each direction, whereas a molecule at the surface will be affected by an unequal distribution of forces. This phenomenon creates an asymmetry responsible for the origin of surface energy, equivalent to surface tension [23].

The surface molecules will be pulled towards the bulk phase by cohesive intermolecular forces, leading to a greater distance between molecules at the surface compared to in the bulk. As depicted in figure 2.6, a larger separation between molecules is correspondent with a larger energy obtained by the molecules. The strength of surface tension is dependent on the interacting cohesive forces between the molecules. The stronger the intermolecular forces between the molecules of a fluid, the stronger the surface tension [23].

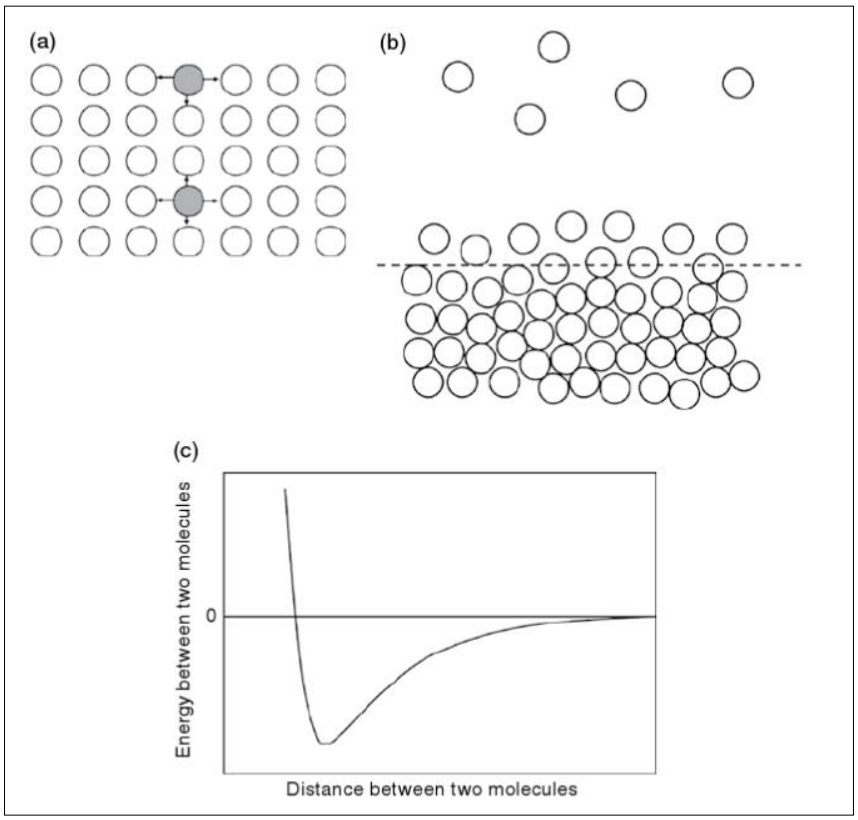

Figure 2.6: (a) Surface tension roots from the imbalance of cohesive forces exerted on molecules at the surface. (b) The molecules close to the surface have a higher energy due to the larger separations, as deduced from the energy versus molecule distance graph in (c) [23].

The *surface tension* term is used for a liquid-air interface. When describing the interface between two immiscible or poorly miscible liquids, the term *interfacial tension* is utilized. In correspondence with surface tension, interfacial tension also originates from an imbalance of attractive forces on interface molecules. Immiscibility between liquids is caused by a significant difference in cohesive forces between molecules of the two liquids, resulting in a net force at the interface. The magnitude of this force is proportional to the difference in cohesive forces [23].

The magnitude of surface- and interfacial tension may be affected by several mechanisms, and added components to an aqueous system may increase or decrease the tension. A surfactant is a molecule acknowledged for its interfacial tension lowering properties, which is of special interest for mobilizing residual oil [24].

2.2.2 Capillary Pressure

Capillary pressure exists when two immiscible fluids are in contact in capillary like tubes, exemplified by the interface between the reservoir fluids oil and water meeting in a pore throat [15]. The understanding of capillary pressure provides knowledge of how immiscible fluids are distributed in a porous media.

The preferential wetting of the capillary walls by one of the immiscible fluids results in a curved interface between the phases, and due to this curvature, the pressure will increase across the interface to balance the interfacial tension forces [25]. Thus, a scenario where the pressure in the phase on the concave side exceeds the pressure in the phase on the convex side will emerge, giving rise to a pressure difference known as the capillary pressure [26].

The curvature of the interface is proportional to the pressure difference across the interface, described by Young Laplace's equation [15]:

$$P_c = \sigma \cdot \cos(\theta) \cdot \left(\frac{1}{r_1} + \frac{1}{r_2}\right) \tag{2.10}$$

Where:

- σ = Interfacial tension between the fluids
- θ = Contact angle
- r_1 = Radius of interface
- r_2 = Radius of interface

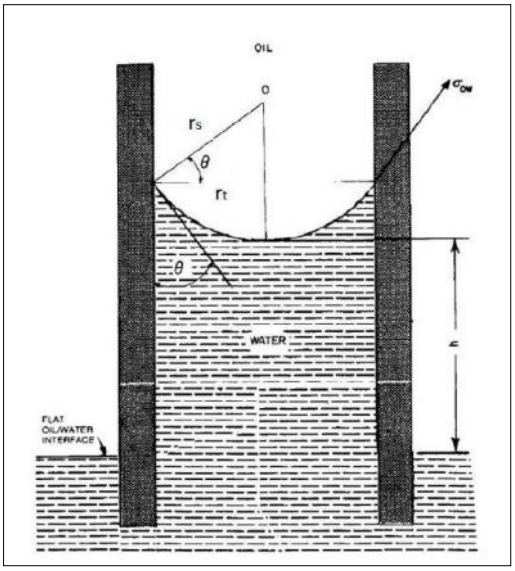

Figure 2.7: Oil/water interface in a capillary tube [26].

The capillary pressure may also be defined as the pressure difference between the non-wetting and wetting phase [15]:

$$P_c = P_{nw} - P_w \tag{2.11}$$

Where P_{nw} and P_w relates to the pressure in the non-wetting and wetting phase respectively.

In general, water wets the capillary walls, and the non-wetting oil rests on a thin water film [25]. Thus, capillary pressure is frequently referred to as the pressure difference between oil and water, P_o and P_w [15]:

$$P_c = P_o - P_w \tag{2.12}$$

Due to this definition, the capillary pressure may be positive or negative, depending on the direction of the radii of curvature [26]. A straight interface yields zero capillary pressure.

The capillary pressure is dependent on local pore geometry, wettability, saturation of reservoir fluids and saturation history (hysteresis) [26]. Therefore, the radii of curvature may vary between pores, and an average macroscopic property of the rock sample is applied [25].

2.2.3 Viscosity

Viscosity is a fundamental characteristic property of all liquids, and is a measure of their internal friction [27]. For liquids, it may also correspond to the informal concept of thickness. The study of viscosity reveals how restrictive the fluid is to flow or shear, which may be visualized by the laminar shear of fluid between two plates [28]:

A layer of a chosen fluid is placed between two horizontal parallel plates at a distance, y, from each other where the position of the bottom plate is fixed and the top plate is moving horizontally at a constant speed, v. During the movement of the upper plate, fluid particles will move parallel to it and a downward velocity gradient will develop; varying from v at the top and zero at the bottom. Each layer of fluid will have a higher velocity than the layer below. When the plate moves right at a constant speed, no net force is acting on the plate. Hence, the fluid exerts a force of friction on the plate, resisting motion. The magnitude of the opposing force equals F.

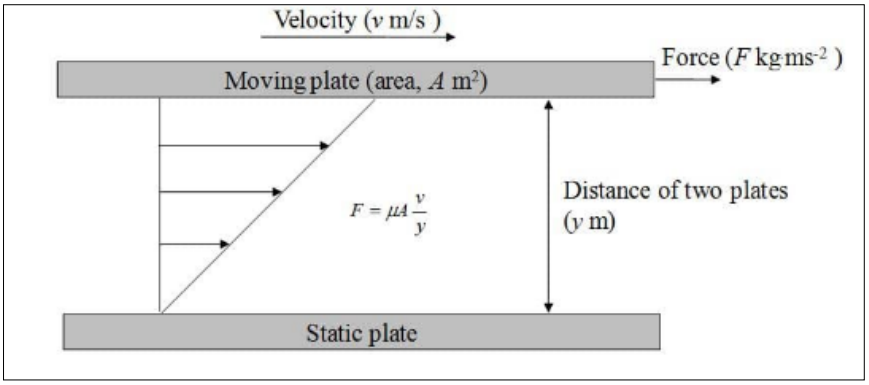

Figure 2.8: Viscosity equals the force of resistance [28].

In mathematical terms, the shear stress, τ, may be expressed by the force, F, required to move the top plate of area, A:

$$\tau = \frac{F}{A} \tag{2.13}$$

The viscosity, μ, of the fluid may be further derived, given as an expression of the ratio between the shear stress to the velocity gradient in the fluid:

$$\mu = \frac{F/A}{dv/dy} \tag{2.14}$$

Where:

- F = External force required to keep plate moving at a constant speed
- A = Contact area of each plate
- dv/dy= Rate of shear deformation

The flow characteristics of a liquid are mainly dependent on the viscosity, and when shear stress is applied, the viscosity of the fluid may change from the initial viscosity [27].

Fluids are characterized by the shear dependency on their viscosity. For *Newtonian* fluids, the shear stress is linear to the shear rate, indicating that the fluid exhibit shear independency and the viscosity will remain constant. However, this is not the case for all fluids. *Non-Newtonian* fluids will experience a change in viscosity as a function of forces exerted on it [27].

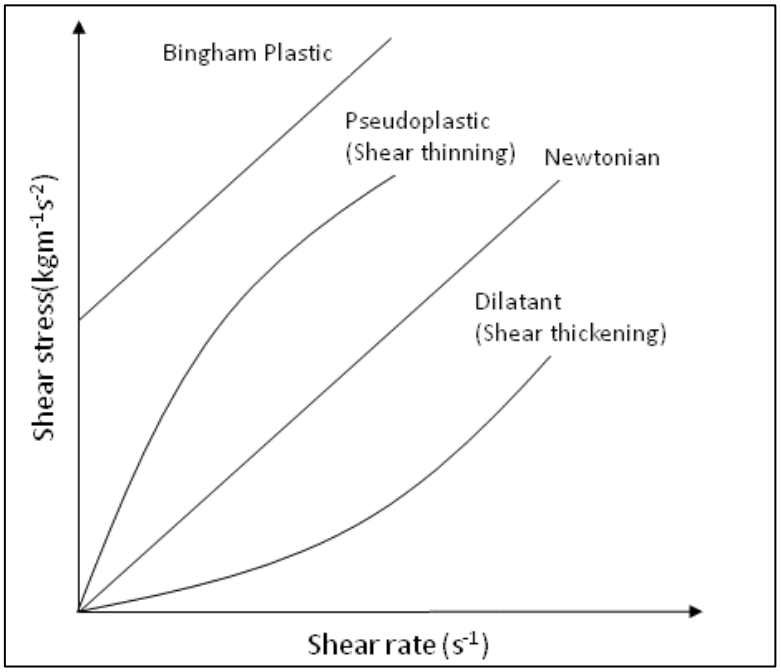

Figure 2.9: The viscosity dependence on external forces [28].

There are assorted types of shear stress/shear rate behavior. *Pseudoplastic* fluids are shear-thinning, meaning that their viscosity will decrease as the shear rate increases. The opposite example is *dilatant* fluids, which display shear-thickening properties and are becoming more viscous as the exerting forces increase. Some fluids may require a certain threshold stress to exhibit a change in viscosity, exemplified by the *bingham plastic* behavior [27].

The viscosity behavior of fluids is of special interest in many fields of science, including the oil industry. The reservoir fluids oil and water exhibit Newtonian behavior, but some chemicals injected into the reservoir during a tertiary recovery process are shear dependent. An example of this is polymers, which viscosify the injection water to form a pseudoplastic fluid. The purpose of this shear-thinning mixture is to reduce the mobility ratio between water and oil in reservoirs where the crude is highly viscous. In cases where the viscosity difference between oil and water is significant, the water may surpass areas of oil and follow high-permeable zones, leading to an early water-cut in addition to a poor sweep efficiency [29].

2.2.4 Ionic Strength

The ionic strength of a solution is a measure its ion concentration, and is given by:

$$I = \frac{1}{2}\sum_{i=1}^{n}(c_i \cdot z_i^2) \tag{2.15}$$

Where:

- c_i = Concentration of ion, i
- z_i = Charge of ion, i
- n = Sum of ionic species present in the solution

2.2.5 pH

The pH is a logarithmic scale ranging from 1-14 used to designate the acidity of basicity of an aqueous solution where neutrality is at pH 7. The pH is a measure of the hydrogen ion concentration of a solution, and may be found from the following correlation:

$$pH = -log_{10}[H_3O^+] \tag{2.16}$$

Solutions with pH values below 7 have a high concentration of H_3O^+, and is considered acidic. If the pH is above 7, the solution is considered basic.

2.3 Fundamentals of Oil Recovery and Flooding Performance

2.3.1 Prediction of Hydrocarbon Recovery

The estimation of the hydrocarbon volume initially in place is an important factor in the planning phase to examine whether the field development is economically viable [15]. The volume of hydrocarbons contained within a reservoir is dependent on the total pore volume and water saturation (S_w). The total pore volume is determined by the reservoir size, and the total size of pores and pore throats.

OOIP is the volume of oil originally in place [30], and is given by:

$$OOIP = \frac{A \cdot h \cdot \varphi \cdot (1 - S_w)}{B_{oi}} \tag{2.17}$$

Where:

- A = Reservoir area (m^2)
- h = Reservoir thickness (m)
- φ = Reservoir porosity
- S_w = Water saturation
- B_{oi} = Initial oil formation volume factor (Rm^3/Sm^3)

The recovery factor – defined as the percentage oil recovered from the total oil volume in place – is dependent on which recovery method is implemented [15]. Primary recovery mechanisms often yield low production rates and recovery factors due to an unavoidable decline in reservoir pressure. Oil and gas are extracted by the creation of a pressure gradient within the reservoir that cause the hydrocarbons to flow towards producing wells [2]. The drainage of reservoir fluids will eventually lead to a pressure drop that greatly reduce the production driving force. Additionally, pressure has a large impact on reservoir fluid volume and composition [15]. If the pressure falls below the bubble point, light oil components may vaporize and leave a heavy oil behind with a reduced mobility.

To maintain a significant reservoir pressure, the most commonly applied secondary recovery method is waterflooding, yielding recovery factors of above 40% in the North Sea [9]. Water injection is an inexpensive recovery method, with an emphasis on the implementation and the accessibility of large quantities of seawater offshore. However, the injection of water may lead to a poor sweep efficiency in heterogeneous reservoirs and for highly viscous crudes [31].

Despite the incremental oil produced by secondary recovery techniques, significant hydrocarbon volumes left behind may be recoverable by the deployment of tertiary recovery techniques. To optimize the recovery factor further, EOR-techniques can be introduced in a tertiary mode and maximize oil recovery in both contacted and uncontacted zones. For instance, surfactants may enhance microscopic sweep efficiency in flooded areas while polymers can increase the macroscopic sweep efficiency considerably. The ambition of EOR-implementation is to escalate the recovery factor. EOR typically rises the recovery factor by 5-15% [32].

The recovery factor, E_R, is the proportion of oil produced from the oil originally in place, and is given by the following correlation [15]:

$$E_R = \frac{N_p}{N} = E_D \cdot E_{vol} = E_D \cdot E_A \cdot E_v \tag{2.18}$$

Where:

- N_p = Oil volume produced
- N = Oil volume originally in place (OOIP)
- E_D = Microscopic displacement efficiency = $\frac{Volume\ oil\ displaced}{Volume\ oil\ contacted}$
- E_{vol} = Volumetric displacement efficiency = $\frac{Volume\ oil\ contacted}{Volume\ oil\ in\ place}$
- E_A = Areal sweep efficiency = $\frac{Area\ contacted\ by\ displacing\ fluid}{Total\ area}$
- E_v = Vertical sweep efficiency = $\frac{Cross{-}sectional\ area\ contacted\ by\ displacing\ fluid}{Total\ cross{-}sectional\ area}$

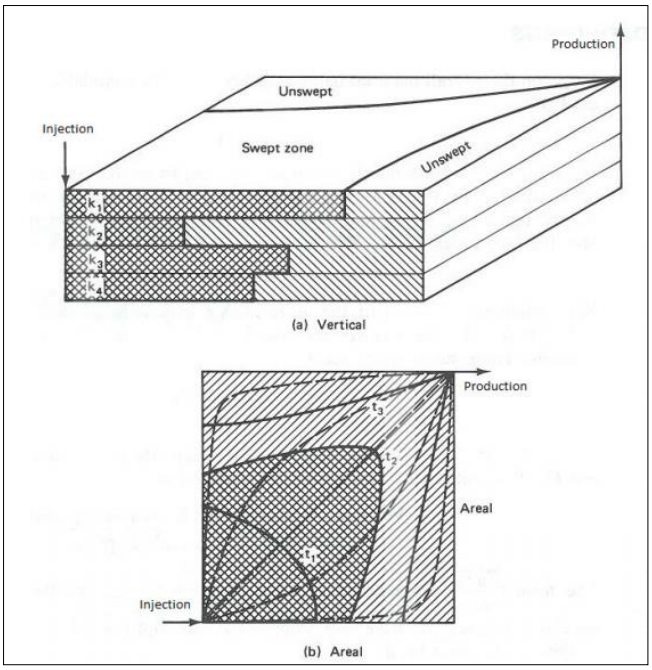

Figure 2.10: Volumetric sweep efficiency is the product of vertical displacement efficiency (a), and areal displacement efficiency (b) [33].

2.3.2 Displacement Efficiency

The mobility ratio is directly related to immiscible flooding performance. The displacement efficiency is a measure of the oil fraction recovered from a zone swept by a waterflood or similar. The Buckley and Leverett equation [34] describes fractional flow, f_w, based on the relationship between water production and total production, expressed through the fractional flow equation:

$$f_w = \frac{1}{1 + \frac{1}{M_{wo}}} \tag{2.19}$$

Assumptions:

- Steady-state flow
- Homogenous system
- Immiscible displacement
- Incompressible fluids

A graph displaying the relationship between fractional flow and water saturation may be utilized to find several parameters important for oil recovery.

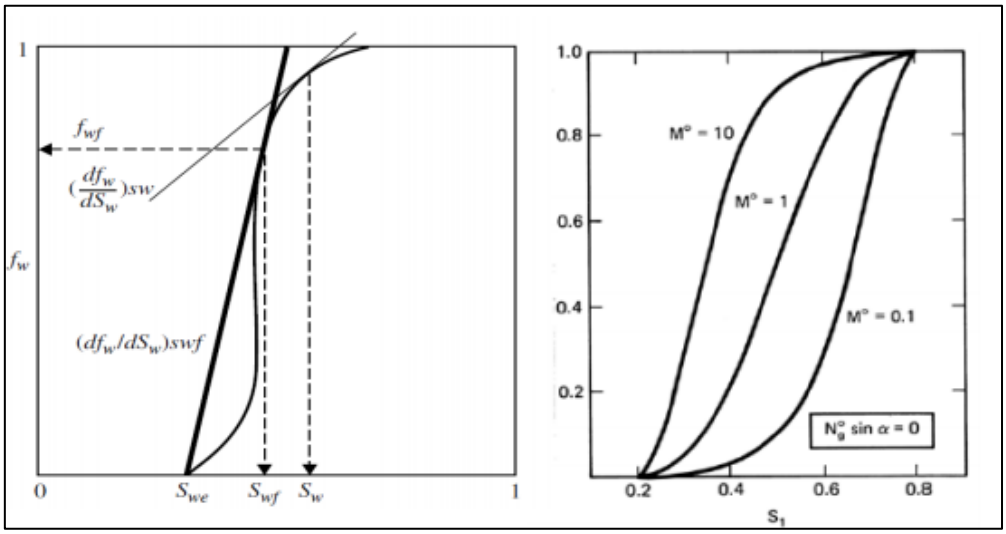

Figure 2.11: Left: The water fractional flow curve may be used to find water saturation at breakthrough (S_{wf}) and average water saturation behind the front (S_w). Right: The shape of the fractional flow curve depends on mobility ratio [34].

From the above figures, the water saturation at water-breakthrough and average water saturation behind the front may be found. The shape of the fractional flow curve is highly dependent on the mobility ratio between the immiscible oleic and water phases. In order to achieve a piston

like displacement, a mobility ratio of 1 or less is desired. In cases where the oil is highly viscous, the water is significantly more mobile, yielding an early water breakthrough and a long tail production of oil. For low oil viscosities generating a mobility ratio of ≤ 1, the oil is equally mobile or more mobile than water, and can move towards a producing well more easily. Theoretically, in a homogenous system, a piston like waterfront may be formed with a saturation of S_{iw} at the front and S_{or} behind the waterfront. Hence, only residual oil will be left behind at water breakthrough [34].

During a displacement of oil by water in a waterflooding process, the *displacement efficiency* is a measure of residual oil saturation, S_{or}, of the swept region at the instant of the first water produced [15].

$$E_D = \frac{(1 - S_{or} - S_{wi})}{(1 - S_{wi})} \tag{2.20}$$

During waterflooding, the stability of the waterfront in a homogenous system is related to the mobility ratio between the immiscible displacing and displaced fluids. High mobility ratios – exemplified by cases with high viscous oil – yield unfavorable displacement scenarios in regards to an early water breakthrough and large unswept oil zones. In reservoirs with undesirable mobility ratios, the development of viscous fingers counteracts the displacement efficiency [35]. The water follows high-permeable zones, resulting in large bypassed oil areas by the time of water breakthrough, as illustrated in figure 2.12.

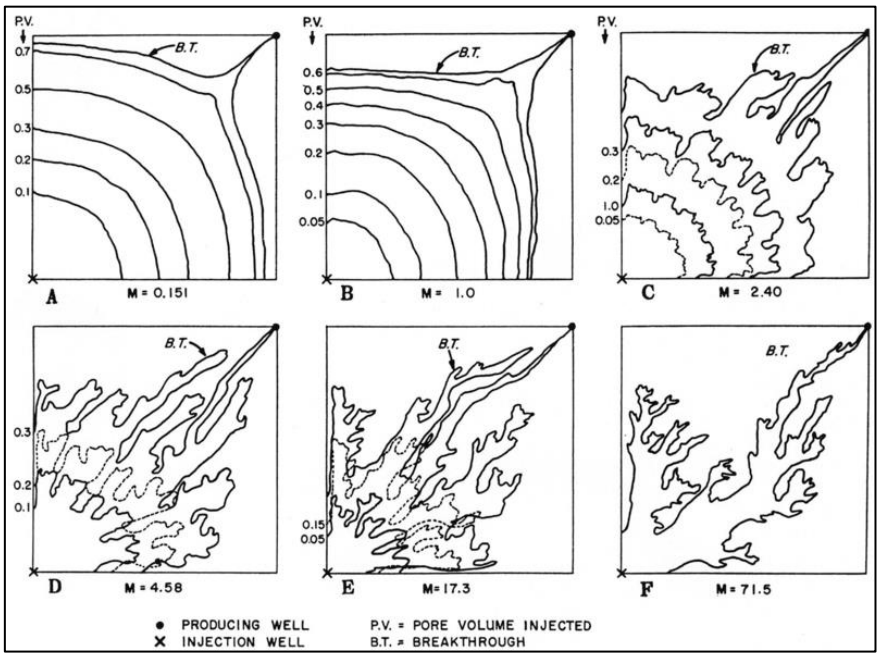

Figure 2.12: Macroscopic sweep efficiency is dependent on mobility ratio. From figure A to F, the mobility ratio increases inversely proportional to the sweep efficiency [35].

In summary, the mobility ratio greatly affects the displacement efficiency. Thus, EOR-techniques may be applied for reservoirs with high mobility ratios to reduce the bypassed oil saturation and postpone water breakthrough. For instance, polymers can be added to injection water and reduce water mobility, which will further reduce the mobility ratio [29].

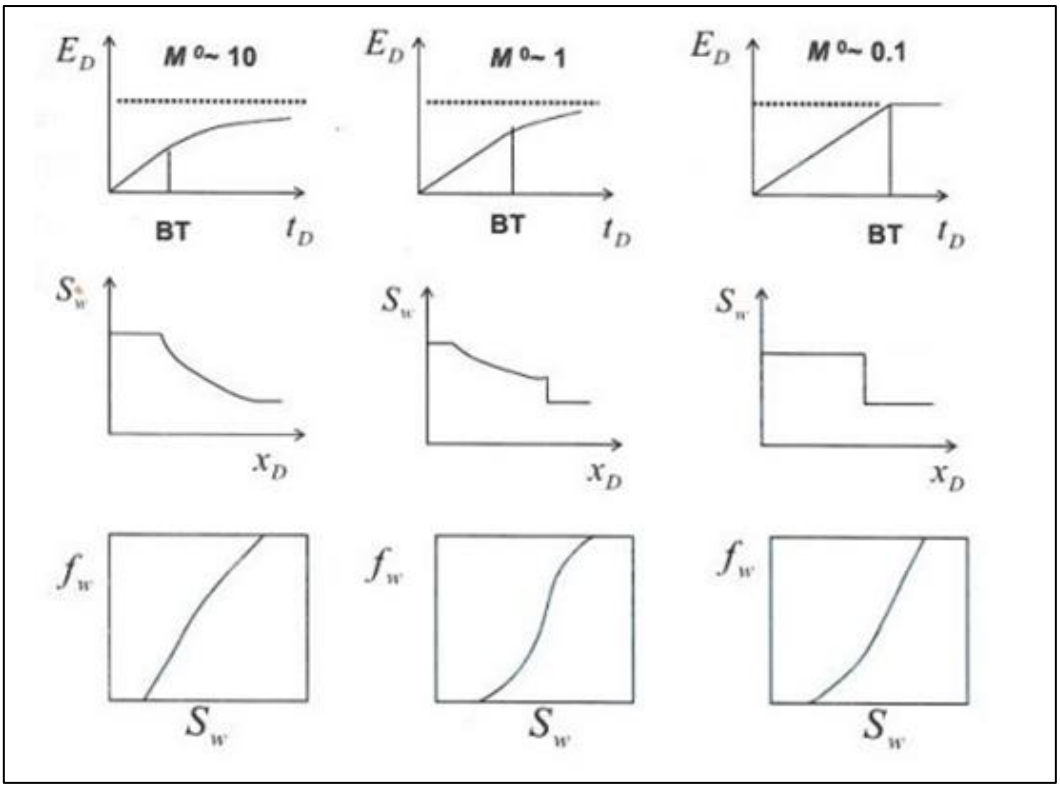

Figure 2.13: Effect of mobility ratio on displacement efficiency (upper), shape of waterfront (middle) and shape of fractional flow curve (lower) [36].

2.3.3 Wettability

The wettability of pore walls is a highly central topic in this thesis, as it is dependent on the chemical composition of reservoir fluids [11]. The initial wetting regime can be altered by several processes, exemplified by the injection of low salinity water with a different ionic composition than connate water, which will be discussed later.

Wettability is a term used to describe the preferential tendency of one fluid to spread on a solid surface in the presence of one or more immiscible fluids. The property is one of the most important factors in reservoir engineering as it affects the rate of oil recovery and residual oil saturation [25]. In the scenario of a liquid drop being placed on a solid surface, the descent to which it spreads on the surface reveals many properties of the two materials. Some liquids may coat the surface entirely, whereas other liquids prefer as little contact with the surface as possible; forming spherical droplets.

In equivalence to immiscible liquids, there also exists a surface tension between a fluid and a solid. The extent to which a liquid drop will spread on a surface is dependent on the intermolecular forces between the molecules of the same material, and the forces working between the solid surface and liquid phase. If the liquid molecules form strong bonds with the surface molecules – stronger than the ones with its own kind – it will spread on the surface. On the contrary, if the bonds formed between the two interacting materials are weak, the molecules within the liquid will prefer contact with themselves [15].

By studying the angle the droplet forms when it approaches a surface – the contact angle – the wettability of the surface may be determined. The Young equation describes the contact angle as a relationship with the interfacial tensions between the solid-oil, σ_{so}, solid-water, σ_{sw}, and water-oil, σ_{wo} [25]:

$$cos\theta = \frac{\sigma_{so} - \sigma_{sw}}{\sigma_{wo}} \tag{2.21}$$

The relationship between the contact angle and interfacial tension is illustrated in figure 2.14:

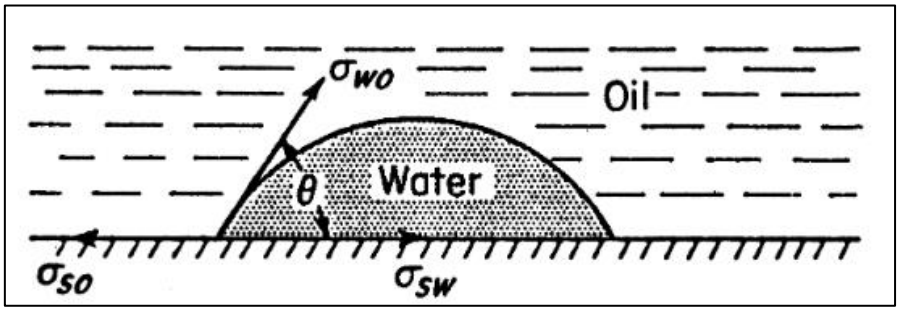

Figure 2.14: The contact angle is an indicator of the system wettability [25].

If a water drop spreads entirely on a solid surface, yielding a contact angle of zero degrees, the surface is referred to as hydrophilic, exemplifying a perfect wetting scenario. The contradictory scenario is a 180-degree contact angle that represents a non-wetting surface, often called hydrophobic. Furthermore, neutral wettability is exhibited when the contact angle is 90 degrees [37].

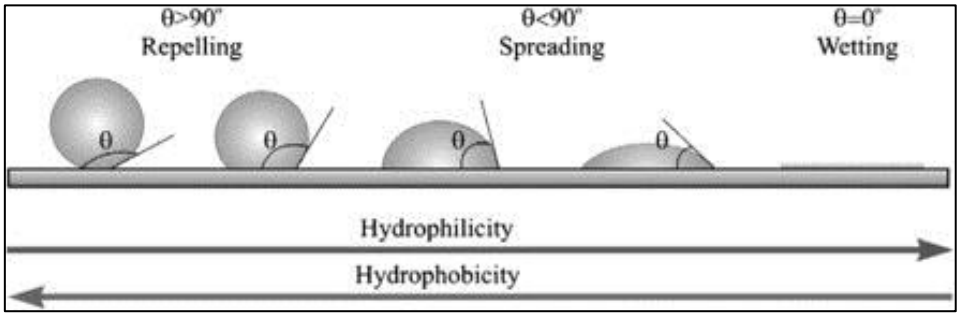

Figure 2.15: The degree of wetting [37].

The understanding of wettability is crucial for reservoir scientists as the wetting of the surface controls the location, flow and distribution of fluids inside the reservoir. The wettability will also affect several parameters, such as capillary pressure, relative permeability and residual oil saturation [38].

The scientific definition of wettability is "the tendency of one fluid to spread on or adhere to a solid surface in the presence of other immiscible fluids" [39]. In a strongly water-wet reservoir, the water will coat the pore walls and the smallest pores will be filled with water. Under these conditions, the oil will flow in the middle of the pores and not have access to the smallest pores due to capillary forces. In strongly oil-wet reservoirs, the distribution of fluids will be the opposite [40].

However, it is seldom that a reservoir possesses a strong wetting preference of either water or oil. Wettability is often referred to as the wetting preference of a rock, and does not necessarily indicate that the wetting fluid will be in contact with the surface at all given times. Hence, the wetting of a rock may be given as a degree of wetting, ranging from strongly water-wet to strongly oil-wet. Rock surfaces that show no preference of either fluids portray neutrality. Many reservoirs have a mixed wetting or fractional wetting where different areas show a wetting preference of either fluids [38].

Intermediate wettability is divided into three sub-groups; fractional-wet, mixed-wet large and mixed-wet small, as illustrated in figure 2.16 [41].

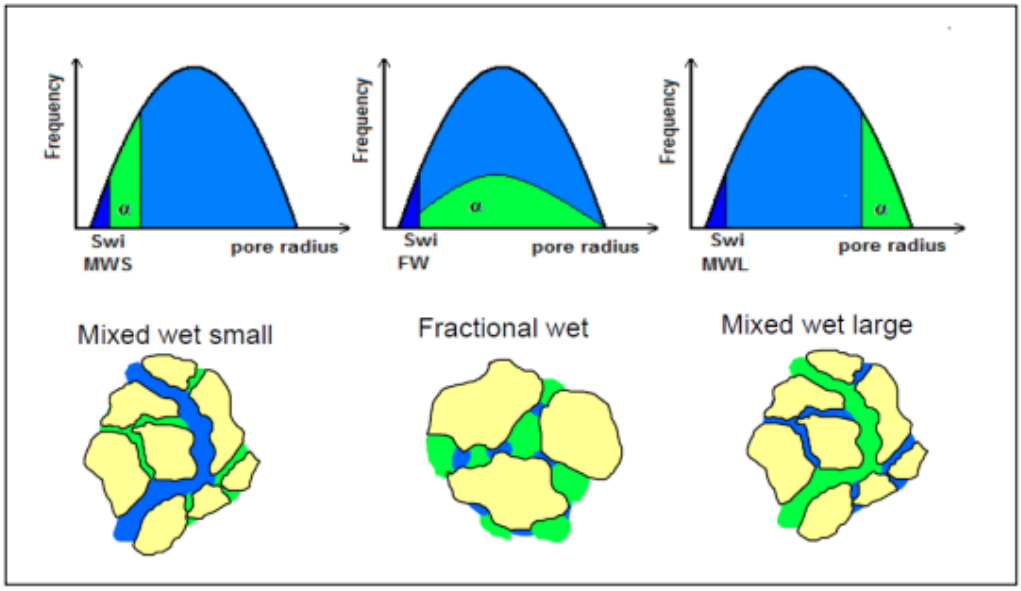

Figure 2.16: Subgroups of intermediate wettability [41].

In fractional wet rocks, some areas of the surface will be water-wet whereas other will be oil-wet. If the rock possesses a mixed wettability, the smallest pores will be wetted with one phase while the large pores will be wetted with the other phase. If the smallest pores are water-wet and the largest pores are oil-wet, the rock is referred to as mixed-wet small. In the opposite case it is termed mixed-wet large [41].

When a surface prefers contact with water, the water will imbibe spontaneously, and occupy the smallest pores and the majority of the rock surface. This affects flow patterns of the reservoir fluids [38].

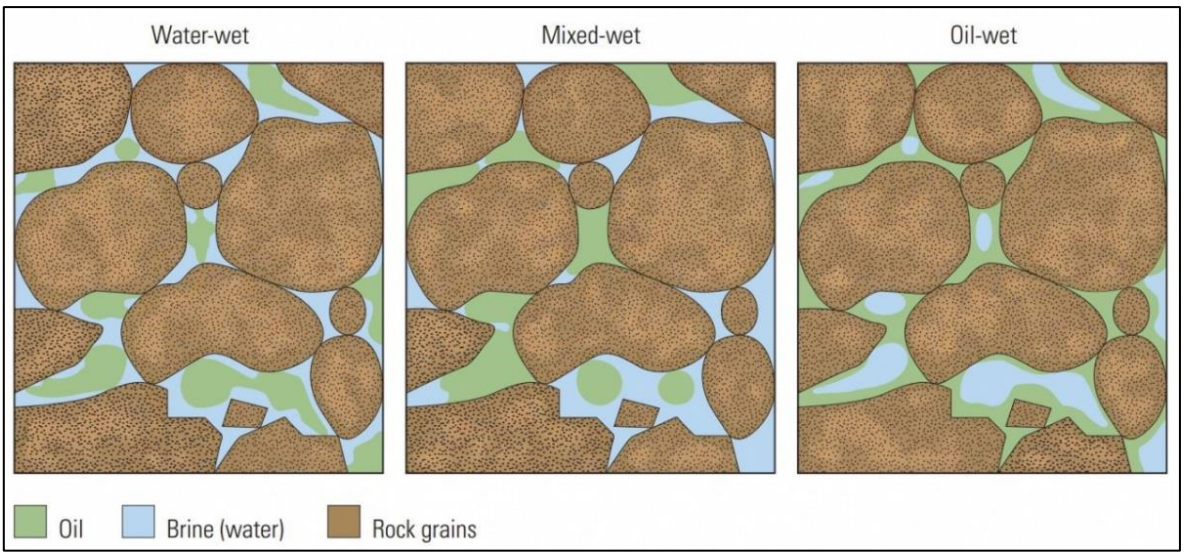

Figure 2.17: In a water-wet rock (left), oil adheres to the surface and fills the smallest pores. The opposite case yields if the rock is oil-wet (right). The mixed-wet rock portrays areas of various wetting preferences (middle) [38].

The importance of wettability gives rise to the question of what determines the wetting preference of a rock. Although the geological processes and mineralogy governing wettability are not yet fully understood, there are some general observations leading to a few rules of thumb. Clastic sandstones portray a tendency of being water-wet while an abundance of carbonates prefer oil as a wetting phase [42]. Nevertheless, there are several exceptions. The initial wettability may also be altered, exemplified by the exposure to crude oil over time, which may change the wettability to oil-wet. Originally, most reservoirs were water-wet since water usually is the first fluid the rock is subject to, but crude oil migrating into the rock at a later time may alter the wettability [38].

Other than studying the contact angle, there are several methods to measure the wettability at a laboratory. The Amott-Harvey Index, I_{AH}, and the US Bureau of Mines Index, I_{USBM} are two commonly used examples [43].

2.3.3.1 Amott-Havey Index

The Amott-Harvey Index is based on the study of spontaneous and forced imbibition processes. The wetting fluid is the only fluid that will imbibe spontaneously, and hence, the study of the ratio between spontaneous and total imbibition of either fluid can reveal the wettability of the rock. Based on this study, capillary pressure versus water saturation curves may be constructed. The index ranges from -1 for strongly oil wet to +1 for strongly water-wet rocks [43].

$$I_{AH} = \frac{Spontaneus\ Water\ Imbibition}{Total\ Water\ Imbibition} - \frac{Spontaneus\ Oil\ Imbibition}{Total\ Oil\ Imbibition} \tag{2.22}$$

2.3.3.2 US Bureau of Mines Index

I_{USBM} is a measure of the work required to imbibe the fluids, and is based on the area under the capillary pressure curves [43].

$$I_{USBM} = log\frac{A1}{A2} \tag{2.23}$$

If A1>A2, the rock is water-wet, and if A2>A1, the rock is classified as oil-wet.

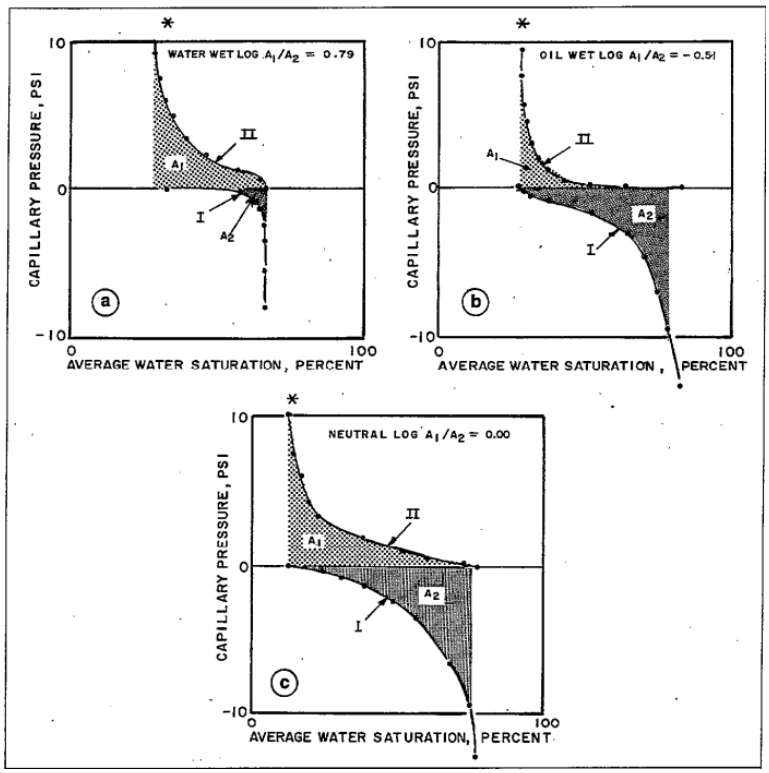

Figure 2.18: USMB wettability measurement [43].

2.3.4 Drainage and Imbibition

The concept of capillary pressure proves significant importance when observing how the immiscible reservoir fluids are distributed throughout a heterogeneous rock. In accordance with the Young Laplace equation (eq. 2.10), the capillary pressure is inverse proportional to the pore radii, indicating that the smallest pores obtain the highest capillary pressures [26].

According to Anderson (1987), imbibition is a displacement process where a non-wetting phase is expelled from of a porous rock by the wetting fluid. It is distinguished between spontaneous and forced imbibition. The forced imbibition takes place due to external work that aids in displacing the non-wetting fluid. On the contrary, spontaneous imbibition is governed by capillary actions. When a wetting fluid imbibes a porous media, the smallest pores will fill first in accordance with the Young LaPlace equation. The smallest pores yield the lowest capillary entry pressures for the wetting phase, and the non-wetting fluid will be displaced towards the larger pores and eventually abandon the rock [26].

Drainage is the opposite process, and exemplifies a scenario where a wetting fluid is displaced by a non-wetting phase. During drainage, the pores of largest radii will fill first as the threshold capillary entry pressure is lower and consequently faster matched by the pressure within the non-wetting phase. Thenceforth, pores of decreasing radii will fill as a function of increasing non-wetting pressure until the irreducible saturation of the wetting fluid is reached. The drainage and imbibition mechanisms may be visualized in the capillary pressure curve for a water-wet system [26].

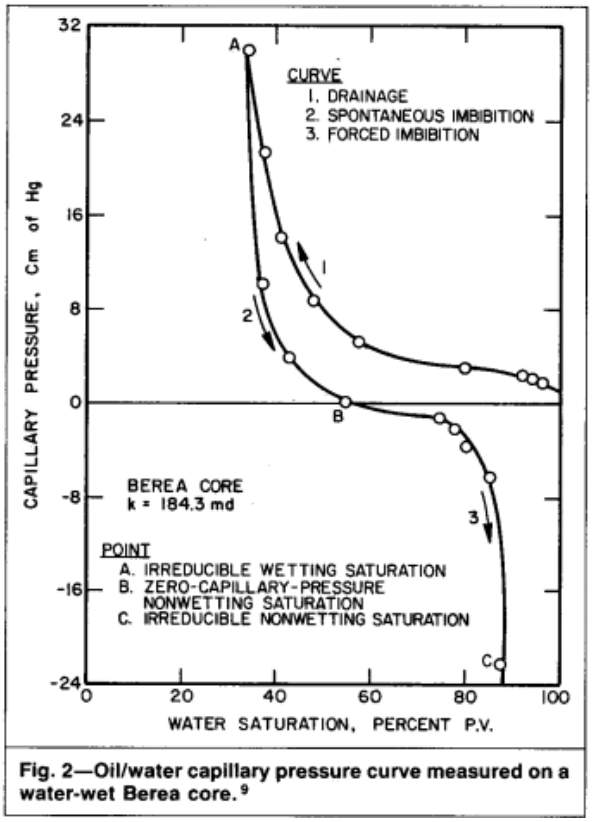

Fig. 2—Oil/water capillary pressure curve measured on a water-wet Berea core.[9]

Figure 2.19: Capillary pressure curve for a water-wet system [26].

2.3.5 Residual Oil Saturation

The purpose of oil recovery is to extract as much oil from a reservoir as possible at lowest potential cost. During production, some of the oil will remain trapped in the reservoir. The residual oil is denoted S_{or}, and two common models describing why oil is trapped after water injection in water-wet systems is the *snap-off model* and the *pore doublet model*:

2.3.5.1 The Snap-Off Model

In water-wet reservoirs, the oil will flow in the middle of the pores with a thin water film separating the oil from the pore wall. Due to capillary imbibition forces, the water film will increase in the pore throats and the oil phase will become thinner [44]. Ultimately, the oil may snap-off and become discontinuous. The oil trapped by capillary snap-off will be left behind as immobile oil globules [36], as illustrated in the figure below:

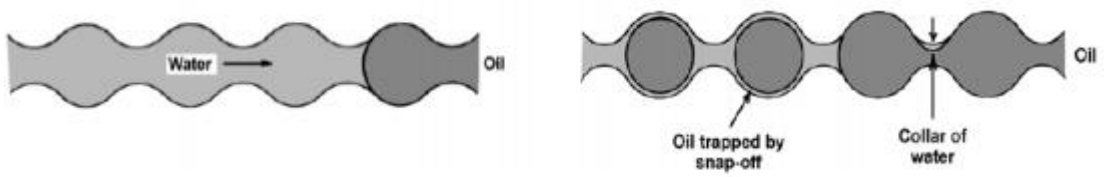

Figure 2.20: Trapping of oil by capillary snap-off [36].

2.3.5.2 The Pore Doublet Model

In cases where a pore splits into two channels, the wetting phase will intrude the narrower channel more rapidly due to capillary imbibition forces. Hence, oil will be trapped in the broader pore channel [36], as visualized in figure 2.21:

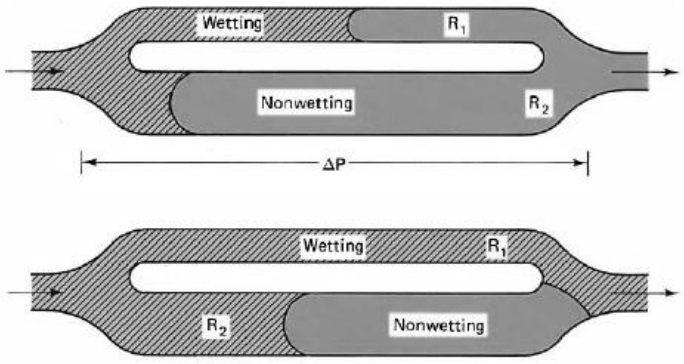

Figure 2.21: Trapping of oil in a pore doublet model [36].

2.3.6 Wettability Effects on Waterflooding

Obtaining knowledge in regards to wettability of a reservoir rock is crucial for optimizing oil recovery. The preference of a solid to be in contact with either water or oil greatly affects many aspects of the reservoir, and is of special importance when applying oil recovery techniques [38].

The wetting preference of a reservoir rock – ranging from strongly water-wet to strongly oil-wet – significantly affects the production history and residual oil saturation. The spatial distribution and location of fluids under the different wetting regimes is in control of the fluid flow of the system. Hence, wettability is in charge of relative permeability and waterflooding behavior [40].

Waterflooding is a frequently used secondary recovery technique. Water injection is implemented in order to maintain a high pressure within the reservoir and displace the oil towards a producing well, yielding higher oil recoveries. For uniformly wetted systems, experimental data reveals that water-wet rocks yield higher recoveries during waterflooding than oil-wet rocks. In water-wet rocks, the water coats the surface and fills the smallest pores, whereas the oil is distributed in the middle and in the largest pores. During imbibition, capillary forces will imbibe the water and displace oil towards the larger pores. Theoretically, in a homogeneous system, the water phase will form a piston like front, and after water breakthrough, none or little additional oil is recovered. The residual oil is a target for EOR-techniques [40].

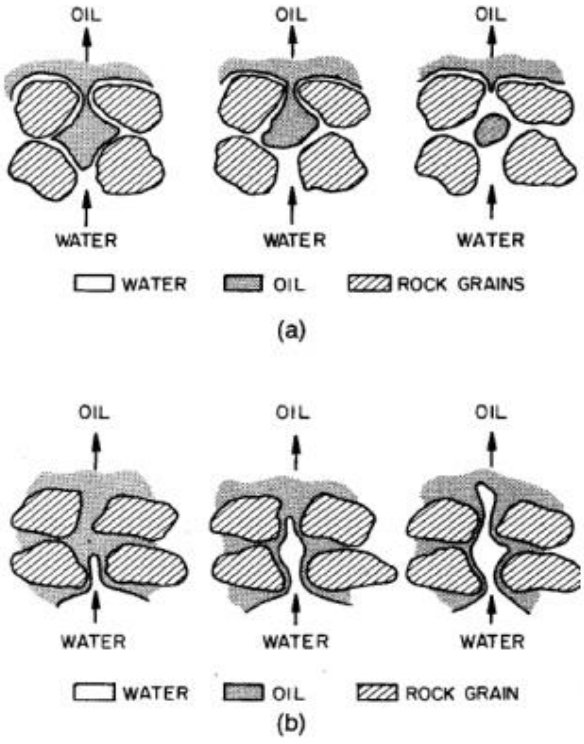

Figure 2.22: Water displacing oil from a pore during waterflooding in a strongly water-wet reservoir (a) and a strongly oil-wet reservoir (b) [45].

Due to the reversed fluid distribution in oil-wet systems, the water will flow more easily and avoid friction with the pore walls. Additionally, the water will form continuous channels or fingers throughout the center of the largest pores. Due to capillary forces, the water will not be able to reach the oil trapped in narrower crevices and pores. An unstable waterfront will be formed, and at water breakthrough, little oil is produced. A long tail production of oil follows, and the reservoir will produce water and oil simultaneously. Water injection in oil-wet reservoirs is less efficient since it requires injection of higher water volumes to produce the same amount of oil, making the economical residual oil saturation higher in oil-wet systems in comparison with water-wet systems [40].

Researchers have not yet come to a consensus regarding the optimal wettability for oil recovery by waterflooding, but the majority of documented laboratory work demonstrate that strongly oil-wet rocks yield the lowest recoveries [46]. However, oil recovery is not necessarily proportional to the degree of water-wetness. According to studies conducted by Jadhunandan (1990), the optimum oil recovery by waterflooding is achieved at intermediate to slightly water wet conditions [47]. Water-wetness yields better waterflooding performance, but if the degree of water-wetness is too excessive, oil tends to snap-off when approaching constrictions and pore throats. The capillary trapped oil globules are left as residual oil.

As reported by Wardlaw and Yu (1986), the displacement efficiency was least for strongly wetting regimes (contact angle $< 30^{o}$), and greatest for conditions approaching intermediate wettability. Their studies claimed that the oil snap-off process does not occur in a system with advancing contact angles greater than 70^{o} [48].

Figures 2.23 and 2.24 illustrate the results from studies carried out by Jadhunandan (1990) obtained from 48 waterflooding tests, showing oil recovery and residual oil saturation as a function of wettability index. The figures clearly suggest that the intermediate to weakly water wet cores yield the most favorable oil displacement [47].

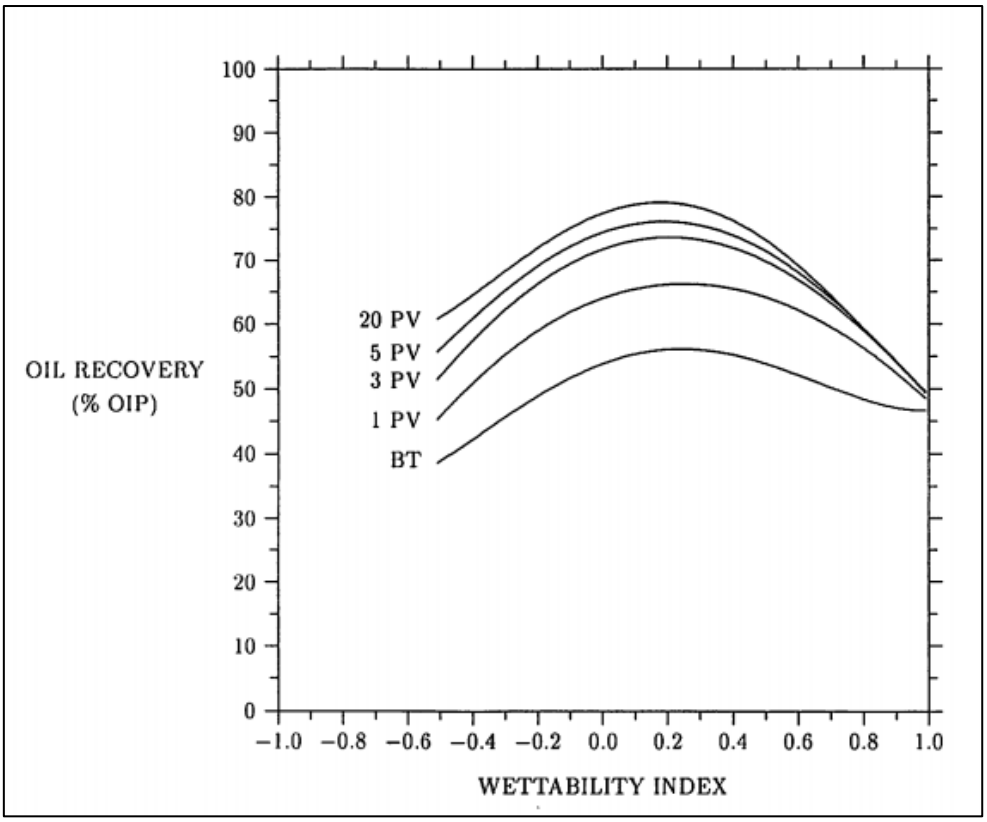

Figure 2.23: Neutral to slightly water-wet conditions yield maximum oil recovery at breakthrough, 1, 3, 5, and 20 pore volume throughput [47].

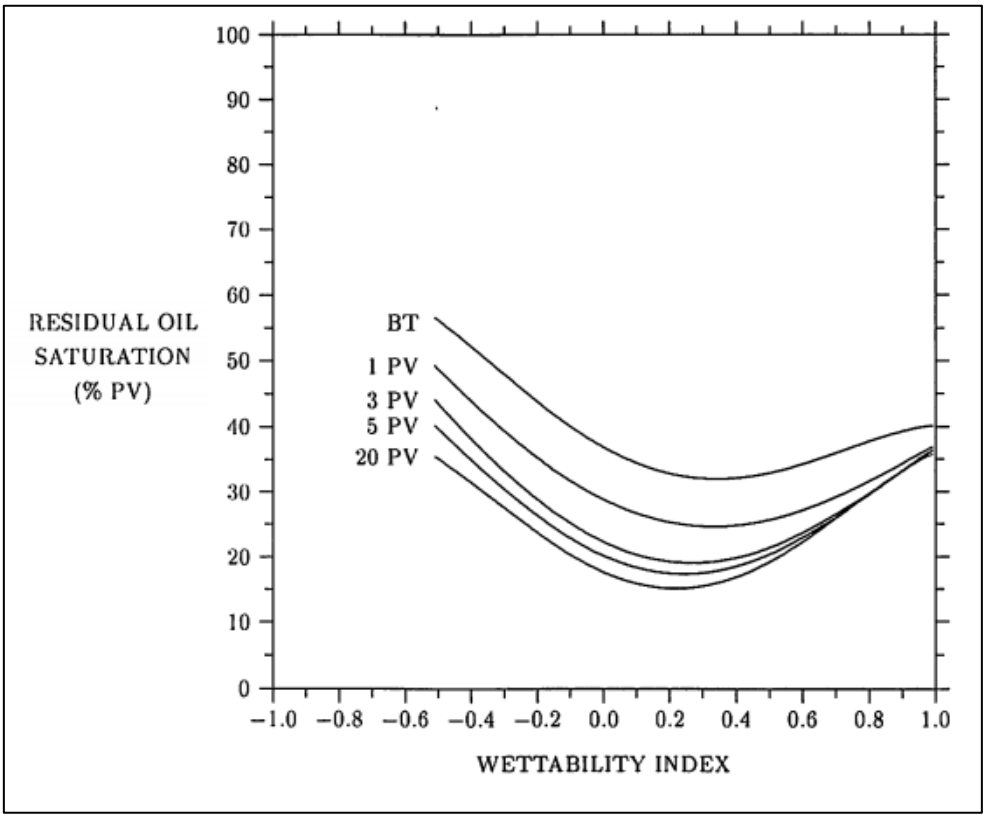

Figure 2.24: Residual oil saturation versus wettability at breakthrough, 1, 3, 5 and 20 pore volumes injected [47].

2.3.7 Breakthrough, Economical, and Ultimate Residual Oil Saturations

During waterflooding, it is distinguished between three different residual oil saturations; namely the residual oil saturation at water breakthrough, the economical (practical) residual oil saturation, and the ultimate residual oil saturation. In a uniform strongly water-wet system with a moderate to small mobility ratio, all these saturations are approximately equal [40]. On the contrary, these saturations can differ significantly in intermediate and oil-wet systems.

The residual oil saturation at breakthrough indicates how much oil is left behind at the instant when the first water is produced. In uniform strongly water-wet reservoirs with a moderate to small mobility ratio, a stable piston like waterfront will be established within the rock, pushing only oil in front of it. Before breakthrough, a volume of oil is produced for every volume of water injected, yielding a highly economical attractive scenario. In intermediate to oil-wet reservoirs, the water breakthrough will occur faster, leaving a higher residual oil saturation at breakthrough [40].

After water breakthrough, oil and water will be produced simultaneously. The water-oil-ratio, WOR, will increase continuously with time, and more water must be both injected and produced for every additionally barrel of oil recovered. Eventually, the WOR will reach a level where the expenditure of injecting and producing more water overreaches the profit of the additional oil produced. The system is then at the economical residual oil saturation. In general, this saturation will be lower in water-wet systems [40].

In intermediate and oil-wet systems, there may still be continuous connections between the oil throughout the porous media after the economical cut-off [40]. If the production of additional oil was maintained at a very high water/oil-ratio after the economical saturation was reached, it would be theoretically possible to extract more oil from intermediate and oil-wet systems than for water-wet systems. In water-wet systems, the oil remains within the larger pores where it may become disconnected from a continuous mass of oil. However, in intermediate and oil-wet formations, the oil adheres to the surface as thin films, which increase the probability of a continuous path towards a producing well. The volume of residual oil trapped in water-wet formations will in theory be larger than the volume of oil left as thin films in intermediate to oil-wet rocks, hence yielding a lower ultimate residual oil saturation [38]. Nevertheless, it may require the injection of thousands of pore volumes of water to reach this saturation [40].

Chapter 3

Enhanced Oil Recovery (EOR)

Hydrocarbon reservoirs face major challenges regarding ultimate field recoveries. Easily recoverable oil is declining, and large oil volumes remain in the reservoirs after implementing conventional recovery techniques [49]. In many cases, more than 60% of hydrocarbons are unrecoverable by primary and secondary recovery methods [2], hence the growing interest concerning chemical additives that may optimize production. The utilization of chemicals in a recovery situation falls under the category of tertiary recovery methods, and are crucial to guarantee a continuous oil supply.

Primary recovery techniques usually indicate the initial production stage where pressure depletion and compression of bedrock works as the displacing effects. Eventually, the production from the primary techniques reaches a decline, and secondary recovery techniques are introduced. Secondary recovery concerns the utilization of injected water or hydrocarbon gas where the aim is to maintain a significant pressure within the reservoir and displace the oil towards a producing well [8].

Even though secondary recovery techniques significantly increase production, there are still strong forces keeping immobilized hydrocarbons trapped in the reservoir, unreachable by injection fluids. Consequently, the petroleum industry has devoted years of research to discover new methods that can improve oil recovery efficiency. Recovery of oils retained due to capillary forces (light oils) and immobility due to high viscosities (heavy oils and tar sand) may be achievable by implementation of EOR-methods [50].

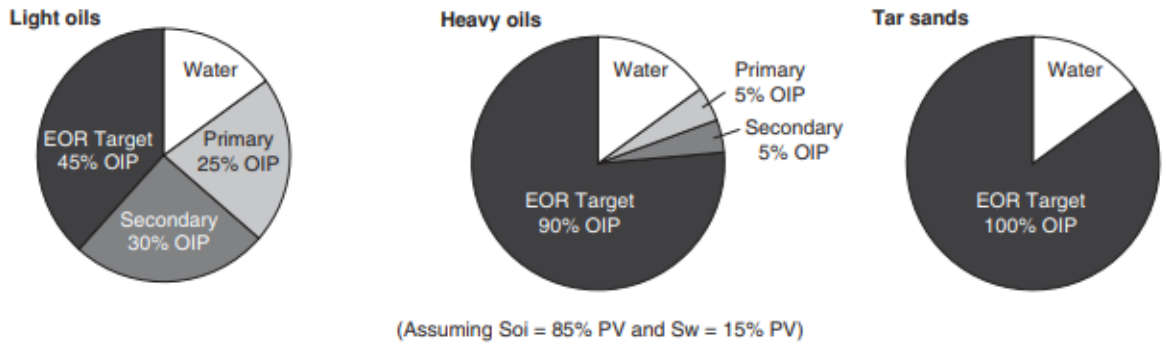

Figure 3.1: EOR-target for different types of hydrocarbons. The EOR-target for light oils is typically 45% OIIP, while heavy oils and tar sand respond poorly to primary and secondary recovery methods [50].

3.1 Capillary Number

When looking for new methods to increase oil production, the *capillary number* plays an important role. The capillary number is a dimensionless measure of viscous forces over capillary forces [15]:

$$N_c = \frac{\mu V}{\sigma} \tag{3.1}$$

Where

- μ = Dynamic viscosity of fluid
- V = Characteristic velocity
- σ = Interfacial tension between two fluid phases

To mobilize residual oil, it is necessary to increase the capillary number several orders of magnitude by either reducing capillary forces or increasing viscous forces [15]. This is further portrayed in the capillary desaturation curve below:

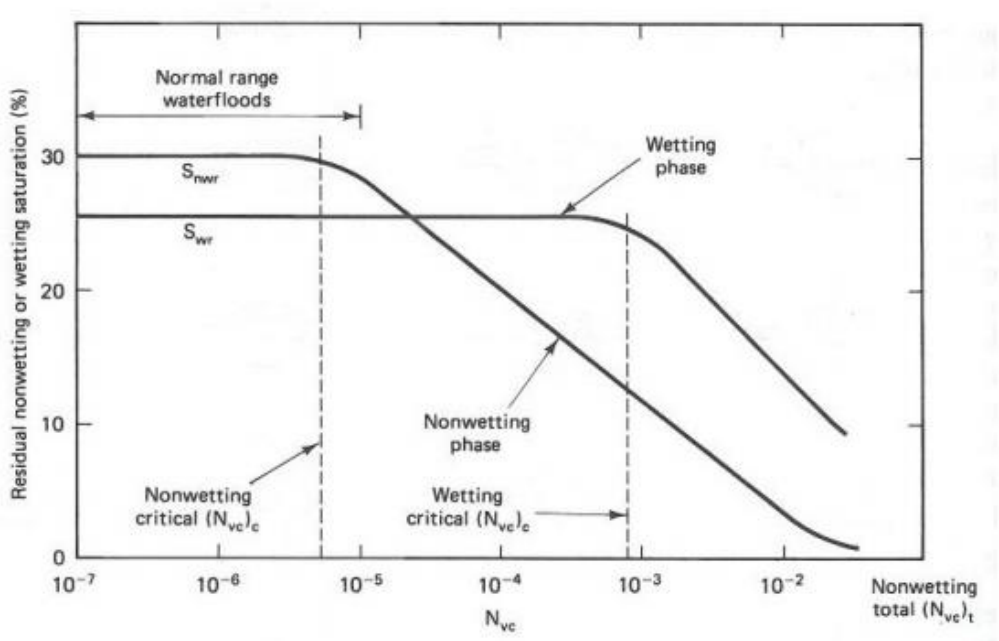

Figure 3.2: Capillary desaturation curve for wetting and non-wetting phases [51].

The figure above displays the relationship between the capillary number and the residual oil saturation. The starting point of declination of S_{or} depends on the wettability of the rock and its pore size distribution. If a wide pore size distribution is present, the initial S_{or} will be larger, and the "knee" constituting $N_{c,crit}$ will be less sharp and appear faster than for narrow pore size distributions. This is due to a larger variation in pore volumes, and the volume of oil trapped in the larger pores will be released first without a relatively high change in capillary number.

The “knee” for narrow pore size distributions will generally be sharper and appear for a greater change in N_c. Since most pores are of similar size, they all require approximately equivalent values of N_c to release trapped oil.

Wettability is also essential for the shape of the capillary desaturation curve. The initial residual volume of a non-wetting fluid will usually be higher since it is trapped as immobile globules surrounded by the other fluid. In water-wet rocks, the $N_{c,crit}$ will appear faster than in oil-wet rocks because it requires a smaller increase in N_c for volumes of immobile fluid-islands to form a continuous flow than for the thin layer of fluid that smooths the bedrock (wetting fluid).

To mobilize residual oil, the capillary number must be increased by several orders of magnitude compared to the initial value after a waterflood (N_c~10^{-6}). To enhance the capillary number, either surfactants must be added to lower the capillary forces, or polymers for viscosity reduction. However, increased viscous forces are usually not sufficient to mobilize residual oil, as polymer flooding is unable to improve the capillary number by more than one order of magnitude. The target for polymer flooding is providing a better macroscopic sweep. Surfactants are far superior on improving microscopic sweep and the reduction of residual oil [29].

3.2 Surfactants

One of the main inhibitors of hydrocarbon recovery involves capillary forces. When displacements are carried out by immiscible fluids such as oil and water, interfacial tension between the injected fluids and oil stands responsible for trapping oil within small pores [14].

A higher microscopic displacement efficiency may be enabled by the injection of surfactants. The term *surfactant* is a widely used contraction for *surface active agents*, meaning active at a surface. The purpose of surfactants is to reduce the surface free energy, enabled by their self-assembly at interfaces. Surfactants are amphiphilic molecules that exhibit both hydrophobic and hydrophilic properties. A surfactant consists of a polar head group that prefers contact with water and a non-polar tail that wishes to avoid contact with water. Its dual nature and the fact that the molecule as a whole will never thrive in a pure water phase or a pure oil phase, makes it adsorb at interfaces where the molecule will orient itself with its head in the water phase and the tail in the oleic phase. At the interface they form a monolayer which drastically changes the interface character, ultimately leading to an interfacial tension reduction [23].

3.2.1 Surfactant Types

There are different types of surfactants dependent on the chemical properties of the polar head group. Ionic head groups carry an electrical charge; either a negative charge – characterized as an anionic surfactant, or a positive charge – acknowledged as a cationic surfactant. The head group may also be non-ionic, meaning that the head group exhibit neutrality in terms of charge. Amphoteric surfactants signify the presence of both opposing charges in the head group [23].

3.2.1.1 Anionic Surfactants

A surfactant in which the hydrophilic part carries a negative charge is called an anionic surfactant. Common examples of anionic surfactants are sulphates, sulphonates, carboxylates and phosphates. When dissociated into water, they split into an anionic monomer and a cation; commonly Na^+, Mg^{2+} or K^+. Anionic surfactants are most frequently used for increasing oil recovery. This is due to them being relatively cheap, stable, retention resistant and soluble in an aqueous phase. Additionally, they efficiently reduce interfacial tension [52].

3.2.1.2 Cationic Surfactants

A cationic surfactant carries a positive charge, and dissociates into a cationic monomer and an anion when contacted with water. Alkyltrimethylammonium salts and alkyldimethylbenzyl-ammonium salts are examples. Due to the positive charge of the head group, they are highly adsorbed on negatively charged clays present in the rock surface. Their high retention prevents them from being frequently used in an oil recovery setting [52].

3.2.1.3 Non-Ionic Surfactants

Non-ionic surfactants are characterized by uncharged head-groups, and they do not ionize in an aqueous solution. Examples of non-ionic surfactants are fatty alcohols and alkylphenol ethoxylates. Due to their lack of charge, they are less sensitive to salinity than ionic surfactants. Non-ionic surfactants are mainly used as co-surfactants during oil recovery [52].

3.2.1.4 Amphoteric Surfactants

Amphoteric or zwitterionic surfactants contain two charged head groups of opposing signs. Examples of such surfactants are alkylaminipropionates and alkylbetaines. Due to their dual charge, amphoteric surfactants may be anionic at a high pH and cationic at a low pH, whereas some surfactants are insensitive to pH. Amphoteric surfactants are not frequently used in the oil industry much due to their high cost [52].

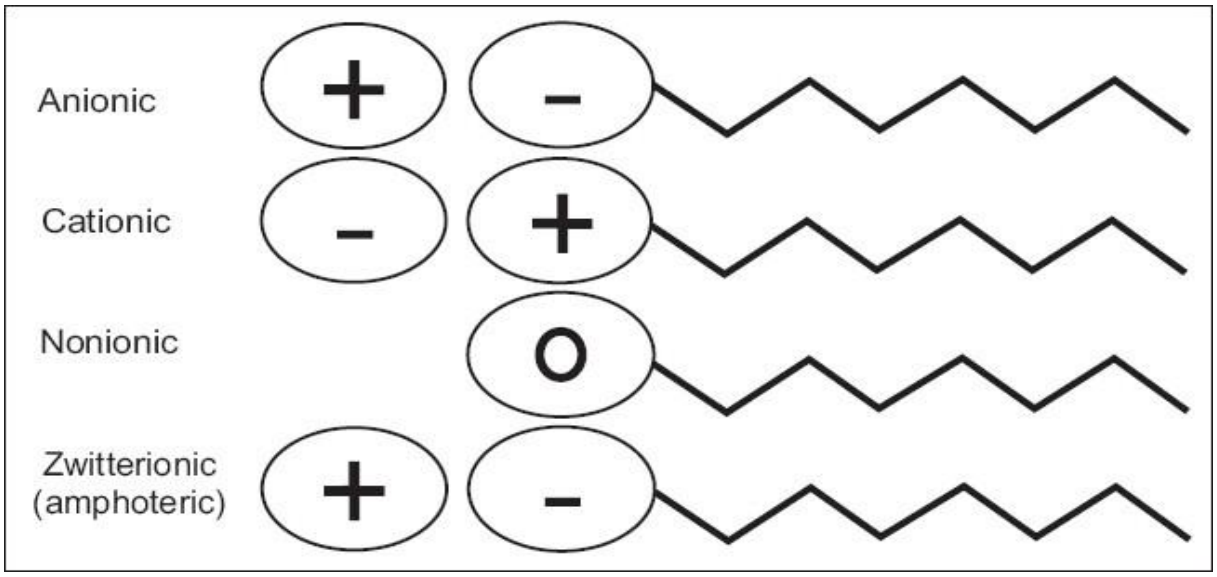

Figure 3.3: The different surfactant types with a hydrophilic head group and a hydrophilic tail [53].

3.2.2 The Formation of Micelles

After a certain concentration of surfactants is added to a system, the drop in surface tension will cease, and a constant plateau will be attained. The concentration of surfactants where this plateau occurs is called the CMC; short for *critical micelle concentration*, and is a unique property for each surfactant at a given temperature and pressure regime. The surfactants added to the solution after the CMC is reached will no longer adsorb at the interface as it is fully saturated of surfactants, but instead aggregate in micelles [23].

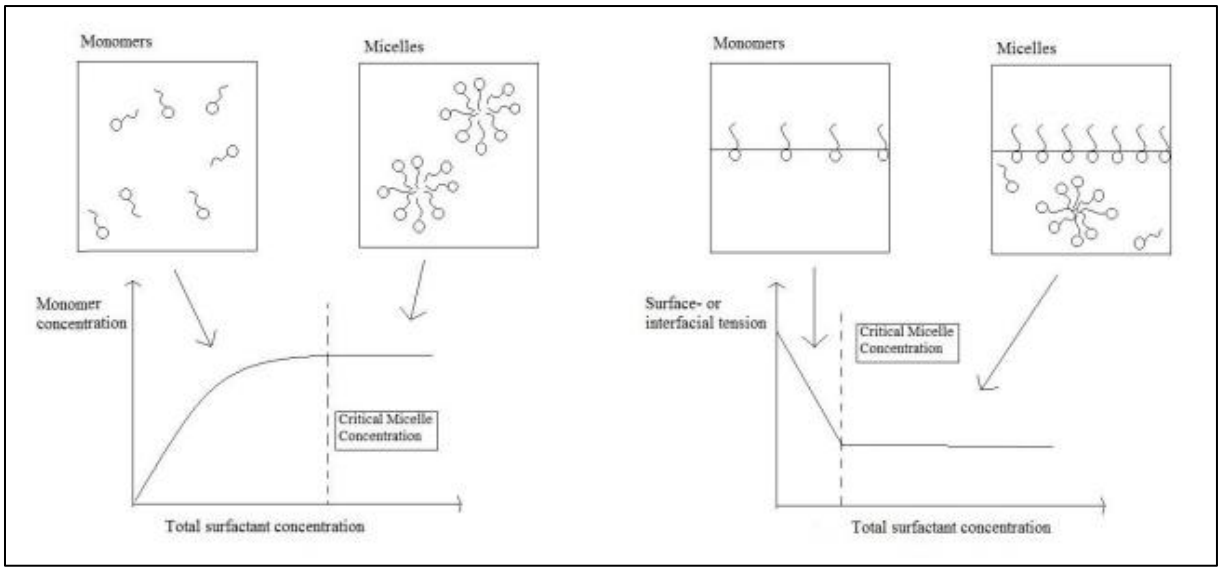

Figure 3.4: At the critical micelle concentration, monomers will aggregate into micelles [54].

3.2.3 Phase Behaviour

Surfactants are sensitive to the salinity of the brine, and three different phase systems can occur depending on the salt concentration. In brines of low salinities, the surfactants will form oil-in-water microemulsions within the aqueous phase (Windsor Type I system). If the salinity level is high, surfactants form water-in-oil microemulsions in the oil phase (Windsor Type II system). The most optimal reduction of surface tension occurs at intermediate salt levels. In this case, the surfactants form microemulsions in a separate phase between water and oil (Windsor Type III system). This phase is continuous, and contain surfactant, water and dissolved hydrocarbons [23].

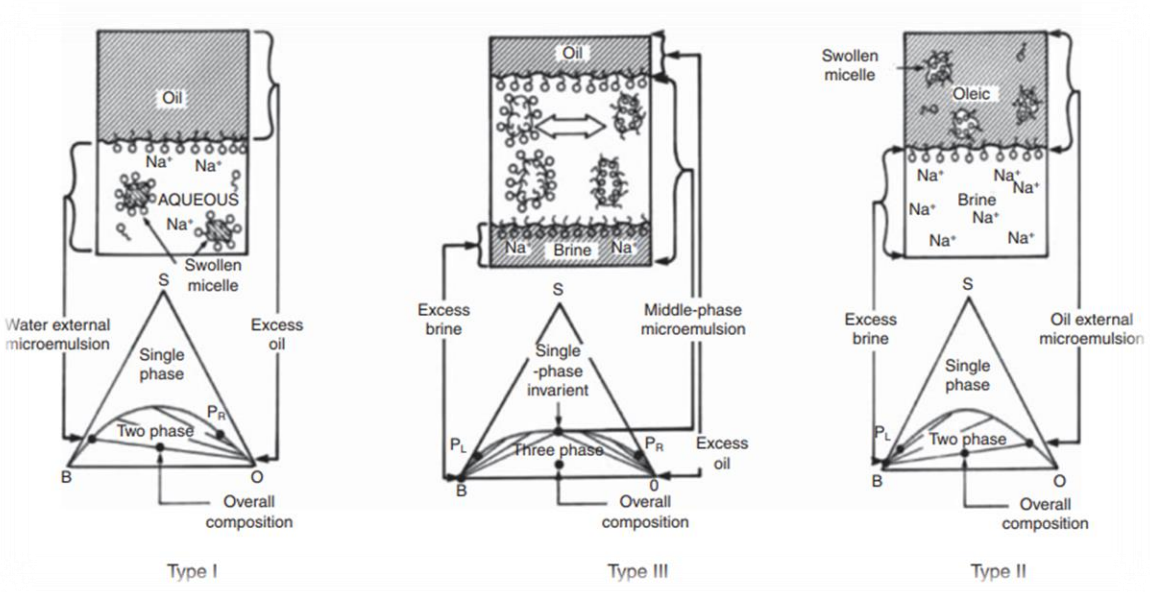

Figure 3.5: Relationship between surfactants and salinity illustrated through the three Windsor types [55].

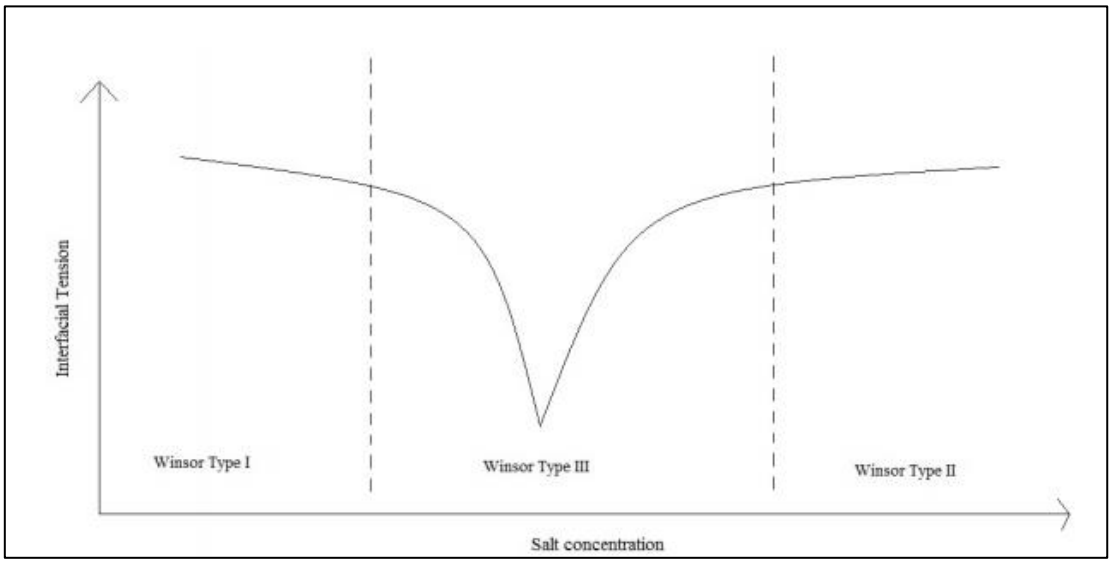

Figure 3.6: Illustration of the interfacial tension dependence on salinity. The IFT is lowest at intermediate salinity levels where the surfactant possesses an equal solubility in both water and oleic phases [56].

3.2.4 Surfactant Retention

In order to investigate whether surfactant flooding is economically viable, the degree to how surfactants are adsorbed at solid surfaces must be known. Loss of surfactants due to retention greatly affects the expenditure of oil recovery [36]. Four mechanisms leading to surfactant retention are:

- Phase Trapping: Loss of surfactants due to capture in an oil-external microemulsion phase, which occurs in a Windsor type II environment.
- Precipitation: Divalent ions present in hard brines may form surfactant-divalent ion complexes that can precipitate and lead to a loss of surfactants.
- Adsorption: Monomers can bond ionically or through hydrogen bonds to the charged surface sites.
- Ion Exchange: In hard brines, ion exchange between the clay surface and the brine/surfactant system may ultimately lead to retention.

3.2.5 Surfactant Flooding

The chemical nature of surfactants that enables them to lower interfacial tension between immiscible fluids can be utilized for oil recovery purposes. Posterior to waterflooding, the residual oil left behind is mainly trapped due to capillary forces. The addition of surfactants to the injection water may enhance the capillary number to the extent that additional oil will be recovered [4, 14, 57].

When subject to an immiscible fluid, liquids tend to minimize the surface area of contact, and thus, form spherical droplets. The decrease in interfacial tension proposed by surfactants aids in mobilizing trapped oil by deforming the spherical oil droplets such that migration through narrow pores may be enabled [57].

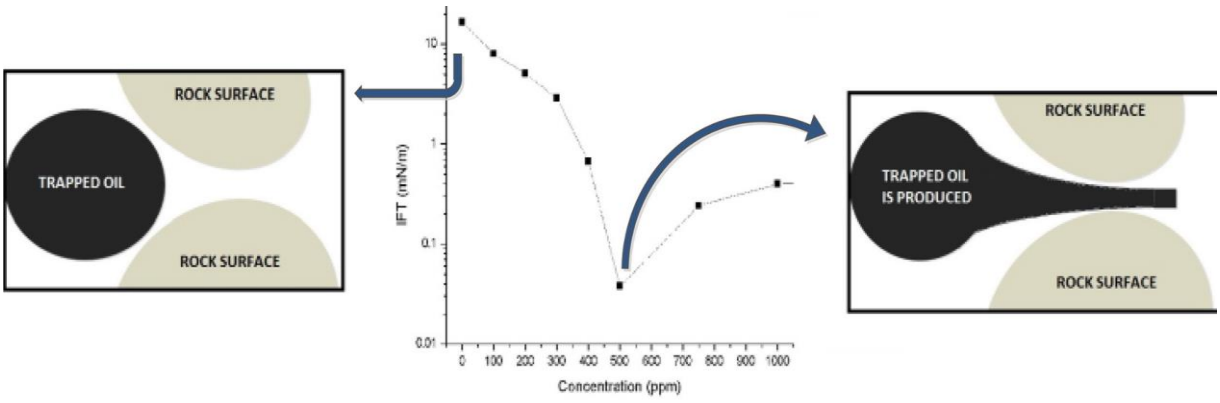

Figure 3.7: The reduction of interfacial tension induced by surfactants can be utilized to mobilize capillary trapped oil [57].

3.2.6 Summary of Surfactants and Their Applicability in This Thesis

The ability of surfactants to reduce residual oil saturation by lowering the interfacial tension between water and oil is utilized in this thesis. Due to the sensitivity of surfactants towards salinity, they will be diluted in low salinity injection water in this simulation study. According to experiments conducted by Spildo et al. (2014), the diluted environment reduces the probability of adsorption, retention and solubility issues. The surfactants form oil-in-water emulsions (Windsor type I), which prevent trapping of surfactants in the oleic phase. Although intermediate salinities (Windsor type III) yield the minimum interfacial tension, surfactants diluted in low salinity water still generate a low interfacial tension. Consequently, the residual oil saturation is reduced in contacted zones, and the microscopic sweep efficiency is increased [4].

3.3 Polymers

Several studies have demonstrated that the production performance is enhanced by adding polymers to the displacing fluid. In comparison to conventional waterflooding, polymers yield a faster production time and additional oil produced [49]. Polymers are principally used as thickening agents for aqueous solutions, which may lead to a higher macroscopic sweep in heterogeneous reservoirs or reservoirs containing heavy oil. By increasing the viscosity of injection water, the mobility ratio decreases to a more desirable value, resulting in an improved vertical and areal sweep efficiency. Polymers may also be used as a gel that clogs high-permeable layers and diverts the injection water into unswept zones. This can aid in preventing an early water breakthrough [29].

3.3.1 Polymer Chemistry

Polymers are large molecules, or macromolecules, consisting of long chains of repeating monomers linked together by covalent bonding [58]. The word *polymer* itself has a Greek origin meaning *many members*, referring to the union of the single monomers constituting the polymer molecule [59]. The synthesis of polymers from monomers is called polymerization. The number n is referred to as the degree of polymerization, and too meet the definition of a polymer, the number of repetitive structural units must be sufficiently high such that the physicochemical properties of the polymer do not change significantly with each new unit addition. The polymer properties are highly variable, depending on the type of monomers, chemical bonding, the degree of polymerization, and the architecture of the chain [58].

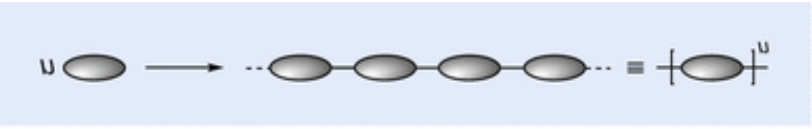

Figure 3.8: A polymer molecule consists of repeating monomers [58].

Polymers are complex molecules of a high molecular weight, and the viscosity is closely related to the size and extension of polymer molecules in a particular solution. When molecules interact, they dissipate energy, and large polymer molecules will spend more energy than low molecular weight solutions. Thus, the higher viscosity of polymer solutions [29].

3.3.2 Polymer Types

It is distinguished between two groups of polymers; synthetic polymers and biopolymers [29]. Natural biopolymers have existed since the earliest times, and can for instance be found in DNA and proteins. The design of synthetic polymers is a relatively recent form of science, but an interesting one due to the fact that the possibilities of building polymers are only restricted by chemical and thermodynamical laws, giving rise to an abundance of creativity [59].

Biopolymers originate from living organisms. Examples of biopolymers are xanthan and sclerogutan. Xanthan is frequently used in waterflooding due to its high viscosifying effect and tolerance to high salinities. Disadvantages of biopolymers are their sensibility to bacteria degradation, expensive price tag and the limited production capacity [36].

In comparison, synthetic polymers are cheaper and easier to produce in large quanta. The most commonly used synthetic polymers are polyacrylamide (PAM) and hydrolyzed polyacrylamide (HPAM). HPAM is the most used one due to its higher tolerance towards mechanical stress and high salinities in comparison to PAM. Unfortunately, synthetic polymers are not ecologically friendly [36].

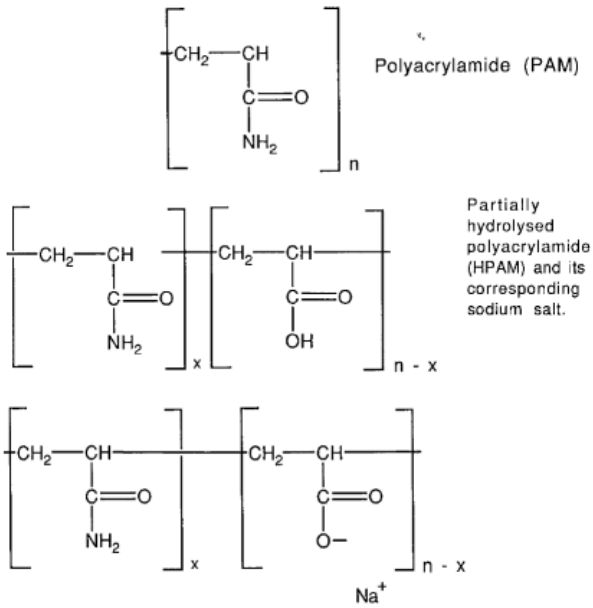

Figure 3.9: Chemical structure of PAM and HPAM molecules [29].

3.3.3 Polymer Rheology

The understanding of the rheological nature of polymers is of great importance when handling polymer-processing operations, exemplified by polymer injection into a reservoir. Polymers are designated viscoelastic fluids, exhibiting shear-thinning behavior. In rheological terms, polymer solutions are non-Newtonian fluids, indicating that the shear stress and shear rate are not linearly proportional [29]. The shear-thinning polymer solution does not obtain a constant viscosity, as displayed in figure 3.10:

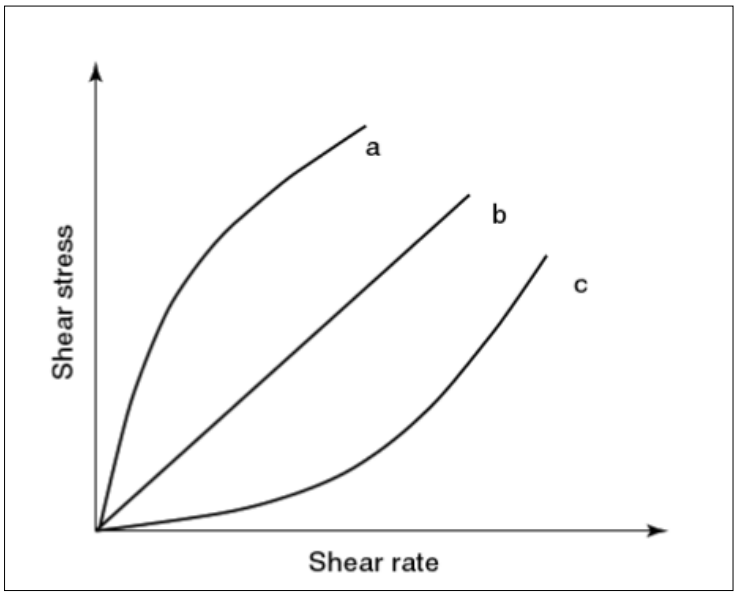

Figure 3.10: Shear stress versus shear rate behavior for shear tinning (a), Newtonian (b), and shear thickening fluids [59].

At increasing shear rate, the coiled polymer molecules will untangle and align themselves in the direction of flow, as illustrated in figure 3.11 [29]:

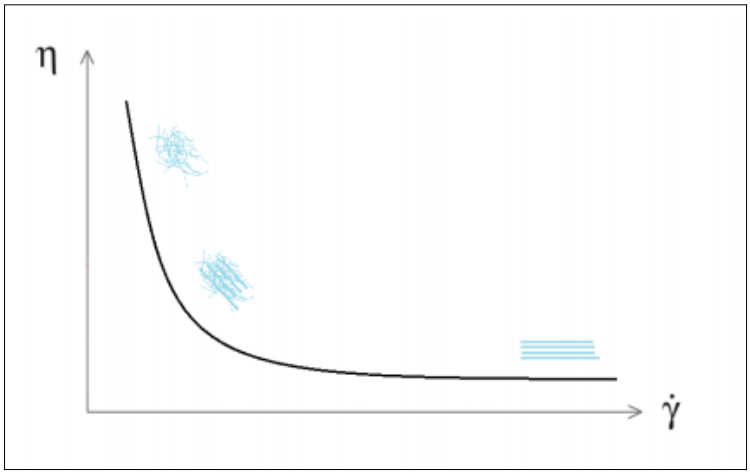

Figure 3.11: The flexible polymer molecules will deform and align at high shear rates [29].

The viscosity behavior of polymer solutions proves more complex in a porous media consisting of pore bodies and pore throats, and is named *in-situ viscosity*. In contradiction to bulk viscosity measurements conducted by viscometers, a polymer molecule will flow through numerous channels of varying radii in a porous reservoir, forcing the molecules to contract and expand. If the polymer is not allowed enough relaxation time following each deformation, the rheological behavior of the polymer might change. Ultimately, the average viscosity of the fluid will differ from the initial bulk viscosity. The prediction of in-situ viscosity is therefore crucial when designing a polymer flood through a porous media [60].

3.3.4 Inaccessible Pore Volume

The inaccessible pore volume, denoted IPV, implies the sum of all pore volumes where the entrance radii of the pore is smaller than the polymer particles. Due to the high molecular weight of many polymers, they are unable to access smaller pores. These pores are mostly occupied by irreducible or connate water, and considering the inaccessibility of this total pore volume to polymers, the polymers will not displace this water, leading to an absence of a highly mobile connate water bank. Conclusively, the polymers may advance and displace oil at a rate higher than predicted on the basis of total pore volume [36].

According to Lund et al. (1991), IPV is affected by the presence of clay, temperature, reservoir heterogeneity and differences in water saturation. For instance, at residual oil saturation, oil will occupy pores that were accessible for polymers at 100% water saturation, increasing the IPV for polymers in the water-filled volume [61].

The IPV phenomenon results in a few advantages. A study conducted by Dawson et al. (1972), revealed that close to one third of the pore volume was not contacted by polymers. From an economic perspective, this indicates less polymers needed for the flooding process. Because of the inaccessible pore volume, the contact between rock and polymer will be greatly reduced, ultimately yielding less polymer adsorption and retention. However, if oil droplets are trapped within the small pores inaccessible by polymers, they will remain as residual oil, which is not a desired outcome [62].

3.3.5 Polymer Degradation

Polymers are sensitive to temperature, salinity, bacteria and shear rate. Both bacteria and high shear rates can lead to degradation, while temperature and salinity may reduce the viscosity of the polymer solution [29]. Additionally, polymer retention presents an injectivity problem. Polymers adsorb well on solid surfaces, exemplified by rock surfaces within a hydrocarbon reservoir. The adsorbed macromolecules represent additional resistance to flow and loss of valuable chemicals. Furthermore, mechanical entrapment of polymers may occur [63].

3.3.5.1 *Salinity Effect on HPAM*

Zhang et al. (2008) investigated the effect of electrolytes on HPAM. The anionic polymer molecule obtains numerous charges along its chain, and the electrostatic repulsion between the anions hinder the molecule from coiling up [64].

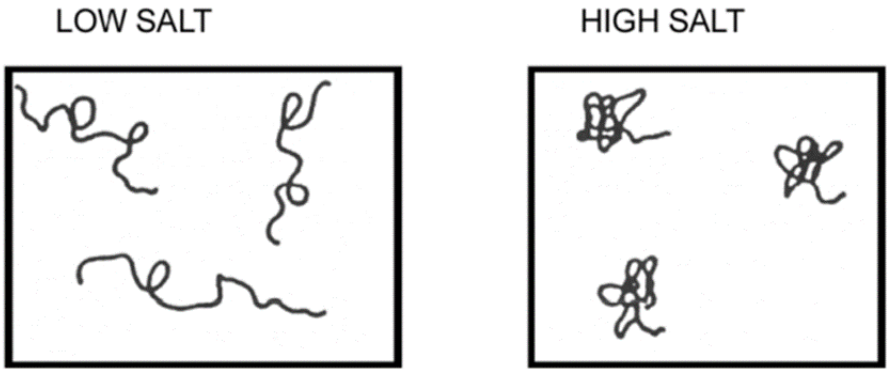

Figure 3.12: The effect of ionic strength on molecular conformation of HPAM [49].

The studies proved that the presence of monovalent inorganic salts could effectively neutralize the negative charges on HPAM, which will shrink the polymer molecule chain and decrease its hydrodynamic radius. According to the study, the mean-square radius of gyration, R_z, decreased by 25% when the concentration of Na^+ increased from 0.02 to 0.2 mol/L [64], as illustrated in figure 3.13:

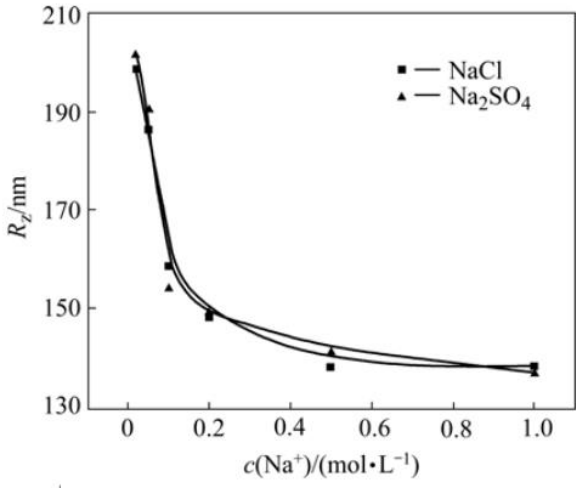

Figure 3.13: Na^+ dependence of Rz of HPAM [64].

HPAM molecules contain carboxylic acid groups, which analogous to the anion repulsion also aid in expansion of the polymer chain. The addition of Ca^{2+}-ions shields the electrostatic repulsion among the anions and reduce charge densities around the macromolecule chain, ultimately leading to shrinkage of the polymer molecule [64].

Figure 3.14 displays the relationship between R_z and Ca^{2+}, illustrating an overall inverse proportional relation between the two. The contracted polymers due to an increase in ionic components in the brine may ultimately result in a lower viscosity [29].

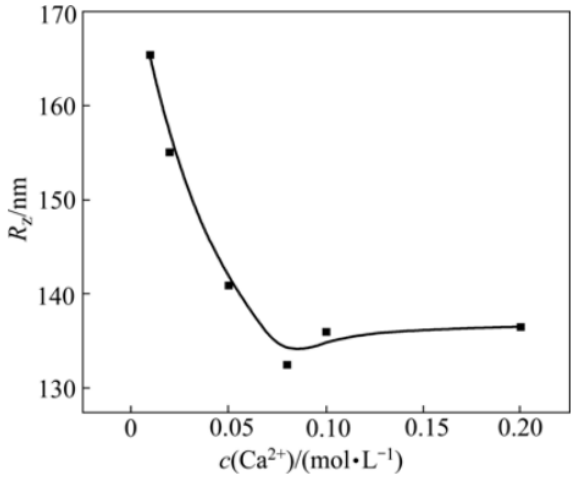

Figure 3.14: Ca^{2+} dependence of Rz of HPAM [64].

3.3.5.2 Polymer Retention

A common phenomenon nearly unavoidable during polymer flooding, is the retention of polymers by the porous media. Simultaneously as a polymer bank propagates through a reservoir, the front of the bank is gradually stripped from the viscosifying chemicals [62]. The total loss of polymers due to retention varies with the type of polymer, its molecular weight, flow rate, temperature, brine salinity and rock composition [36]. The presence of silica and calcium carbonate in the reservoir rock is usually significant factors [65].

The two dominant retention mechanisms are adsorption of polymer onto the rock surfaces of large pores, and mechanical entrapment in small pores. Polymer molecules are attracted to charged active sites throughout the porous media, and may adsorb onto the rock. Mechanical trapping occurs due to accumulation of polymers in pore channels similar to or smaller than the polymer molecule size. Polymers are highly flexible molecules, and can be forced into smaller pores by the solvent [65]. Retention causes an undesired loss of polymers, and leads to a delay of the generated oil bank propagation. It is of great importance to obtain a perception of the extent of polymer retention in a practical field case application to enable estimates of the polymer slug size needed to prevent breakdown of the polymer slug before breakthrough [36].

A study by Lund et al. (1991) deduced the wettability effect on retention, claiming that polymer adsorption is increasingly proportional to the water-wetness of rock surfaces. During a core flood, retention at S_{or} in the water-wet core was 30 μg/g. In comparison, the oil/mixed – wet core only retained 5 μg/g [61]. When a major part of the potential active surface is wetted by oil, less surface is accessible for polymer adsorption.

3.3.6 Polymer Flooding

Bypassed oil can arise from an unfavorable mobility ratio or due to heterogeneities present within the reservoir. In a reservoir scenario of fluid displacement, it is desirable that the mobility ratio between water and oil equals 1 or less. In a two-dimensional flood through a homogenous rock, a piston-like displacement approaching full oil recovery at water-breakthrough will be shown at mobility ratios equal to or less than unity. Therefore, it is not necessary to consider polymer injection unless the mobility ratio is sufficiently high. These elevated mobility ratios form front instabilities, leading to an early water breakthrough and a following two-phase tail production. The areal flood may be stabilized by a polymer addition, which will effectively increase water viscosity and perhaps reduce water permeability [29].

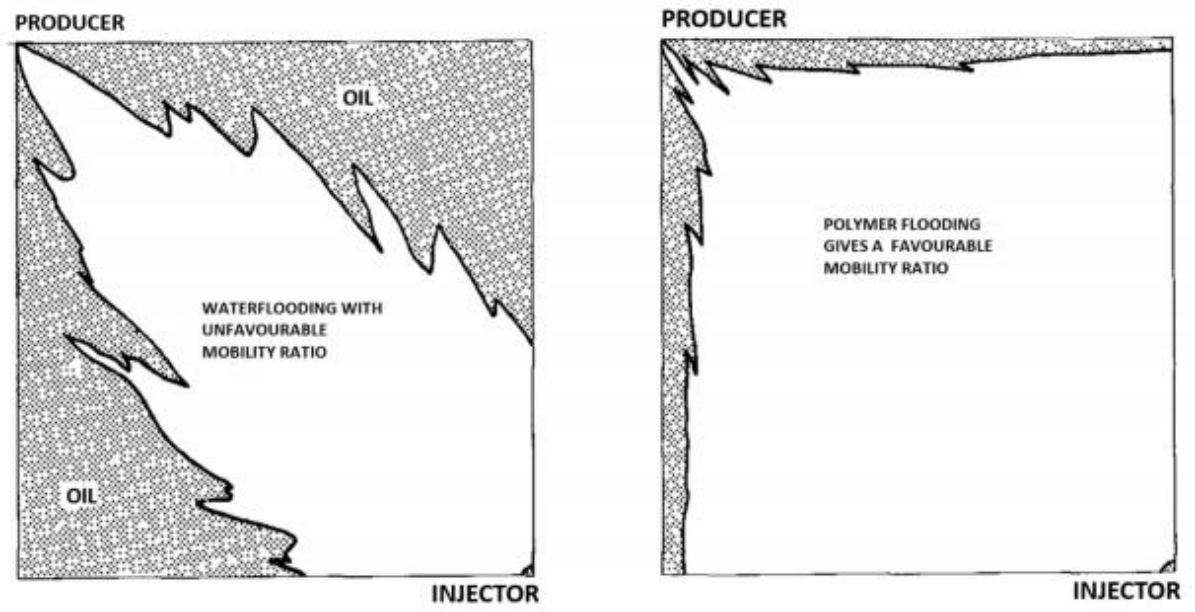

Figure 3.15: Illustration of how areal sweep may be improved by polymer flooding [29].

Reservoir large scale heterogeneities can give rise to a poor vertical sweep, exemplified by the presence of adjacent layers of contrasting permeabilities or geological irregularities. Although a favorable mobility ratio may be present (M=1), the heterogeneities can still lead to an early water breakthrough. Water will follow the high permeable layers and leave zones of lower permeability uncontacted. In these systems, polymers are added to further reduce the mobility ratio to values of 0.1-0.3, and block the high permeable zones such that the injection water is diverted into the whole reservoir. The polymers will not affect residual oil saturation, as its purpose is to enhance the macroscopic sweep of waterflooding [29].

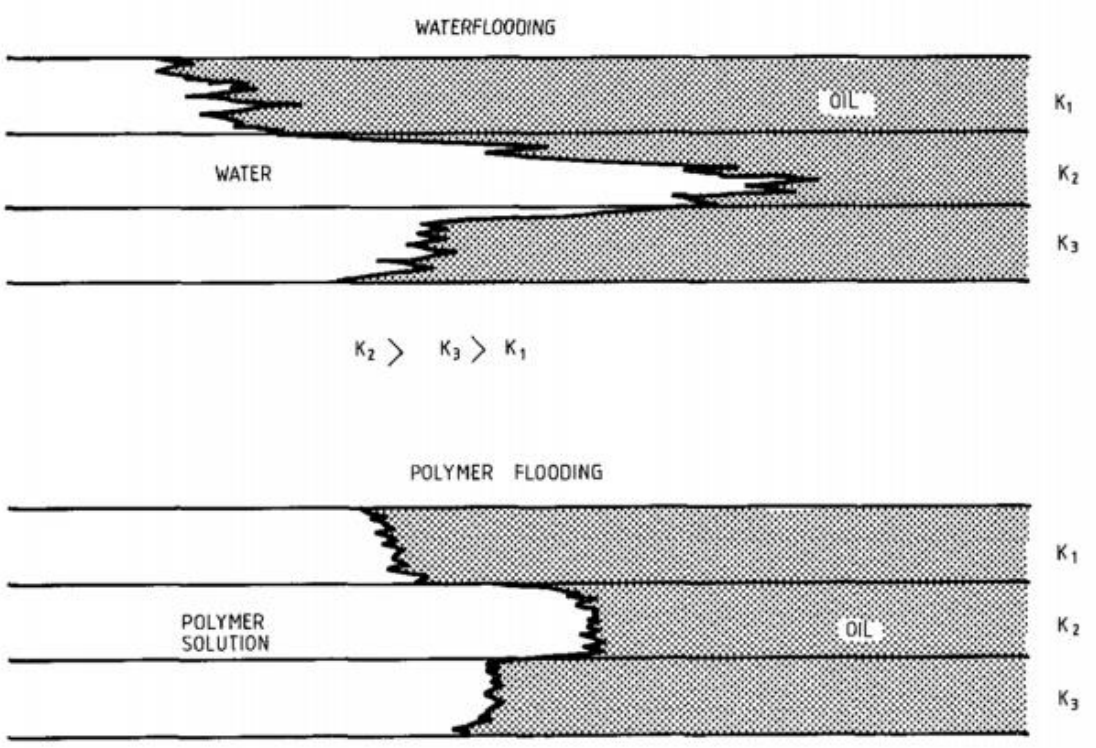

Figure 3.16: Improvement of vertical sweep by the polymer blockage of high permeable zones [29].

3.3.7 Summary of Polymers and Their Applicability in This Thesis

Polymers are added to the injection water to ensure a stable oil displacement and accelerate oil production. The macromolecules effectively enhance the viscosity of the water phase, which can reduce the probability of viscous fingering and other frontal instabilities that leave zones of bypassed oil [29]. Due to their sensitivity towards brine salinity, the polymers are diluted in low salinity water in this simulation study to ensure that the viscosity of the polymer phase is maintained during the polymer propagation through the porous media. In a composite low salinity surfactant polymer injection, the polymers ensure a stable displacement of the surfactant slug, and prevents the low salinity chase water from creating fingers in the surfactant slug.

3.4 Low Salinity Waterflooding

Although water injection has been the most practiced recovery method for nearly a century, little consideration has been bestowed upon the chemistry of injection water, and how it may affect crude oil/brine/rock (COBR) – interactions. The salinity of the seawater used during regular waterflooding is typically around 35 000 ppm [66]. By reducing the brine salt content below 6000 ppm, it will be regarded as low salinity water [12]. Low salinity waterflooding has gained severe ground the past decades due to its proposed effects on oil recovery.

3.4.1 Previous Laboratory Studies

Low salinity waterflooding has been an increasingly prominent EOR-method in recent years, but the first documented work on low salinity injection extends back to the 1940s, when Smith (1942) compared the oil recovery potential of cores saturated with Kansas crude oil with the injection of brine and fresh water [67]. At the current time, his studies concluded that the fresh water was not beneficial, but a decade later, Martin (1959) proved the opposite scenario in sandstone cores. He explained his results with the theory of swelling, emulsification and migration of clay particles [68]. Bernard (1967) also confirmed the potential of low salinity water injection a few years later, where he discovered that fresh water yielded higher recoveries in both secondary (S_{wi}) and tertiary (S_{or}) modes. During his studies, he discovered incremental oil recovery in addition to an increased differential pressure, which he blamed on the release of fines blocking pore throats. Nevertheless, the release of fines mobilized residual oil – increasing the microscopic sweep [69].

Despite the early work on low salinity brine injection, the recovery technique took a few decades longer to gain severe interest in the petroleum science industry. In the decade of 1990, Morrow and his companions were studying wettability effects on oil recovery, and discovered that the recovery was dependent on the preferential wetting of rocks which could be altered by the ionic composition of water [46, 70]. The pioneering publications of Morrow and his co-workers gave low salinity brine injection a revolutionary status.

In the following years, several laboratory tests were conducted, addressing the brine salinity effect on oil extraction. Most studies confirmed that when the salinity of the injection brine was reduced to a concentration significantly lower than the initial connate water, more oil was produced [68-71]. However, all researchers did not support this outcome. According to Sharma and Filico (1998), the primary factor controlling oil recovery was the salinity of the connate water, and they argued that injection brine salinity had no effect on oil recovery [72]. Some studies also implied that the lowering of injection brine salinity would have a negative effect on oil production [73]. Regardless of the publications giving low salinity waterflooding discredit, the majority of published experiments declares that diluted brine injection will enhance oil recovery significantly.

3.4.2 Field Scale Observations

The fortunate laboratory studies on low salinity waterflooding have encouraged scientists to upscale the experiments into full field trials. Many of the trials proved a close relation between laboratory and field experiments; both of them leading to incremental oil recovery.

A log-inject-log test executed by Webb et al. (2004), ended up with a 25-50 % reduced residual oil saturation after low salinity brine injection. The tests were conducted as a comparison of waterflooding performance with varying brine salinities in a sandstone reservoir [74]. However, the prosperity of low salinity water injection is highly case-dependent. On the Snorre field on the Norwegian Continental Shelf, Statoil implemented a low salinity water injection project in 2011 which met all screening criteria necessary to be able to conduct a successful project. Despite the promising forecasts, the results of the field trial indicated a poor potential for low salinity water injection [75].

Low salinity water injection is still a researched topic, which may optimize waterflooding performance significantly in qualified reservoirs. The water based EOR by wettability modification is an environmentally friendly technique, and it is reported that oil amounting to 5-20% OOIP extra may be produced, both in laboratory experiments and field pilots [11].

3.4.3 Proposed Mechanisms for Low-Salinity Waterflooding

Subsequent to the observed incremental oil production due to low salinity water injection, several hypotheses have been proposed to explain the success. Although the mechanisms of diluted brine injection are still debated, it is believed that various mechanisms with their individual contributions are acting together [13].

The predominant theory is the wettability alteration of the reservoir rock. Two principal hypotheses to justify the wettability alteration is multicomponent ion exchange (MIE) and expansion of the double layer. Furthermore, fine migration, an increased pH and reduced interfacial tension analogous to alkaline flooding also obtain significant roles in the increased oil recovery [13].

3.4.3.1 Factors Controlling Initial Wettability

The initial wetting of a reservoir rock is a result of millions of years in a chemical equilibrium between formation water, oil and rock. If the injection water has an ionic composition closely related to the formation water composition, no significant change in wetting properties shall be expected, but if the injection water salinity is modified, the chemical equilibrium will be disturbed and wetting alteration may be a product [11].

The amount of clay is a good indicator of the wetting properties of a reservoir rock. Clay minerals have a high affinity towards active polar components in crude oil, and as the pH decreases below neutrality, the adsorption of both acidic and basic polar organic components increases. Reactive cations in the brine such as H^+ and Ca^{2+} will also adsorb onto the negative clay sites at the same acidic conditions, and initiates an adsorption competition with the polar oil components [11].

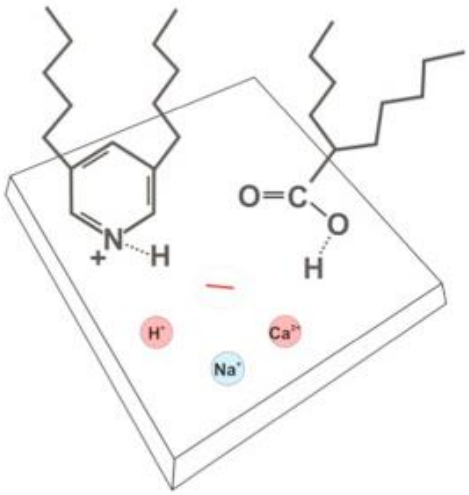

Figure 3.17: Active cations in the brine phase competes with polar components in crude oil towards the negative sites on the clay surface [11].

During the formation of an oil reservoir, oil enters a porous rock initially filled with formation water in a process driven by gravity forces. Before the oil enters, active cations such as Ca^{2+}, Mg^{2+}, Na^{2+} and H^+ are adsorbed onto clay minerals. The degree of adsorption is dependent on the salinity and pH of formation water. As the oil enters, polar components may expel the adsorbed cations from their clay sites. The oil will coat the surface and the wetting conditions will be altered towards more intermediate- to oil-wet [11].

3.4.3.2 Wettability Alteration by Low Salinity Waterflooding

The adsorption of organic compounds may be reversed or accelerated following the injection of low salinity water, and ultimately lead to incremental oil recovery. Shifts towards both more water-wet conditions and oil-wet conditions are reported, both having potential to increase oil production. The direction of wettability alteration is related to proton exchange reactions which lead to a change in pH of the formation water. Escalated pH-levels are in general linked to water-wet conditions whereas decreased pH-levels promote oil-wetness. The change in pH is governed by whether Ca^{2+} ions exchanges polar compounds or protons from the active clay sites [11].

In rocks that are naturally oil-wet to intermediate-wet, a change towards more water-wet conditions is a reasonable theory to explain incremental oil recovery. Water-wet reservoirs theoretically yield the highest oil production due to the distribution and flow of the immiscible reservoir fluids [40]. In strongly oil-wet systems, oil occupies the smallest pores in addition to wetting the surface. When water flooded, fingers form quickly, and water- breakthrough occurs nearly simultaneously as the first oil is produced. This unstable displacement leads to surpassed pockets of oils that will require huge amounts of injected water to be produced, - thus, not an economically preferable scenario. The oil trapped in water-wet reservoirs will be small isolated pockets, whereas residual oil in oil-wet systems can be traced throughout the system [76]. Hence, the wettability alteration caused by dilute brine injection is a desired outcome.

Moderate to strongly water-wet rocks are usually recognized by a low clay content, few polar compounds in crude oil, high content of Ca^{2+} and a formation water pH close to neutral or slightly alkaline. It can be an advantage to reduce the water-wetness to release capillary trapped oil and increase recovery. Some studies report a shift towards more oil-wet conditions following a low salinity water injection. A reason behind these observations may be the adsorption of organic material onto clay, which is enabled by the replacement of H^+ by Ca^{2+} that leads to a decrease in pH. The degree of water-wetness decreases as organic material adsorbs onto clay, and less oil will be trapped by capillary forces during waterflooding. Thus, a small increase in oil recovery is possible [11].

3.4.3.3 Multicomponent Ionic Exchange

The chemistry of rocks and its saturating fluids is essential knowledge for the investigation of how low salinity waterflooding may enhance oil recovery. Sandstone is mainly consistent of quartz, feldspar and clay that obtain a zero point of charge inferior to the typical pH in sandstone reservoirs [77]. Thus, the rock surface is negatively charged. Multivalent or divalent metal cations such as Ca^{2+} and Mg^{2+} are strongly adsorbed on the negatively charged rock surface sites, and they may further bond to negatively charged polar compounds, like resin and asphaltene, present in the oil phase. Hence, the cations work as bridges between the negatively charged clay and oil surfaces. This leads to the formation of organo-metallic complexes that have proven to promote oil-wetness of the rock surface. Concurrently, some organic polar compounds are also absorbed directly to the mineral surface, increasing the oil-wetness further [78].

Dependent on the characteristics of the clay surface and organic functional group, there are in accordance with the extended DLVO-theory eight possible mechanisms of organic matter adsorption onto clay minerals. Four of these mechanisms are involved in the multicomponent ionic exchange, and they are illustrated in figure 3.18 [78].

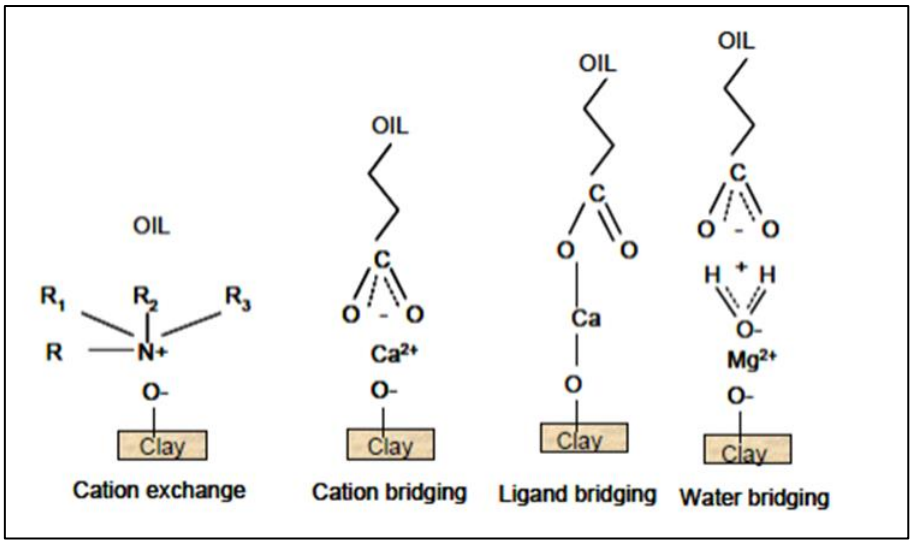

Figure 3.18: Mechanisms describing the adsorption to clay minerals during MIE [78].

According to Lager et al. (2008), the adsorption of organic matter by cation exchange takes place by molecules containing quaternized nitrogen or heterocyclic rings that may replace exchangeable metal cations initially bound to clay the surface. Furthermore, cation bridging is a weak adsorption mechanism between a polar functional group and exchangeable cations on the clay surface. Ligand bonding is exemplified by the formation of a direct bond between a multivalent cation and a carboxylate group. These bonds are stronger than cation bridging and cation exchange bonds, and may lead to the detachment of organo-metallic complexes from the mineral surface. Occasionally, the cation is strongly solvated and water bridging can occur. Water bridging involves the complexation between the water molecule solvating the exchangeable cation and the polar functional group of the organic molecule [78].

The key to understanding the chemical mechanisms occurring during the injection of low salinity brine is to obtain detailed knowledge regarding the interactions between clay, polar components within the oil phase and active cations in the brine [13]. As reported by Lager et al. (2008) [78], the higher oil recovery during low salinity waterflooding is much due to the multi-component ionic exchange, between the injected brine and rock surface. The MIE theory bases on the disruption in thermodynamic equilibrium of the COBR-system caused by the injection of brine with a different electrolyte concentration than formation brine [79].

During low salinity waterflooding, the variations in ionic concentration between injected water and connate water will result in a substitution of divalent cations by monovalent cations [79]. The clays will not be in ionic equilibrium with the injected low salinity water, and ions will be exchanged until an equilibrium is established. Theoretically, the exchange of Ca^{2+} and Mg^{2+} cations adsorbed on the clay surface with free Na^{+} ions may release crude oil since the cation binding the oil and clay disappears. Many experiments in regards to both laboratory and field scale have been conducted to further evaluate the effect of multicomponent ionic exchange. Lager et al. (2008) confirmed the effect by the detection of Ca^{2+} and Mg^{2+}- ions in the produced water immediately after breakthrough, indicating an ionic exchange within the rock core [78].

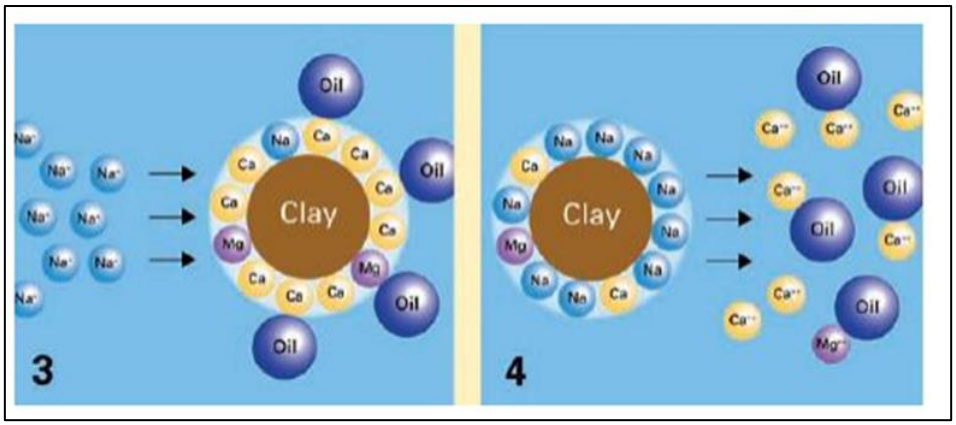

Figure 3.19: COBR-system before MIE (left), and after MIE (right).

3.4.3.4 Double Layer Expansion

When subject to high salinity levels, sufficient positively charged cations are able to screen off the negative electrical charges of the clay and oil, consequently neutralizing the repulsive forces between them. As long as the binding forces by the cations exceed the repulsive electrostatic interactions, the bond between oil and clay remains secured [80]. The Derjaguin-Landau-Verwey-Overbeek (DLVO) - theory approximates the total interaction energy between charged particles by the summation of the repulsive and the attractive contributions. The attractive contribution originates from van der Waals forces, whereas the repulsive contribution originates in the interaction between the electric double layers of the two particles [81].

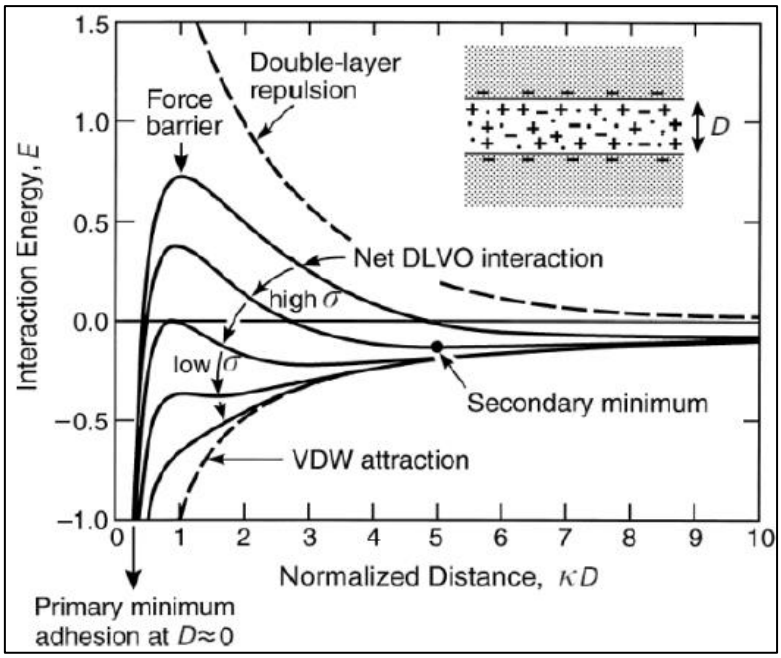

Figure 3.20: Schematic plots illustrating how the sum of the attractive van der Waals forces and repulsive electrostatic layer forces determines the total interaction potential between two objects of charge in an aqueous electrolyte. The force barrier prohibiting flocculation is highly dependent on the surface charge densities, σ, and the ionic strength of the electrolyte solution [82].

An electrical double layer is existent around any object of charge exposed to a fluid. The inner layer is called the Stern layer, and is consistent of ions of opposite charge adsorbed directly onto the object due to chemical interactions. The second layer, the Guoy-Chapman diffuse layer, is composed of free ions attracted to the object surface charge, and its electric potential is decreasing exponentially away from the object surface [81].

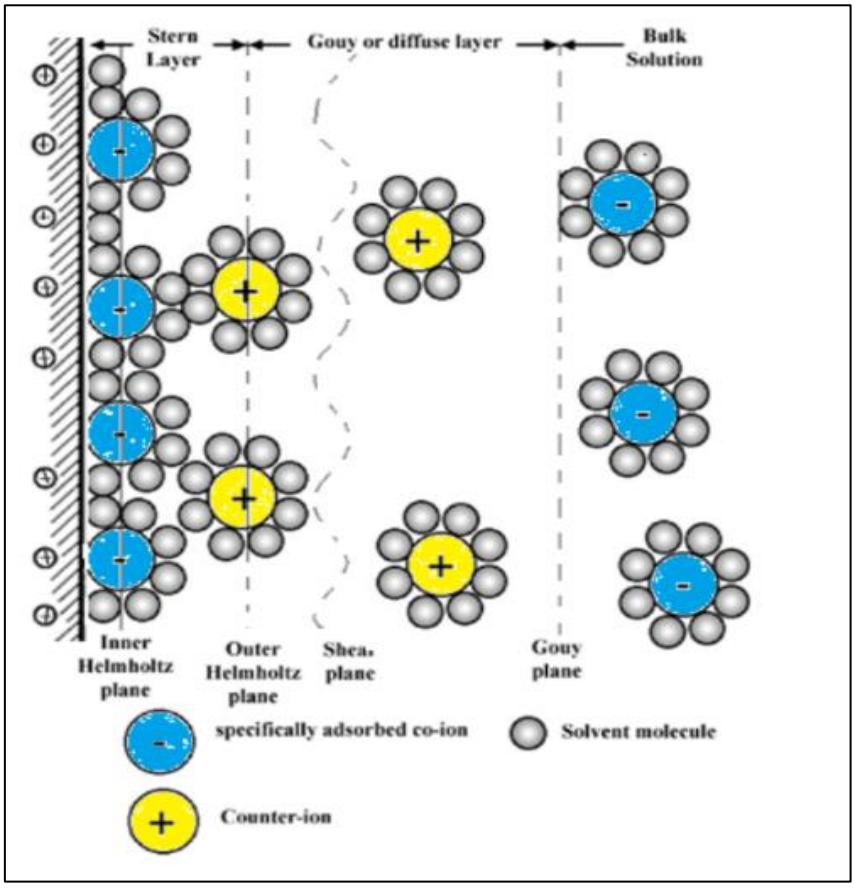

Figure 3.21: A representation of the electrical double layer surrounding objects of charge in an aqueous electrolyte. The inner layer consists of strongly adsorbed counterions, lowering the electrical potential at points adjacent to the object. The diffuse outer layer consists of free ions attracted to the surface charge [82].

The thickness of the double layer determines the stability of the objects. Hence, a thin double layer leads to a higher risk of flocculation. The double layer thickness is dependent on many factors, including the concentration and valency of electrolytes. The diffuse double layer have a screening length that is inversely proportional to the square root of the electrolyte concentration [80]. The injection of brine with a reduced salinity level, hence a lower electrolyte concentration, leads to an increase in the screening length [83]. This generates expansion of the double layer surrounding the oil particles and clay surface, and may ultimately separate the adsorbed oil from the charged clay surface. The desorption of oil reduces the fraction of rock surface coated by oil and may promote water-wetness [80].

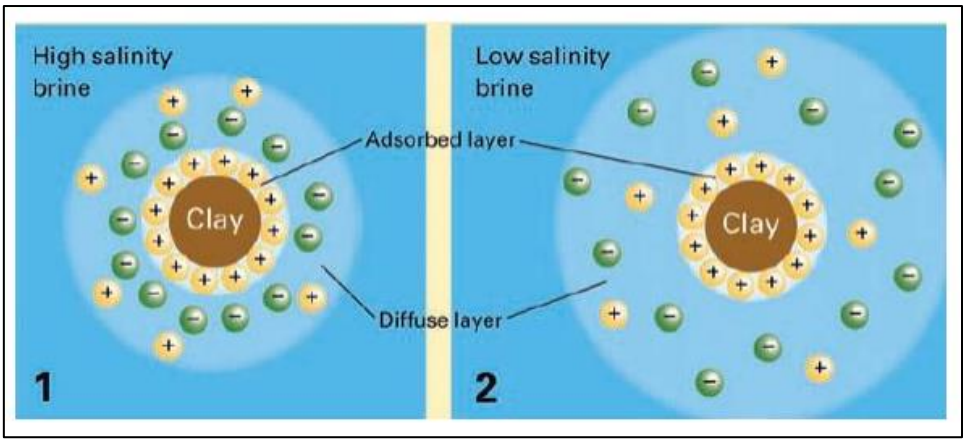

Figure 3.22: The double layer concept.

3.4.3.5 Fine Migration

During a low salinity injection experiment on Berea core samples, Tang and Morrow (1999) noticed produced fines (primarily kaolinite). Furthermore, it was observed an increase in differential pressure over the core, indicating a permeability reduction. The observations ultimately led to the hypothesis that clay particles were detached from the rock surface and migrated with the flowing water where some of them were produced and some were stuck in pore throats or pore constrictions – causing a permeability reduction. Fines migration is assumed to be explained by the DLVO-theory of colloids. Divalent cations such as Ca^{2+} and Mg^{2+} stabilize the clay by screening the repulsive forces between them. The injection of low salinity brine with an ionic strength equal to or less than the critical flocculation concentration (CFC), may conclusively lead to clay particles being stripped off the pore surface, yielding an exposure of the underlying surface. This may eventually lead to an increased water-wetness of the rock. The detached fines will also mobilize oil attached to them, and hence, increase the oil production [71].

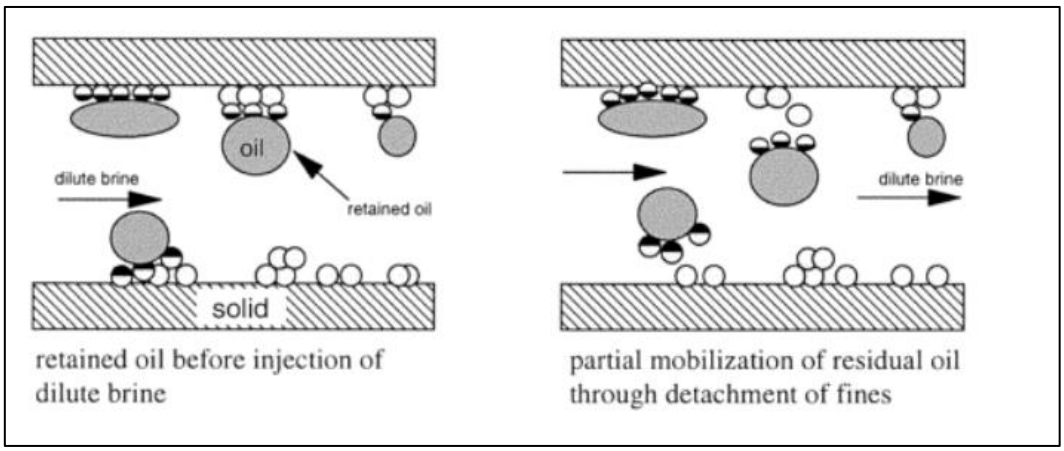

Figure 3.23: Fine migration leads to mobilization of trapped oil [71].

3.4.3.6 pH variation

Studies have revealed a rise in pH levels as a result of low salinity water injection, causing an increased alkaline climate within the rock of interest. Most connate waters are considered acidic due to dissolved sour molecules - exemplified by CO_2 and H_2S - and the pH is usually at 5-6. As the diluted injection brine displaces the high saline formation water, an increase in pH at the clay-water interface is observed [78]. This increase is a result of two concomitant reactions occurring, namely the carbonate dissolution and cation exchange:

$$CaCO_3 \leftrightarrow Ca^{2+} + CO_3^{2-} \tag{3.2}$$

$$CO_3^{2-} + H_2O \leftrightarrow HCO_3^- + OH^- \tag{3.3}$$

The excess of OH^- ions following carbonate dissolution, in addition to the cation exchange where clay minerals exchange H^+ atoms from the water with previously adsorbed cations, both lead to an increased alkaline environment. However, absorbed CO_2 works as a buffer inhibiting the pH to increase above 10. Hence, the pH usually levels at a maximum of 9. In many ways, the pH increase following low salinity water injection resemble the principles behind alkaline waterflooding [78]. Alkaline waterflooding is especially acknowledged for the decrease in interfacial tension between water and oil and an increased water wettability - both yielding an increased oil recovery [84].

The reduction of interfacial tension is due to the formation of surfactants when the residual oil is approached by alkaline low salinity water. Polar or acid components within the oil phase are saponified when contacted by an increased alkaline brine, which essentially is an in-situ generation of surfactants. The surfactant molecules, due to its hydrophilic and lipophilic properties, are known for reducing the capillary forces trapping residual oil. Moreover, the oil may act as emulsifying agents to disperse oil droplets into the continuous water phase. The mobilization of oil enabled by surfactants in addition to increased water-wetness of the rock all contribute to an incremental recovery of oil originally in place [85].

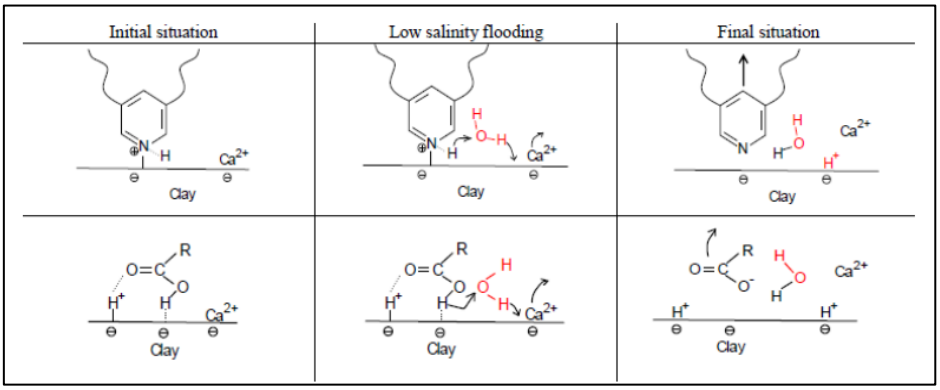

Figure 3.24: Proposed mechanisms for low salinity flooding. Desorption of basic material (upper) and desorption of acidic material (lower) [13].

3.4.4 Summary of Low Salinity Water and Its Applicability in This Thesis

Low salinity waterflooding is a relatively recent EOR-technique proved to enhance oil recovery beyond the capability of high salinity water. The introduction of water of another ionic concentration than connate water will disturb the ionic equilibrium within the reservoir and induce mechanisms that alter the initial wettability and release trapped oil. By these actions, the macroscopic and microscopic sweep efficiencies may be enhanced [11, 71, 78]. In this simulation thesis, the effects of low salinity water on oil recovery in a reservoir model will be examined. Moreover, the low salinity water provides a beneficial environment for surfactants and polymers, which will be further discussed in the following chapter.

3.5 Low Salinity Waterflooding in Combination with Surfactants and Polymers – A Literature Review

Although researchers have not yet come to a full consensus regarding the mechanisms behind the low salinity water effect, most experimental studies and field trials confirm an incremental oil recovery, mostly due to wettability alteration in intermediate- to oil-wet clastic rocks and destabilization of oil layers [5]. The topic is still enduring systematic research, and has been increasingly evolving all since Tang and Morrow (1999) published their pioneering work on increased oil recovery by modified injection water composition nearly 20 years ago [71].

Recent studies demonstrate that the effects of the diluted brine can benefit from being combined with surfactants and polymers for incremental oil recovery. The low salinity environment is beneficial for both surfactants and polymers in terms of their physicochemical properties, increasing their stability and reducing retention [5, 14].

The surfactants that give rise to low interfacial tension at lower salinities are less expensive compared to the surfactants designed to cope with a highly saline water. The diluted ionic concentration of low salinity water typically yields Windsor type I behavior, and the surfactants remain in the aqueous phase. At regular seawater salinities, the surfactants may form water-in oil microemulsions (Windsor type II), and remain trapped in the continuous oleic phase - resulting in loss of active surfactants [14]. An obtained stabilized low salinity environment is also beneficial for polymer flooding, where a longer-lasting desirable mobility ratio may be attained, as high salinity levels are preventing polymers of reaching their full viscosifying potential [5].

Publications show that the composite effect of several EOR-fluids may be larger than the sum of the individual fluids by themselves [6], which is a part of the reasoning why hybrid EOR-injection is presumed to gain significant ground in the next upcoming years.

3.5.1 Low Salinity Surfactant Flooding

The aim of a hybrid LSS-process is to combine the benefits of low salinity waterflooding and surfactant flooding in an attempt to generate a higher oil production. Addition of surfactants prevents retrapping of oil that was initially mobilized by low salinity brine [86]. Anionic surfactants - which are typically utilized in oil recovery settings - are sensitive to temperature, pH and salinity of the water phase. Moreover, the loss of surfactants due to adsorption, precipitation and mechanical trapping presents major challenges. An increasing amount of studies reveal that several factors regarding the implementation and flooding behavior of surfactants are improved when the ionic composition of the water is reduced. For instance; surfactant adsorption is greatly reduced, the physicochemical properties of surfactants are improved, and environmental – and safety regulations regarding surfactant implementation are more easily met [14].

In order to investigate whether an LSS-process escalated oil recovery, Alagic et al. (2010) conducted core flooding experiments of combined low salinity water injection and surfactant flooding. The study was executed in four samples cut from the same block of Berea sandstone, which were aged to establish a non-water wet state. The cores were initially filled with synthetic seawater (high salinity brine) at a salinity of 36 321 ppm, and later drained with the highly viscous oil Marcol 152 until S_{wi} was established. The concentration of the low salinity brine was set to 0.50 wt% NaCl, and the surfactant used was internal olefin sulfonate [14].

The displacement tests were conducted in both secondary (at S_{wi}) and tertiary (at S_{or}) modes, involving various steps of high salinity brine injection, low salinity brine injection and a combined low salinity- and surfactant injection. Results revealed incremental oil recovery in both secondary and tertiary modes following the low salinity waterflooding in comparison with high salinity waterflooding [14]. Figure 3.25 illustrates the recovery difference of low salinity waterflooding and high salinity waterflooding.

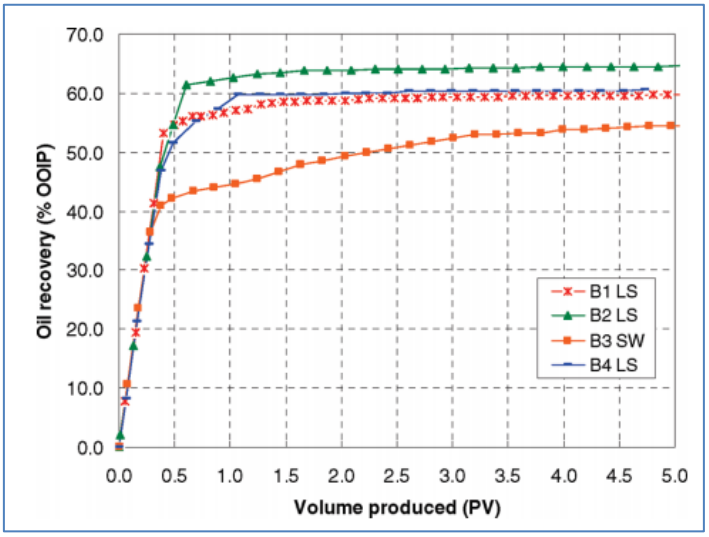

Figure 3.25: Oil production for secondary LS floods in cores B1, B2 and B4, and SW flood in core B3 [14].

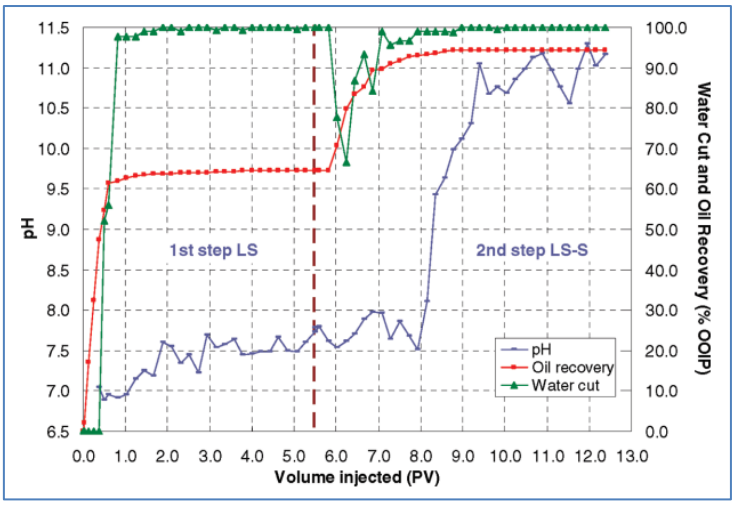

Figure 3.26: pH, oil recovery and water cut for core B2 [14].

As deducted from figure 3.26, core B2 was first flooded with low salinity water at S_{wi}, followed by a second step of low salinity water and surfactants. The oil recovery at water breakthrough was 54.7%, and elevated to 94.4% after the introduction of surfactants.

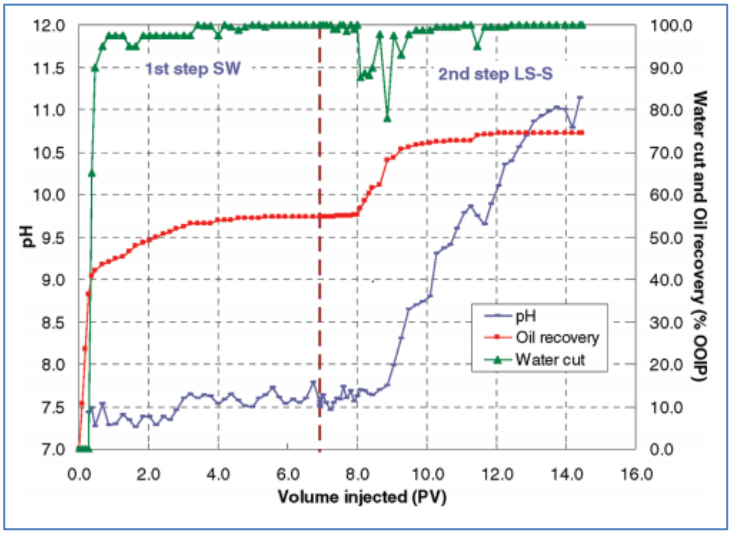

Figure 3.27: pH, oil recovery and water cut for core B3 [14].

Figure 3.27 displays a low salinity surfactant slug injected after seawater flooding. Oil recovery after the first step was 54.6%, and after the LSS injection, 74.5% OOIP was recovered.

During the experiments with low salinity water injections, it was noticed that the LS-floods reached a plateau in oil production earlier than the seawater flooding, in addition to reaching lower residual oil saturations and a later water breakthrough. The end-point relative permeability values of the LS-floods were also significantly lower than in the SW-flood, indicating a shift in wettability towards a more water-wet state after the LS-floods. The surfactants were more successful in reducing the interfacial tension in pre-established low salinity environments than in a high salinity environment, much due to the presence of divalent

ions in the high salinity brine that makes surfactants less effective. According to the experiments, tertiary oil recovery was reduced when the surfactants were injected without a pre-flush of low salinity water. In low-salinity environments, the surfactants form oil-in-water microemulsions (Windsor type I), and when the surfactants are dissolved in a high-salinity environment, the surfactants are trapped in the oil phase (Windsor type II) [14].

In order to obtain a minimum interfacial tension, the optimal salinity is found at intermediate salt levels (Windsor type III). Nevertheless, solution solubility can be poor, and the retention can be high at these salinities. The Windsor type I behavior also yields moderately low IFTs, and can therefore be a compromise between the desired IFT-reduction, and the unwanted retention and solubility issues. This exemplifies why the combination of low salinity water and surfactants is advantageous [4].

3.5.2 Low Salinity Polymer Flooding

Polymers are added to injection water to increase the viscosity of the displacing fluid, which in theory will recover the oil that is bypassed by brine during traditional waterflooding. The addition of polymer molecules will however not recover residual oil over the capability of traditional waterflooding [29]. Nevertheless, polymers will help the injection water to reach a broader specter of the reservoir by improving the macroscopic sweep.

Polymer injection may meet several challenges. The chemicals can be technically, chemically and economically difficult to implement, and the wrong approach may result in injectivity issues and polymer retention/adsorption. Polymers are sensitive to the salinity of the connate water, pH, reservoir temperature and wettability of reservoir rock. The dependence of polymer retention on wettability is an interesting study, especially due to the fact that low salinity water is acknowledged for its wetting alteration abilities. Polymers may adsorb at a larger scale in water-wet rocks due to the absence of competing organic oil components that adsorb on the rock surface under intermediate- to oil wet conditions [5]. However, the absence of a dense electrolyte concentration in the injection water is known for stabilizing the polymer molecules, making them more resistant towards retention [36].

Studies conducted by Mohammadi et al. (2012) reported that the usage of polymer chemicals are reduced to one third if the solvent is low salinity water rather than high salinity water, yielding an economically preferable scenario. The viscosity will increase as salinity levels decline, and less polymer chemicals are therefore required. Furthermore, the high concentration of divalent ions in seawater accelerate precipitation of polyacrylamide polymers, a process that is reversible by low salinity water. Low salinity brine can be beneficial for the usage of polyacrylamide at high temperatures, in addition to hydrolyzed polymers [87].

Shiran et al. (2013) attempted to investigate the evidence for improved oil recovery by low salinity polymer flooding further, and the studies reveal that polymers - similar to surfactants - are more effectively able to mobilize trapped oil when a low salinity environment is established at initial water saturation (S_{wi}) rather than at the residual oil saturation (S_{or}). A potential reason

may be that a tertiary low salinity flood will encounter oil that is already trapped and burdensome to mobilize, whereas a secondary low salinity flood will approach a continuous oil phase and prevent further trapping. Polymers aid in stabilizing the LS-flood which further improves the oil banking due to a better mobility ratio and inaccessible pore volume [5].

Figure 3.28 illustrates the oil recovery increase after low salinity polymers are injected in an already established low salinity environment.

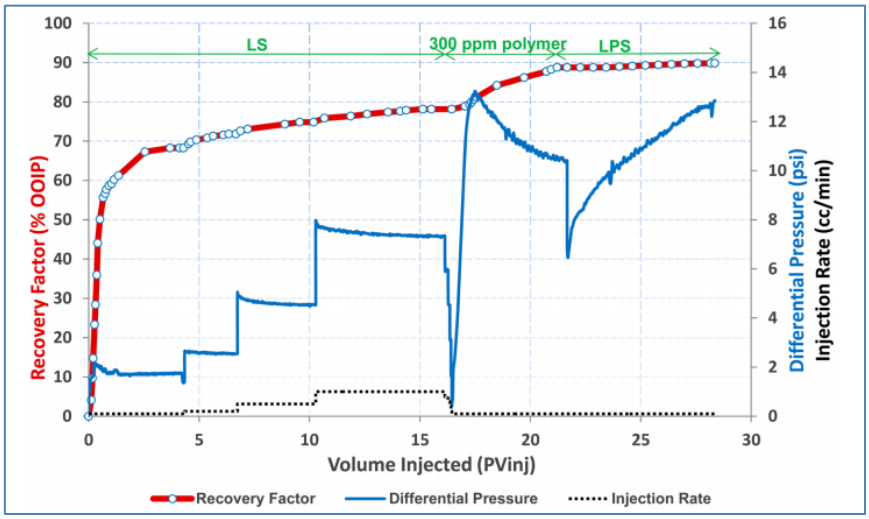

Figure 3.28: Cumulative oil recovery, differential pressure and injection rate versus pore volumes injected [5].

3.5.3 Polymer and Surfactant Interactions

Common concerns of the hybrid LSSP-process may regard the interactions and compatibility of surfactants and polymer molecules. Although the chemicals may not be injected in the same slug, there can be mixing at the interface due to dispersion and diffusion. Additionally, polymers may also mix with surfactants due to the inaccessible pore volume phenomenon occurring when polymers are injected after surfactants, causing them to penetrate into the surfactant slug ahead [88].

The chemicals can be injected in the same slug (SP), or separately. Due to a chromatographic separation of polymers and surfactants caused by the inaccessible pore volume for polymers, polymers are likely to be absorbed since they flow ahead. Polymers may be injected first as sacrificial agents for adsorption, or injected after the surfactant slug to make sure that the chase water does not create fingers in the surfactant slug. General observations regarding the chemical behavior of the EOR-chemicals, is that while the polymer principally stays in the water phase, surfactants can be traced through the aqueous, oleic and the middle microemulsion phases [89].

The purpose of polymers is to increase the viscosity of water, while the job of surfactants is to reduce interfacial tension. Therefore, it proves interesting to investigate if the blending of the chemicals has any effect on the ability of polymers and surfactants to viscosify water and reduce interfacial tension, respectively.

3.5.3.1 Polymer Effect on Surfactants

Studies find that the presence of polymers does not affect the interfacial tension much. The phase behavior – from type I to type III to type II as a function of salinity – is shifted slightly to the left when polymers are present, indicating that the optimum salinity for ultralow interfacial tension is somewhat decreased [90]. Furthermore, the CMC marginally increases when polymers are present [89].

Trushenski (1977) reported that surfactant loss may be an outcome following the presence of polymers. Due to the inaccessible pore volume phenomenon, polymers may bypass surfactants, ultimately leading to phase trapping. A laboratory core test revealed that the trapping and remobilization of the surfactant phase were profoundly governed by the polymer concentration. According to the study, a peak in polymer concentration dramatically reduced sulfonate concentration, and when the polymer concentration decreased, the sulfonate concentration increased again, indicating a remobilization of surfactants. Even though the trapped surfactants may be displaced by a chase water at a later stage, the surfactants were no longer competent in displacing oil [88].

3.5.3.2 Surfactant Effect on Polymers

The effect of surfactants on polymers is highly variable with the type of polymer and surfactants used. In general, surfactants obtain abilities to both reduce and increase water viscosity. When the CMC is reached, micelle aggregates form, which can add to the water viscosity. Surfactants also brings Na^+ -ions known for reducing the polymer viscosity. In regards to HPAM, these two effects cancel each other, so the overall viscosity is not significantly affected. However, hydrophobic associate polymers are known to interact more with micelles, and are for that reason more sensitive towards the presence of surfactants. According to a study conducted with the associating polymer AP-P, the presence of surfactants led to an increase in viscosity. This is caused by the hydrophobic group on the polymer, which is solubilized into micelles [89].

3.5.3.3 Surfactant-Polymer Interaction in a Low Salinity Environment

An experimental study conducted by Trushenski (1977) proclaims that lowering the electrolyte concentration increases the stability of polymers and surfactants, causing them to interact less - ultimately leading to a higher oil recovery [88]. This may be explained by the DLVO-theory introduced earlier. Due to the negative charge on polymers and anionic surfactants, an increase in electrolyte concentration will screen the repulsive charges and compress the electrical double layers of both chemicals. A reduced zeta-potential makes the chemicals vulnerable for aggregation, decreases the system stability and ultimately leads to phase separation [89].

3.5.4 Composite Low Salinity Surfactant/Polymer Injection

Studies have shown that a combination of low salinity waterflooding with surfactant, polymer, or surfactant-polymer flooding leads to incremental oil recovery. In laboratory experiments combining the tertiary fluids, some of the studies revealed that the composite effect of the injection scheme exceeded the individual contributions of low salinity water, surfactants and polymers. Many of these laboratory studies have been successfully history matched [6].

Figure 3.25 visualize a typical injection scheme of a hybrid LSSP-process, illustrating the individual contributions of each slug on oil recovery. The LSSP-fluids are injected in a tertiary mode after seawater injection. Initially, a low-salinity environment shall be established by low salinity waterflooding. Thenceforth, a slug of low salinity surfactant is injected to enhance the microscopic sweep. The following low salinity polymer ensures a stable displacement of the surfactant slug, and prevents the establishment of viscous fingers in the surfactant slug by chase water. Ultimately, low salinity waterflooding is commenced.

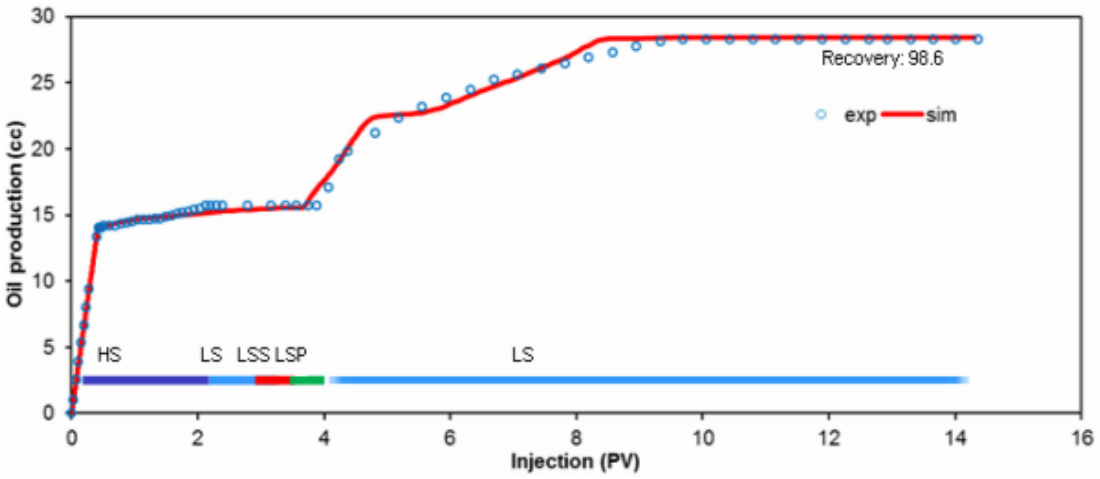

Figure 3.29: Experimental and history matched oil production from a composite lab experiment [6].

The experiment displayed in figure 3.29 is a typical representative of how a composite EOR-experiment may be conducted, where the sequence of the LSSP fluids is the following [6]:

- Injection of high salinity sea water (HS, 4% salt)
- Injection of low salinity brine (LS, 0.4% salt)
- Injection of low salinity surfactant (LSS)
- Injection of low salinity polymer (LSP)
- Injection of low salinity brine (LS, 0.4% salt)

Chapter 4

Simulation Models

4.1 Reservoir Simulator

For reservoir behavior predictions, a simulation tool will be utilized. Simulation studies enable the investigation of several recovery scenarios, which greatly optimizes the reservoir development [91].

In this thesis, the advanced reservoir simulator STARS will be used. STARS is a compositional simulator developed by the Computer Modelling Group (CMG), and is a sensible choice when managing advanced EOR-processes such as low salinity waterflooding. The simulator has several advantages in terms of managing dispersion and chemical composition in a flood. STARS accounts for complex phenomena required to accurately model chemical EOR-mechanisms, exemplified by the modelling of geochemical reactions which occur during low salinity water injection. Furthermore, STARS provides accurate effects of IFT-reduction following surfactant injection due to a recurrent relative permeability interpolation. In regards to polymer flooding, STARS enable characterization of polymer shear, retention and inaccessible pore volume [91].

To run a simulation, STARS requires an input data file defining important parameters concerning the reservoir and fluid properties, in addition to a planned recovery technique and schedule. The data file used for the simulations in this thesis will be presented in the appendix section.

Following the completion of each simulation run, the results are ready for analysis in the "Results 3D" and "Results Graph" features. Results 3D can be utilized to view the grid properties for any output time in 2D and 3D. The Results Graph feature enables plotting of various well data over time, in addition to special history parameters defined in the input data file.

4.2 EOR-Simulation

This part presents the theoretical background for the simulation of tertiary hybrid EOR-processes for a component simulator, namely STARS. In this thesis, the effect of the following fluids is tested:

- Low salinity brine (LS)
- Surfactants diluted in low salinity brine (LSS)
- Polymers diluted in low salinity brine (LSP)

The methodology is to examine the contribution and interaction of each tertiary EOR-fluid during a composite experiment. In the simulation study, low salinity brine will first be injected in a tertiary mode to establish a low salinity environment for the forthcoming chemicals. Thenceforth, surfactants diluted in low salinity brine is introduced, followed by a slug of low salinity brine with polymers. Ultimately, a chase slug of low salinity brine is injected. Based on previous simulation work on hybrid EOR, the expected influence from the tertiary fluids are the following:

4.2.1 Low Salinity Brine (LS)

In regards to previous modelling of low salinity waterflooding, Skauge et al. (2011), and later confirmed by Tavassoli et al. (2016), report that the relative permeability is dependent on salinity. The water will obtain a lower relative permeability at the endpoint, there will be a small shift of cross-over point, and a lower residual oil saturation, S_{or}, - indicating an increase in water-wetness [86, 92]. The reduced water relative permeability is due to a higher resistance to flow for the water phase following the wettability change, in addition to the release and trapping of fines. These mechanisms may be portrayed through an increase in pressure [86].

4.2.2 Low Salinity Surfactant (LSS)

As reported by Skauge et al. (2011), Pettersen et al. (2016) and Tavassoli et al (2016), the residual oil saturation, S_{or}, is expected to be reduced significantly or completely due to the lowering of interfacial tension between the water and oleic phases [6, 86, 92]. Skauge et al. (2011) declares that the relative permeability curves will be significantly straightened, and the capillary pressure is assumed to be zero. Furthermore, the interfacial tension is dependent on the surfactant concentration. The salinity determines the phase behavior for surfactant concentrations larger than the CMC. In a low salinity environment, there will exist two phases; one microemulsion phase with water, electrolyte, surfactant and solubilized oil, and an excess oil phase (Windsor type I). The water viscosity may be increased due to the formation of

micelles at CMC, which will increase reservoir pressure [6, 86, 92]. Surfactant adsorption and solubility issues may portray an obstacle when conducting surfactant flooding experiments. However, these complications are reduced at low salinities (Windsor type I) [93].

4.2.3 Low Salinity Polymer (LSP)

According to Mohammadi et al. (2012) and Khorsandi et al. (2017), the polymers and low salinity water can cooperate in increasing oil recovery by sweep improvements due to a viscosity increase and wettability alteration, respectively. The water viscosity will be dramatically increased by the polymers, which will reduce the relative permeability of water and the mobility ratio. Polymer entrapment can reduce permeability dependent on the initial heterogeneity of the reservoir, and will increase the field pressure. The polymer solution viscosity is a function of concentration, shear rate and salinity, and high salinities may reduce the viscosity of the polymer phase. Factors such as polymer adsorption, inaccessible pore volume and permeability reduction are features associated with polymer flooding, and should be accounted for by the simulator [87, 94]. The correct description of polymer implementation may present the largest challenge of the tertiary fluids due to the lack of a proper macroscopic model in the current generation simulators [6].

4.2.4 Low Salinity Surfactant Polymer (LSSP)

The modelling of a composite low salinity waterflooding, surfactant flooding and polymer flooding process is a topic requiring more research. Previous publications by Skauge (2015) and Pettersen et al. (2016) addresses the modelling approach of hybrid EOR-processes [6, 93]. According to their studies, the simulation of the complex EOR-process yields satisfactory results. The double relative permeability interpolation mechanism in STARS allows the definition of two relative permeability sets, which enables the description of relative permeability dependence on salinity and surfactant concentration. However, it is not yet possible to define a third set of polymer relative permeability [6].

4.3 Overview of Reservoir Model and Initial Properties

This thesis concerns a reservoir model of the dimensions 195, 155 and 25 grid blocks in I, J and K directions, respectively. There are two wells in the model, one injector located in blocks 27, 25, 16-17, and one producer located in blocks 160, 120, 1-13, the wells are approximately 2500 meters apart. Both wells are controlled by a maximum volumetric rate of 7500 m^3/day. The model is rather homogenous and has an overall porosity of 23%. The horizontal permeability in I and J directions is 2000 mD, and the vertical permeability is at 100 mD; enabling cross-flow between layers and the analysis of gravitational effects on fluid displacement and dispersion of dissolved components. Figure 4.1 visualizes the 3-dimensional reservoir model.

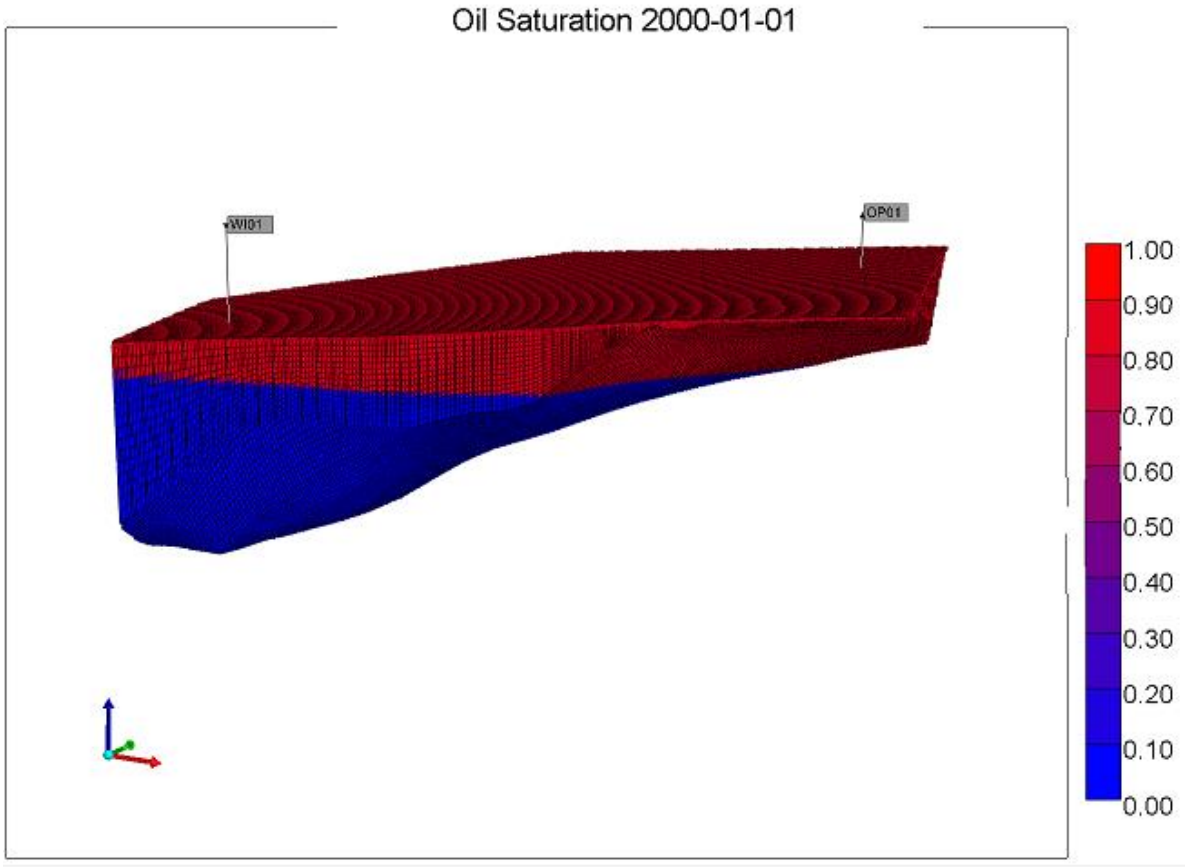

Figure 4.1: The reservoir model used in this study, illustrating the initial distribution of reservoir fluids. The scale is a measure of the oil saturation within the reservoir. The injector is to the left and producer is on the right side.

4.3.1 Initial Conditions

Initially, the active phases initially in the reservoir are oil, water and dissolved hydrocarbon gas. The connate water initially in place obtains a salinity of 40 000 ppm, and the irreducible water saturation, S_{wi}, in the oil zone is 12.3%. The total volume of oil originally in place (OOIP) is $6.6092 \cdot 10^7$ m^3.

The reference case demonstrates regular seawater flooding, where high salinity water at a salt concentration of 40 000 ppm is injected throughout the entire production stage.

Table 4.1 presents the properties of the initial components in the reservoir.

Table 4.1: Properties of initial reservoir fluids and components.

Component	***Molecular Mass (kg/gmol)***	***Density (kg/m^3)***	***Compressibility (1/kPa)***
Water	0.018	1038.80	$4.15 \cdot 10^{-7}$
Salt	0.058	991.00	$4.94 \cdot 10^{-7}$
Oil	0.444	846.30	$1.66 \cdot 10^{-6}$
Gas	0.022	1.15	$1.80 \cdot 10^{-6}$

The initial relative permeability curves for oil and water during high salinity conditions are illustrated in figure 4.2.

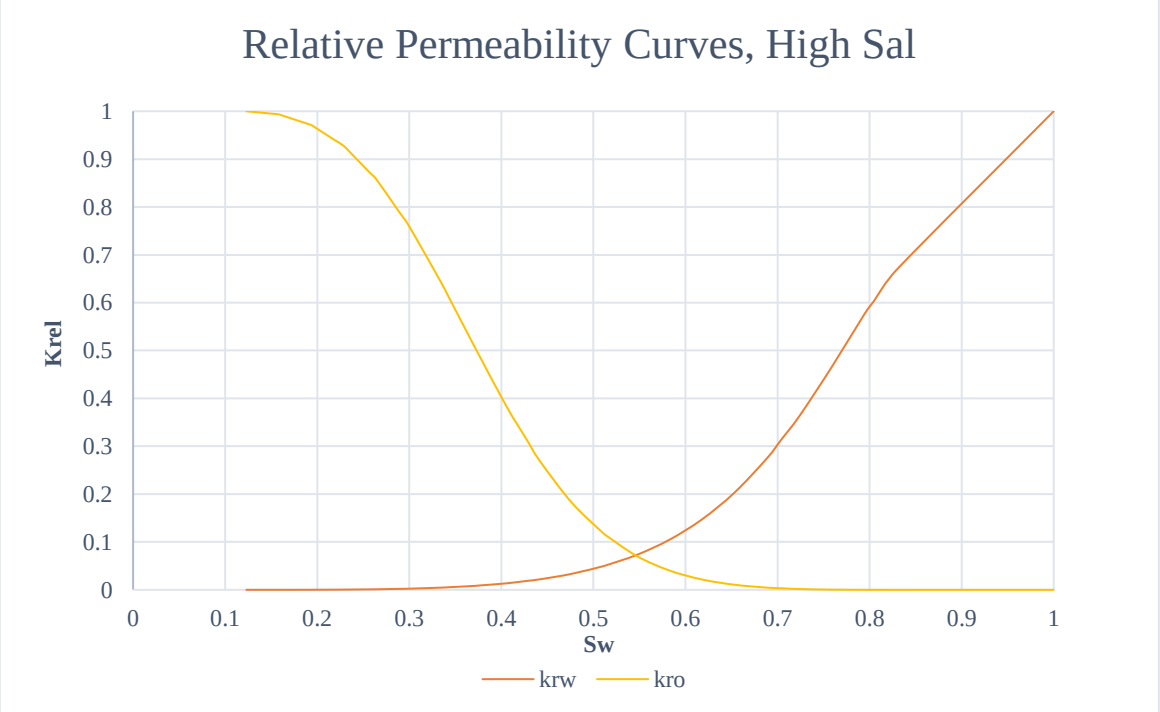

Figure 4.2: Water- and oil relative permeability curves for high salinity water (initial case).

4.4 Low Salinity Water Surfactant/Polymer Modelling

4.4.1 Properties of Surfactants and Polymers in an Aqueous Solution

The surfactants and polymers alter the characteristics of the water phase, and the properties of the chemicals diluted in water are presented in table 4.2.

Table 4.2: Properties of surfactants and water in an aqueous solution.

Chemical	***Molecular Mass (kg/gmol)***	***Density (kg/m^3)***	***Compressibility (1/kPa)***
Surfactant	0.548	991	$4.94 \cdot 10^{-7}$
Polymer	8.000	1000	$4.94 \cdot 10^{-7}$

4.4.2 Defining Injection Components

There are six components that are included in this study, namely water, salt, surfactant, polymer, oil and solution gas. Salt, surfactants and polymers are diluted in the water phase while the gas can be dissolved in the oil.

In the Run section, the injection composition for each injection well must be defined. The concentration of each of the six components shall be given in mole fractions where the total value of the injection stream must equal 1.

The keyword INCOMP is used to define the injection stream composition, and is followed by six entries describing the mole fractions of each component in water; m_{water}, m_{salt}, m_{surf}, m_{poly}, m_{oil} and m_{gas}.

4.4.3 Defining Relative Permeability Curves

Figures 4.3 and 4.4 illustrate the water- and oil relative permeability curves for high salinity waterflooding (4% salt), low salinity waterflooding (0.4% salt), and surfactant flooding given as input in the simulation data file. The low salinity relative permeability curves are based on unpublished internal work, and the relative permeability curves for maximum surfactant concentration is given based on an assumption of an “extreme process” with straight relative permeability curves and a residual oil saturation, S_{or}, of 0.

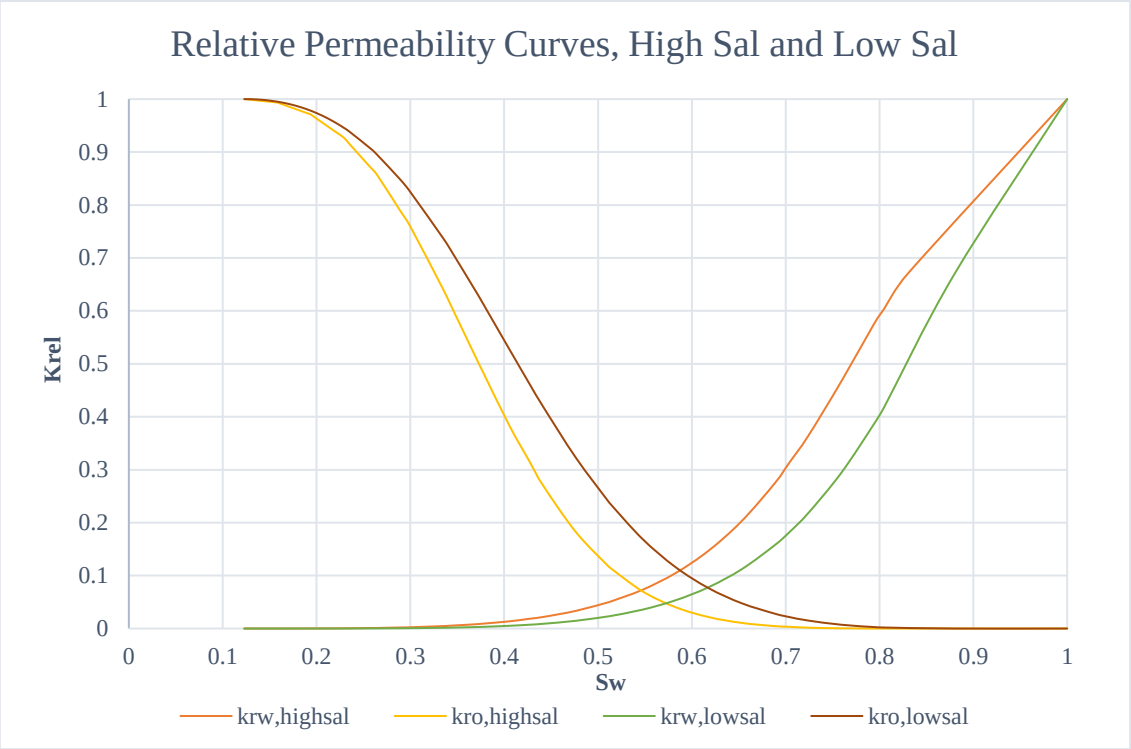

Figure 4.3: Input water- and oil relative permeability curves for high salinity water and low salinity water.

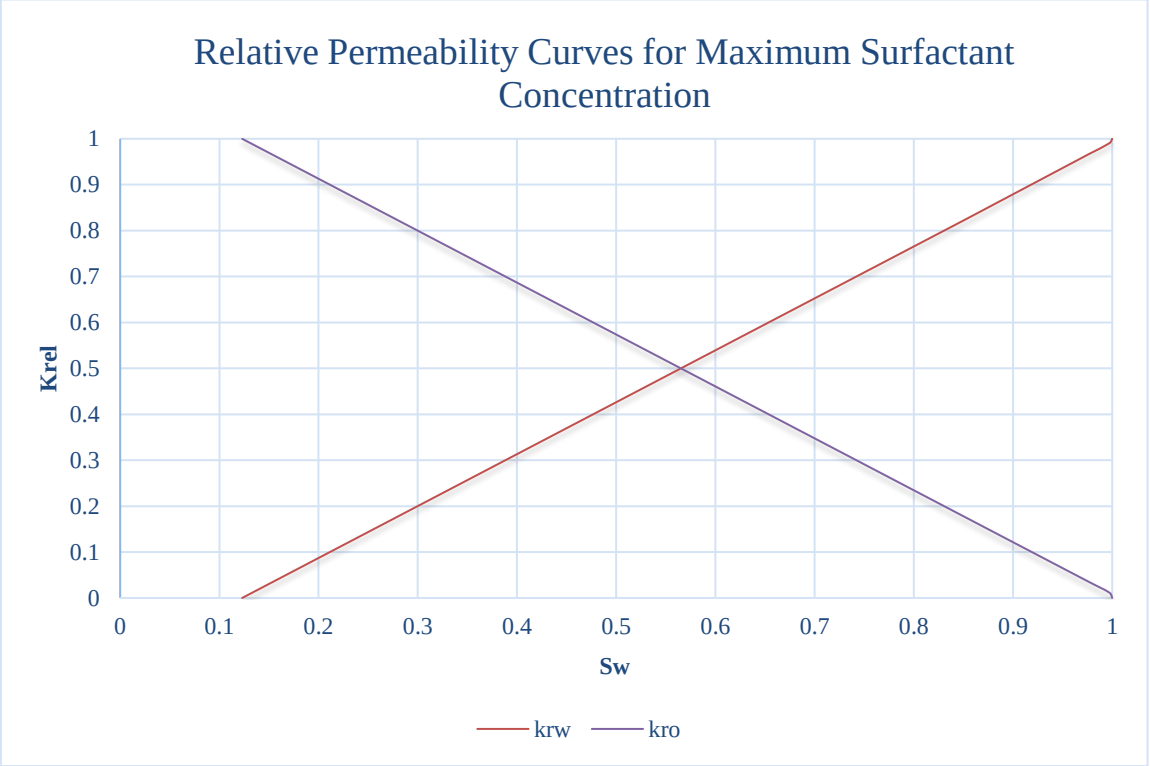

Figure 4.4: Input water- and oil relative permeability curves for maximum surfactant concentration.

4.4.3.1 Relative Permeability Interpolation

The assumption that rock fluid properties only depend on fluid saturations and hysteresis proves insufficient to describe flow behavior under certain circumstances [95]. During the LSSP process, the relative permeability will change due to the physiochemical mechanisms occurring within the reservoir. The relative permeability will for example be affected by the wettability change due to the diluted water injection, IFT reduction and release of capillary trapped oil following the surfactants, and the mobility ratio-reducing effect of polymers.

STARS obtain useful features enabling the use of interpolated relative permeability curves, and the flexibility in terms of interpolation parameters, enables a variety of reservoir phenomena to be managed [95]. Interpolation is a procedure where new data points within a range of known values are constructed. Relative permeability data for maximum and minimum concentration of a component diluted in water is given in the input data file, but for all concentrations between these boundaries, STARS interpolates relative permeability values.

The interpolation in STARS can be based on the concentration of the key component in water, or the capillary number. The capillary number is a dimensionless ratio of viscous forces and interfacial tension forces:

$$N_c = \frac{\mu v}{\sigma} \tag{4.1}$$

If an interfacial tension table has been defined (INFTABLE) in the Rock-Fluid section, the interpolations will be based on the logarithm of the capillary number. Otherwise, the concentration of the component in water will be the basis of the interpolations. However, the interfacial tension is a function of concentration, and hence, the interpolations should be equivalent. Nevertheless, the interpolations do not equal, because STARS does not compute the capillary numbers from the common formula, but in another way that neglects the velocity term. The simulator substitutes the velocity with Darcy's Law, and consequently, the viscosity cancels and N_c yields [95]:

$$N_c = \frac{K_{abs}\Delta P}{\sigma_{ow}\Delta x} \tag{4.2}$$

It proves complicated to calculate exact values for capillary number in advance of running the simulation model, as a differential pressure value, ΔP is required. The concentration-based interpolations become linear whereas the capillary number-based interpolations become exponential. For salinity interpolations, the concentration-based option is the best approach, while the capillary number-based method seem better for surfactant interpolations.

4.4.3.2 Interpolation of a Single Relative Permeability Set

As input in a STARS data file, the maximum and minimum component concentrations are defined; these are regarded as the upper and lower interpolation bounds. This example regards the relative permeability dependence on salinity, where 4% and 0.4% salt concentrations are used for the high salinity water and low salinity water, respectively. There are different relative permeability curves belonging to the high salinity brine and low salinity brine. To handle this situation, the STARS interpolation mechanism works like the following:

For salinity levels higher than 4% (upper bound), the high salinity curve is utilized, and for salt levels lower than 0.4% (lower bound), the low salinity curve is used. If the salinity is between 0.4 and 4%, an interpolated relative permeability value is chosen. For example, a salinity of 1.6% corresponds to 40% high salinity and 60% low salinity. Thus, an intermediate relative permeability is interpolated with 0.4 high salinity + 0.6 low salinity.

One set of relative permeability tables are given for both high salinity water and low salinity water, and the following parameters are used to estimate the relative permeability and capillary pressure for any concentration value between the extremes:

$$k_{rw} = k_{rw}^{HS} \cdot (1 - wtr) + k_{rw}^{LS} \cdot wtr \tag{4.3}$$

$$k_{ro} = k_{ro}^{HS} \cdot (1 - oil) + k_{ro}^{LS} \cdot oil \tag{4.4}$$

$$P_{cow} = P_{cow}^{HS} \cdot (1 - pcw) + P_{cow}^{LS} \cdot pcw \tag{4.5}$$

Where:

$$wtr = \left(\frac{\log_{10}(N_c) - \mathrm{DTRAPW}^{LS}}{\mathrm{DTRAPW}^{HS} - \mathrm{DTRAPW}^{LS}}\right)^{WCRV} \tag{4.6}$$

$$\mathrm{oil} = \left(\frac{\log_{10}(N_c) - \mathrm{DTRAPN}^{LS}}{\mathrm{DTRAPN}^{HS} - \mathrm{DTRAPN}^{LS}}\right)^{OCRV} \tag{4.7}$$

$$\mathrm{pcw} = \left(\frac{\mathrm{wtr} + \mathrm{oil}}{2}\right) \tag{4.8}$$

wtr and oil are dimensionless interpolation parameters for water and oil. N_c denotes the capillary number, and $DTRAPW$ and $DTRAPN$ are values describing the wetting and non-wetting phase interpolation parameters respectively. $WCRV$ and $OCRV$ are curvature interpolation parameters ranging between 0 and 1, which allow additional flexibility in interpolating between sets of curves if experimental evidence requires it.

4.4.3.3 Double Interpolation

In order to determine the actual relative permeability values at a given concentration, STARS interpolates between the limiting curves for minimum and maximum concentration of the component in water. When an additional chemical is introduced, STARS shall compute intermediate relative permeability values; an advanced feature called double interpolation.

In a reservoir initially filled with high salinity brine and oil, low salinity water is first injected followed by a slug of low salinity brine and surfactants. There will be relative permeability values based on the salinity level, k_r^{salt}, and relative permeability values based on the surfactant concentration, k_r^{surf}. The final relative permeability, k_r, is found by the interpolation of those two.

In order to perform double interpolation, two rock regions must be defined:

- Rock type 1: Relative permeability curves for component A as a function of the concentration of A in water.
- Rock type 2: Relative permeability curves for component B as a function of the concentration of B in water.

To STARS, it matters which component (salt, surfactant) is designated to Rock type 1 and 2. Simulation studies reveal that surfactant must be Rock Type 1, and salt Rock Type 2 in order for the graphs to seem reliable. It is unclear why the graphs in STARS rely on the order of the defined salinity and surfactant relative permeability sets, as this should not matter.

STARS does only handle two interpolation regions at the same time. In the case of an LSSP injection with a following polymer slug after the surfactant injection, it is not possible to define the polymer relative permeability as a third set. This is an issue that CMG hopefully finds a solution for in the nearest future.

4.4.3.4 Modelling of Relative Permeability

Relative permeability curves are defined in the Rock-Fluid section under the keyword SMOOTHEND QUAD. Two rock types must be defined, one regarding surfactant and the latter regarding salt. It is critical that this exact definition sequence is complied. The keyword RPT describes these rock types, and is followed by the number 1 or 2.

After a rock type has been specified, the INTCOMP keyword indicates which component is chosen to interpolate with, and the phase it is diluted in. Each rock type has two sets of relative permeability tables designated to the maximum and minimum component concentration in water. The keyword KRINTPR 1 or 2 denotes each of these curves.

DTRAPW defines the concentration value relevant for each curve. This value is given as the logarithm of the capillary number for the surfactant curves, and as a mole fraction of the concentration in water for the salinity curves.

Below DTRAPW follows a water-oil relative permeability table with corresponding capillary pressure values (SWT), and a liquid-gas relative permeability table (SLT). The sequence of these tables must be obeyed, because SLT has an endpoint check which depends on an endpoint in SWT.

The following diagram from the STARS manual illustrates the required ordering of each keyword.

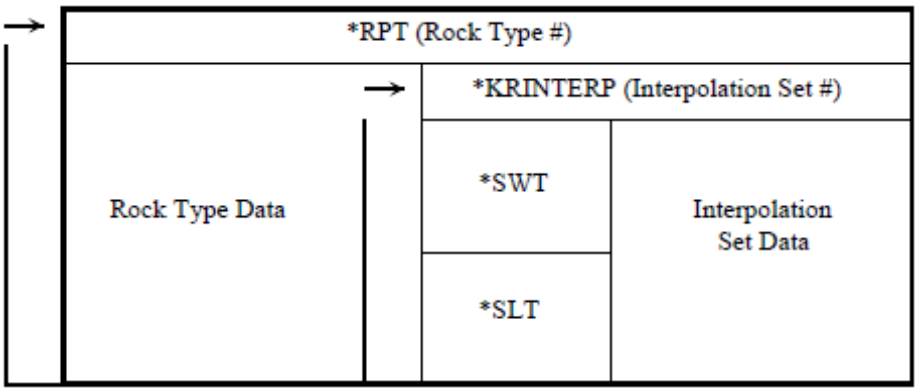

Figure 4.5: Diagram displaying the sequence of the keywords used [95].

4.4.4 Viscosity Mixing

The viscosity of water is assumed to be relatively constant at a value of 1 cp, although it may decrease when subject to higher temperatures. However, the concentration of diluted salt and EOR-chemicals may affect the viscosity of the water phase. The default setting considers a linear relationship between component concentration in water and corresponding viscosity [95], based on the following equation:

$$\ln(\mu) = \sum_{i}^{n} x_i \ln(\mu_i) \tag{4.9}$$

Where μ represents the phase viscosity, μ_i denotes the viscosity of the pure phase, and x_i symbolize the mole or mass fraction of the diluted component.

In some cases, linear viscosity mixing may not be assumed. Hence, a nonlinear mixing approach shall be applied for each component applicable. In the Fluid Description section, the components must be divided into two groups; the components specified in the VSMIXCOMP keyword (set S), and those not. The total fraction, x_i, of these two groups must sum 1. The keyword VSMIXENDP describes abscissas corresponding to the first and last table entries. Ultimately, the keyword VSMIXFUNC are followed by eleven table entries describing the nonlinear mixing rule function.

Each table entry is found from the following correlation:

$$f_a(x_a) = \frac{\ln(\mu - M)}{\ln(\mu_a - M)} \tag{4.10}$$

Where the subscript a denotes the key component specified by VSMIXCOMP, and M is found from the following formula:

$$M = \left[\sum_{i \neq S}^{n} x_i \ln(\mu_i)\right] / (1 - x_a) \tag{4.11}$$

4.4.5 Component Adsorption

Adsorption of surfactants and polymers can cause loss of the chemicals, and therefore reduce the performance of the flooding processes. The adsorption of chemicals onto rock is inevitable and assumed to commence instantaneously. STARS obtain features that accounts for the component adsorption, and can be included in both tabular form or in terms of the Langmuir adsorption isotherm. The tabular form has been utilized in this thesis.

In the Rock-Fluid section, the keyword ADSCOMP is followed by the component name and the continuous phase. The keyword ADSMAXT specifies the maximum adsorption capacity given in gmol/m^3. ADRT describes the residual adsorption level. A value of zero indicates a completely reversible adsorption whilst ADRT = ADSMAXT specifies a completely irreversible adsorption.

Thereafter, the dependence of adsorption on composition must be defined. A table describing the adsorption, ADSTABLE, must be present for each adsorbing component. ADSTABLE specifies a table of adsorption versus composition. *cpt* is the mole fraction of the component in the continuous phase, ranging from 0 to 1. *adt* denotes the adsorbed moles per unit pore volume at the given composition *cpt* in gmol/m^3.

4.4.6 Interfacial Tension

The change in interfacial tension between water and oil as a function of surfactant concentration in water is modelled in the Rock-Fluid section. The keyword INFTABLE designates the drop in interfacial tension as the concentration of surfactants increases. The interfacial tension table consists of *cift*, which is the composition of the component/phase given by INTCOMP. The concentration of the surfactants is given as its mole fraction in water. *cift* is accompanied with *sigift*, which describes the interfacial tension given in dyne/cm. The table must have at least two entries, where each entry is given in a new line.

As clarified in table 4.3, the interfacial tension decreases as the interfacial tension increases. The initial interfacial tension is 16 dyne/cm.

Table 4.3: The water-oil interfacial tension as a function of surfactant concentration.

Surfactant Concentration (mole fraction)	**Interfacial Tension (dyne/cm)**
0.000	16.00
0.001	0.01
0.005	0.05

4.4.7 Numerical Dispersion

The propagation of diluted salt and EOR-chemicals in the continuous water phase is affected by heterogeneity and tortuosity in the porous media. The term “dispersion” refers to the mixing of fluids caused by diffusion, local velocity gradients, heterogeneous streamline lengths, and mechanical mixing [55]. In addition to the physical dispersion of a component within another, numerical dispersion must also be accounted for when analyzing simulation results. The numerical dispersion is a result of simulator calculations, where the simulated system have a different behavior than the intended physical system. This can be visualized by examining how the front of the component develops through each grid block from the injector towards the producer. The front is likely to become more diffuse and loose its initial squared shape, and a mixing zone will be developed where the component concentration decreases progressively. Even though the reservoir may be uniform, numerical dispersion can have an effect on the simulation results.

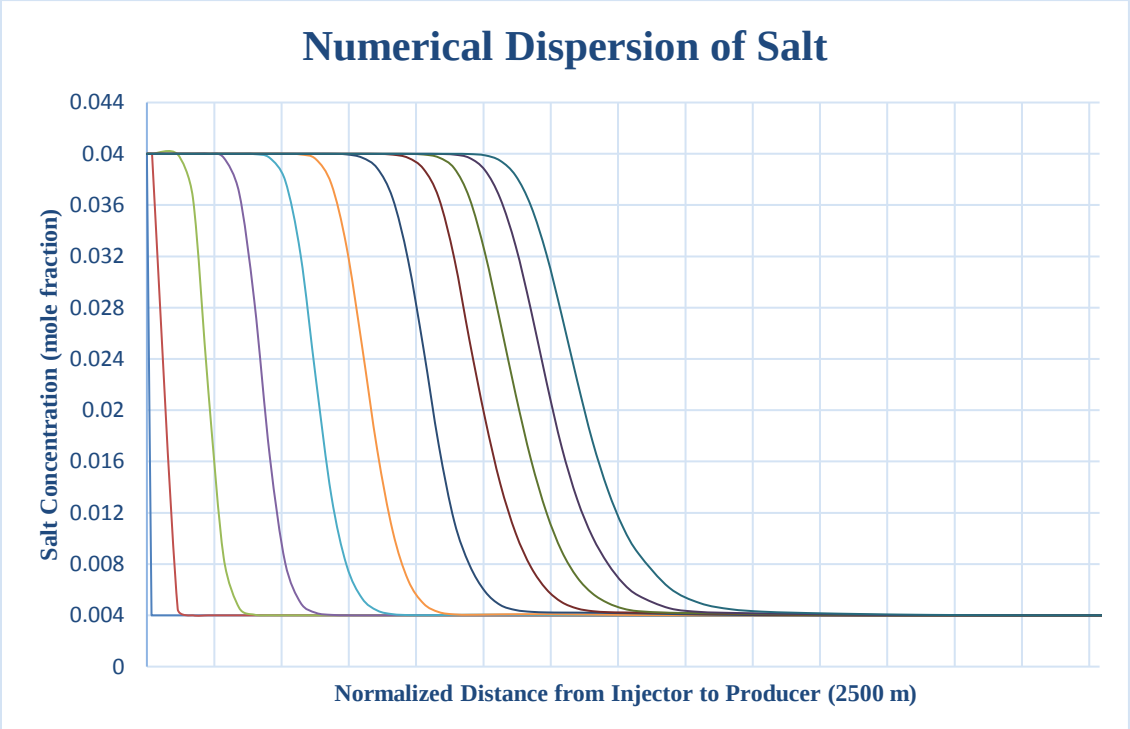

Figure 4.6: Numerical dispersion of salt with increasing distance from injector.

Figure 4.6 illustrates an example of an expanding mixing zone of salt throughout the reservoir. The connate water is initially at a salinity of 40 000 ppm (0.04), and is flooded with low salinity brine at 4000 ppm (0.004). The plots represent the concentration of salt in grid cells from the injector towards the producer, and it is apparent that it requires a longer time period for the grid cells closer to the producer to reach the minimum salinity level of 4000 ppm. Hence, dispersion increases over distance from injector.

Chapter 5

Simulation Results and Discussions

5.1 Base Case

The reference case presents conventional seawater flooding over a time span of 30 years. It is assumed that the formation water salinity equals the injection water salinity, which is 40 000 ppm, therefore no salt mixing will occur. Table 5.1 summarizes the production results for the reference case on the last production date, and figures 5.1 and 5.2 display the cumulative oil recovery, water cut, oil production rate and bottom-hole pressure as functions of time.

Table 5.1: Production results for the reference case.

Case Study	Oil Produced (m^3)	Oil Recovery (%OOIP)	Water-Cut (%)	Oil Rate (m^3/day)	Bottom-hole Pressure (kPa)
High Salinity Flooding	$1.60 \cdot 10^7$	61.25	99.15	63.23	21 290.7

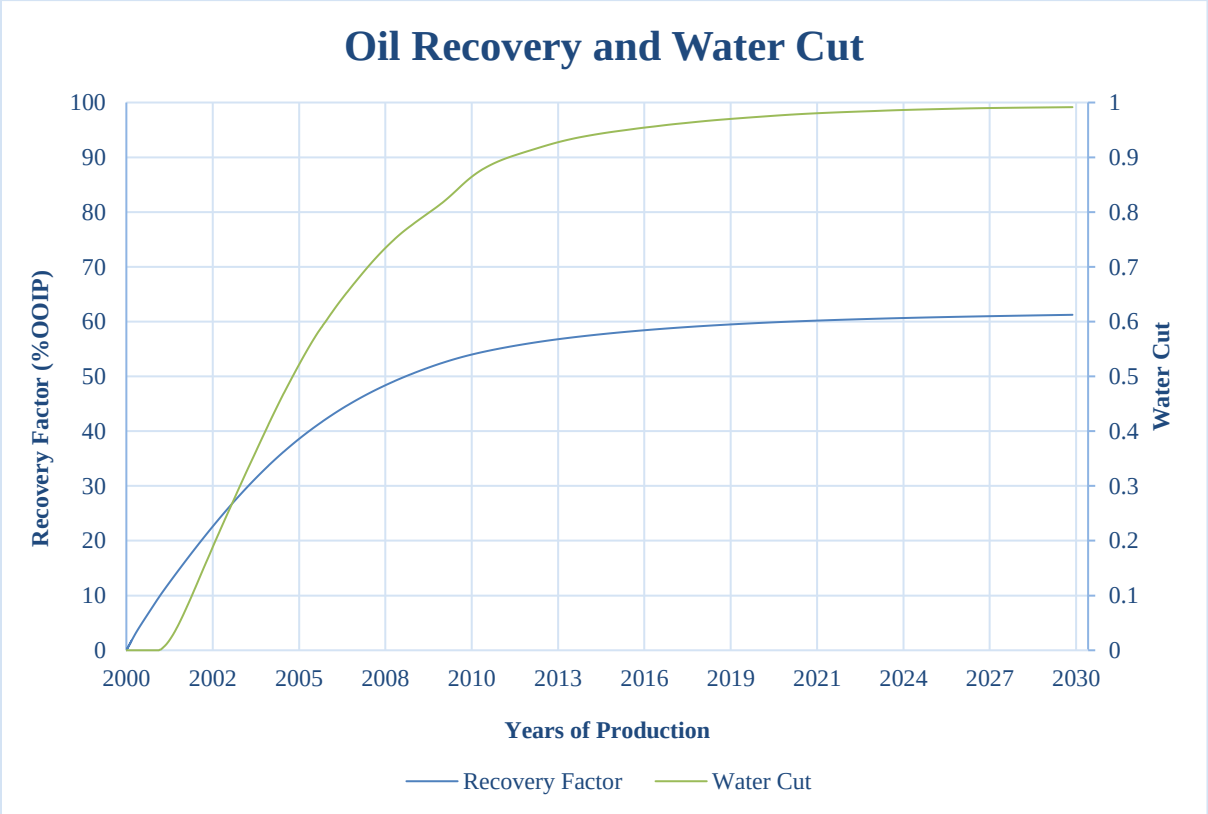

Figure 5.1: Cumulative oil recovery and water cut for the reference case of high salinity waterflooding.

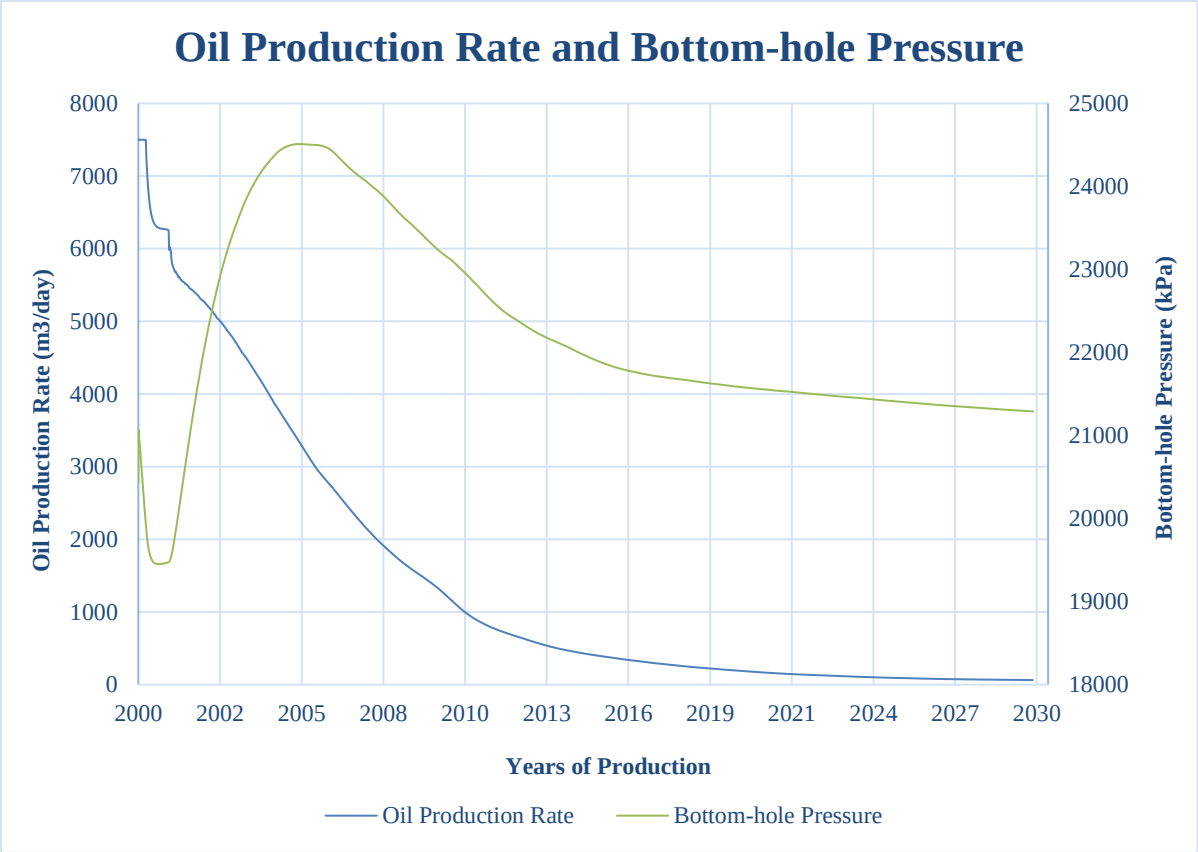

Figure 5.2: Oil production rate and bottom-hole pressure for the reference case of high salinity waterflooding.

The total oil volume produced after 30 years is $1.60 \cdot 10^7$ m^3, corresponding to a recovery factor of 61.25% of OOIP. The oil production rate does not remain constant for long, only for the first 90 days. Thereafter, it sinks rapidly and stabilizes at lower rates towards the end of the production time due to an increasing water cut. At the last day of production, the oil rate is 63.23 m^3/day.

The water cut has the opposite trend of the oil rate, and increases expeditiously until reaching a plateau at 99.22% at the end of the field lifetime, yielding a highly uneconomic scenario. Already after 15 years, the water cut exceeds 95%, and the expenses of continuing production may surpass the profits. The bottom-hole pressure increases initially due to the injected water, and reaches a maximum of 24 510.2 kPa before it starts to decline and reaches 21 248.4 kPa at the end of the field lifetime.

5.2 Comparison of Low Salinity Water Injection Potential to Conventional High Salinity Waterflooding

In order to investigate if a low salinity water injection is effective in this particular reservoir model, its potential is compared to conventional high salinity waterflooding in a secondary mode (S_{wi}). Low salinity brine was injected into the reservoir under the same initial conditions as for the high salinity waterflooding for an equal amount of years. The initial salinity of the brine within the reservoir is 40 000 ppm, and the injected water salinity obtains a salinity of 4000 ppm. Due to the difference in brine salinity, salt mixing will occur. The aim is to examine what effect the salinity reduction has on cumulative oil production. The comparison of the production results from the high salinity waterflooding and low salinity waterflooding processes on the last production date is displayed in table 5.2, and the cumulative oil recovery, water cut, oil production rate and bottom-hole pressure are visualized in figures 5.3 and 5.4.

Table 5.2: Comparison of high salinity waterflooding and low salinity waterflooding potential

Case Study	**Oil Produced (m^3)**	**Oil Recovery (%OOIP)**	**Water-Cut (%)**	**Oil Rate (m^3/day)**	**Bottom-hole Pressure (kPa)**
High Salinity Waterflooding	$1.60 \cdot 10^7$	61.25	99.15	63.23	21 290.7
Low Salinity Waterflooding	$1.73 \cdot 10^7$	66.20	96.79	239.50	20 965.8

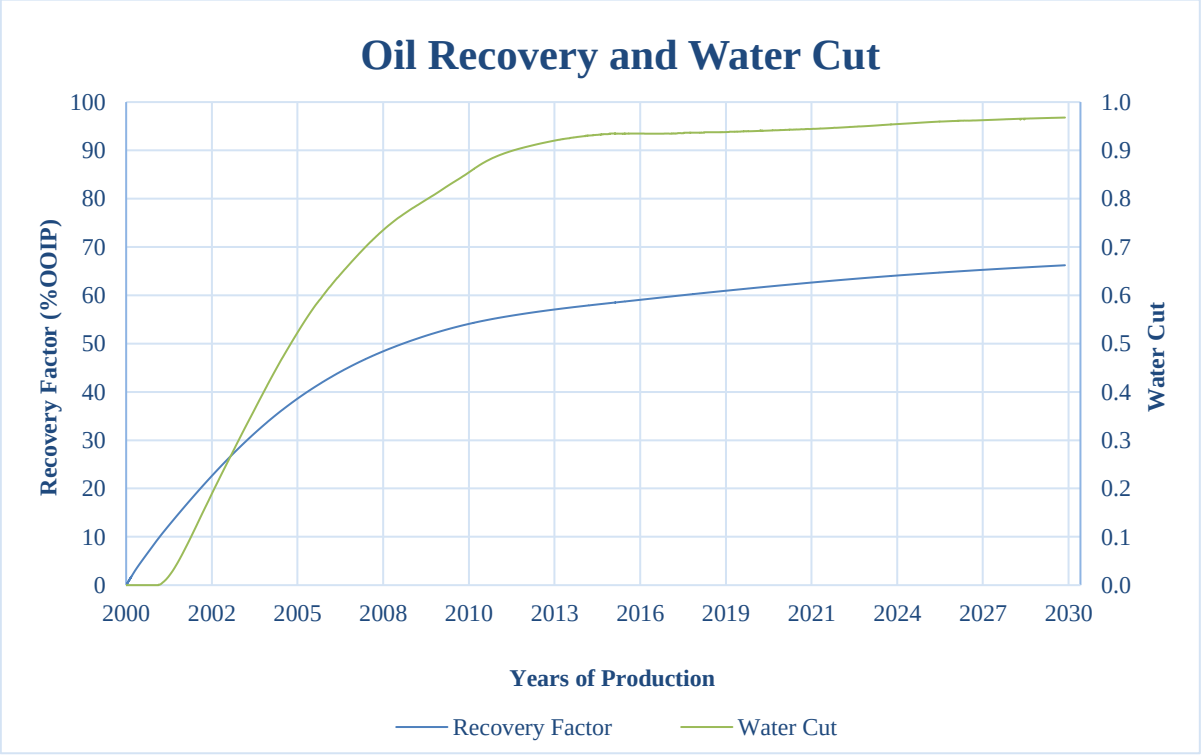

Figure 5.3: Cumulative oil recovery and water-cut for the low salinity waterflooding process.

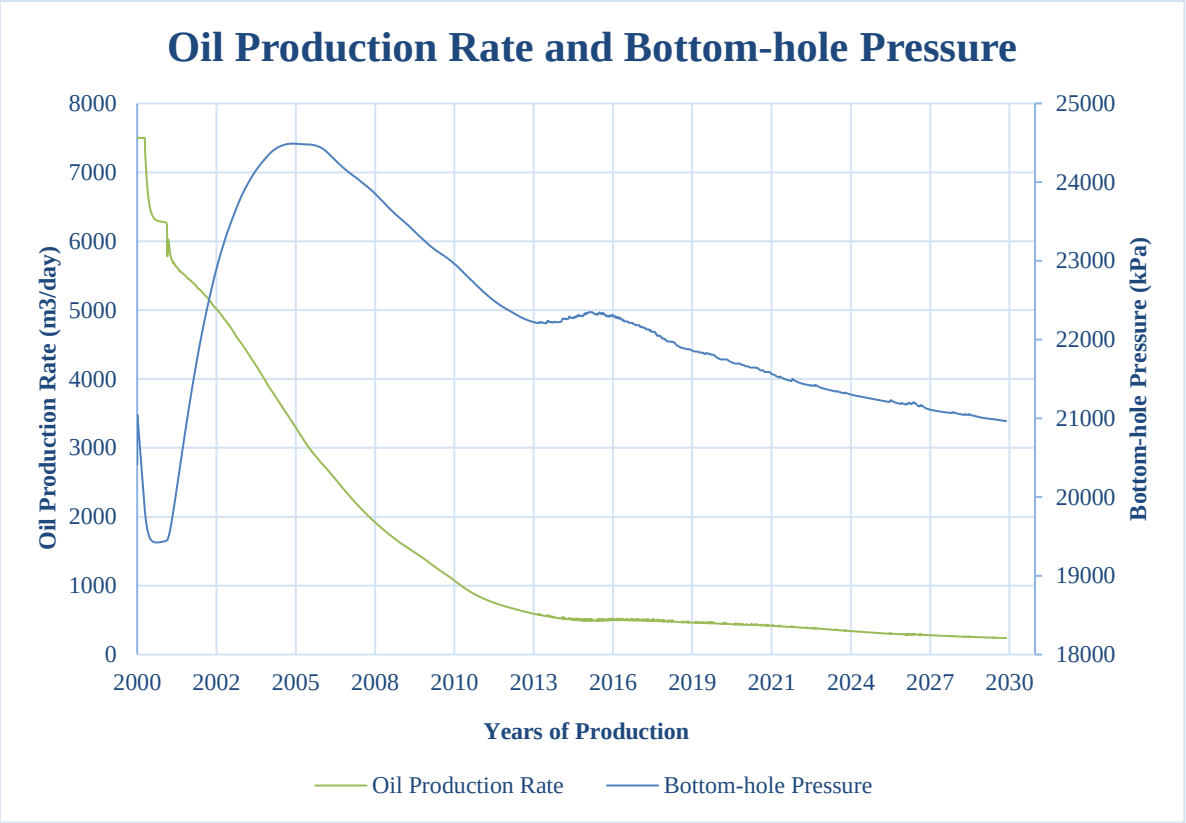

Figure 5.4: Oil production rate and bottom-hole pressure for the low salinity waterflooding process.

The total oil volume produced by the continuous low salinity water injection is $1.73 \cdot 10^7$ m^3, corresponding to a recovery factor of 66.20%. The oil production rate is maintained at 7500 m^3/day for 90 days, similar to the reference case, before it gradually starts to decline. Eventually, it ends up at 239.50 m^3/day.

The water cut increases as the oil production rate decreases, and in year 30, the water cut has risen to 96.79%.. The bottom-hole pressure increases to 24 480.3 kPa after injection commencement. Thereafter, it decreases steadily before it reaches a new local maximum at 22 353.6 kPa after 1 PV of low salinity water has been injected. Towards year 30, the pressure declines and eventually reaches 21 290.7 kPa.

5.2.1 Oil Recovery Comparison

Figure 5.5 displays the cumulative oil recovery comparison between the high salinity waterflooding and low salinity waterflooding processes. The production of oil increases equally for both processes in the first decade. Thenceforth, the high salinity curve approaches a plateau while the low salinity oil production curve continues to increase further. It takes approximately 11.5 years to inject one pore volume, and therefore the same amount of years until the full effect of low salinity water can be properly observed. After 30 years of production time, the recovery factor for the high salinity waterflooding study ends up at 61.25%, while the low salinity water has recovered 66.20% of the oil originally in place (OOIP). The difference amounts to $1.3 \cdot 10^6$ m^3 additional oil produced by the low salinity water.

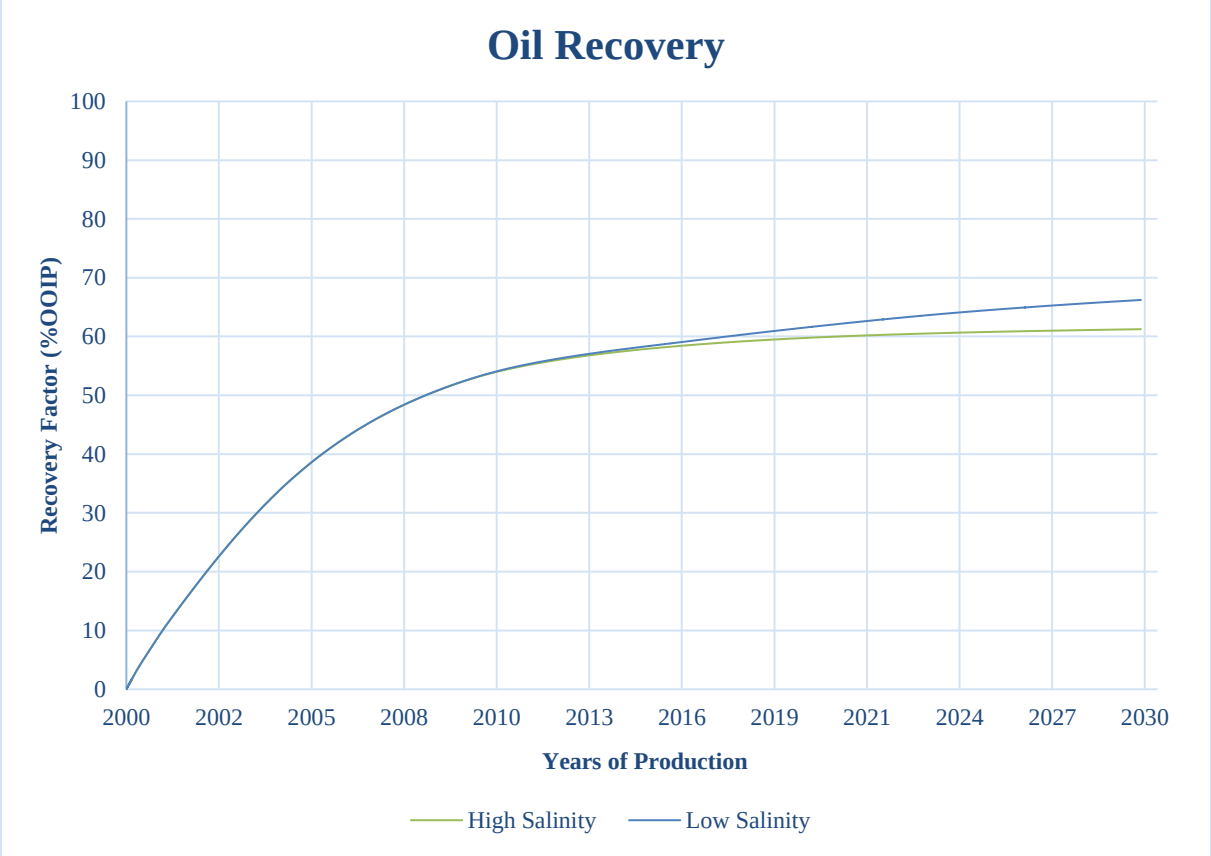

Figure 5.5: Cumulative oil recovery comparison between the high salinity- and low salinity waterflooding processes.

5.2.2 Water Cut Comparison

The water cut for both high salinity waterflooding and low salinity waterflooding are shown in figure 5.6. From the graphs, it may be deducted that the water cut obtains a significantly lower value after 30 years of production in the low salinity waterflooding process. The wettability altering effects of the diluted injection water yield better flooding performance and an enhanced macroscopic sweep [40], which may explain why the water cut is 2.38% lower for low salinity waterflooding, as the water is distributed more evenly throughout the reservoir. It takes 8 years longer for the low salinity waterflooding process to reach a water cut of 95% compared to the base case, indicating that an economic production can be maintained for a longer period of time.

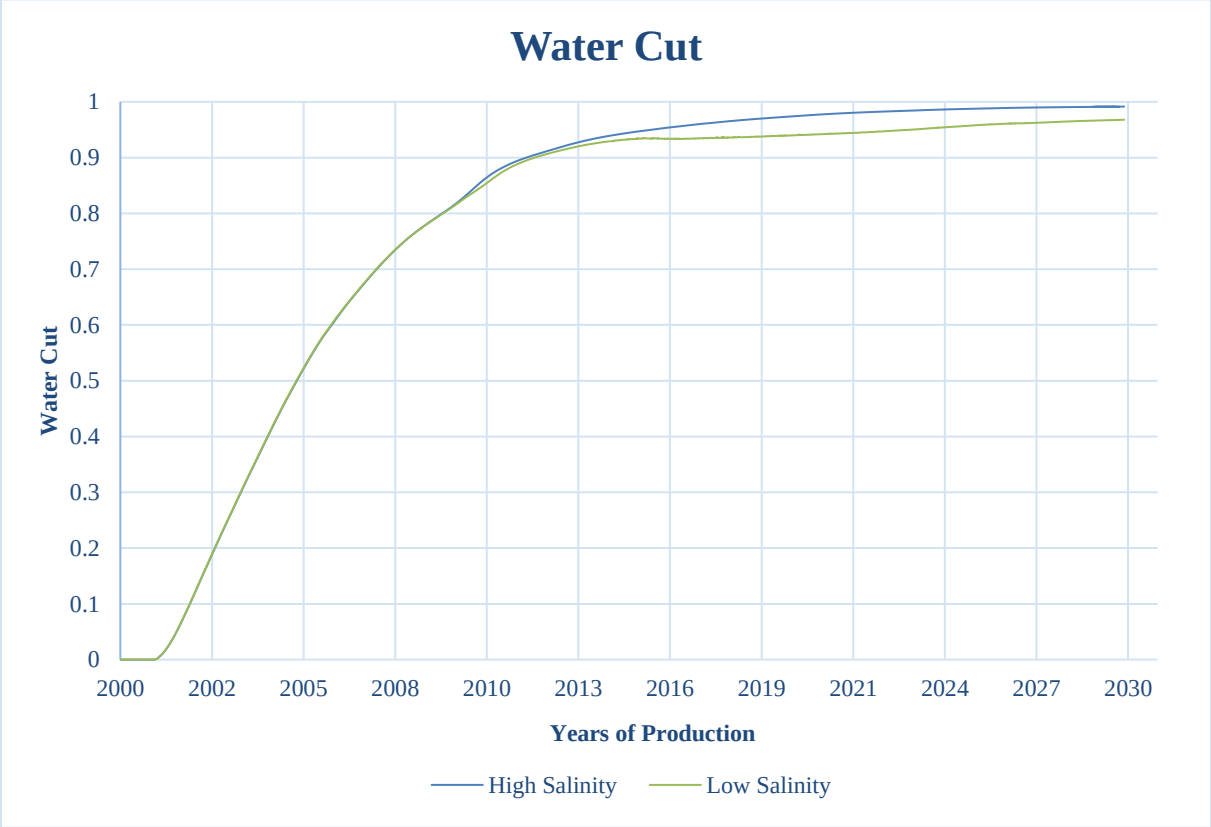

Figure 5.6: Comparison of water cut between the high salinity- and low salinity waterflooding processes.

5.2.3 Oil Production Rate Comparison

The oil production rates for the high salinity and low salinity waterflooding processes are displayed in figure 5.7. The two rates are aligned initially until approximately 1 PV is injected. From this point forward, the oil rate levels at significantly higher rates for the low salinity case. The low salinity waterflood maintains a higher oil production rate for a longer time, and after 30 years of production, the oil production rate is 279% higher for the low salinity waterflooding process.

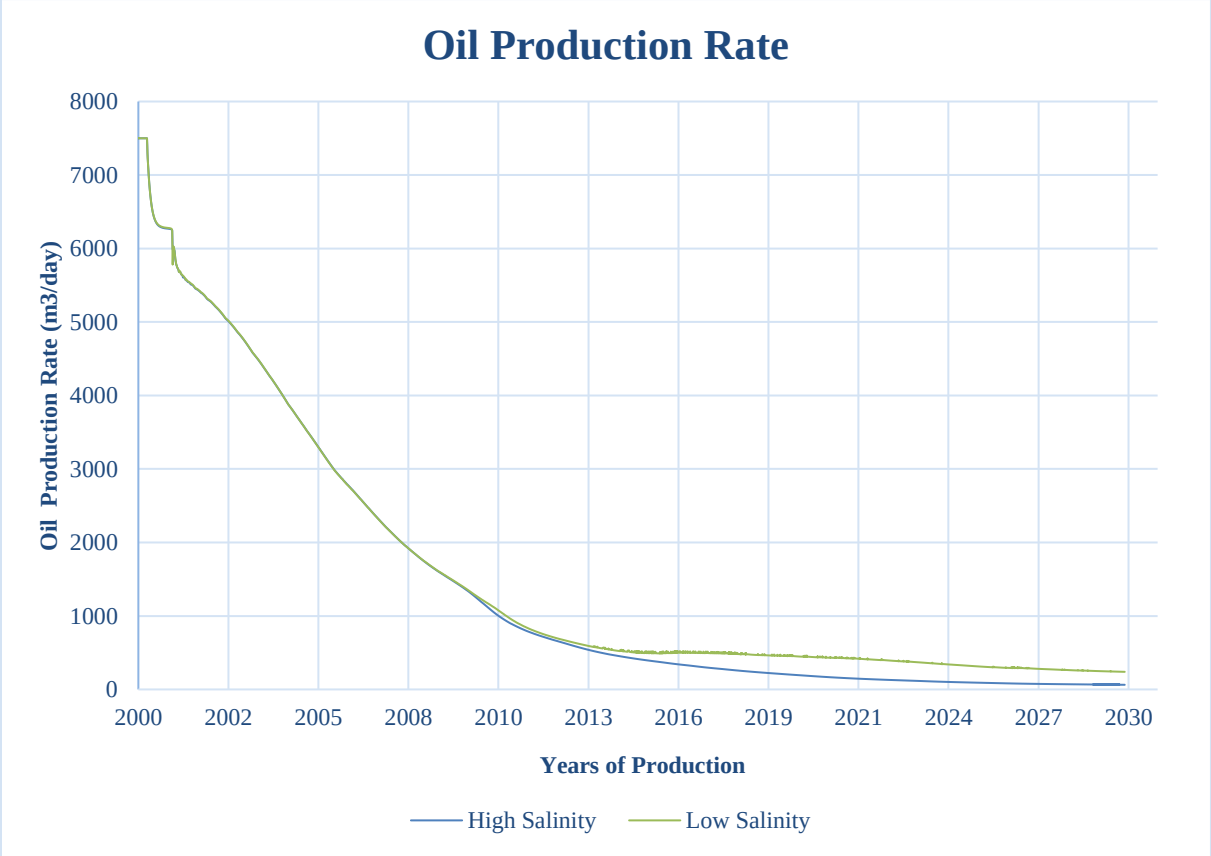

Figure 5.7: Comparison of oil production rate between the high salinity- and low salinity waterflooding processes.

5.2.4 Bottom-Hole Pressure Comparison

The comparison of the low salinity pressure behavior to the base case is presented in figure 5.8. The pressures for the two trials are initially equivalent until 1 PV of the low salinity water has been injected. At this point, there is a pressure buildup within the reservoir for the low salinity waterflooding process, and according to published papers, this increase is caused by the blockage of pores induced by ionic interactions between crude oil, brine and rock [71, 96]. Furthermore, the increased water-wetness reduces the relative permeability of water, which can affect reservoir pressure.

The pressure does not increase for long, and eventually it starts to decline at a faster rate than the high salinity curve. The elevated pressure decrease for the low salinity case may be due to a declining oil saturation within the reservoir, which increases the relative permeability of water.

Figure 5.8: Comparison of bottom-hole pressure between the high salinity- and low salinity waterflooding processes.

5.2.5 Low Salinity Water Propagation

STARS obtains visualization tools that enable inspection of the whole reservoir for a wide range of properties. By examining how the low salinity water advances in the reservoir, it gives a more thorough understanding of the simulation results. Below follows the progression of the low salinity waterfront at ½ PV injected, 1 PV injected, and injection closure. The low salinity waterfront is displayed in an IK-cross sectional view.

Figure 5.9 visualizes well locations and the propagation of low salinity water after approximately ½ PV of the diluted water is injected. Thenceforward, figure 5.10 illistrates how the low salinity water has spread after 1 PV is injected. Lastly, figure 5.11 shows the salinity distribution within the reservoir on the last day of low salinity water injection.

In front of the pure low salinity water, a salt mixing zone develops. Due to gravitational forces, the denser water will flow towards the reservoir bottom before it reaches the reservoir top. The low salinity water gradually spreads towards the producer, and by year 2030, almost all the water within the reservoir obtains the low salinity concentration value of 4000 ppm. The upper and lower leftmost corners have not yet reached the minimum salinity concentration.

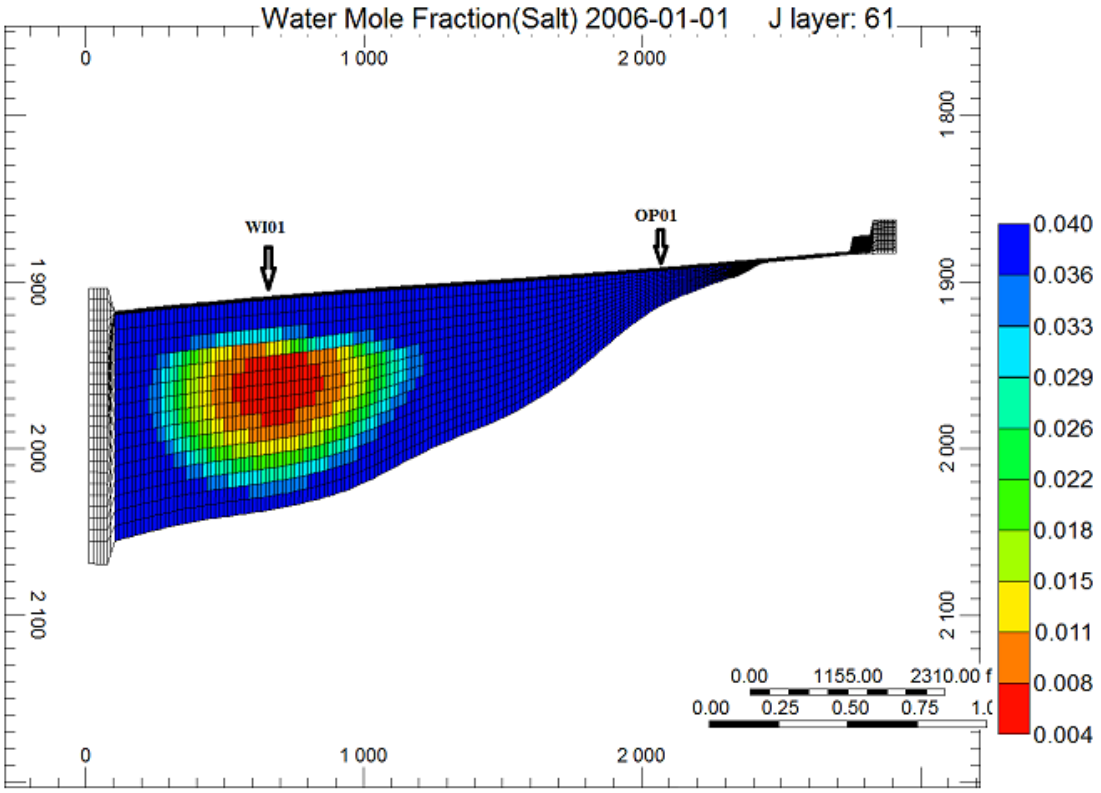

Figure 5.9: The water salinity distribution after 6 years (approximately ½ PV injected). The injector (WI01) and producer (OP01) are marked.

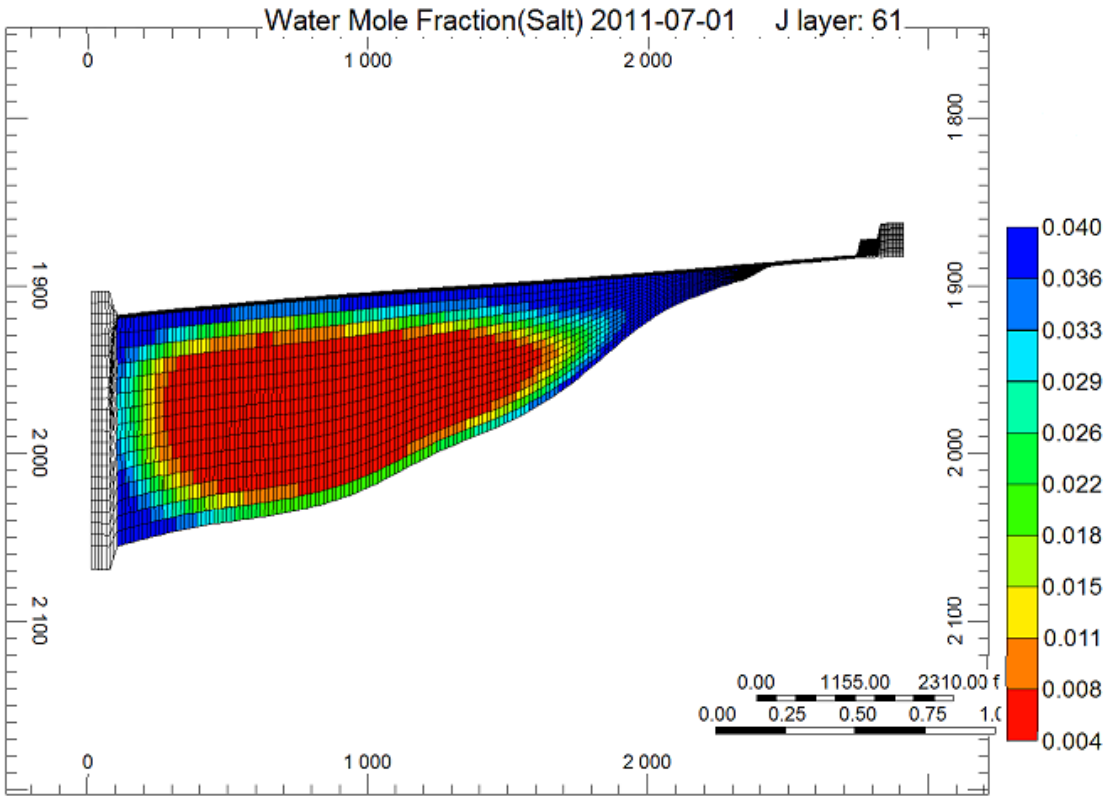

Figure 5.10: The water salinity distribution after 11.5 years (approximately 1 PV injected).

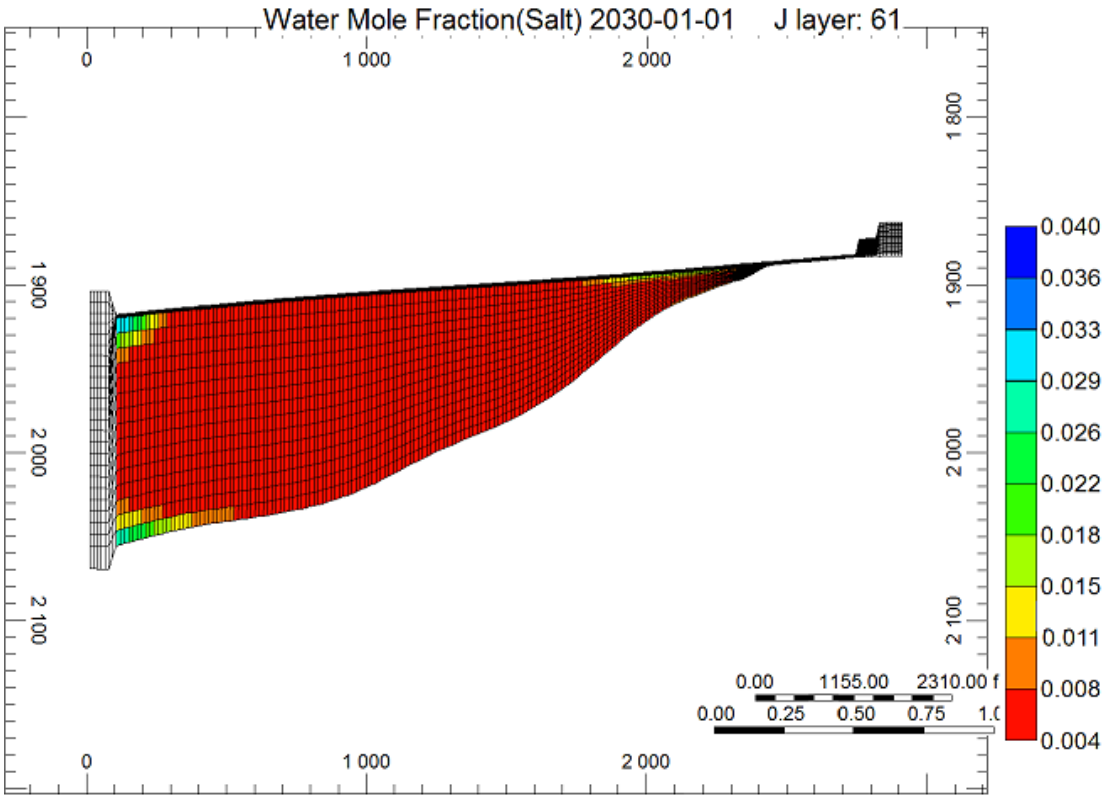

Figure 5.11: The water salinity distribution at the final stage of low salinity water injection.

5.2.6 Residual Oil Comparison

Figure 5.12 visualizes the residual oil saturation after the high salinity waterflooding and low salinity waterflooding. Even though the low salinity waterflooding process leaves zones of residual oil, the residual oil saturation is much larger after the conventional seawater flooding. A large portion of the residual oil after the low salinity injection may be mobilized if the flooding process is prolonged, since the cumulative oil recovery curve is still slightly increasing at production termination. However, it is not likely to extract the same amount of trapped hydrocarbons from prolonging the high salinity waterflooding process. The rate of oil production for the base case was considerably lower after the 30 years, and the reservoir was mainly producing water. The residual oil left behind is a target for EOR.

If the distribution of residual oil after the low salinity waterflooding in figure 5.12 is compared to the salinity concentration distribution from figure 5.11, it may be observed a correspondence. By year 30, the upper and lower leftmost corners of the reservoir model have not yet reached the minimum salinity concentration of 4000 ppm, although the majority of the reservoir obtains that concentration. The low salinity waterflooding process does not properly sweep the corners.

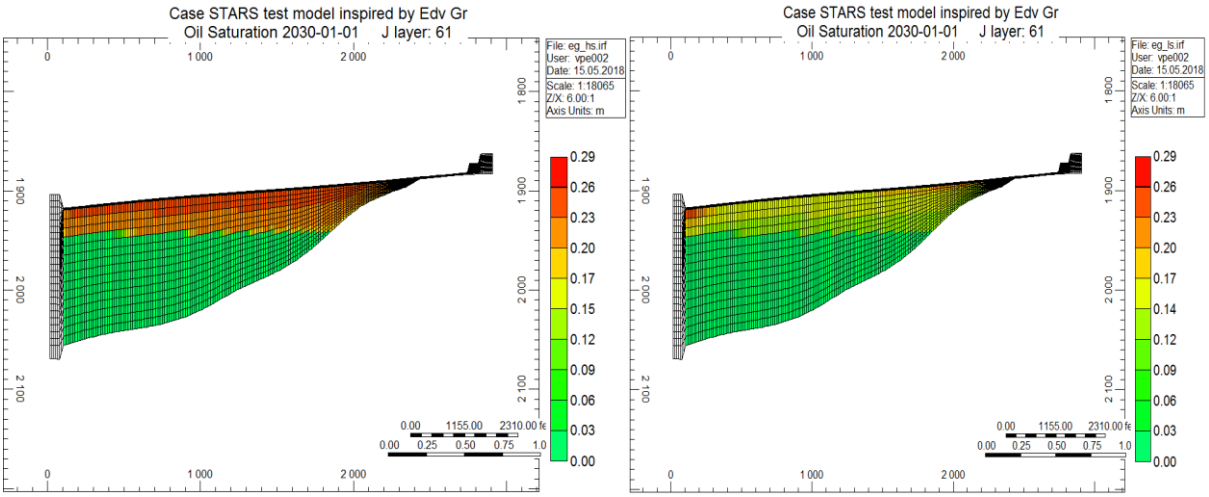

Figure 5.12: Residual oil after high salinity waterflooding (left) and low salinity waterflooding (right).

5.2.7 Summary

The continuous low salinity waterflooding process yields a higher oil recovery than the high salinity waterflooding process under the same initial and production conditions in a secondary mode (S_{wi}). By the end of the production time, an incremental $1.3 \cdot 10^6$ m^3 additional oil has been produced, and the oil recovery is increased to 66.20% from 61.25% in the reference case. The water cut is also significantly reduced, and it requires approximately 8 years longer for the low salinity water case to reach a water cut of 95%, which often represents an economical production limit. Furthermore, the oil production rate is 279% higher for the low salinity water case on the last production date. The bottom-hole pressure increases once 1 PV of low salinity water has been injected, but declines faster than the base case pressure towards the end of production.

Although researchers have not yet come to a consensus regarding the mechanisms behind incremental oil recovery by low salinity waterflooding, the main theory regards the wettability alteration towards a more water-wet state [13]. Water-wetness is in general interlinked with better flooding performance due to the distribution and flow of reservoir fluids. The risk of viscous fingering and other front instabilities are greatly reduced when the reservoir rock shifts towards a more water-wet state, and the low salinity injection water is diverted into oil zones that may be bypassed by the high salinity water. Consequently, the macroscopic sweep is enhanced [40].

The lower endpoint water cut for the low salinity waterflooding process signifies the wettability change towards water-wetness. The low salinity water is directed into a broader specter of the reservoir. Thus, it requires more time for the injection water to reach the producer. The improved macroscopic sweep is also exemplified through the improved cumulative oil recovery and the higher oil production rate at the last day of production.

Moreover, clay swelling and the migration of fines may release trapped oil, which can lead to an enhanced microscopic sweep. These phenomena can lead to a pressure buildup within the rock. After 1 PV of low salinity water is injected, a pressure increase is observed (figure 5.4). Several published papers confirm an increased pressure due to the injection of diluted brine [69, 71, 96, 97]. This pressure increase is attributed to clay swelling, the mobilization, migration and pore throat blocking by fines, and the flux diversion into nonswept zones. Subsequent to the initial pressure buildup, the pressure decreases at a faster rate than the pressure decline during the reference case for high salinity waterflooding. Since the oil saturation will be less in the low salinity waterflooding case, the water relative permeability will increase, which can reduce the field pressure.

A study of the distribution of residual oil in the reservoir after the two different flooding processes, demonstrate that the grids with the highest residual oil saturation are the same grids that has not reached the minimum salt concentration of 4000 ppm after the low salinity flooding process, indicating a poor sweep by the low salinity water in the corners of the reservoir model.

5.3 Timing of Low Salinity Water Injection

To introduce low salinity brine as an injection fluid already in a secondary mode, may cause the project economics to rise to undesirable heights, with an emphasis on equipment and operational costs. Hence, it proves more reasonable to implement low salinity waterflooding in a tertiary recovery phase.

This part focuses on the interval sizes of regular high salinity waterflooding and low salinity waterflooding. The reservoir is first flooded with seawater for three varying time intervals, and thenceforward flooded with low salinity water until year 50. These trials are regarded as case studies 1, 2 and 3. In the first trial, 1 PV of high salinity water will be injected, followed by low salinity water throughout the rest of the production stage. In the following trial, 1 ½ PV of seawater will be flooded through the reservoir prior to the commencement of low salinity waterflooding. In the last trial, 2 PV of high salinity water will be injected first, before the low salinity water is introduced.

Table 5.3 displays the production results for the three different HS-LS case studies.

Table 5.3: Production results for the tree different HS-LS studies.

Case Study	**Year of LS -Start**	**Oil Produced (m^3)**	**Oil Recovery (%OOIP)**	**Water Cut (%)**	**Oil Rate (m^3/day)**	**Bottom-Hole Pressure (kPa)**
(1) 1 PV HS	2011	$1.78 \cdot 10^7$	70.58	98.48	113.91	20 790.7
(2) 1 ½ PV HS	2017	$1.76 \cdot 10^7$	67.48	97.96	152.23	20 799.4
(3) 2 PV HS	2023	$1.70 \cdot 10^7$	65.19	96.82	237.48	21 268.2

A general observation regarding the onset of low salinity waterflooding, is that the earlier the diluted water is introduced, the higher cumulative oil recovery is achieved. Additionally, the water cut and oil rate are lower – indicating that the oil volumes in place are produced at a shorter time range, and less injection water is required. Moreover, the bottom-hole pressure increases for a shortened tertiary phase.

5.3.1 Results for Case Study 1

In the first trial, 1 PV of seawater is flooded through the reservoir prior to the commencement of low salinity water injection. The low salinity brine is thenceforth injected from the middle of year 11 throughout the remainder of years until production end. The injection scheme is described in table 5.4, and the simulation results can be observed in figures 5.13 and 5.14:

Table 5.4: Injection scheme for the EOR-process with corresponding concentrations and slug sizes.

Injection Fluid	**Concentration (ppm)**	**Slug Size (years)**
High Salinity Water (HS)	40 000	11.5
Low Salinity Water (LS)	4000	38.5

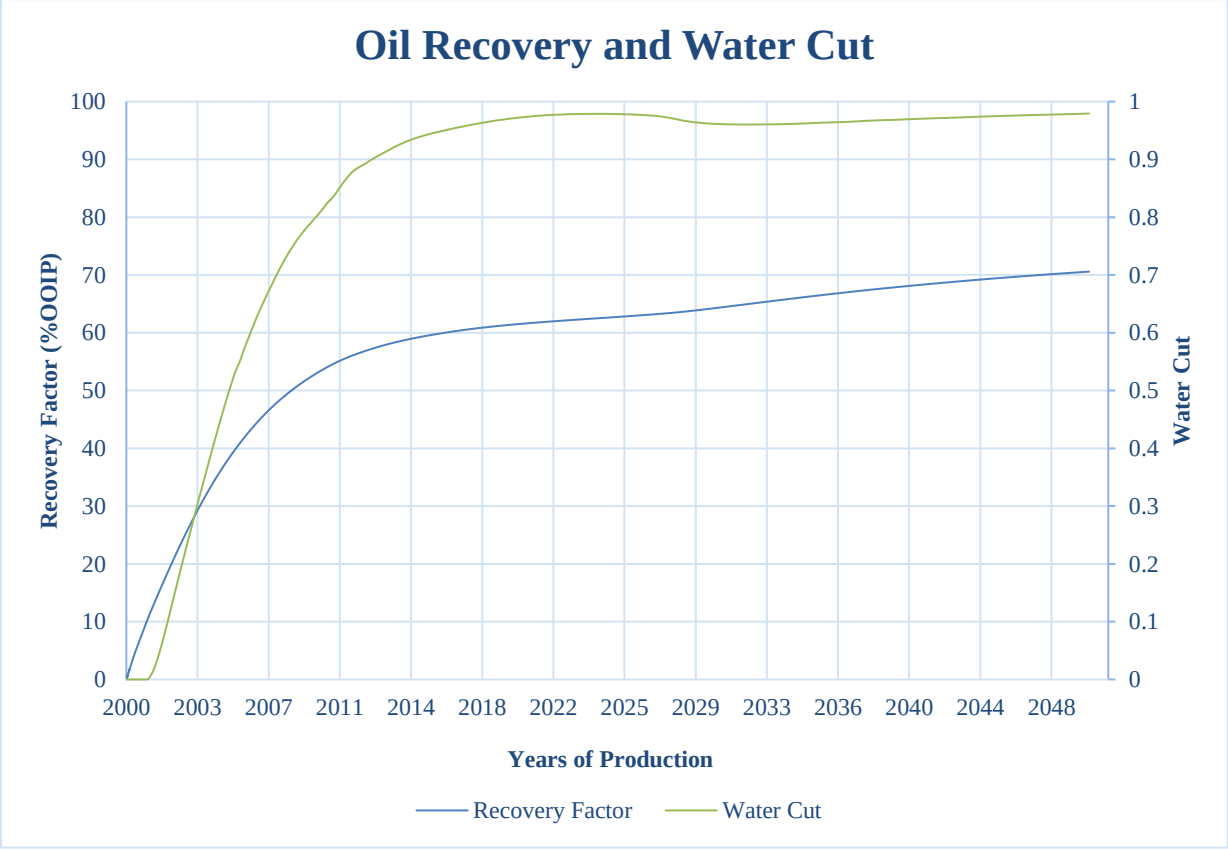

Figure 5.13: Cumulative oil recovery and water cut for case study 1.

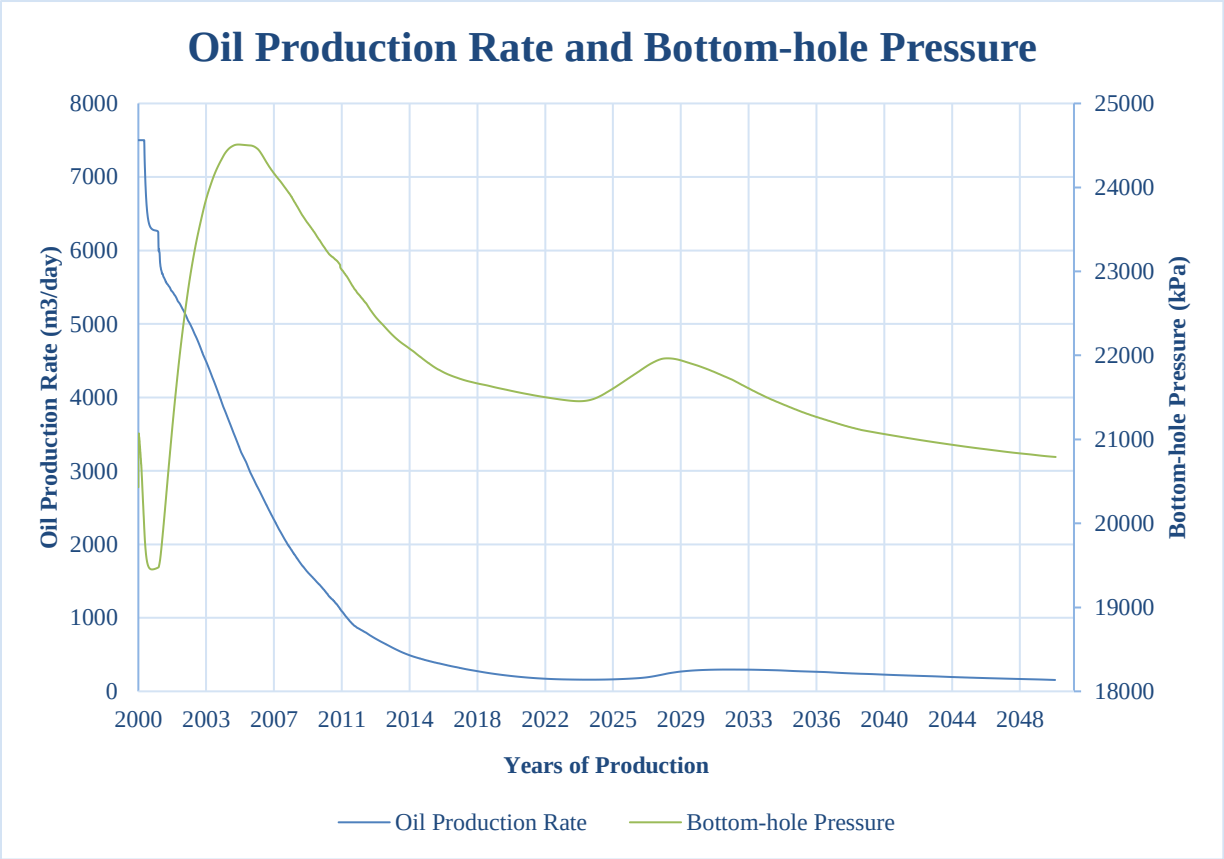

Figure 5.14: Oil production rate and bottom-hole pressure for case study 1.

The low salinity effect is visible in year 23, after 1 PV of low salinity water has been injected. At this time, it is observed a sudden decrease in water cut and increase in oil production rate. Moreover, the slope of the cumulative oil production curve is also steadily increasing around the same period, and the pressure increases.

The total cumulative oil produced at the finalization of production time is $1.78 \cdot 10^7$ m^3, corresponding to a recovery factor of 70.58%. The oil production curve is still increasing in year 2050, but the rate at which the oil is produced is reducing, levelling at 113.91 m^3/day on the last production date. The water cut has been continuously increasing towards the end of the production time, and ultimately reaches 98.48%. The bottom-hole pressure increases by 2.37% due to the low salinity effect, and gradually sinks towards the end of production time where it eventually reaches 20 790.7 kPa.

5.3.2 Results for Case Study 2

The next study case examines the production results when 1 ½ PV of seawater is injected into the reservoir prior to the onset of low salinity waterflooding. The reservoir is flooded with high salinity brine for 17.25 years, before low salinity water is injected for the following years. Table 5.5 summarizes the injection scheme, and the results are visualized in figures 5.15 and 5.16:

Table 5.5: Injection scheme for the EOR-process with corresponding concentrations and slug sizes.

Injection Fluid	**Concentration (ppm)**	**Slug Size (years)**
High Salinity Water (HS)	40 000	17.25
Low Salinity Water (LS)	4000	32.75

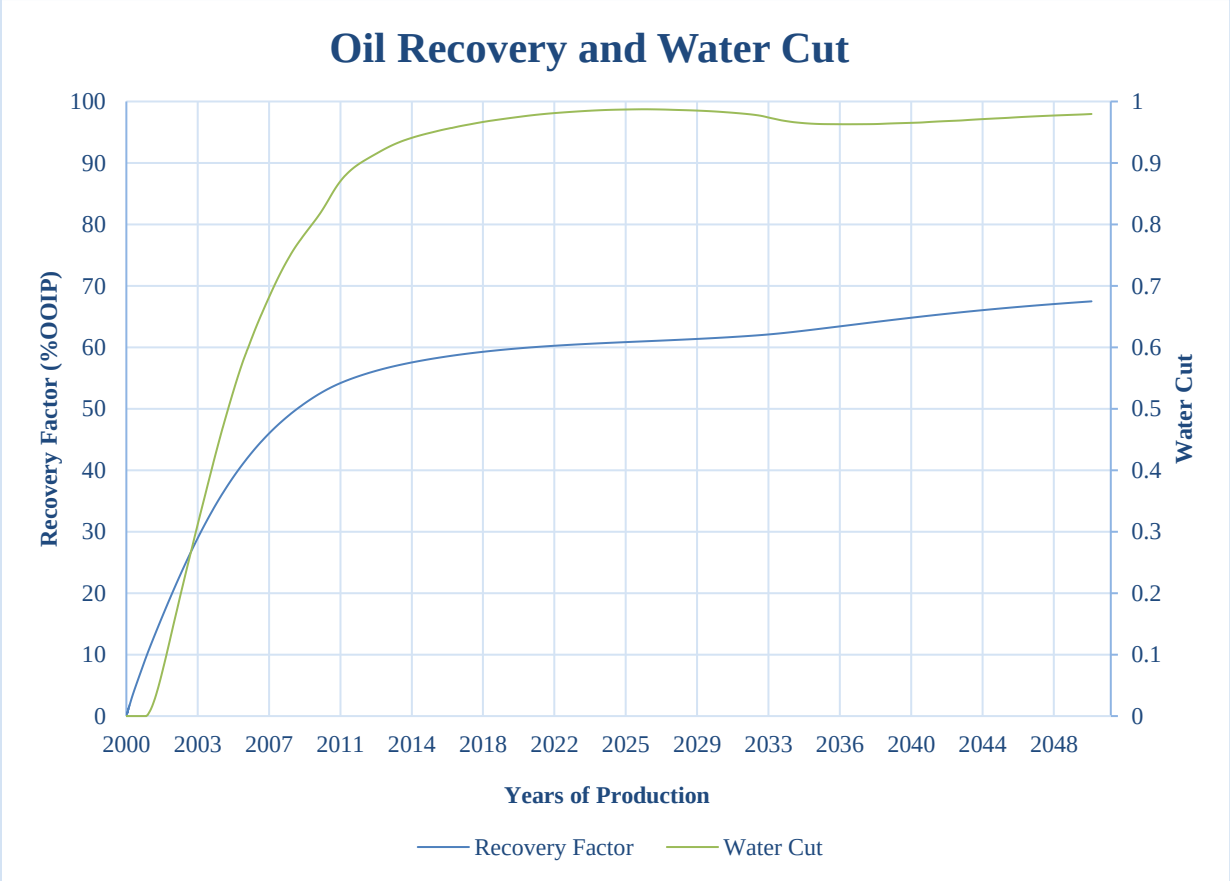

Figure 5.15: Cumulative oil recovery and water cut for case study 2.

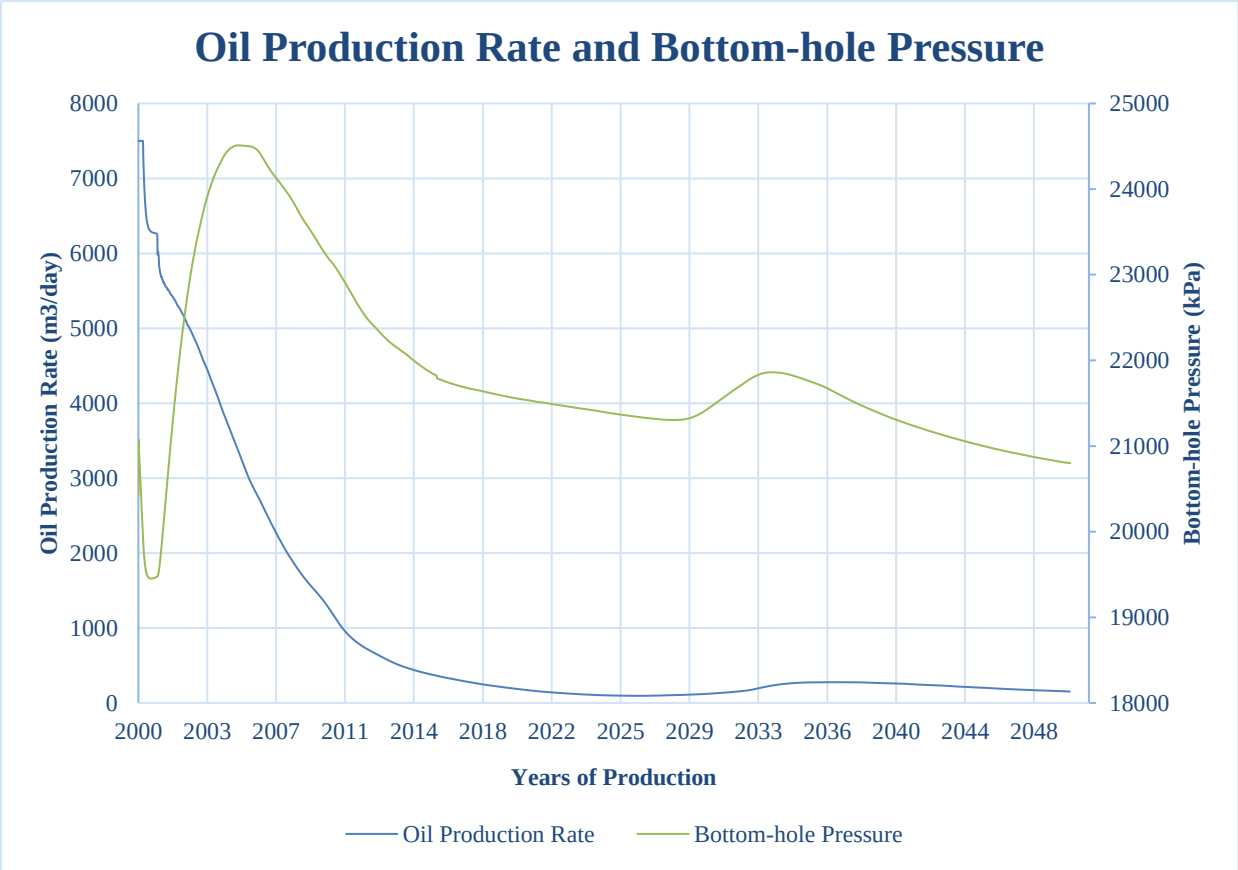

Figure 5.16: Oil production rate and bottom-hole pressure for case study 2.

At the end of the production period, $1.76 \cdot 10^7$ m^3 oil is recovered, corresponding to an oil recovery of 67.48%. The water cut levels at 97.96%, and the oil production rate ceases at 152.23 m^3/day. In year 2028, after 1 PV of low salinity water is injected, the effects of the diluted water are portrayed through an increased rate of oil recovery and reduced water cut. Additionally, the field pressure increases by 2.60% and reaches a local maximum when 1 PV of low salinity water has been injected. Thereafter, it declines and ends up at 20 799.4 kPa at the end of production time.

5.3.3 Results for Case Study 3

The last trial investigates the production results when 2 PV of seawater is injected primarily, followed by a low salinity waterflood throughout the remaining production time. High salinity water is injected first continuously for 23 years, chased by 27 years of low salinity injection water. The injection scheme is shown in table 5.6, and the production results are displayed in figures 5.17 and 5.18:

Table 5.6: Injection scheme for the EOR-process with corresponding concentrations and slug sizes.

Injection Fluid	**Concentration (ppm)**	**Slug Size (years)**
High Salinity Water (HS)	40 000	23
Low Salinity Water (LS)	4000	27

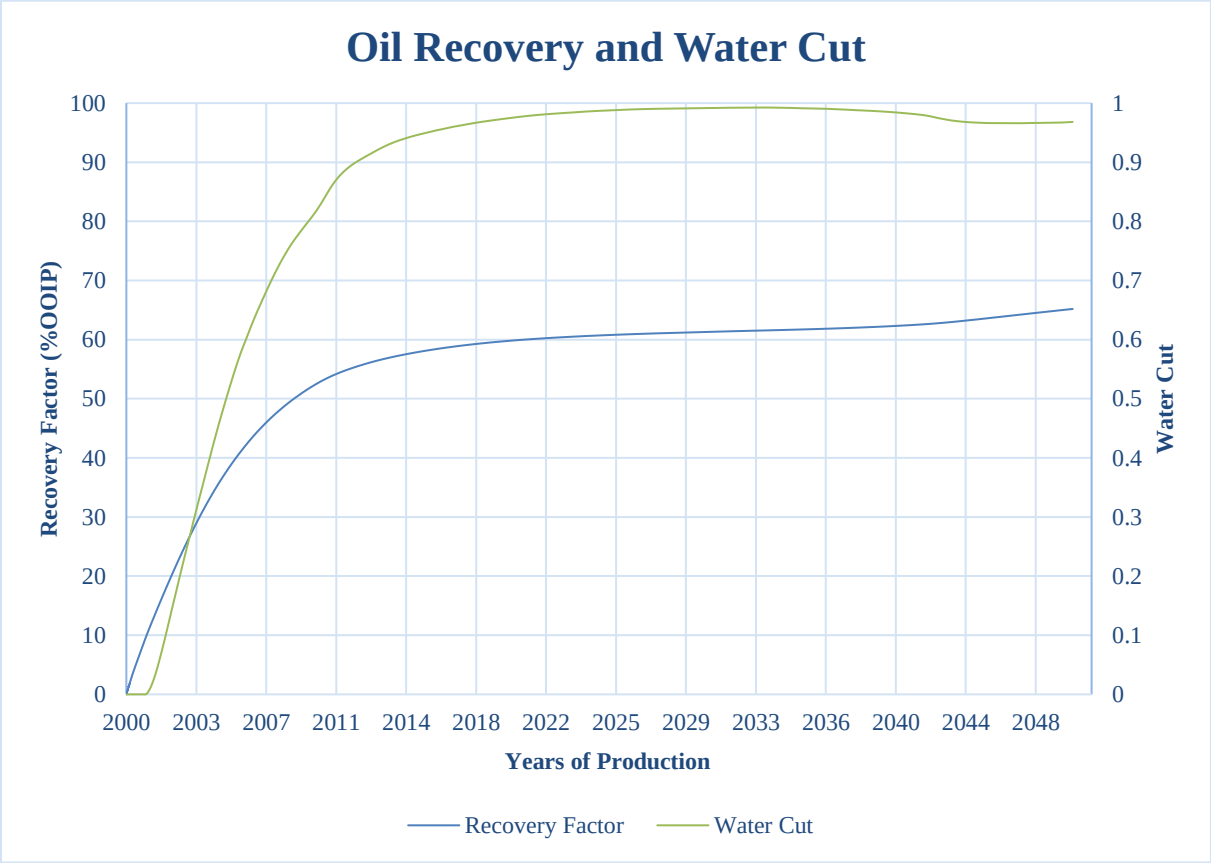

Figure 5.17: Cumulative oil recovery and water cut for case study 3.

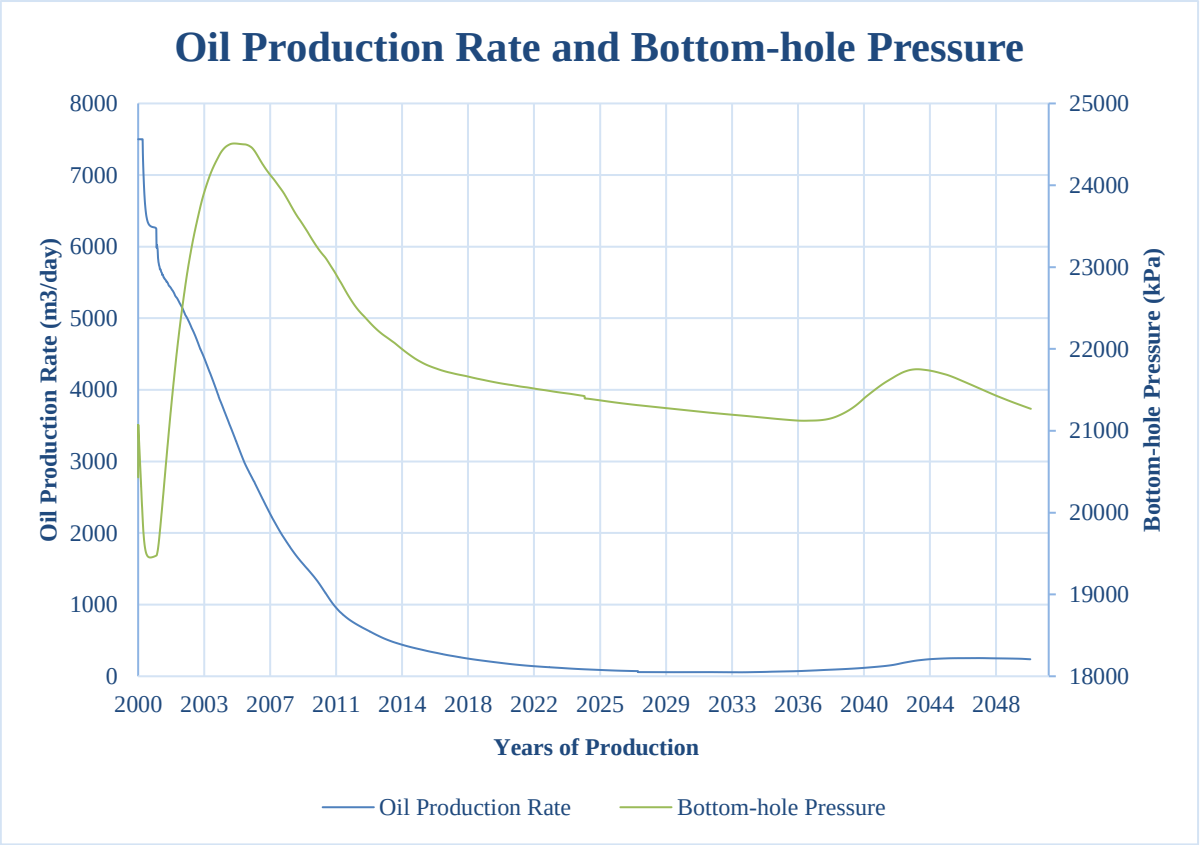

Figure 5.18: Oil production rate and bottom-hole pressure for case study 3.

At the termination of production, a total of $1.70 \cdot 10^7$ m^3 cumulative oil is produced, indicating an oil recovery of 65.19%. At the same time, the water cut has reached 96.82%, and the oil production rate has levelled at 237.48 m^3/day. The low salinity effect becomes visible around year 2034, when approximately 1 PV of low salinity water is injected. From this point forward, the slope of the cumulative oil production curve steepens, indicating an enhanced sweep by the diluted water. Moreover, the oil production rate increases simultaneously as the water cut decreases, before both stabilizes approximately 11.5 years later. The pressure declines until 1 PV of low salinity water has been injected. Thereafter, it builds up by 2.98% before commencing another decline. At the end of the production, the pressure has sunk to 21 268.2 kPa.

5.3.4 Oil Recovery Comparison

Figure 5.19 illustrates the cumulative oil recovery for the three trials. It may be deducted that the case study 1 displays the earliest effect of the diluted water, end ends up with the highest total oil recovery. Thereafter follows case study 2, and lastly case study 3.

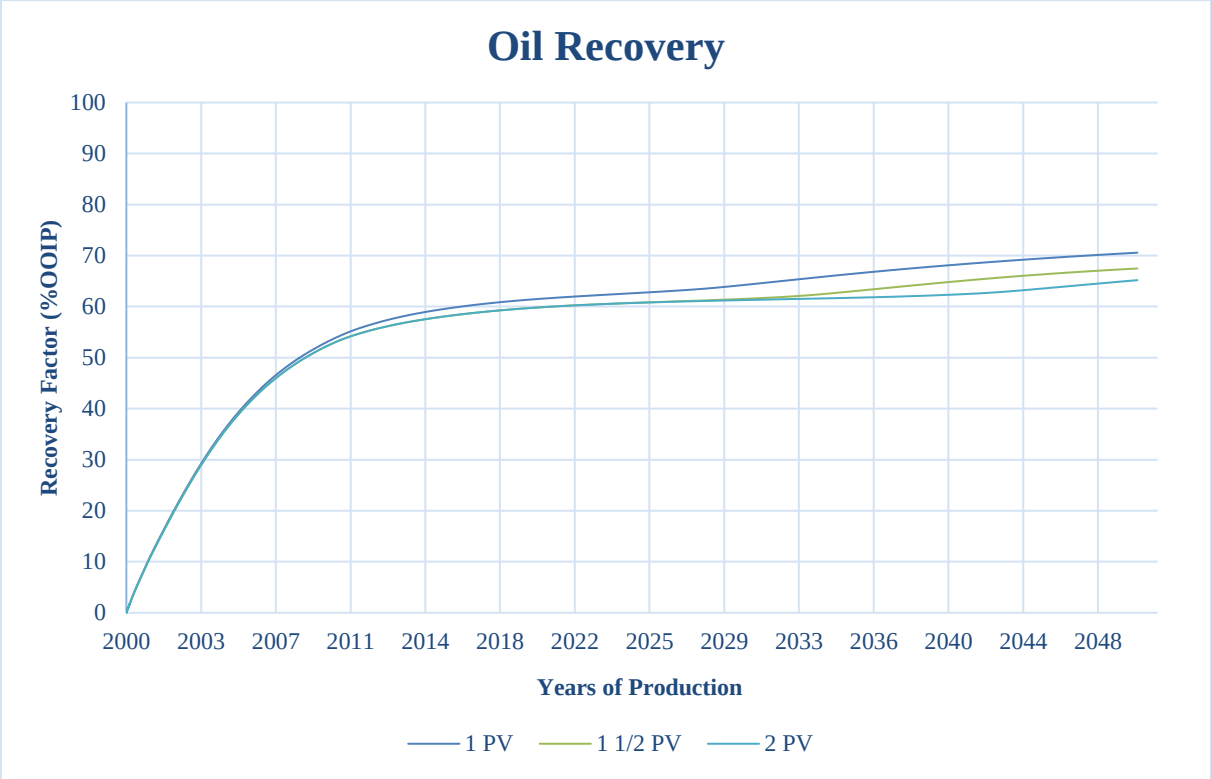

Figure 5.19: Comparison of cumulative oil recovery for case studies 1 (1 PV), 2 (1 ½ PV) and 3 (2 PV).

The oil recovery of the three different trials is dependent on the length of continuous low salinity waterflooding, and total oil production is proportional to the interval size of the low salinity waterflooding period. Wettability alteration is assumed the major reason behind these observations [13]. In the first case, the low salinity water is granted more time to interact with the formation and reservoir fluids. Therefore, it has more prerequisites in terms of enhancing the sweep, which ultimately leads to a higher oil recovery. It takes approximately 11.5 years to inject one pore volume. Thus, the same amount of time may be required to observe the effects of the injection fluids.

5.3.5 Water Cut Comparison

Figure 5.20 illustrates the water cut for the three different trials. It may be observed an offset in water cut behavior for the three studies, dependent on the timing of low salinity water injection. The endpoint water cut decreases for shorter flooding periods of low salinity water.

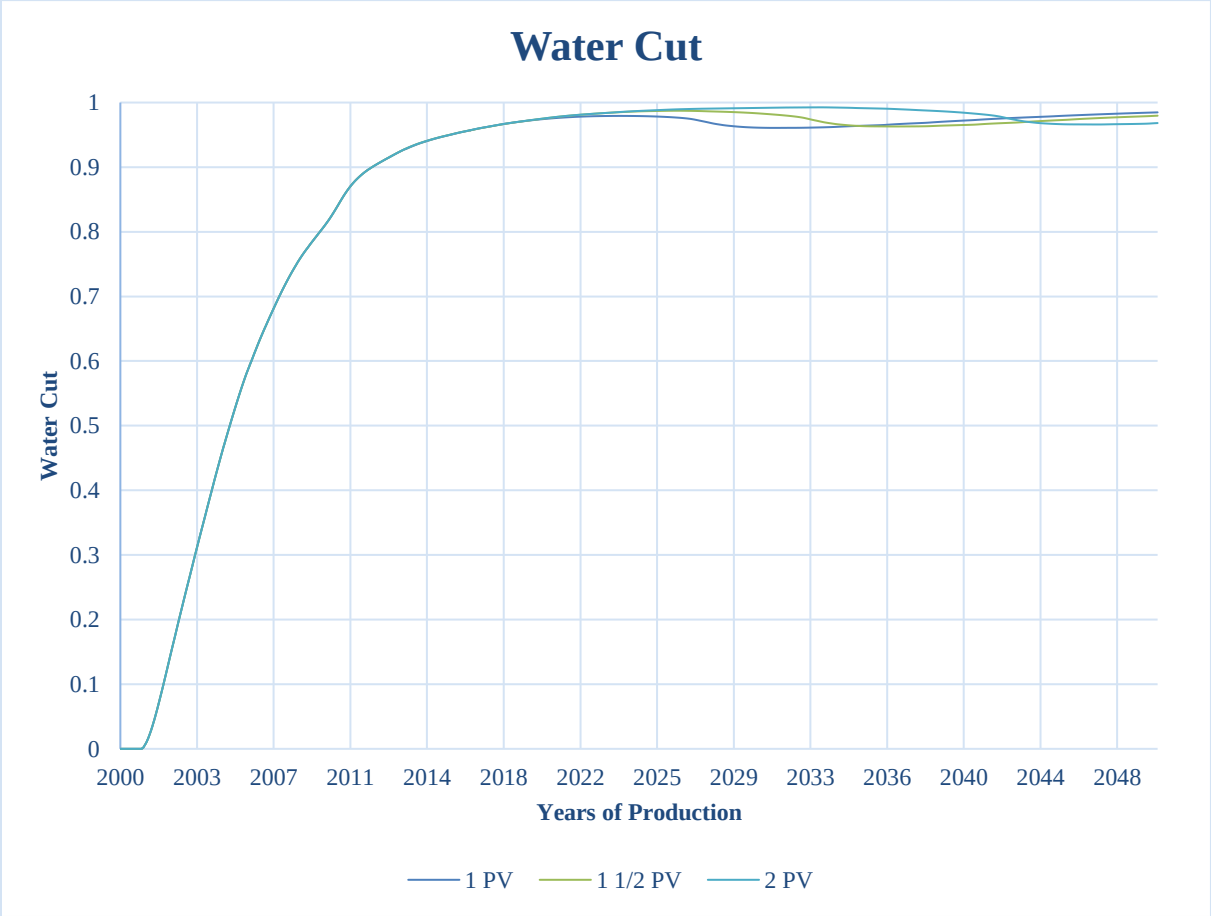

Figure 5.20: Comparison of water cut for case studies 1 (1 PV), 2 (1 ½ PV) and 3 (2 PV).

After 1 PV of low salinity water has been injected, the water cut drops due to mobilization of oil. The first case has the highest endpoint water cut of the three different cases. The enhanced macroscopic sweep improves oil banking and reduces the length of oil-tail production. In year 2050, the water-cut will therefore be higher for case study 1 considering that most of the oil has already been produced at this time. The water cut is lower for the latter trials due to a prolonged tail production of oil, and the field will continue to inject and produce water for a longer period in order to attain the same total oil recovery as case study 1.

5.3.6 Oil Production Rate Comparison

The production rate of oil in the final year of production is highest for case study 3 and lowest for case study 1, while case study 2 holds the intermediate oil rate. The oil production rate is in harmony with the water cut, as a high water cut is interlinked with low oil production rates. The three different studies are illustrated in figure 5.21.

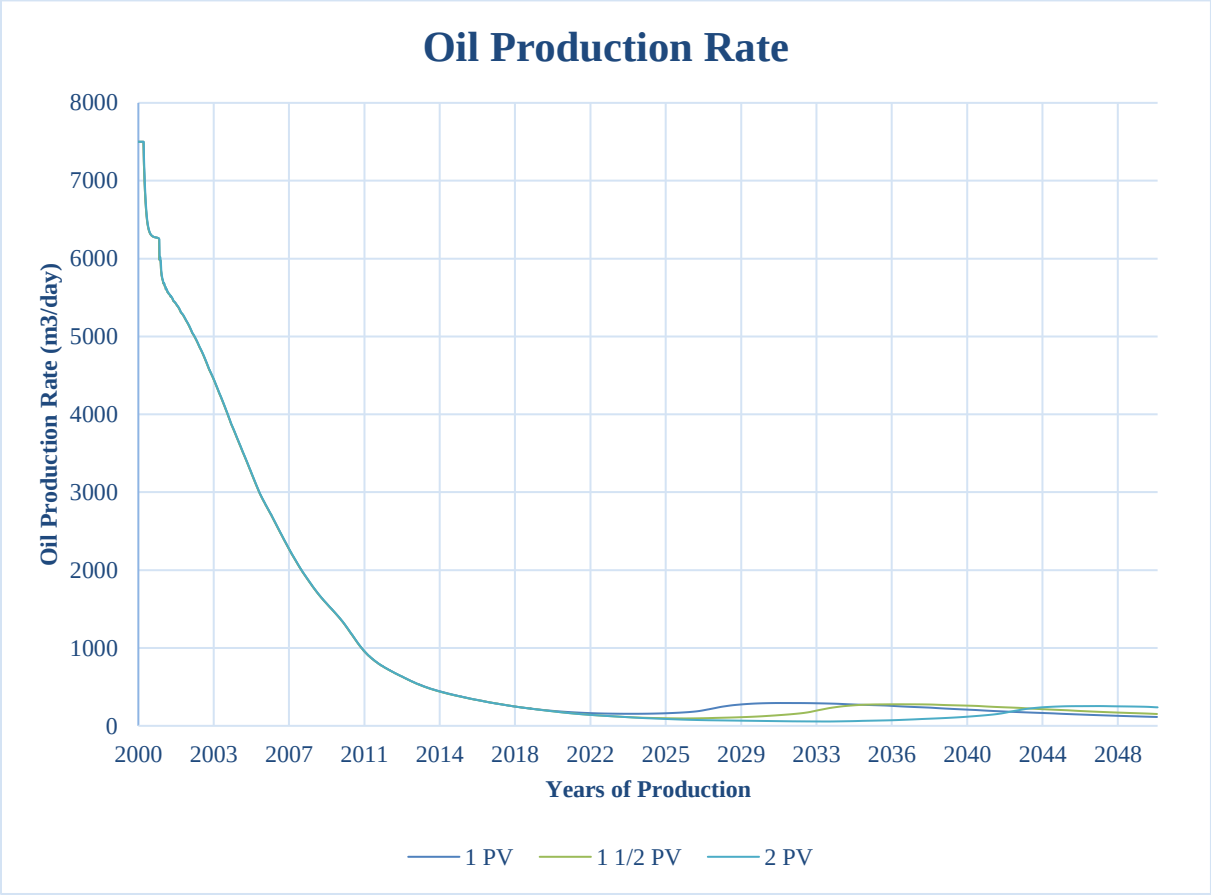

Figure 5.21: Comparison of the oil production rate for case studies 1 (1 PV), 2 (1 ½ PV) and 3 (2 PV).

The enhanced macroscopic sweep by low salinity water ensures that less volumes of injection water is necessitated in case study 1 to produce an equal volume of oil. This is also reflected in the total cumulative oil recovery and water cut. Case studies 2 and 3 will continue to produce oil at higher rates for a longer period, but large volumes of water will also be produced.

5.3.7 Bottom-hole Pressure Comparison

The comparison of the reservoir pressure for the three different studies is presented in figure 5.22. The low salinity effect that causes an increase in the bottom-hole pressure is delayed with an offset dependent on the start of low salinity water injection. The pressure buildup is due to clay swelling, pore blockage by fines, diversion of injection water into uncontacted zones and a reduced water relative permeability [71, 96, 97]. At the end of the production time, the pressure is the least for case study 1, and increases with the length of the secondary phase. This pressure behavior may be explained by the lower oil saturation for the prolonged tertiary phase, which enhances flow properties of water and consequently reduces field pressure.

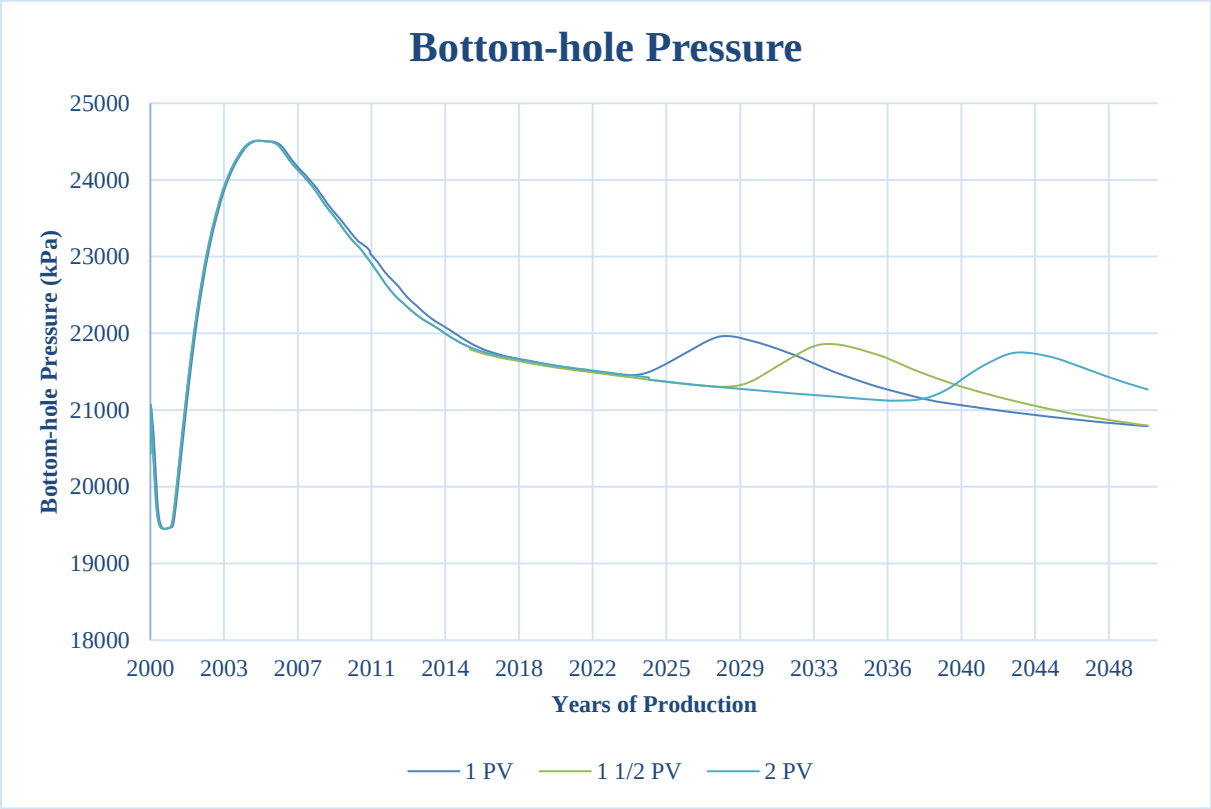

Figure 5.22: Comparison of the bottom-hole pressure for case studies 1 (1 PV), 2 (1 ½ PV) and 3 (2 PV).

5.3.8 Discussion and Summary

In terms of cumulative oil recovery, it proves more beneficial to have a short secondary phase of seawater flooding and long tertiary phase of low salinity waterflooding. The total cumulative oil recovery in case study 1 is 70.58%; 1.33% higher than case study 2 and 4.89% higher than case study 3. The low salinity slug yields similar effects in all trials, only that the effects have an offset dependent on the onset of low salinity water injection. The latter cases will continue to produce oil at higher rates for a longer time, but the oil will be produced at a very high water cut, which will ultimately affect project economics.

The pressure buildup after 1 PV of low salinity water has been injected is likely due to a water permeability reduction induced by ionic interactions between the diluted injection water and COBR-system. The change towards a more water-wet state reduces the water relative permeability, which can increase the reservoir pressure. Previous studies validate an increase in pressure, and place the responsibility on release of fines blocking pore throats [71]. The swelling of clays and water flux into unswept zones may also obtain significant roles in the pressure buildup [97].

The results from the three trials are in correspondence with theory, as case study 1 yields the best production results. The low salinity water is injected earlier, and has more time to interact with the reservoir rock and its saturating fluids. When injected into a highly saline environment, the low salinity water disrupts the chemical equilibrium within the reservoir, and the ionic exchanges between the diluted water and COBR-system eventually lead to an increase in the degree of water-wetness, and release of trapped oil [11, 96].

According to studies conducted by Shiran et al. (2013), the introduction of low salinity water at an earlier stage is more effectively able to mobilize oil, considering that the waterflood may approach a continuous oil phase and prevent further trapping. When the low salinity water is injected at a later stage, it may encounter oil that is already trapped and burdensome to mobilize [5]. The latter trials will have a longer tail-production of oil, which will require more injection water to mobilize [40].

Despite the additional oil produced in case study 1, the implementation of low salinity water injection at an early stage presents major expenses. The first trial clearly yields the most optimal production results, but the costs of the elongated low salinity waterflood may not exceed the additional profits. Therefore, a thorough evaluation with regards to the additional oil produced by the case study 1 versus the costs of injecting low salinity water for a longer time period, is required. Case study 2 is not far behind on oil recovery, producing 1.33% less oil than case study 1. It is possible that this strategy is a decent alternative considering that it necessitates 6.25 less years of low salinity water injection.

5.4 Full Surfactant Potential

The aim of surfactant flooding is to reduce residual oil by lowering the interfacial tension between the displaced and displacing phases, and ultimately release capillary trapped oil [57].

In order to test if surfactant flooding is effective in this reservoir model, an "extreme process" is simulated. It is assumed that the surfactant chemicals reach their full potential in terms of lowering the interfacial tension; giving rise to straight relative permeability curves and a residual oil saturation, S_{or}, of 0. Additionally, no adsorption of surfactants onto rock is assumed in this trial. The surfactants are injected without a pre-established low salinity environment.

5.4.1 Injection Scheme

The injection scheme is displayed in table 5.7. The surfactants accompanied with low salinity water were injected in year 15 after a water cut of 95% was established after the initial high salinity waterflooding process. Thereafter, the EOR-chemicals were injected continuously for 65 years.

Table 5.7: Injection scheme for the EOR-process with corresponding concentrations and slug sizes.

Injection Fluid	**Concentration (ppm)**	**Slug Size (years)**
High Salinity Water (HS)	40 000	15
Surfactants (LSS)	5000	65

5.4.2 Results

Figures 5.23 and 5.24 illustrate the production results from the continuous surfactant flooding, visualizing the full oil recovery potential by an increased microscopic sweep. At the end of the production in year 2080, $2.19 \cdot 10^7$ m^3 oil is produced, corresponding to a recovery of 83.36% of the oil originally in place (OOIP).

The surfactant effects are visible in year 2026, after 1 PV of surfactants is injected. However, after approximately two additional pore volumes of surfactants are injected, the oil production curve approaches a plateau. From this point forward, very little additional oil is produced.

Simultaneously as the oil production curve is levelling, the water cut approaches high values, and eventually ends up at 99.98%. In a corresponding manner, the oil production rate is also

very low towards the last simulation date, and finish as 1.60 m^3/day. Hence, the reservoir is producing almost entirely water.

The effects of the surfactants are also exemplified through the bottom-hole pressure, which increases after 1 PV of the tertiary fluid is injected. According to a study by Tavassoli et al. (2016), the increase in pressure after the starting of LSS may occur due to the two-phase flow of oil and water in front of the surfactant slug [86]. As deduced from figure 5.24, the pressure increase occurs simultaneously as the increase in the oil production rate, and can be a result of oil banking due to the LSS-fluid. A viscosity increase due to the formation of microemulsions at surfactant concentrations above CMC may also lead to a higher pressure [6, 93]. Subsequent to the initial pressure increase, a steep pressure decline is observed, and at the last date of production, the pressure is 19 293.2 kPa. The mobilization of oil by the surfactants effectively decreases the oil saturation within the reservoir, which increases the water relative permeability and consequently reduces the field pressure.

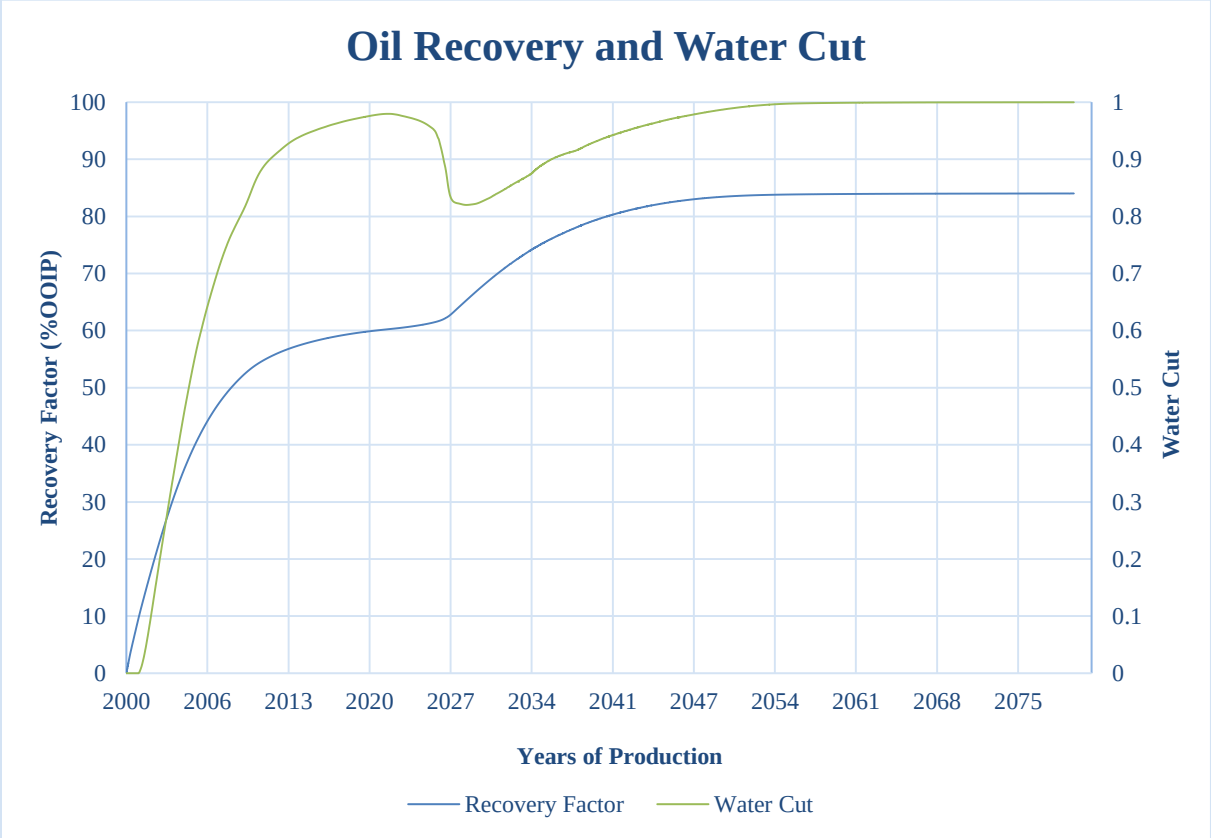

Figure 5.23: Cumulative oil recovery and water cut for the surfactant flooding process.

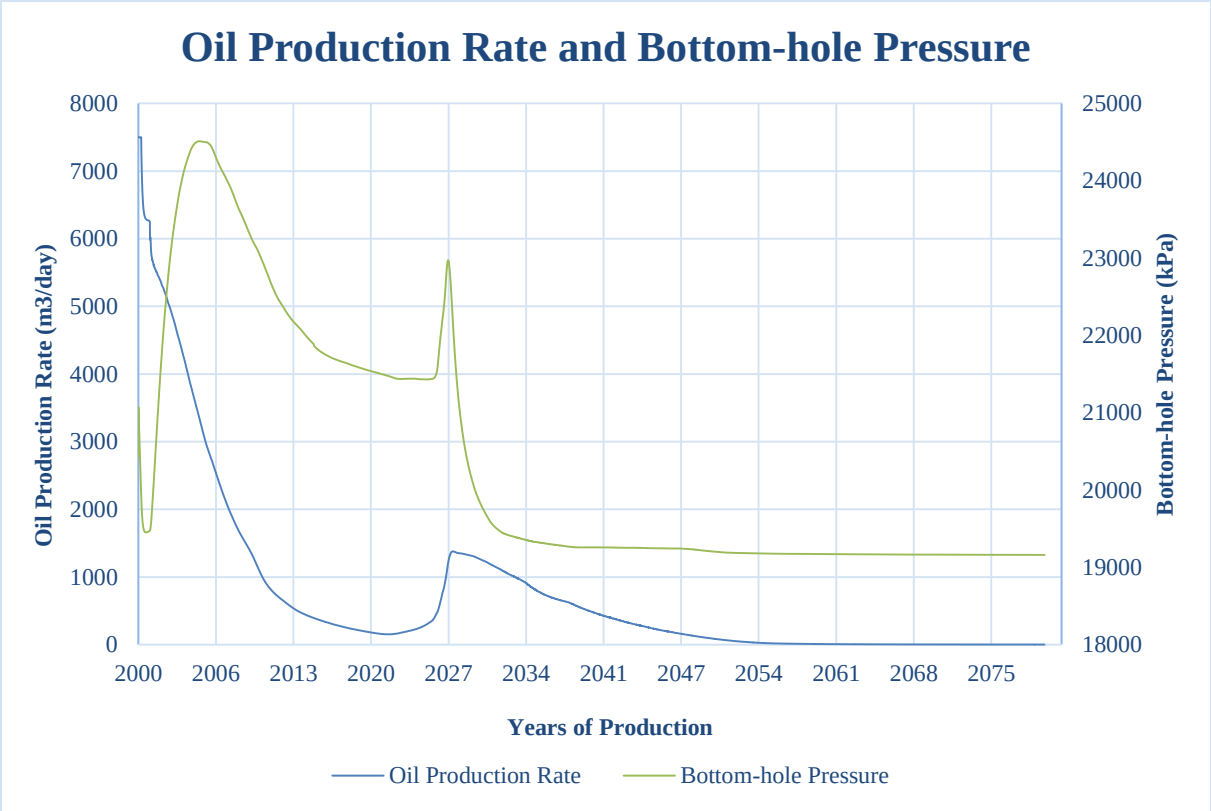

Figure 5.24: Oil production rate and bottom-hole pressure for the surfactant flooding process.

5.4.3 Discussion and Summary

The maximum oil recovery by the continuous surfactant flooding process is 83.36%, amounting to an oil volume of $2.19 \cdot 10^7$ m^3. At the end of the production time, the reservoir is mainly producing water, with a water cut of 99.98%, and an oil production rate of 1.60 m^3/day. Once the LSS-phase is injected, there is an initial pressure buildup. The pressure increase occurs simultaneously as the rise in oil production. The higher pressure may be caused by a two-phase oil and water flow in front of the surfactant slug [86]. Additionally, the formation of microemulsions due to surfactant mixing with the reservoir fluids can increase the viscosity of the surfactant flood, which can build up the reservoir pressure [6, 93].

The surfactant phase effectively reduces interfacial tension, which releases volumes of oil trapped by strong capillary forces. According to a previous laboratory study, a pre-flush of low salinity water could have enlarged the maximum oil recovery by surfactants further. The surfactants are sensitive to electrolytes in the brine, which make them vulnerable for destabilization and retention. Additionally, it is an increased probability of surfactant trapping in the oleic phase (Windsor type II behavior) at high salinities [14]. In addition, the wettability alternating effects of the low salinity water that leads to a higher macroscopic sweep could have distributed the surfactants into a larger part of the reservoir.

Nevertheless, this simulation study demonstrates that surfactants diluted in low salinity water are able to increase oil recovery without a preflush of low salinity water.

5.5 Full Polymer Potential

The purpose of polymer flooding is to increase the viscosity of the displacing injection water and reduce the mobility ratio between water and oil. If the implementation of polymer flooding is successful, it will establish a stable displacement front, and prevent viscous fingering and other front instabilities that lead to bypassing of oil zones. Ultimately, the oil production will be accelerated and the macroscopic sweep will be greatly enhanced [29].

This trial will examine the effects of polymers in this reservoir model when injected without a pre-established low salinity environment, and the ultimate recovery potential proposed by the viscosifying chemicals. No polymer adsorption onto rock is assumed, and the polymers will be injected continuously over a long period.

5.5.1 Injection Scheme

The injection scheme is described in table 5.8. In equivalence with the previous trial with surfactants, polymers will also be injected continuously after the secondary high salinity phase has reached a water cut of 95%. Conventional seawater is flooded through the reservoir for the first 15 years, before polymers are injected for the next upcoming 65 years.

Table 5.8: Injection scheme for the EOR-process with corresponding concentrations and slug sizes.

Injection Fluid	**Concentration (ppm)**	**Slug Size (years)**
High Salinity Water (HS)	40 000	15
Polymers (LSP)	350	65

5.5.2 Injection Rate Sensitivity

Due to an upper pressure limit of 42 500 kPa for the reservoir, a sensitivity study of the polymer injection rate is conducted. The polymer macromolecules viscosify the water, and thereby reduce the mobility of the water phase [29]. Ultimately, this can lead to a severe pressure buildup within the reservoir. The pressure increase induced by polymer flooding can be controlled by the injection rate, where high rates are interlinked with higher pressures. Hence, it may be necessary to reduce the injection rate to avoid an excessive pressure buildup, and to ensure that the pressure remains below 42 500 kPa throughout the entire production stage.

The previous simulations have an injection rate of 7500 m^3/day. In addition to a trial with this rate, two more simulations will be conducted with the reduced rates 5000 m^3/day and 3500 m^3/day, as summarized in table 5.9:

Table 5.9: Injection rate for the three case studies.

Case Study	**Injection Rate (m^3/day)**
1	7500
2	5000
3	3500

5.5.3 Results for Case Study 1

The production results from case study 1 are displayed in figures 5.25 and 5.26. The polymers are injected continuously for 65 years at an injection rate of 7500 m^3/day after an initial 15 years of seawater flooding. At the finalization of production, a total of $1.83 \cdot 10^7$ m^3 oil has been produced, corresponding to a cumulative oil recovery of 70.21%. The effects of the polymers become visible approximately two years before 1 PV is injected. The polymer phase propagates through the reservoir in a dissimilar manner than water due to differing flow properties, and will therefore obtain another velocity. In addition, the polymer macromolecules may be larger than constrictions and pore throats within the porous media, and can accelerate through the reservoir at a faster rate than assumed on the basis of pore volume, in accordance with the inaccessible pore volume theory [36, 62].

After the oil production rate peaks in year 2037, the water production accelerates, exemplified through the increasing water cut and lower oil production rate. In year 2080, the reservoir is producing 99.68% water, and the oil rate has sunk to 13.28 m^3/day.

The reservoir experiences a severe pressure buildup. The pressure increases immediately after injection by 1.43%. Thereafter it increases exponentially, and after 20 years, the upper pressure limit has been reached. The simulator adjusts the water injection rate when the pressure limit is exceeded, as depicted from figure 5.26, and the pressure remains at the upper limit of 42 500 kPa throughout the entire production stage. In conclusion, the injection rate of 7500 m^3/day is too high for the continuous polymer flooding process.

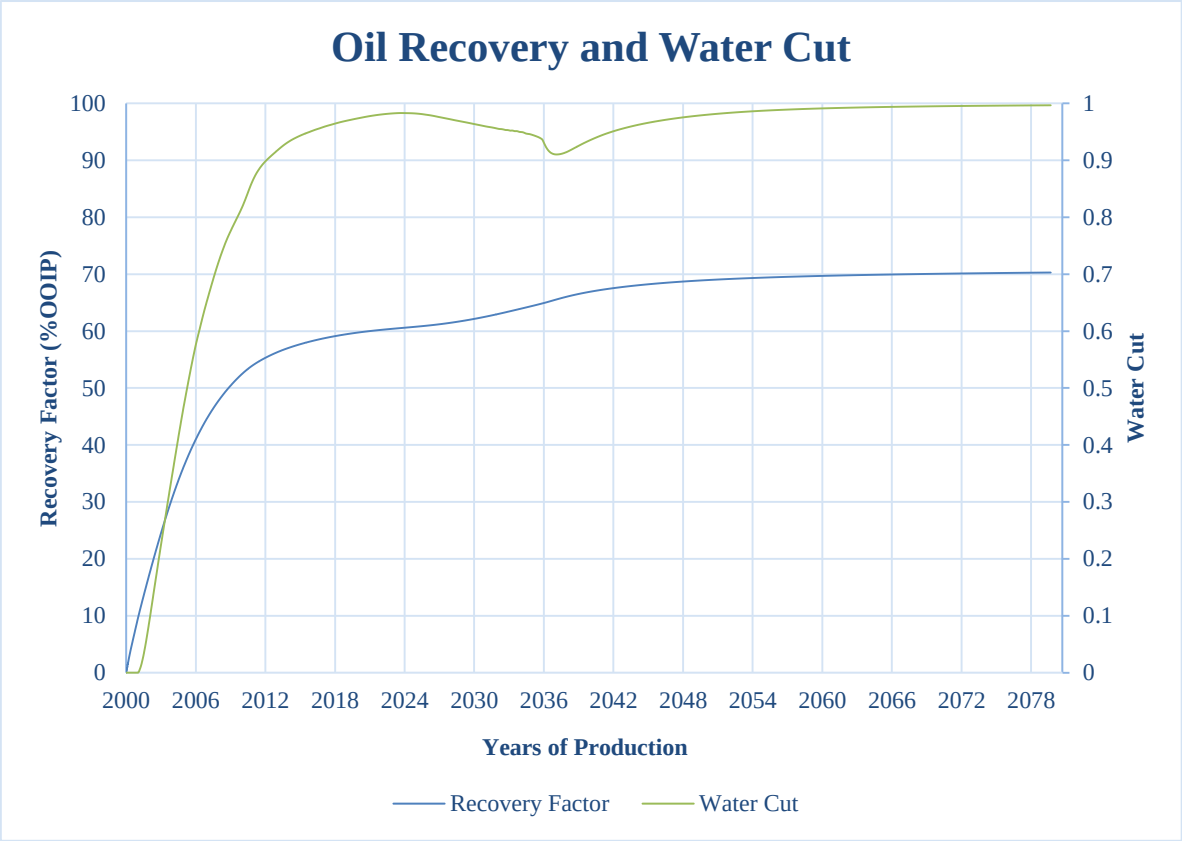

Figure 5.25: Cumulative oil recovery and water cut for the polymer flooding process.

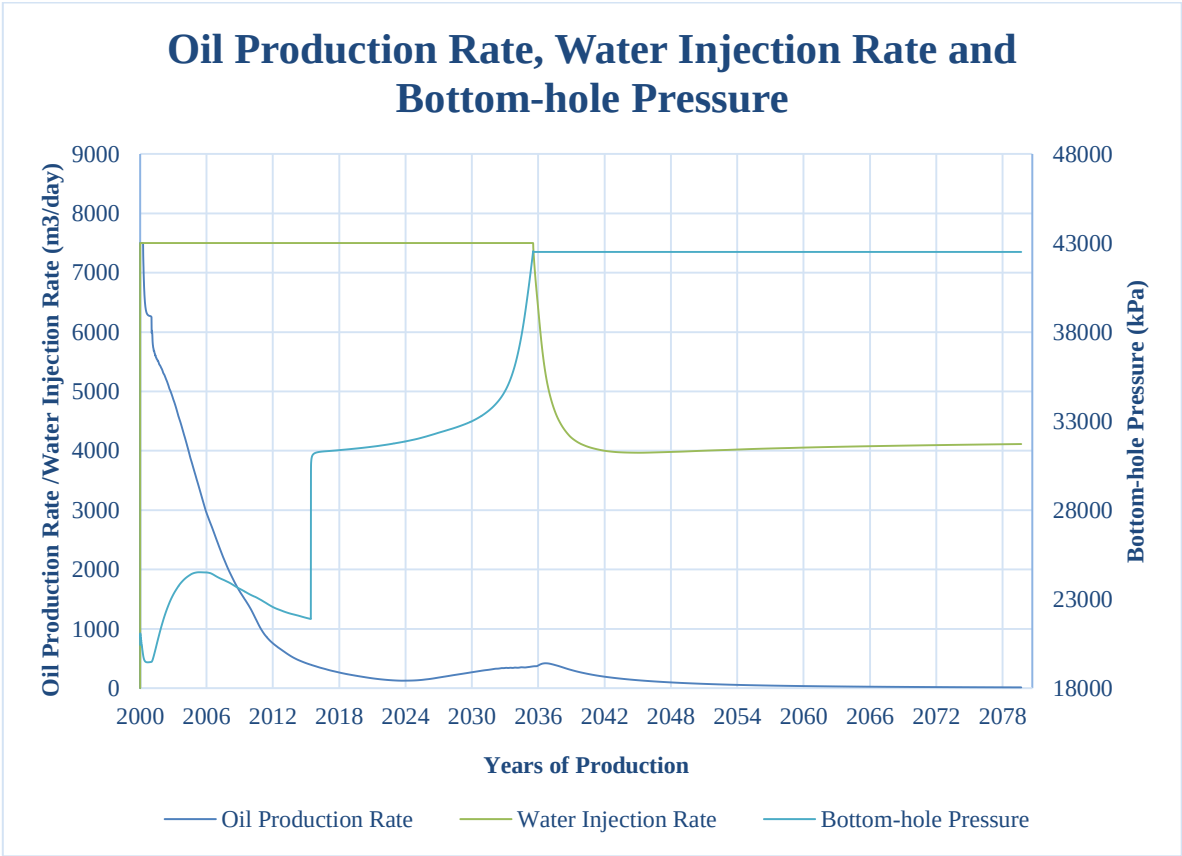

Figure 5.26: Oil production rate, water injection rate and bottom-hole pressure for the polymer flooding process.

5.5.4 Results for Case Study 2

The production results for the injection rate of 5000 m^3/day are presented in figures 5.27 and 5.28. The continuous polymer process is able to recover 70.16% of the oil originally in place, which amounts to an oil volume of $1.83 \cdot 10^7$ m^3. The polymers increase the rate of oil production, and thereby reduce the water cut. Before the polymer effect becomes visible, the reservoir is producing oil at a rate of 100.5 m^3/day, and the water cut levels at 97.98%. The oil production rate is increased to 325.7 m^3/day, and the water cut is reduced to 92.03% by the polymers. In year 2080, the rate of oil production has declined, and the reservoir produces oil at 18.26 m^3/day. In correspondence with the oil production rate, the water cut has reached 99.55%.

Although the injection rate is lowered, the reservoir pressure exceeds the upper limit in this case study. After the immediate pressure buildup, a small pressure decline is observed which may be explained by the change in injection rate from 7500 m^3/day for the initial high salinity waterflooding to 5000 m^3/day for the polymer flooding. Nevertheless, the pressure increases steadily after that time, and by year 33, the pressure has reached the upper limit, and the simulator automatically reduces the injection rate as demonstrated in figure 5.28. Hence, the injection rate of 5000 m^3/day is too large.

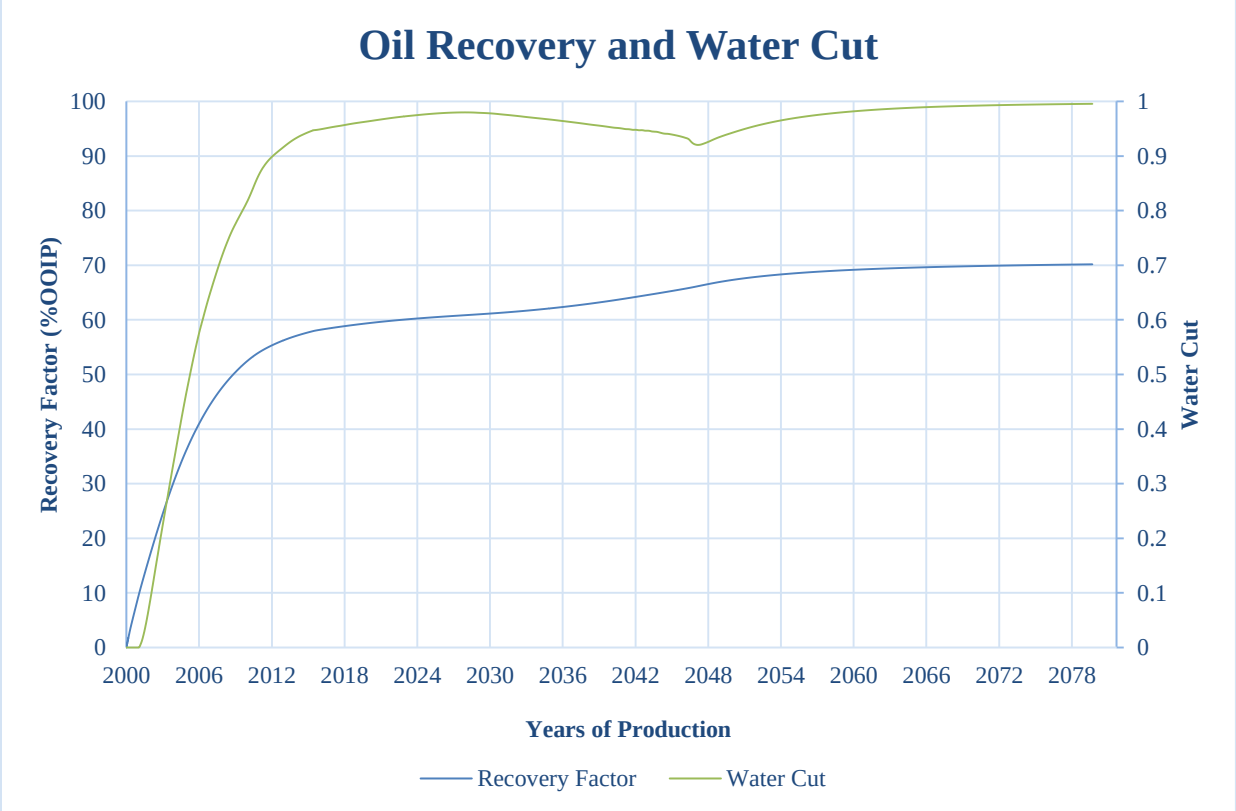

Figure 5.27: Cumulative oil recovery and water cut for the polymer flooding process.

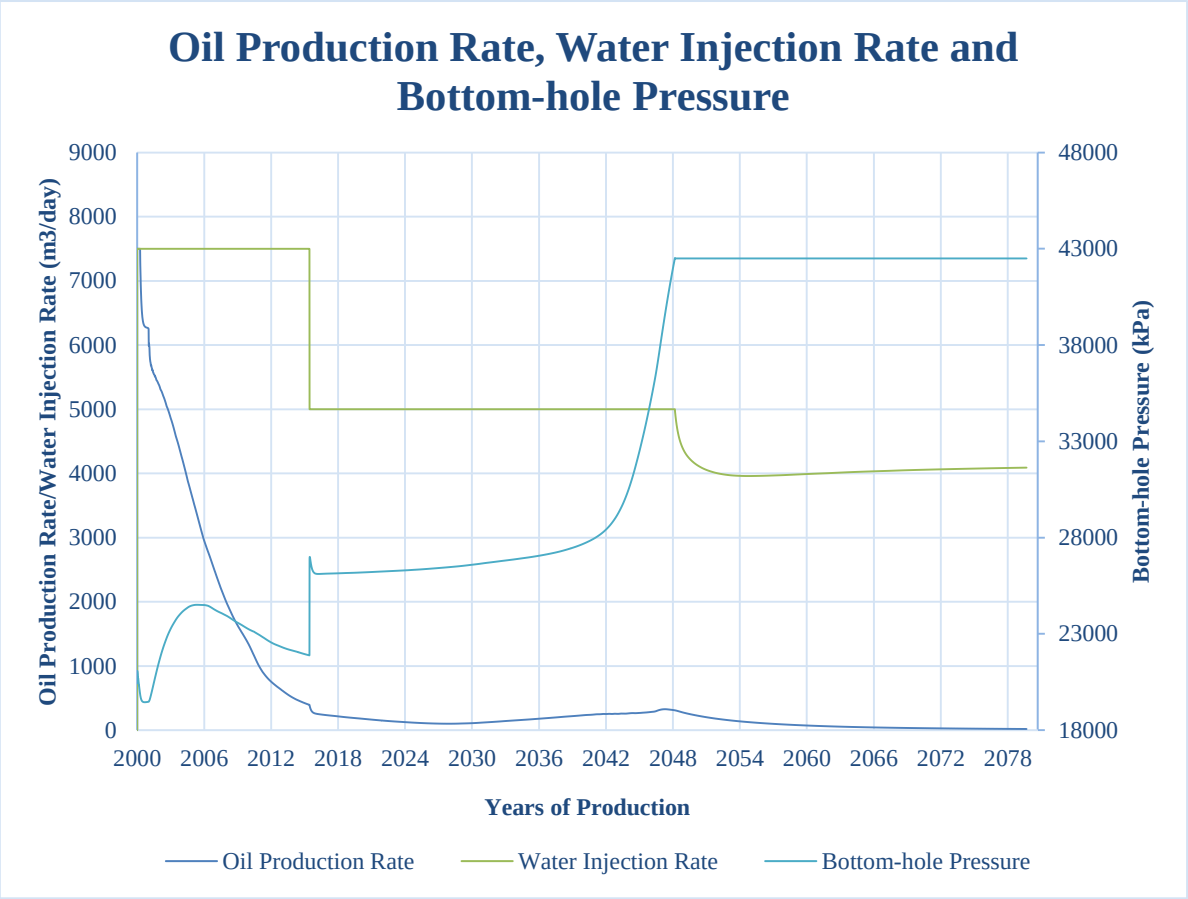

Figure 5.28: Oil production rate, water injection rate and bottom-hole pressure for the polymer flooding process.

5.5.5 Results for Case Study 3

The results from the injection rate of 3500 m^3/day are illustrated in figures 5.29 and 5.30. The polymer process produces 69.81% of the oil originally in place, which corresponds to an oil volume of $1.82 \cdot 10^7$ m^3. The oil production rate increases from 84.58 m^3/day to 235.01 m^3/day, but eventually declines to reach 39.47 m^3/day at the end of production. Correspondingly, the water cut decreases from 97.57% to 92.20% by the polymer flooding, before it eventually increases to 98.87% at the last production day.

The reservoir pressure increases instantly after the commencement of polymer injection, and decreases shortly after due to the shift in injection rate from 7500 m^3/day to 3500 m^3/day. However, it increases again and reaches a maximum of 39 166.0 kPa after 57 years of polymer injection. The pressure never overreaches the upper limit of 42 500, and the injection rate of 3500 m^3/day is therefore a sensible choice for the continuous polymer flooding process.

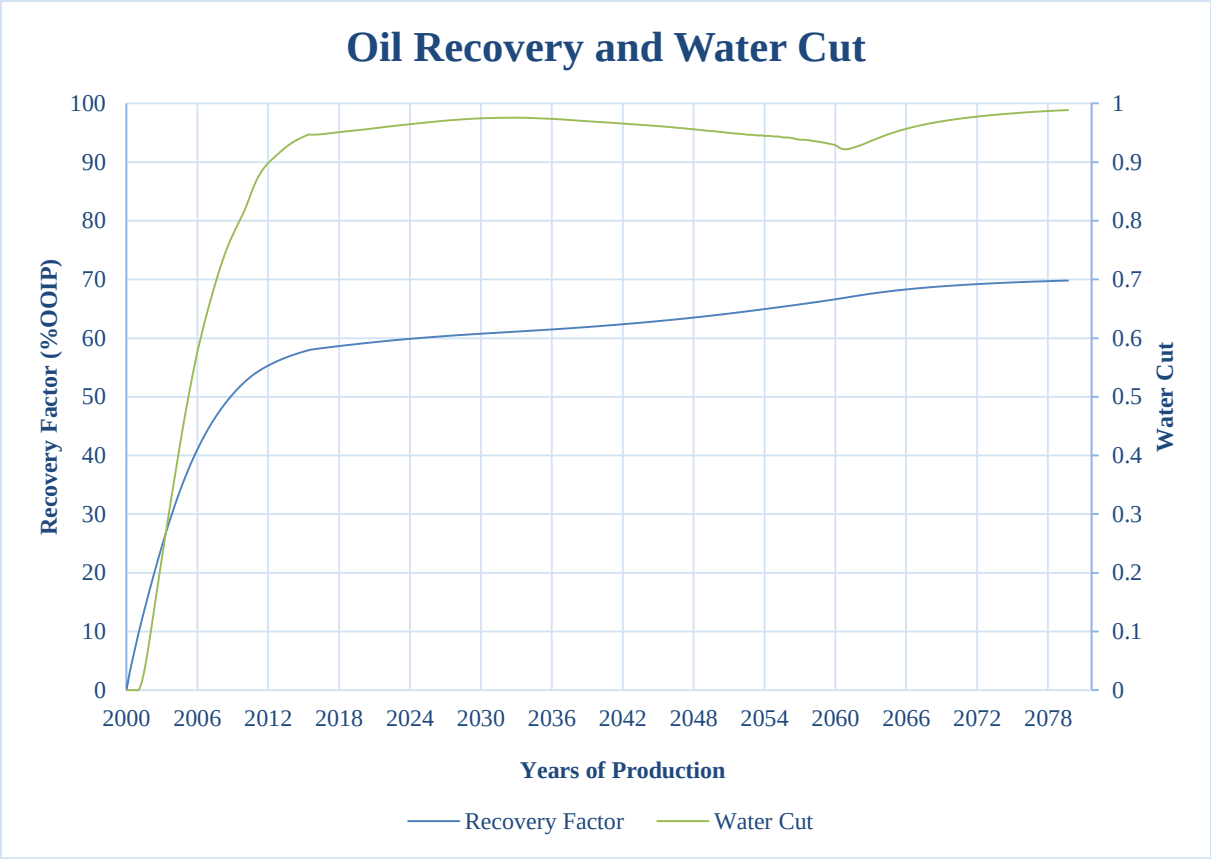

Figure 5.29: Cumulative oil recovery and water cut for the polymer flooding process.

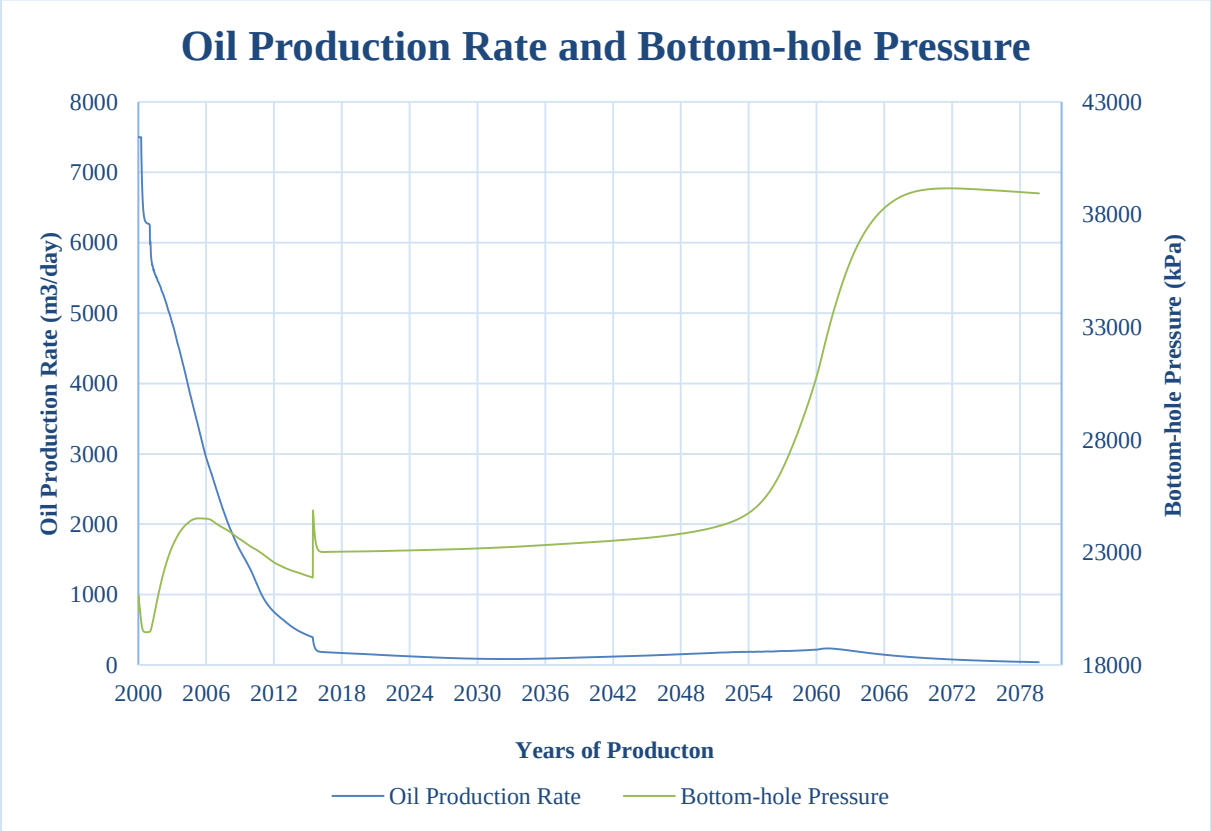

Figure 5.30: Oil production rate and bottom-hole pressure for the polymer flooding process.

5.5.6 Discussion and Summary

The simulation studies reveal that polymer flooding is effective in increasing oil recovery without a pre-established low salinity environment. The viscosifying chemicals are able to enhance the macroscopic sweep by increasing the water viscosity and thereby reduce the mobility ratio between water and oil. Ultimately, this leads to a more stable displacement process [29].

In case study 1, the polymer effect becomes visible before 1 PV is injected. Polymers are in general acknowledged for improving sweep and accelerating oil production, and will have a different flooding pattern than regular waterflooding. Thus, the time required for the polymers to flow through the reservoir is not expected to be equal to the time demanded by waterflooding. Previous studies highlight the inaccessible pore volume phenomena that may occur during polymer flooding [61, 62]. The size of the polymer macromolecules can be larger than the size of pore throats and constrictions within the reservoir, which makes these pores inaccessible for the polymers. Consequently, the polymers may advance through the reservoir at a rate faster than predicted [36]. According to Dawson (1972), close to one third of the total pore volume may not be contacted by polymers [62]. The earlier than expected effects are however not present in case studies 2 and 3. The injection rate is lowered for these trials, and it requires more time to inject one pore volume.

The total cumulative oil recovery after the continuous polymer flooding is 70.30%. 70.16% and 69.81% for case studies 1, 2 and 3, respectively. As expected, an increased injection rate will mobilize the oil in place faster. However, the two first case studies experience a pressure buildup that exceeds the upper pressure limit for the reservoir model. The pressure is dependent on injection rate, where high rates lead to higher reservoir pressures. The pressure buildup by polymers is due to their high molecular weight, which effectively increases the viscosity of the water phase. In order to avoid a pressure that exceeds the upper limit, a reduction in injection rate may be necessary. During the simulation studies, the pressure buildup was delayed for the reduced injection rates, indicating that it takes longer for the pressure to increase. The bottom-hole pressure in case study 3 does not exceed the pressure limit, and is therefore a reasonable choice.

5.6 Low Salinity Waterflooding and Surfactant Flooding

This trial focuses on the maximized recovery by low salinity waterflooding and surfactant flooding in a tertiary mode. The injection start of low salinity water and surfactants are based on the oil production plateau from the previous injected phase, to examine their potential to reduce the residual oil saturation further.

The high salinity flood obtains a salt concentration of 40 000 ppm, matching the connate water salinity. The salt concentration of the low salinity brine is 4000 ppm. Lastly, the surfactant concentration is 5000 ppm. The same "extreme process" from chapter 5.4 is also assumed in this trial, to examine whether the surfactants are effective at the residual oil saturation after low salinity waterflooding, $S_{or,LS}$, and if the surfactants are able to increase oil recovery beyond the capability of low salinity water.

5.6.1 Injection Scheme

Low salinity water injection is commenced after 25 years when the seawater flood becomes inefficient. Thenceforth, surfactant flooding is started 35 years after the low salinity flood. By that time, the oil production by the low salinity waterflood is approaching a plateau. 4 years of surfactant flooding is followed by a low salinity chase flood for another 34 years until a new plateau is established. The injection scheme is summarized in table 5.10.

Table 5.10: Injection scheme for the EOR-process with corresponding concentrations and slug sizes.

Injection Fluid	**Concentration (ppm)**	**Slug Size (years)**
High Salinity Water (HS)	40 000	25
Low Salinity Water (LS)	4000	35
Surfactants (LSS)	5000	4
Low Salinity Water (LS)	4000	36

5.6.2 Results

From figures 5.31 and 5.32, it is evident that both the low salinity water slug and surfactant slug are able to improve cumulative oil recovery compared to the conventional seawater flood. While the cumulative oil production is 60.55% after the initial high salinity waterflooding, the low salinity waterflooding and surfactant flooding are able to rise the production to 67.84% and 83.55%, respectively. Ultimately, the reservoir is mainly producing water. The endpoint water cut is 99.46%, and the reservoir is producing oil by 40.58 m^3/day.

The pressure increases when both low salinity water and surfactants are injected. As deduced from figure 5.32, this pressure increase is accompanied with an increase in oil production and can be caused by oil banking. The low salinity water may lead to trapping of fines in pore constrictions, which can effectively increase the reservoir pressure [71]. Additionally, the reduction in water relative permeability following the wettability alteration may also increase the pressure. Furthermore, microemulsions may be formed as a consequence of the surfactant injection, which can enhance the phase viscosity and induce a pressure increase [6, 93].

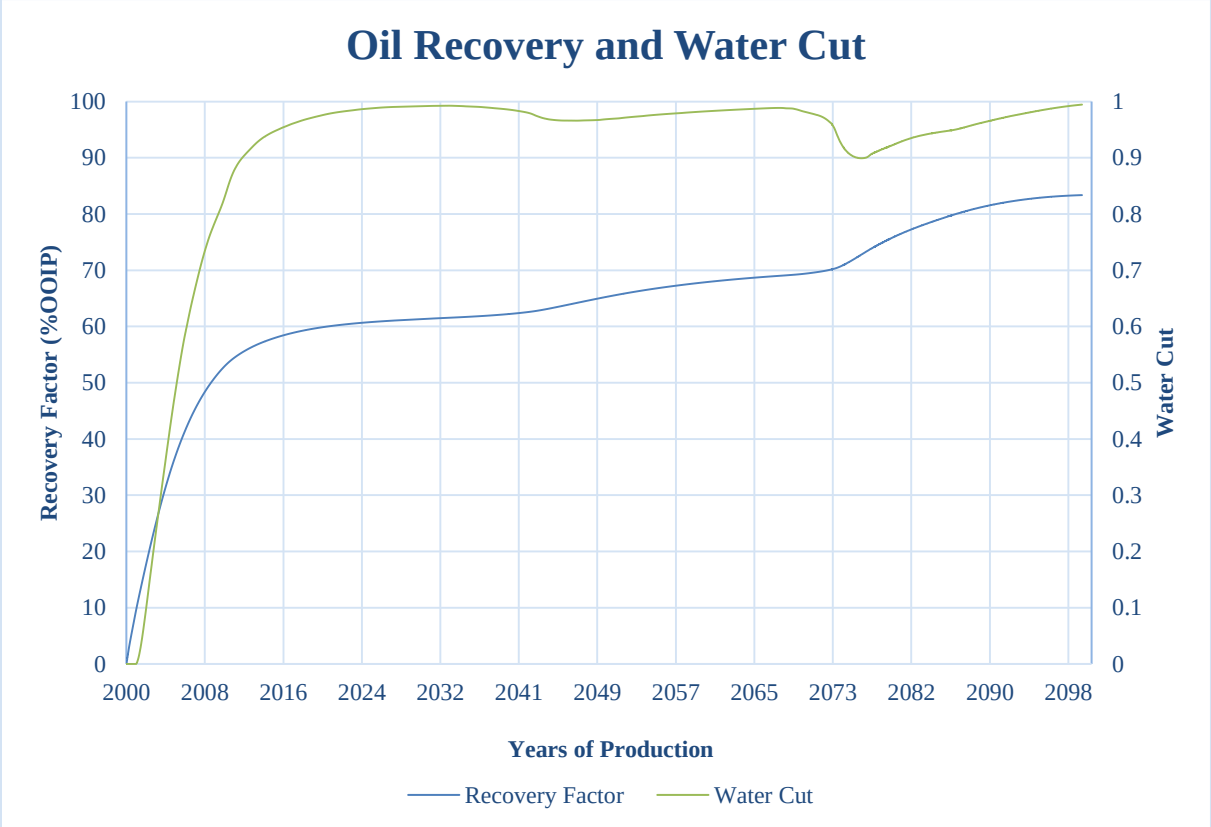

Figure 5.31: Cumulative oil recovery and water cut for the low salinity water – and surfactant flooding processes.

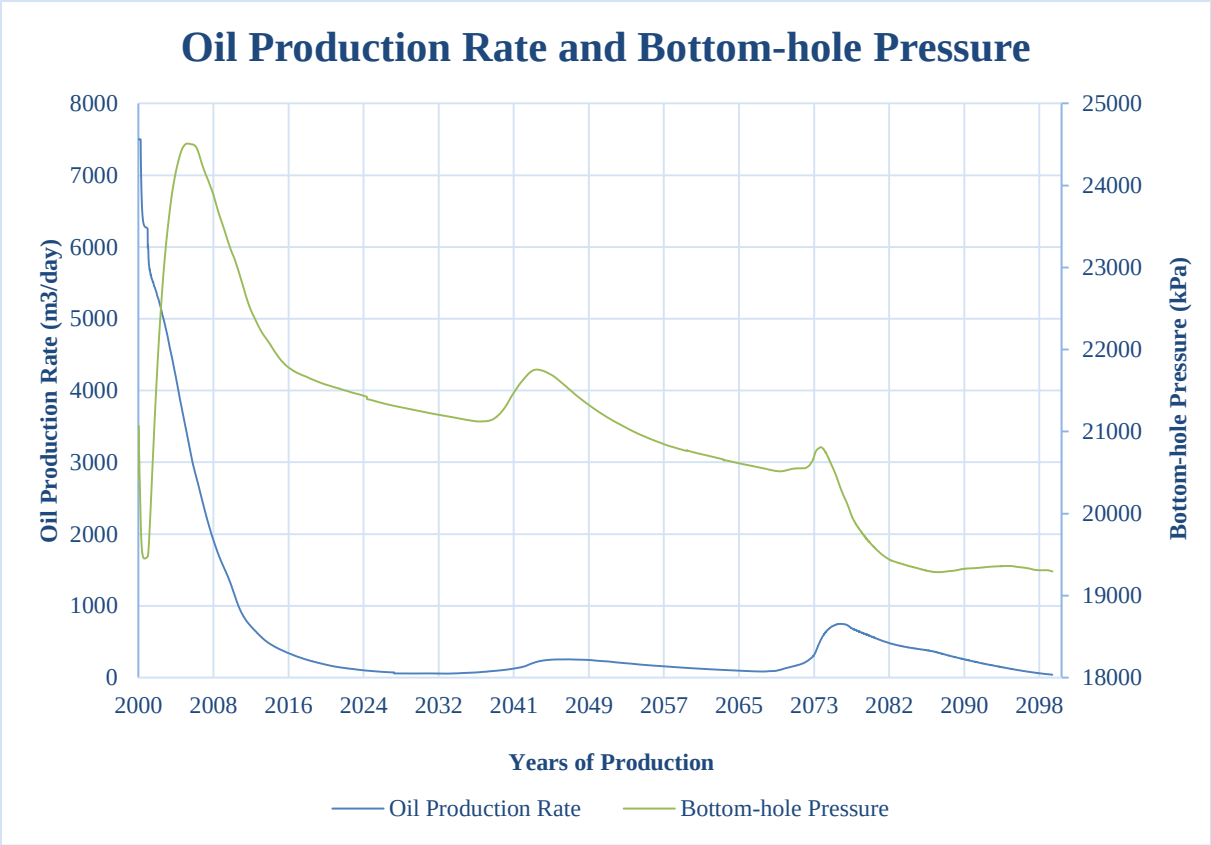

Figure 5.32: Oil production rate and bottom-hole pressure for the low salinity water – and surfactant flooding processes.

The low salinity water contributes with its wettability alternating effect, leading to a higher macroscopic sweep [13]. Clay swelling and release of fines may in addition affect the microscopic sweep [71, 97]. Furthermore, the surfactants successfully reduce the interfacial tension between water and oil due to their adsorption on fluid-fluid interfaces, and mobilize residual oil. The lowering of the interfacial tension effectively increases the capillary number, ultimately leading to an enhanced microscopic sweep [57].

The pre-established low salinity environment within the reservoir has an impact on the function of the surfactants. The wettability shift towards a more water-wet state also helps the surfactants to cover a larger area of trapped oil due to a better flooding performance interlinked with water-wet reservoirs [40]. Additionally, the trapping of surfactants in the oleic phase is prevented in low salinity environments, since the surfactants form oil-in water emulsions. According to a previous laboratory study conducted by Alagic et al. (2010), surfactants were more effective in increasing the oil recovery when a slug of low salinity water was injected prior to the surfactants [14]. Compared to chapter 5.4, this process generated a higher oil production. In addition, the oil production rate was significantly larger during this study at the end of production, indicating that more oil may be recovered if the recovery process is prolonged.

The cumulative oil production after the high salinity waterflooding process, low salinity waterflooding process, and surfactant flooding process is displayed in figure 5.33, illustrating the enhancement of oil production by each flooding process.

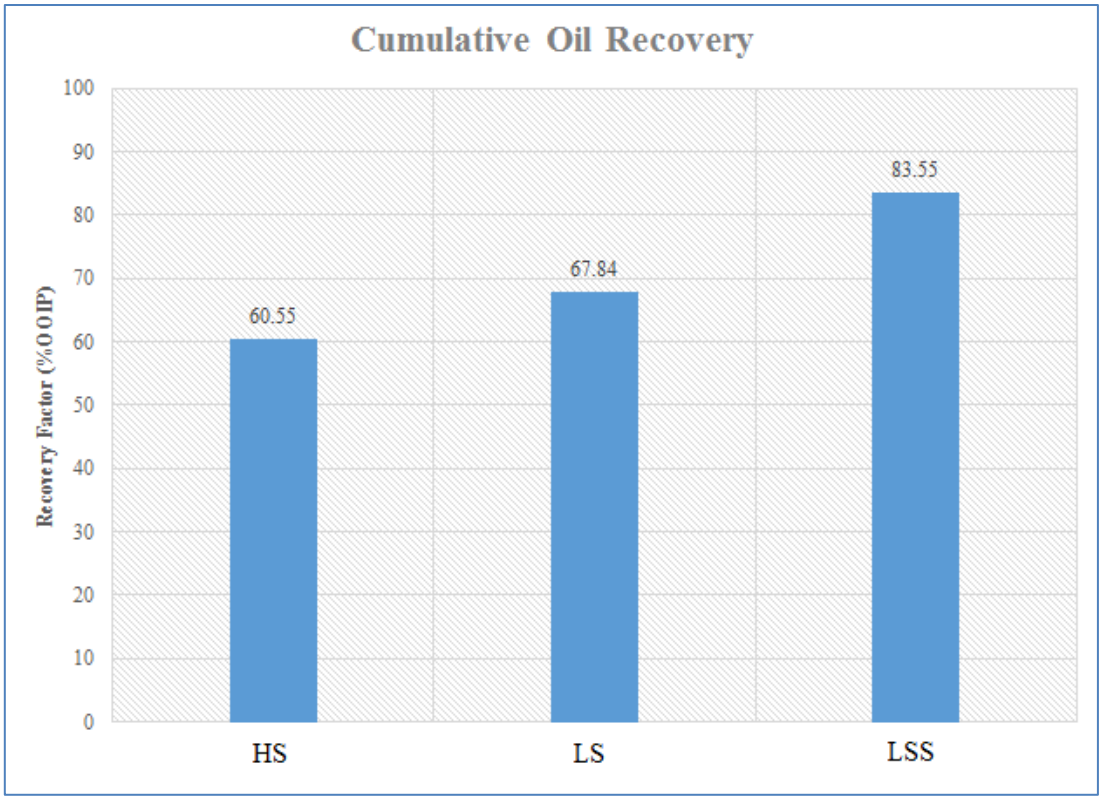

Figure 5.33: Cumulative oil recovery after the HS, LS and LSS processes.

5.6.3 Surfactant Propagation

The surfactants are injected over a time period of 4 years (1/3 PV), from year 2060 to 2064, and is followed by a chase slug of low salinity water until all surfactants are displaced. Initially, a mixing zone is developed surrounding the injector, with gradually decreasing surfactant concentration towards the producer. Figure 5.34 demonstrates the concentration distribution of the surfactants after ½ PV is injected, where the first ¾ of this period consist of surfactant flooding before low salinity chase water injection is commenced. By this time, most of the reservoir is still uncontacted by the surfactants.

Figure 5.35 illustrates the surfactant concentration within the reservoir in year 2072, which is approximately when 1 PV is injected. By this time, the surfactant slug has expanded significantly, and have reached a maximum concentration in a large fraction of the reservoir. The maximum surfactant concentration is surrounded by a mixing zone of gradually decreasing concentration. In addition, the surfactant concentration has started to decrease around the injector due to the low salinity water that is injected to displace and spread out the surfactant slug.

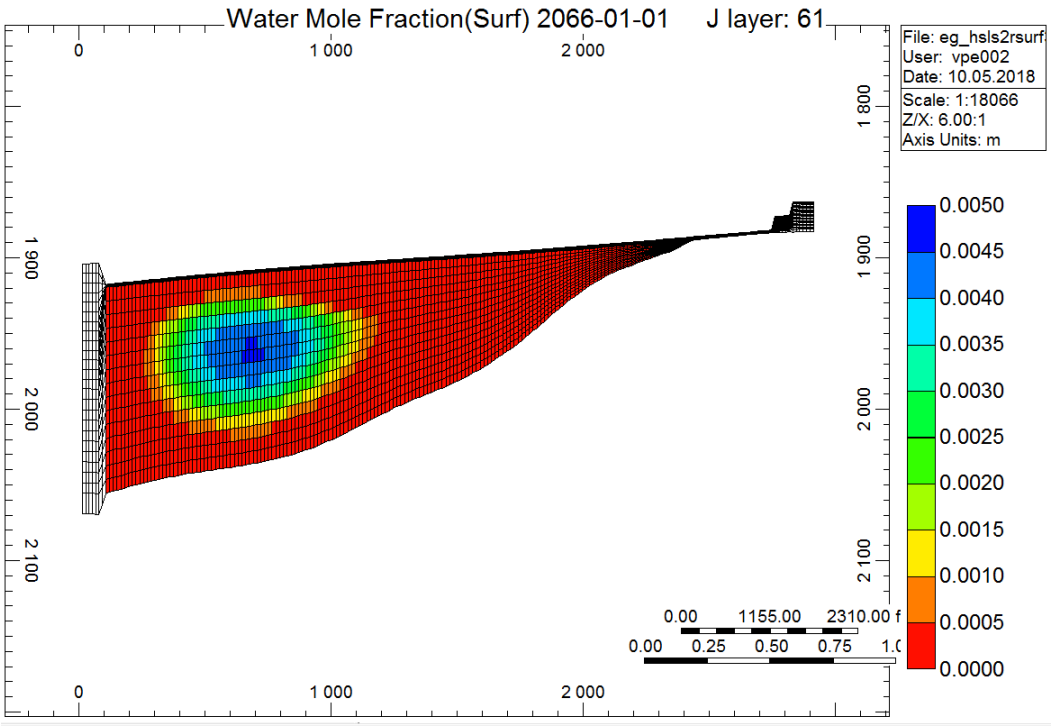

Figure 5.34: Approximately ½ PV injected

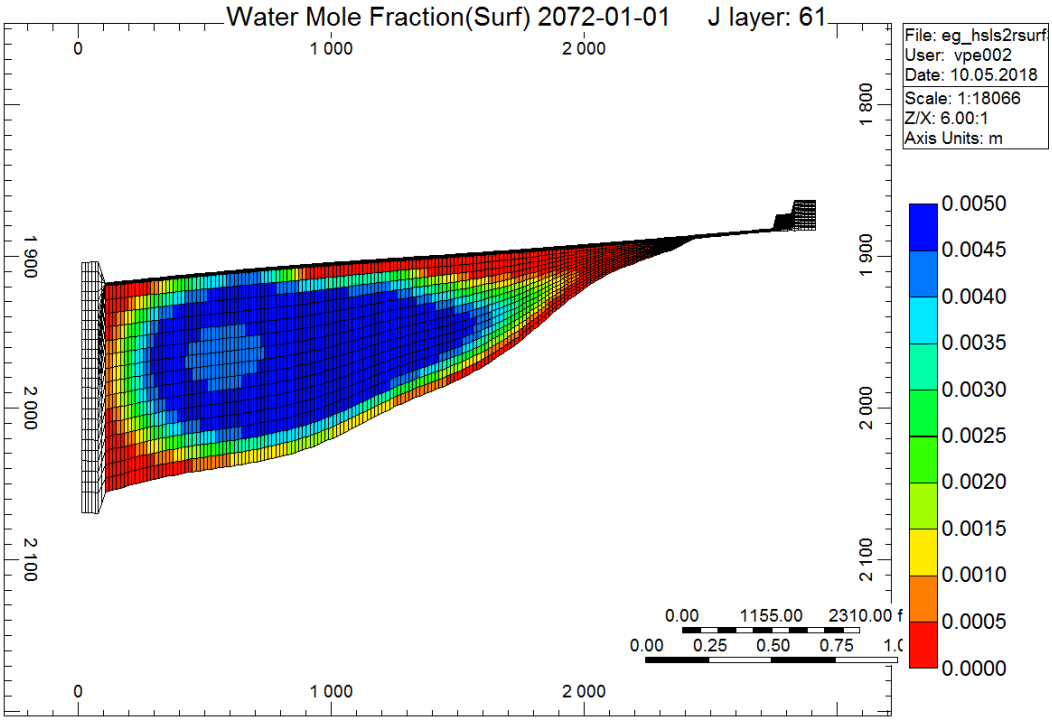

Figure 5.35: 1 PV injected.

The surfactant bank is chased by the low salinity water, and the surfactants are approaching the producer, as illustrated in figures 5.36 and 5.37.

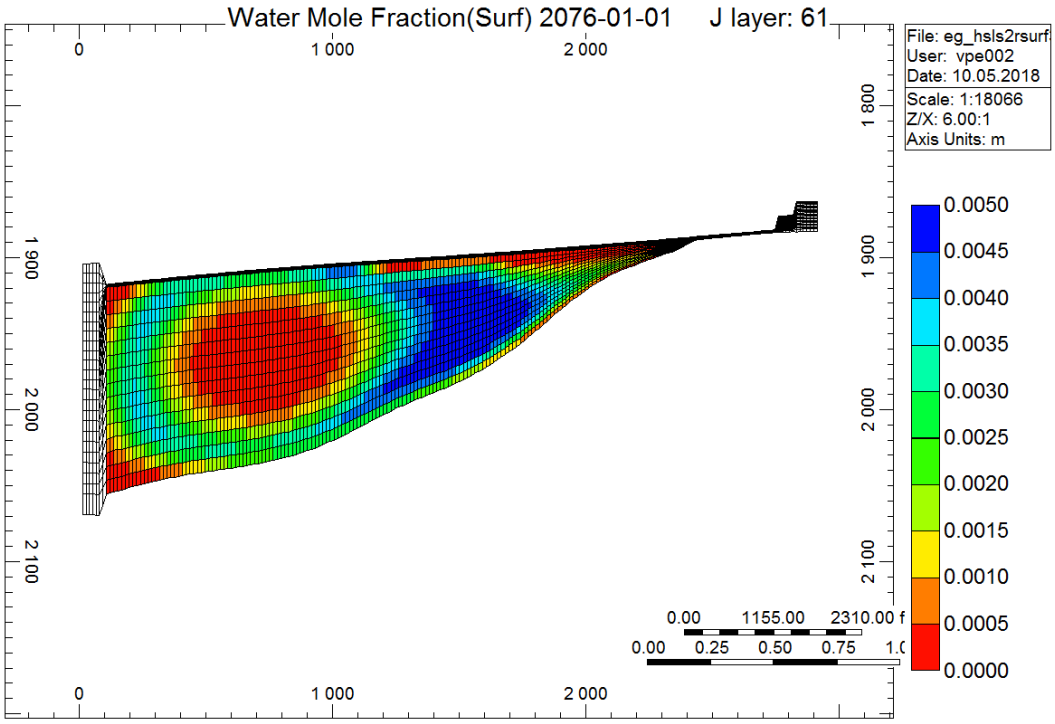

Figure 5.36: The surfactant bank is chased by low salinity water.

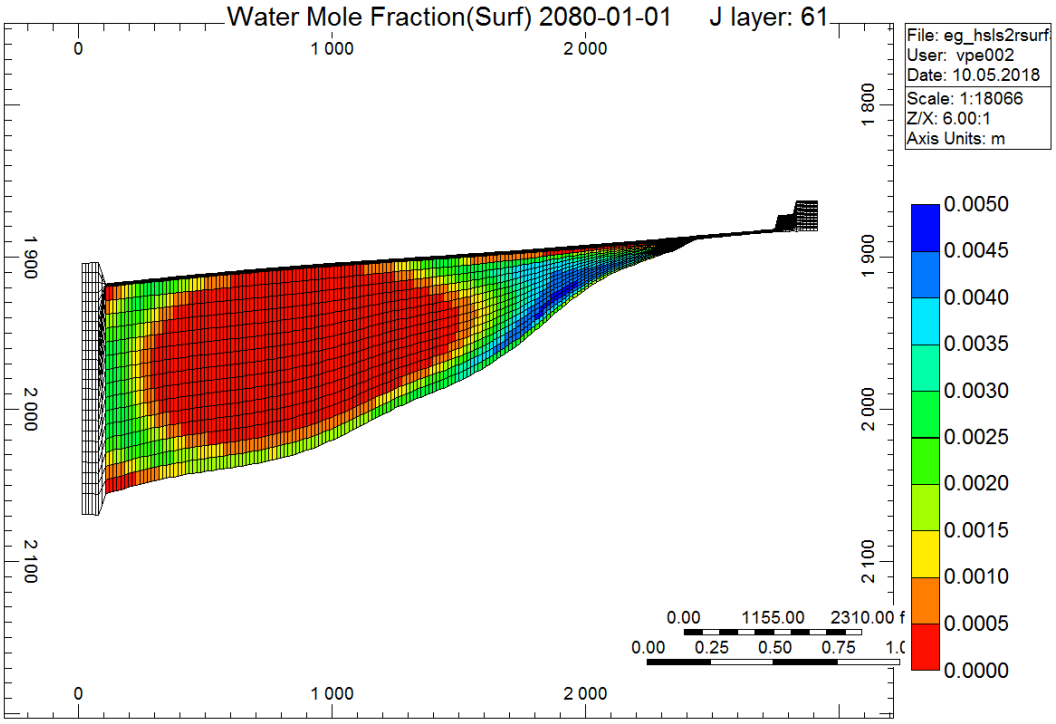

Figure 5.37: The surfactant bank is approaching the production well.

Figure 5.38 displays the surfactant concentration within the reservoir towards the end of production. Ultimately, approximately all surfactants are produced. Hence, they will no longer have an effect in the reservoir. However, the leftmost corners never reach full surfactant concentration.

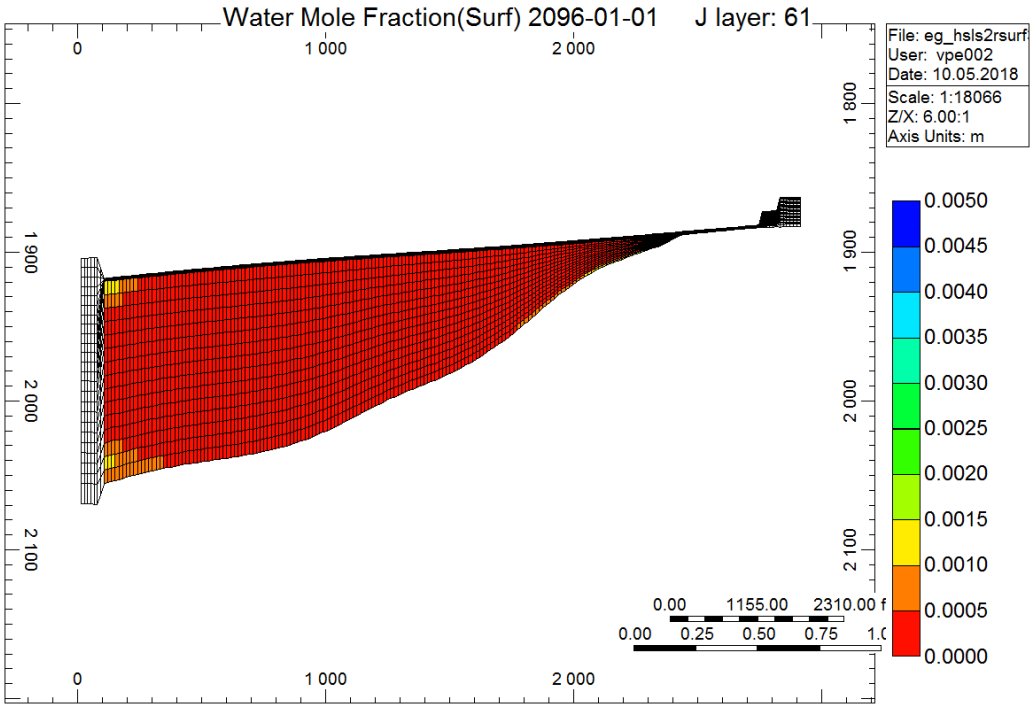

Figure 5.38: Towards the end of the low salinity chase flood, almost all surfactants are produced.

5.6.4 Discussion and Summary

This trial has examined the total potential of combining low salinity waterflooding with surfactant flooding in a tertiary mode. After the oil recovery from the initial high salinity waterflood has plateaued, low salinity water is introduced and flooded through the reservoir until a new oil production plateau is established. At this point, the surfactants are injected to further escalate oil recovery by enhancing the microscopic sweep. After 1/3 PV of surfactants are injected, a chase slug of low salinity water is flooded through the reservoir to displace the surfactant bank towards the producer.

Compared to the oil recovery from the seawater flooding process, low salinity waterflooding and surfactant flooding combined are able to rise the production by a total of $6 \cdot 10^6$ m^3. After the high salinity process, the recovery factor is 60.55%. The cumulative oil recovery is increased by 12% due to the low salinity waterflooding, and thereafter increased another 23% by the surfactant flooding. After the low salinity flooding, the recovery factor has increased to 67.84%, and by the end of the surfactant flooding, the recovery has risen further, and levels at

83.55% of the oil originally in place. Thus, surfactants are able to increase oil production beyond the capability of low salinity water.

The low salinity water enhances the sweep efficiency by altering the reservoir wettability, which leads to a more stable oil displacement [40]. By shifting the wetting preference of the rock towards a more water-wet state, the injection water is diverted more evenly throughout the reservoir. Oil zones that were previously bypassed by the injected water are now contacted and displaced [13]. This is also beneficial for the forthcoming surfactants, since they will be distributed throughout a larger portion of the reservoir. Moreover, the pre-established low salinity environment optimizes the surfactant functioning, and prevents trapping of surfactants in the oleic phase (Windsor type II), which occurs under highly saline conditions [14].

5.7 Hybrid Low Salinity Surfactant/Polymer Flooding

In this part, the composite effect of low salinity waterflooding, surfactant flooding and polymer flooding is examined. The EOR-fluids will contribute with their individual effects, and the combination of them will enhance both the macroscopic and microscopic sweep efficiency, which may result in incremental oil recovered [6, 93]. The low salinity water is injected first to provide a diluted environment for the following chemicals. Low salinity water is acknowledged for its wettability altering abilities, which affects waterflooding patterns [13, 40]. Surfactants effectively reduce the residual oil saturation by adsorbing on fluid/fluid interfaces [57], and the following polymer slug ensures that the low salinity chase water does not create fingers in the surfactant slug. The final low salinity chase water displaces the chemicals throughout the reservoir.

This chapter exemplifies realistic production scenarios, and two different slug sizes for the surfactant phase and polymer phase are tested; 1/3 PV and 1/6 PV. They will be referred to as case studies 1 and 2, respectively. The effects of chemical adsorption onto reservoir rock will be examined for each slug size. Table 5.11 summarizes the scope of work for this chapter.

Table 5.11: Description of the six simulation studies.

Case Study	**Slug Size (PV)**	**Description**
1	1/3	No surfactant or polymer adsorption
		Surfactant adsorption but no polymer adsorption
		Surfactant and polymer adsorption
2	1/6	No surfactant or polymer adsorption
		Surfactant adsorption but no polymer adsorption
		Surfactant and polymer adsorption

5.7.1 Case Study 1

In the following three simulation studies, 1/3 PV of surfactants and 1/3 PV of polymers will be injected, corresponding to 4 injection years for each tertiary fluid.

5.7.1.1 Injection Scheme

The injection fluids relevant in this study are high salinity water, low salinity water, surfactants and polymers. Their concentration and slug sizes are displayed in table 5.12.

The reservoir will first be flooded with high salinity water for 20 years. Thenceforward, low salinity water will be flooded through the reservoir for 2 years to establish a low-salinity environment for the following slugs of surfactants and polymers. The slug sizes of the surfactant flooding and polymer flooding processes are 1/3 PV, which correspond to 4 years for each of the individual EOR-fluids. To chase the chemicals through the reservoir, low salinity water is injected in the end.

This part consists of three simulation studies, where the first one assumes no chemical adsorption. The next study examines the results from surfactant adsorption only, and the last trial investigates the production outcome when both surfactant and polymer adsorption are activated.

Table 5.12: Injection scheme for the EOR-process with corresponding concentrations and slug sizes.

Injection Fluid	**Concentration (ppm)**	**Slug Size (years)**
High Salinity Water (HS)	40 000	20
Low Salinity Water (LS)	4000	2
Surfactants (LSS)	5000	4
Polymers (LSP)	350	4
Low Salinity Water (LS)	4000	30

5.7.1.2 No Surfactant or Polymer Adsorption

In the first simulation, it is assumed that no surfactants or polymers are adsorbed onto the rock surface. Although the presumption of no adsorption is not realistic, it gives a perception of the maximum effect of the two chemicals, and provides a foundation for comparison when adsorption is activated in the subsequential studies. The simulation results are displayed in figures 5.39 and 5.40:

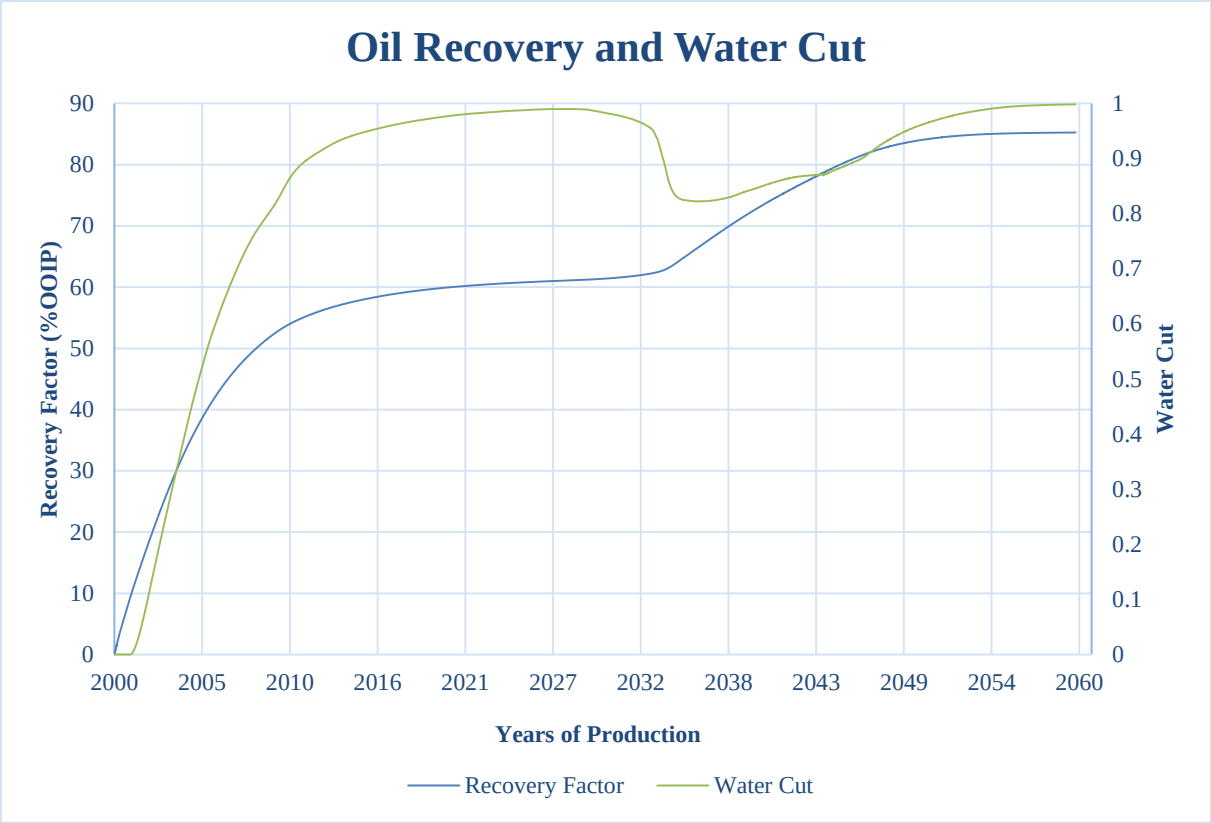

Figure 5.39: Cumulative oil recovery and water cut for the hybrid LSSP-process.

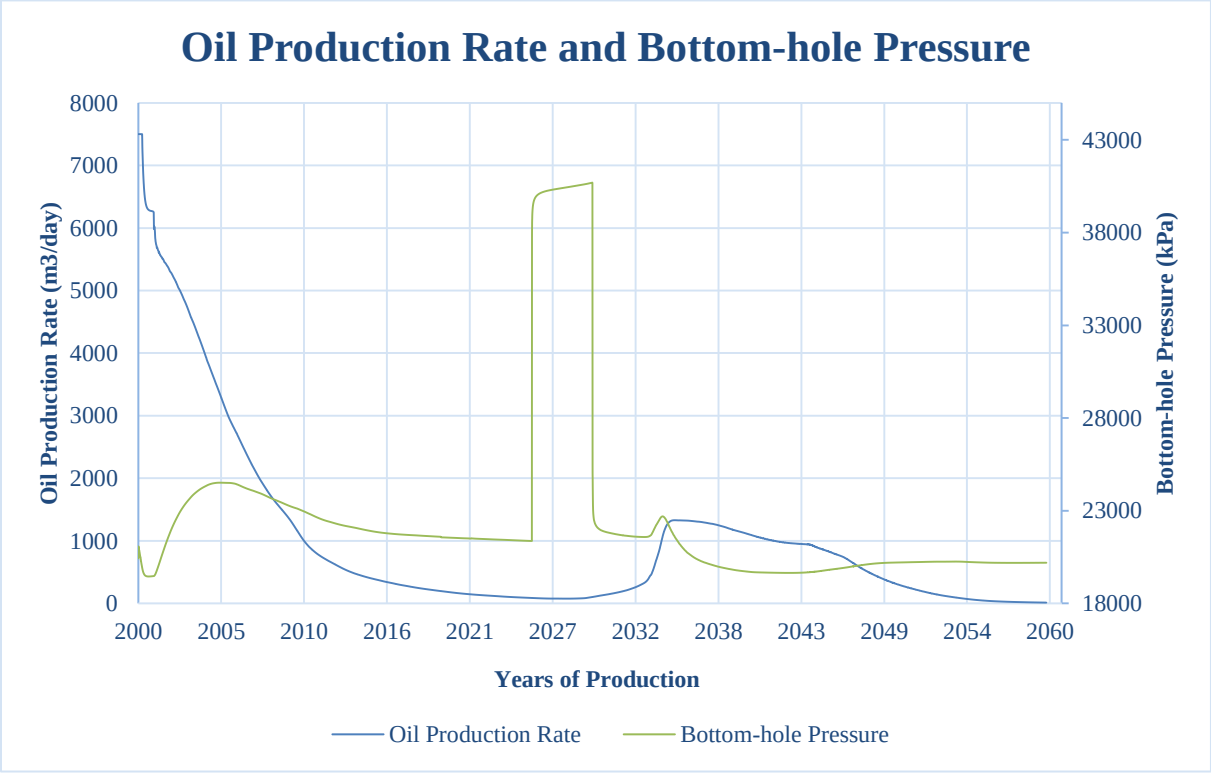

Figure 5.40: Oil production rate and bottom-hole pressure for the hybrid LSSP-process.

From figures 5.40 and 5.41, it is highly evident that the propagation of the tertiary fluids through the reservoir yields an effect on production behavior. The combined effect of the low salinity water, surfactants and polymers rise the oil production to a value of $2.22 \cdot 10^7$ m^3, from $1.60 \cdot 10^7$ m^3 after the seawater phase. The total cumulative oil recovery after the composite tertiary process is 85.25% of the oil originally in place.

The effects of the hybrid EOR-process are also visible in the water cut and oil production rate. The water cut sinks from 98.78% down to 82.23% due to the LSSP-process, before reaching 99.83% at the end of production in 2060. The oil production rate increases from 76.79 m^3/day to 1329.06 m^3/day due to the LSSP-slug, and eventually reaches 12.64 m^3/day in 2060. By this point, the enhanced sweep by the EOR-chemicals have mobilized most of the oil within the reservoir, and the reservoir is producing almost entirely water. The highly viscous polymer slug immediately increases the reservoir pressure to 40 696.9 kPa. Thereafter, the pressure declines again before a new local maximum at 22 692.8 kPa is reached. Ultimately, the reservoir pressure reduces to 20 193.6 kPa.

The local maximum pressure increase is due to change in the salinity level within the reservoir, as depicted from figure 5.41.

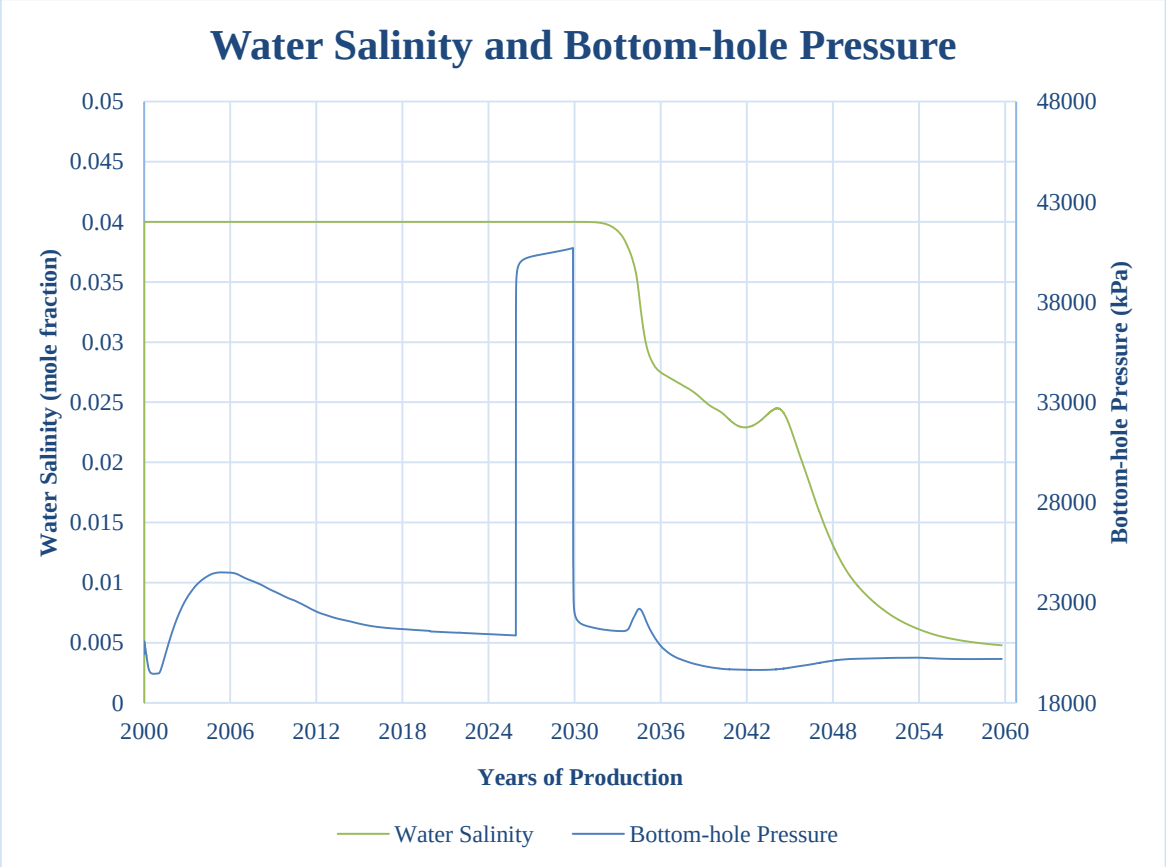

Figure 5.41: The local maximum pressure increase is due to change in water salinity.

5.7.1.3 *Surfactant Adsorption*

This trial is based on the same methodology as the previous study, except that the assumption of no surfactant adsorption is no longer valid. It is assumed an adsorption of 0.1 mg/g surfactant onto reservoir rock, but polymer adsorption is still neglected in this study in order to evaluate the individual effects of surfactant adsorption. The simulation results are presented in figures 5.42 and 5.43:

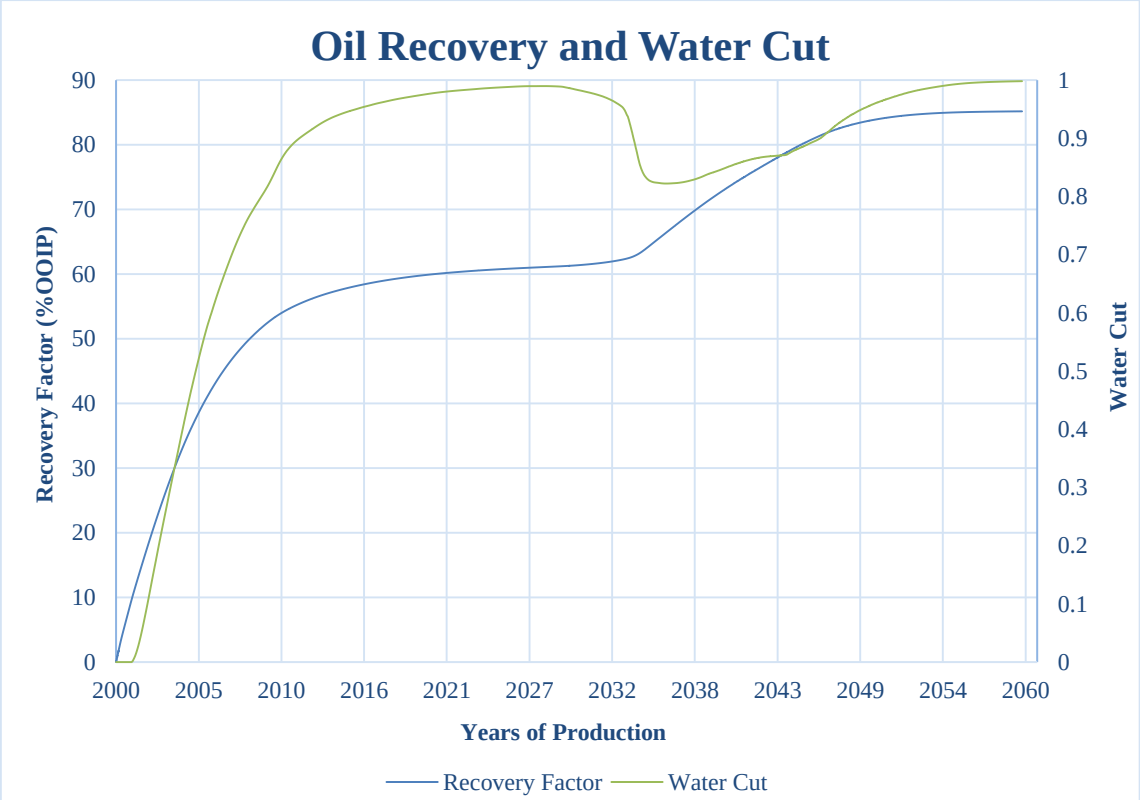

Figure 5.42: Cumulative oil recovery and water cut for the hybrid LSSP-process.

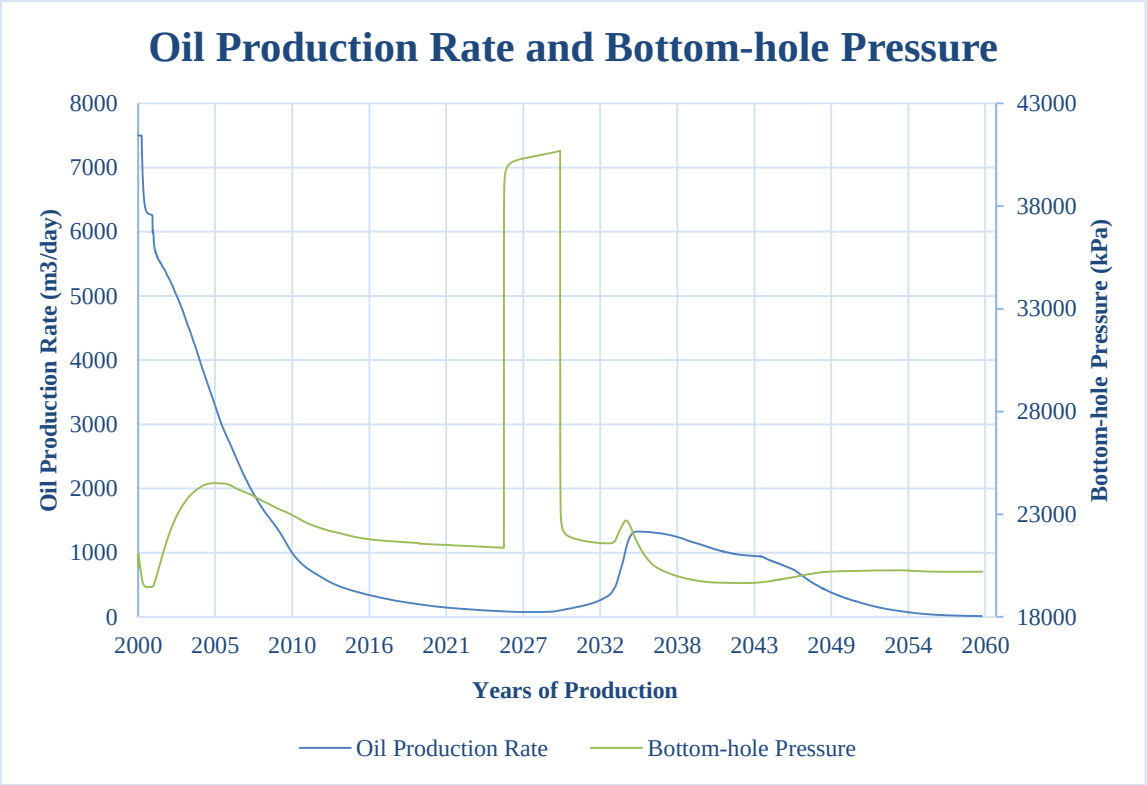

Figure 5.43: Oil production rate and bottom-hole pressure for the hybrid LSSP-process.

Although surfactant adsorption is activated in this study, the simulation results do not differ dramatically from the previous trial. The total cumulative oil recovery is 85.18% of the oil originally in place. Thus, the reservoir produces $1.90 \cdot 10^4$ m^3 less oil than the previous trial without adsorption. Nevertheless, the water cut and oil rate behavior are nearly identical. The water cut is 98.97% before the LSSP-effects activate, and reaches a bottom of 82.23%. From this point forward, it increases steadily until reaching 99.83% at the finalization of production. The oil production obtains a rate of 75.94 m^3/day before the LSSP-slug lifts the oil production rate to a value of 1330.44 m^3/day. Towards year 2060, the oil rate sinks to 12.65 m^3/day.

The pressure increases to a maximum level of 40 697.3 kPa due to the LSSP-fluids. This pressure increase is due to the highly viscous polymer slug. After the abrupt increase in reservoir pressure, it declines again. Thereafter it increases again due to a changed salinity level within the reservoir. and a local maximum of 22 691.5 kPa is established. Eventually, the pressure reduces to 20 194.2 kPa.

Adsorption extracts surfactant molecules from the surfactant slug, and therefore reduces its full potential to lower the interfacial tension and release trapped oil. This was reflected in the cumulative oil production, where $1.84 \cdot 10^4$ m^3 less oil was produced. The endpoint oil rate and pressure are slightly higher, which may be due to a somewhat larger oil saturation within the reservoir. Nevertheless, the differences between the two trials are not exceedingly dissimilar, indicating that the surfactants are still effective despite the adsorption.

5.7.1.4 *Surfactant and Polymer Adsorption*

In this trial, polymer adsorption is also included, and is set as 0.05 mg/g. The surfactant adsorption is the same as in the previous study. The simulation results are illustrated in figures 5.44 and 5.45:

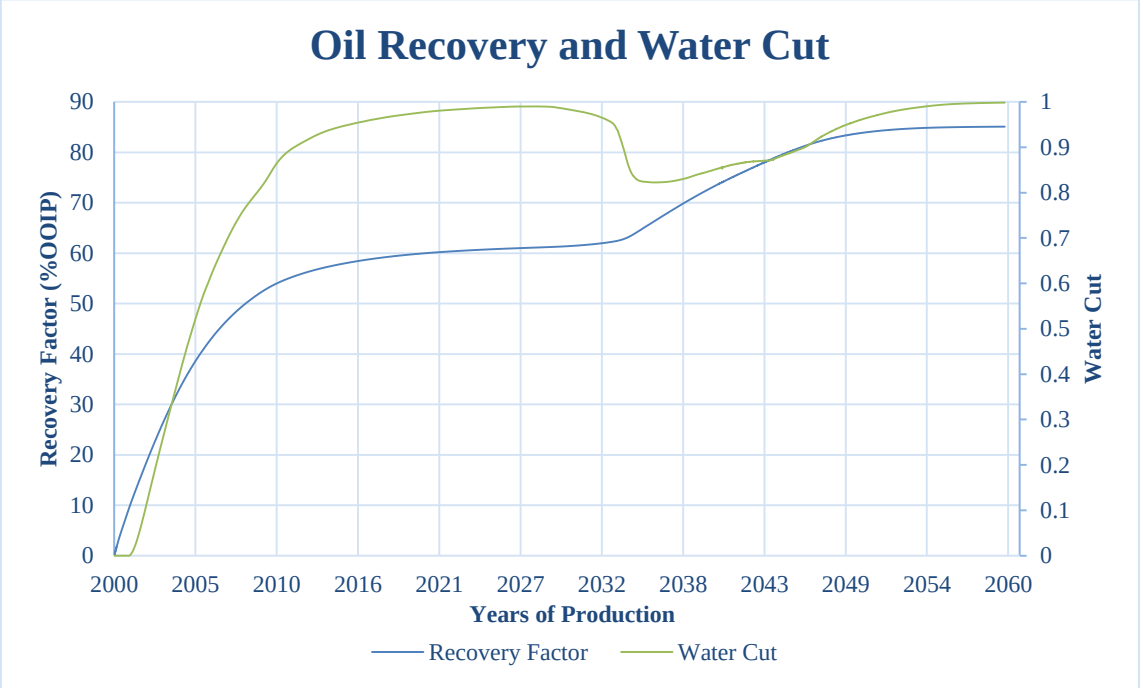

Figure 5.44: Cumulative oil recovery and water cut for the hybrid LSSP-process.

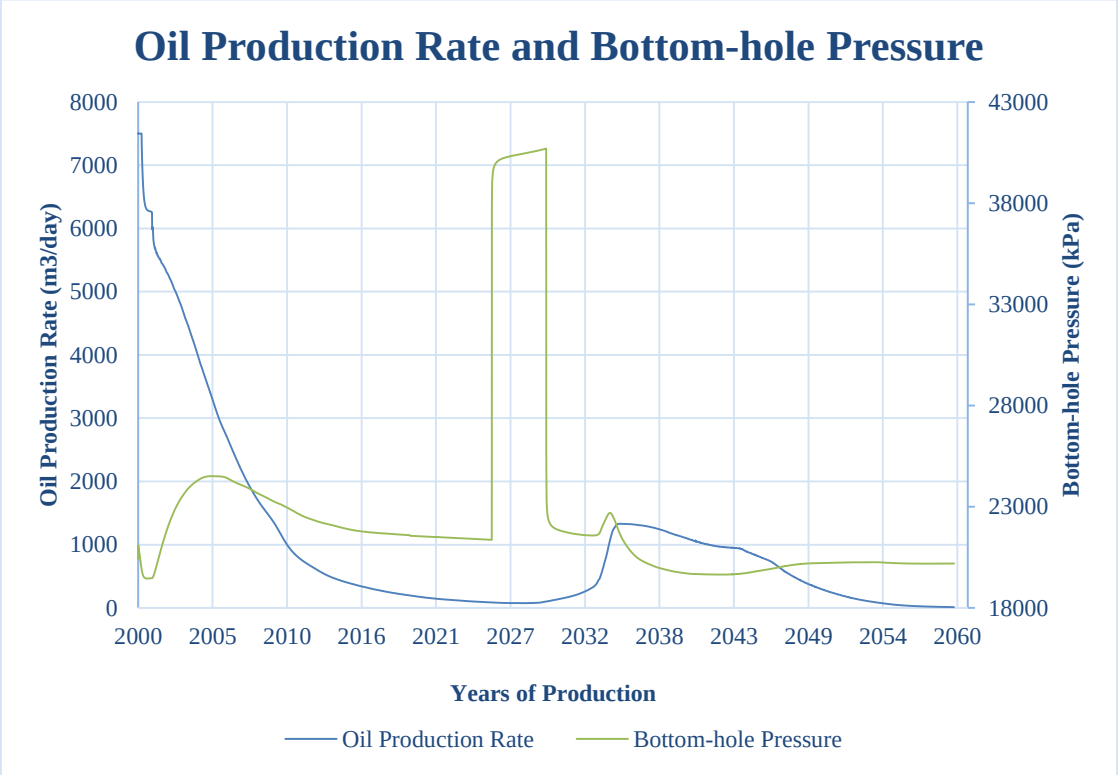

Figure 5.45: Oil production rate and bottom-hole pressure for the hybrid LSSP-process.

The total cumulative oil recovery when both surfactant and polymer adsorption are activated, is 85.08%, and the reservoir produces $4.6 \cdot 10^4$ m^3 less oil than the case study with no adsorption, and $2.7 \cdot 10^4$ m^3 less oil than the case study with surfactant adsorption only. The water cut behavior is nearly identical to the previous studies, and the oil production rate is fairly higher.

In equivalence with the previous studies, the pressure increases abruptly when the LSSP-fluids are injected, due to the viscosifying effects of the polymer molecules. The pressure is increased to a maximum of 40 696.1 kPa, before it decreases again. Shortly after, a new local pressure maximum of 22 692.1 kPa is established. Eventually, the pressure gradually decreases and reduces to 20 202.5 kPa. The endpoint pressure is slightly higher than in the previous studies, and may be connected to a higher oil saturation in this trial which can portray an obstacle to water flow [22].

5.7.2 Case Study 2

This section resembles the previous study in chapter 5.7.1. In this case study, the individual slug sizes for surfactants and polymers are divided in half in order to investigate the effect of slug size on oil production. Both surfactants and polymers are expensive, and it is not desired to inject more than necessary to produce the oil bank [36].

5.7.2.1 Injection Scheme

The concentrations and slug sizes of the injection fluids are displayed in table 5.13. Primarily, the reservoir will be flooded with seawater for 20 years, followed by low salinity water for 2 years. Thereafter, surfactants and polymers will be injected separately for 2 years each (1/6 PV). Ultimately, low salinity chase water will be injected for 34 years. This study will examine the oil production potential from three different scenarios; one without any adsorption of either surfactants or polymers, one with surfactant adsorption but no polymer adsorption, and one with activated adsorption of both chemicals.

Table 5.13: Injection scheme for the EOR-process with corresponding concentrations and slug sizes.

Injection Fluid	**Concentration (ppm)**	**Slug Size (years)**
High Salinity Water (HS)	40 000	20
Low Salinity Water (LS)	4000	2
Surfactants (LSS)	5000	2
Polymers (LSP)	350	2
Low Salinity Water (LS)	4000	34

5.7.2.2 *No Surfactant or Polymer Adsorption*

This simulation study reveals the production results when no adsorption of either surfactants or polymers is assumed. The assumption of no chemical adsorption is not sensible, but it provides comparison data for the later simulations with activated adsorption. The simulation data is displayed in figures 5.46 and 5.47:

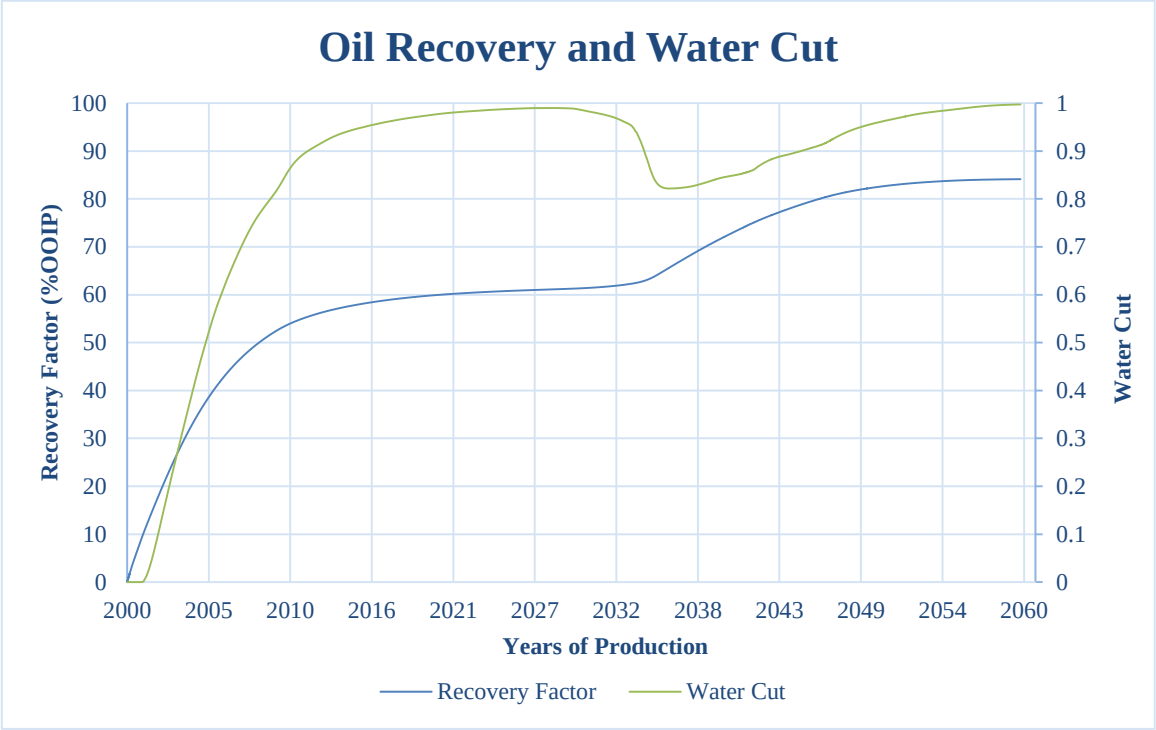

Figure 5.46: Cumulative oil recovery and water cut for the hybrid LSSP-process.

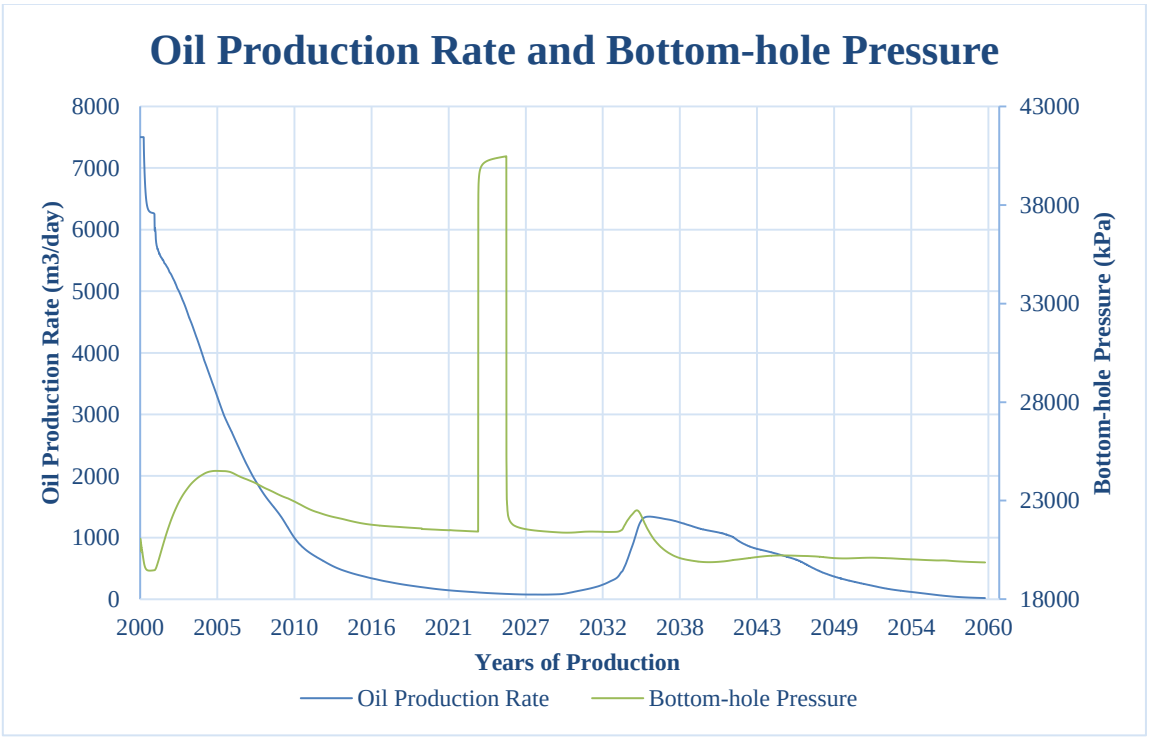

Figure 5.47: Oil production rate and bottom-hole pressure for the hybrid LSSP-process.

The combined effect from the LSSP-fluids elevates the cumulative oil recovery to 84.13%, which amounts to a total oil production of $2.20 \cdot 10^7$ m^3. The hybrid tertiary process is also visible through the water cut and oil production rate, which is significantly reduced and increased respectively as a result of the LSSP-slug. Before the EOR-effects are activated, the reservoir is producing 98.99% water, which is reduced to 82.19% before it increases to 99.74% at production termination. The contrary pattern is shown in the oil production rate. The reservoir is producing oil at 76.09 m^3/day before the effect of the LSSP-fluids lifts the rate up to 1341.42 m^3/day. Eventually, the oil rate reduces to 18.89 m^3/day at the end of production time.

In terms of reservoir pressure, it is heavily increased by the introduction of polymers. The pressure rises to a maximum of 40 468.4 kPa before it declines again. Thenceforth, it increases to a pressure of 22 513.1 kPa. Ultimately, the pressure reduces towards the end of production and ends up at 19 869.0 kPa.

5.7.2.3 Surfactant Adsorption

In this scenario, it is assumed that 0.1mg surfactants will adsorb onto 1g of rock. Polymer adsorption is still disregarded in this trial to study the individual effects of surfactant adsorption. The production results are illustrated in figures 5.48 and 5.49:

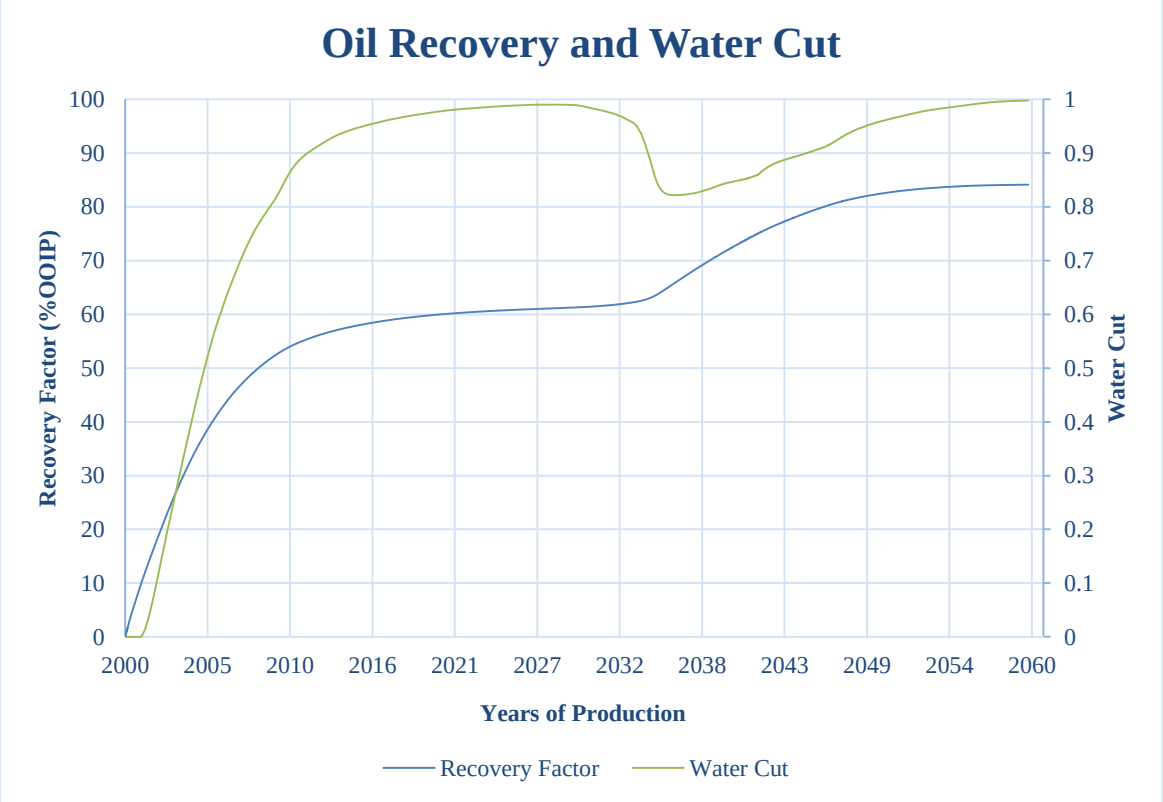

Figure 5.48: Cumulative oil recovery and water cut for the hybrid LSSP-process.

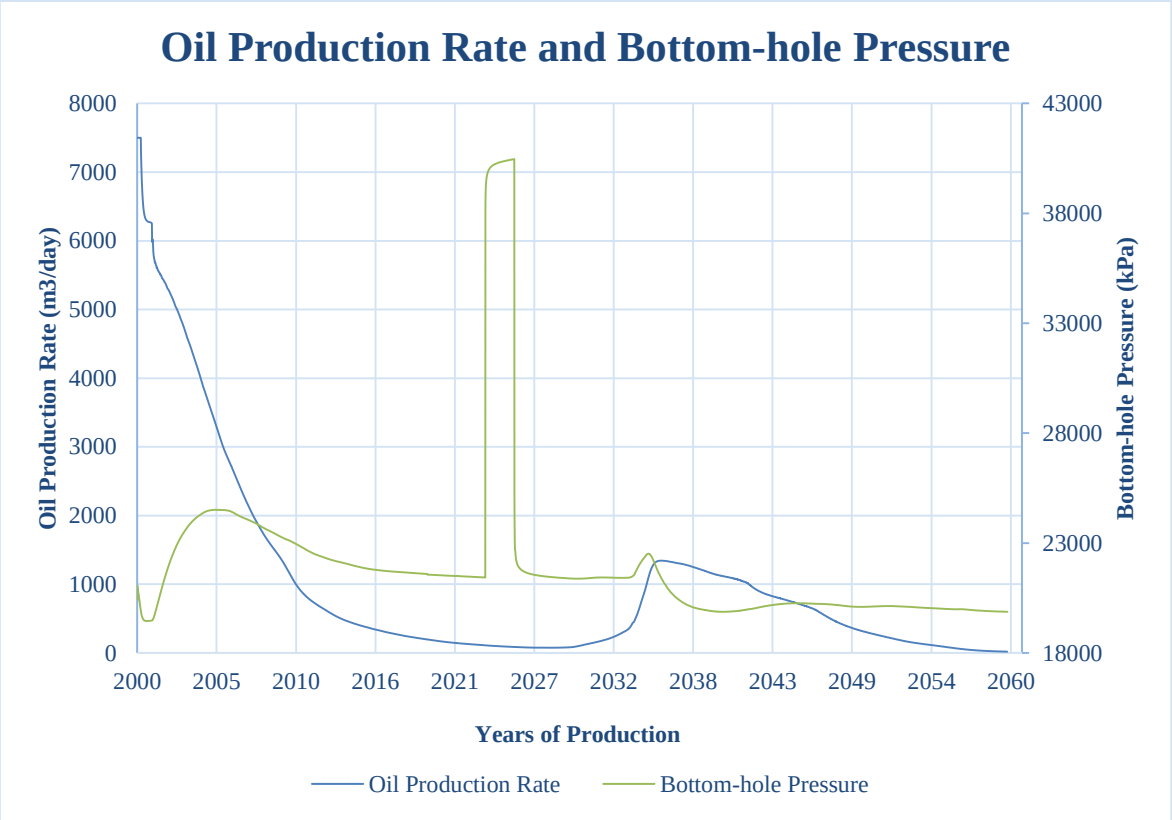

Figure 5.49: Oil production rate and bottom-hole pressure for the hybrid LSSP-process.

In this trial, the surfactant adsorption onto rock is activated, and the cumulative oil recovery is reduced to 84.09%. A total of $9.2 \cdot 10^3$ m^3 less oil is produced compared to the previous case with no adsorption of either chemicals. The oil production difference is not grand, indicating that the injected surfactant slug size is larger than the surfactants adsorbed [36].

The effects from the composite low salinity waterflooding, surfactant flooding and polymer flooding are also exemplified through the water cut and oil production rate. The water cut abruptly decreases from 98.90% to 82.14% due to the LSSP-slug. Thereafter the water cut increases steadily and eventually reaches 99.74%. The oil production rate displays the opposite behavior, and increases from 76.09 m^3/day to 1343.18 m^3/day at its peak, before reducing to 19.43 m^3/day at the end of production. However, both the water cut and oil production rate do not differ excessively from the previous study. The water cut was 0.01% higher when surfactant adsorption is activated, and the reservoir was producing 0.83 m^3 additional oil each day at the last production date, compared to the previous trial.

The reservoir pressure reaches a maximum at 40 468.3 kPa when the LSSP-slug is injected. Thenceforth, it decreases before reaching a new local maximum of 22 515.3 kPa. At the end of production time, the pressure has declined to 19 872.8 kPa.

5.7.2.4 *Surfactant and Polymer Adsorption*

In this simulation study, both surfactant and polymer adsorption are activated. The surfactant adsorption is the same as in chapter 5.7.2.3, and the polymer adsorption is assumed to be 0.05 mg/g. The simulation results are visualized in figures 5.50 and 5.51:

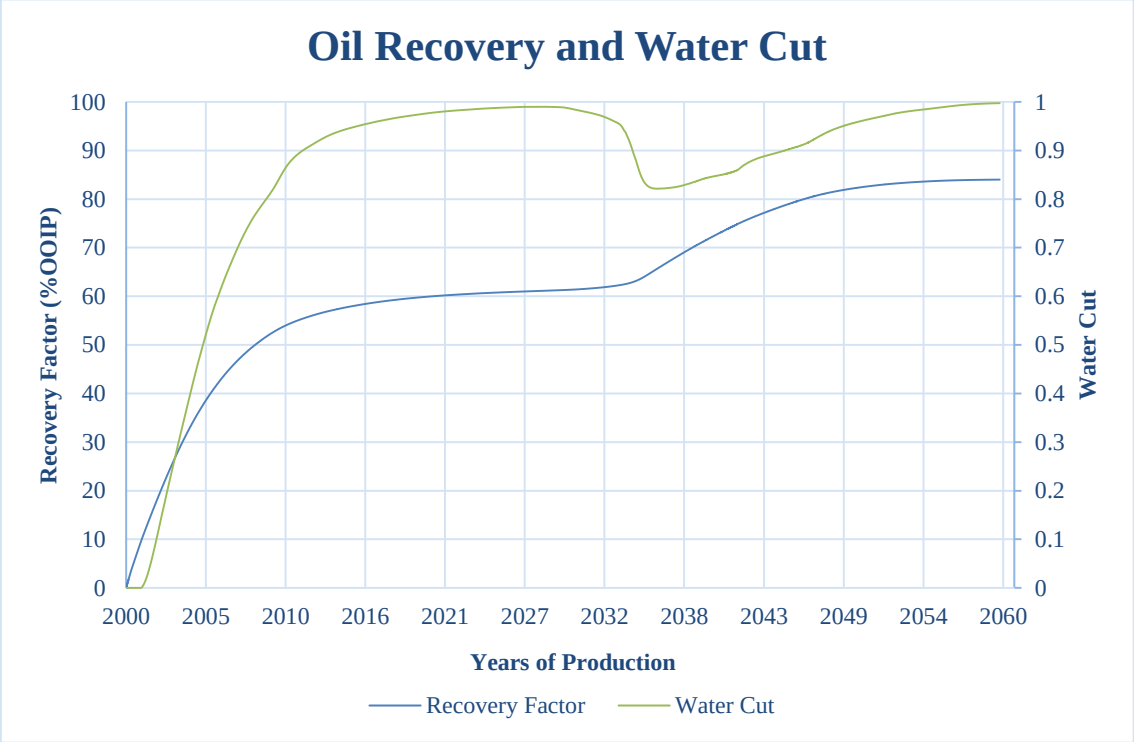

Figure 5.50: Cumulative oil recovery and water cut for the hybrid LSSP-process.

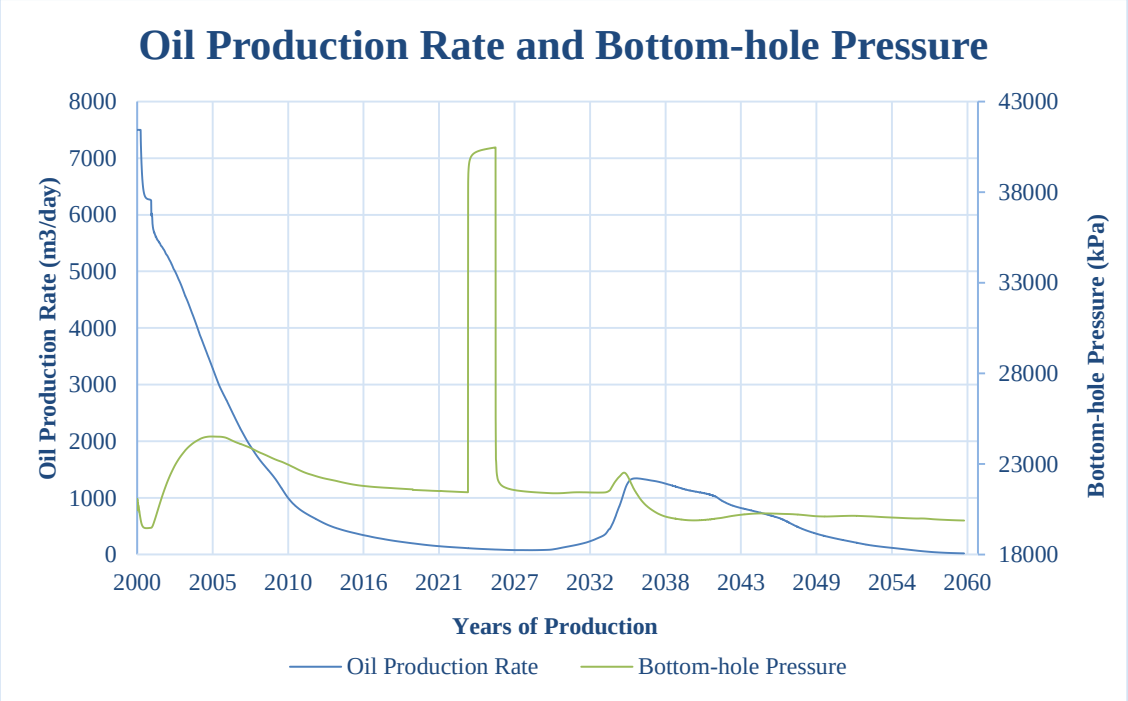

Figure 5.51: Oil production rate and bottom-hole pressure for the hybrid LSSP-process.

The activation of both surfactant and polymer adsorption decreases the cumulative oil recovery to 84.01%. The reservoir produces $3.1 \cdot 10^4$ m^3 less oil than when no adsorption is assumed, and $2.2 \cdot 10^4$ m^3 less oil than when only surfactant adsorption is active.

In regards to water cut, it does not differ from the previous trials. However, the oil production rate is somewhat increased, and at the last production date, the reservoir is producing oil at 19.72 m^3/day. This corresponds to 0.83 m^3 more oil each day than when no adsorption is assumed, and 0.29 m^3 more oil each day than when only surfactant adsorption is activated.

The pressure is highly increased by the polymers, and reaches a maximum of 40 468.2 kPa. Thenceforward, it decreases again, and reaches a new local maximum of 22 513.7 kPa. Ultimately, the pressure declines to 19 873.9 kPa.

5.7.3 Comparison of Simulation Results

This section includes a comparison of the different adsorption scenarios for both slug sizes. A summary is presented in table 5.14:

Table 5.14: Production results for the six simulation studies.

Study Case	**Oil Produced (m^3)**	**Recovery Factor (%OOIP)**	**Water Cut (%)**	**Oil Production Rate (m^3/day)**	**Bottom-hole Pressure (kPa)**
1/3 PV – no ads	$2.2245 \cdot 10^7$	85.25	99.83	12.62	20 193.6
1/3 PV – surf ads	$2.2226 \cdot 10^7$	85.18	99.83	12.65	20 194.2
1/3 PV - surf+poly ads	$2.2199 \cdot 10^7$	85.08	99.83	12.73	20 202.5
1/6 PV – no ads	$2.1952 \cdot 10^7$	84.13	99.74	18.89	19 869.0
1/6 PV – surf ads	$2.1943 \cdot 10^7$	84.09	99.74	19.43	19 872.8
1/6 PV – surf+poly ads	$2.1921 \cdot 10^7$	84.01	99.74	19.72	19 873.9

In summary, the cumulative oil recovery is higher for the 1/3 PV slug size, and the adsorption of each chemical reduces the oil recovery. Since the recovery is less, there is still more oil left in the reservoir. Thus, the oil production rate and reservoir pressure are somewhat higher. In corresponding manner to the oil production rate, the water cut is lower. The differences in cumulative oil recovery are visualized in figure 5.52.

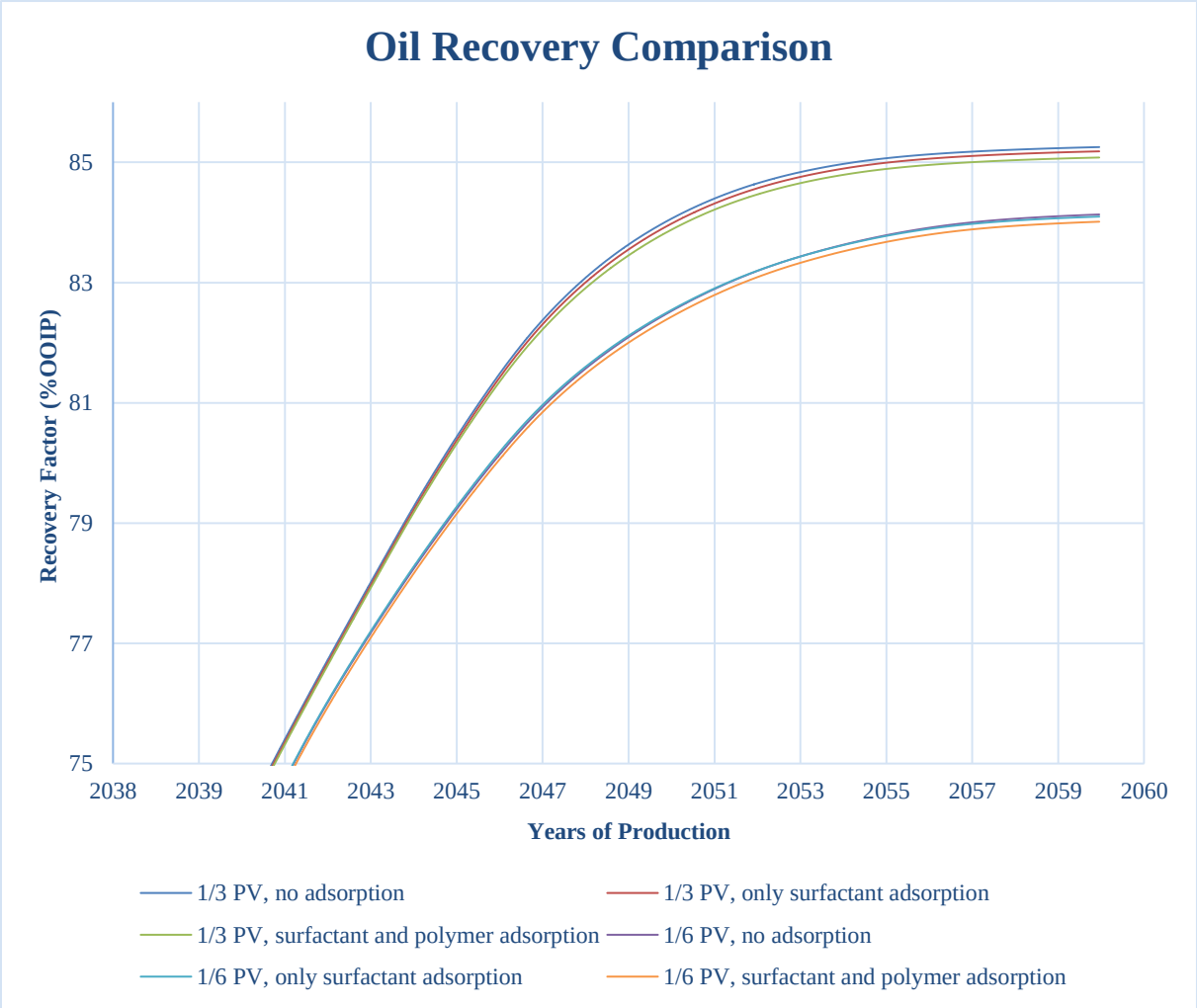

Figure 5.52: Oil recovery comparison.

5.7.4 Discussion and Summary

According to the simulation results, the adsorption of the EOR-chemicals reduces the oil recovery. Nevertheless, the decrease is not severe, indicating that the surfactants and polymers are still active despite the adsorption. Furthermore, the slug size is not broken down by adsorption [36]. The decreased oil recovery indicates a higher oil saturation within the reservoir at the termination of production. Thus, the oil production rate will be somewhat higher for the trials with activated adsorption, and the water cut is for that reason lower. Moreover, an increased oil saturation within the reservoir coincides with a reduced water relative permeability, and the remaining oil globules may be obstacles for the water flow [22]. This can lead to an increase in reservoir pressure.

In terms of slug sizes, the 1/3 slug size yields a cumulative oil recovery 1.27% higher than when the slug size is divided in half for the case studies with activated surfactant and polymer adsorption. This amounts to an oil volume of $2.78 \cdot 10^5$ m^3. Although the larger slug size generates a higher oil production, it is not likely that the additional oil volumes will counteract the expenses of the prolonged chemical injection.

Chapter 6

Overall Discussion

The wettability change towards a more water-wet state and destabilization of oil layers are in general assumed the main contributors to incremental oil recovery during low salinity waterflooding [11, 13, 96, 97]. According to Anderson (1987), water-wet reservoirs yield the highest recoveries during waterflooding due to the distribution and flow of reservoir fluids. Under water-wet conditions, the risk of viscous fingering and other frontal instabilities is reduced, having a significant impact on macroscopic sweep and timing of water breakthrough. In a homogenous water-wet reservoir, the breakthrough-, economical-, and ultimate oil recoveries are nearly identical, meaning that less injection water is required to produce a selected volume of oil [40].

The effects of lowering the injection water salinity concentration from 40 000 ppm to 4000 ppm were demonstrated during simulation studies. The total cumulative oil recovery was improved by 8.13 % compared to conventional seawater flooding in a secondary mode (S_{wi}). Additionally, the water cut remained at lower values for a longer time period, and the oil production rate was significantly higher. These discoveries signify a macroscopic sweep enhancement proposed by an increased water-wetting preference by the reservoir rock.

Incremental oil recovery by low salinity waterflooding was also observed in a tertiary mode (S_{or}), as implemental and operational expenses can be risen to undesired levels during a long low salinity waterflooding process. Sensitivity studies revealed that a short secondary phase (high salinity waterflooding) and a long tertiary phase (low salinity waterflooding) yielded the highest oil recovery. Commencing low salinity water injection subsequent to 1 PV of high salinity waterflooding resulted in a 1.33% higher recovery than when 1 ½ PV of high salinity water was flooded through the reservoir prior to low salinity waterflooding, and a 4.89% higher recovery than for the 2 PV high salinity water preflush. The longer tertiary phase leads to a higher recovery since the diluted water has more time to interact with the COBR-system, and consequently give rise to mechanisms releasing trapped oil, like multicomponent ion exchange (MIE), double layer expansion, fine migration, and an increased pH [13]. Furthermore, the introduction of low salinity water at an early stage may prevent further trapping of oil since it is more likely to encounter a continuous oil phase. When injected at a later stage after a prolonged high salinity waterflood, most of the oil may already be trapped and challenging to mobilize [5].

The initial pressure buildup after 1 PV of low salinity water is injected is mainly due to clay swelling, mobilization and trapping of fines, reduction in water relative permeability due to a wettability change, and the water flux into unswept zones [71, 96, 97]. Nevertheless, the accelerated oil production induced by the low salinity water leaves less oil in the reservoir, which may ultimately increase the water relative permeability and reduce reservoir pressure.

According to a simulation study, surfactants were able to increase oil recovery by enhancing the microscopic sweep without a pre-established low salinity environment. In a similar trial, polymers were also effective in enlarging oil recovery by a macroscopic sweep enhancement after an initial high salinity waterflooding. During the simulations of continuous polymer flooding, the injection rate was reduced due to a severe pressure buildup within the reservoir.

The purpose of surfactant flooding is to lower the interfacial tension between oil and water, leading to a deformation of capillary trapped oil droplets that enables migration through narrow pore constrictions [57]. Polymer flooding ensures a more stable displacement of oil, and diverts the displacing water into oil zones previously bypassed. The purpose of polymer flooding is to optimize the macroscopic sweep of water, and will not affect the microscopic sweep [29]. The simulation studies of continuous surfactant and polymer injection, respectively, confirm that the EOR-chemicals are individually effective in rising oil recovery without a pre-established low salinity environment.

A simulation study revealed that the surfactants are able to further enhance oil recovery after low salinity water injection becomes inefficient. The surfactants were effective at $S_{or,LS}$, and increased the total oil recovery by 23%. When injected after a production plateau for the previous low salinity waterflooding process, the surfactants were able to generate a higher cumulative oil production than when injected after seawater. The endpoint oil production rate was 1.60 m^3/day subsequent to the continuous surfactant flooding injected after high salinity waterflooding, indicating that little additional oil is recoverable. In comparison, the endpoint oil production rate for the low salinity process followed by surfactant flooding was 40.58 m^3/day, indicating that more oil may be recovered. A previous laboratory study conducted by Alagic et al. (2010) confirms that injecting surfactants after a low salinity environment has been established is beneficial for oil recovery. Due to the sensitivity of surfactants towards salinity, they are more able to effectively reduce interfacial tension and increase the capillary number in a low salinity habitat [14]. At low salinities, the surfactants form oil-in water emulsions (Windsor type I), and the loss of surfactants to the oleic phase is prevented. Moreover, studies reveal that the Windsor type I - salinity range may be more beneficial for oil recovery even though the interfacial tension is lower for intermediate salinities (Windsor type III). These claims are based on the retention and solubility issues connected with the Windsor type III behavior [4].

Polymers are also sensitive to high salinities, and their ability to effectively increase water viscosity may be greatly reduced due to screening of the electrostatic repulsions among the anions on the polymer molecule chain [64]. However, simulation studies conducted in this thesis confirm that the viscosifying chemicals are able to increase oil recovery without a pre-established low salinity environment.

Ultimately, low salinity water, surfactants and polymers were injected in a composite experiment. The low salinity water was injected to establish a diluted environment for the upcoming chemicals. Surfactants and polymers were introduced individually before a chase slug of low salinity water was utilized to displace the chemicals towards the producing well. Several simulations were conducted to study the effects of chemical adsorption and slug sizes

of surfactants and polymers. According to the simulations, the inevitable adsorption of surfactant and polymers onto reservoir rock reduced the oil production. However, the reduction was not grand, indicating that the chemicals are effective despite the adsorption, and that the slug sizes were not too small [36]. In comparison to the previous simulation studies of the individual tertiary EOR-processes, the combined low salinity water, surfactants and polymers generated a higher oil recovery. The reduction of surfactant and polymer slug sizes from 1/3 PV to 1/6 PV only led to a 1.27% lower oil recovery factor, amounting to $2.78 \cdot 10^5$ m^3 oil. Although the 1/3 slug size generated a higher oil production, the expenditure of the additional chemicals may exceed the profits.

Chapter 7

Conclusions

This simulation study has examined the feasibility of EOR-implementation in a reservoir model by the usage of the compositional reservoir simulator STARS. The ambition was to study the effects of low salinity waterflooding, surfactant flooding and polymer flooding, and if the composite effect of the tertiary fluids enables mobilization of oil trapped after high salinity waterflooding.

Based on the simulation results, the following conclusions have been established:

1. Low salinity waterflooding proves efficient in this reservoir model based on comparison studies of the EOR-process with conventional high salinity waterflooding in a secondary mode (S_{wi}). The reduction of brine salt content from 40 000 ppm in the high salinity water to 4000 ppm in the low salinity water is able to mobilize an additional 8.13% more oil. The incremental cumulative oil production is due to an increased water-wetness of the reservoir and destabilization of oil layers by reason of ionic interactions between the diluted water and the COBR-system. An increased water-wet state is interlinked with enhanced flooding performance, ensuring that more oil zones are contacted by the displacing injection water. Front instabilities are also reduced, exemplified through the lower water cut and higher oil production rate for the low salinity waterflood after 30 years of production. The initial pressure increase after low salinity water injection is caused by a water relative permeability reduction due to wettability alteration, in addition to clay swelling, fines trapping, and water flux into unswept zones.

2. Due to the additional expenses of low salinity waterflooding compared to conventional seawater flooding, injecting low salinity water in a tertiary mode (S_{or}) is more sensible from an economical viewpoint. Simulation studies of the timing of onset low salinity water injection reveal that the earlier the diluted water is introduced, the more effectively it enhances oil production. The longer time the low salinity water is allotted to interact with the reservoir, the more it is enabled to increase the sweep, exemplified through the higher cumulative oil produced. The case studies where the tertiary low salinity phase was shorter required more volumes of injected water to produce the same amount of oil. However, the optimal start-up time for low salinity water injection requires a comprehensive study of project economics, as the additional oil produced by a long tertiary phase may not exceed the costs of injecting low salinity water throughout the elongated low salinity water process.

3. The full potential of surfactants diluted in low salinity water was tested in order to resolve whether the EOR-process yields any effect without a pre-established low salinity environment. The surfactants were introduced after the initial high salinity waterflood had reached a water cut of 95%, and were injected continuously until almost no further oil production was achievable. By this method, the ultimate oil recovery potential by the surfactants was 83.36% of OOIP.

4. The full potential of oil production by polymer flooding without a pre-established low salinity environment was also examined, and revealed that 69.81% of the oil originally in place was produced by the viscosifying chemicals. The polymers diluted in low salinity water were injected after a water cut of 95% had been attained by high salinity waterflooding, and the results demonstrate that polymers are effective in enhancing the macroscopic sweep. Due to the severe pressure buildup caused by an increased water viscosity, the injection rate was reduced from 7500 m^3/day to 3500 m^3/day.

5. The ability of surfactants to further enhance oil recovery beyond the capability of low salinity water was tested. The surfactants were injected when the previous low salinity waterflooding was approaching a plateau, and the simulations demonstrated that the surfactant flooding process was able to mobilize 23% more oil by reducing interfacial tension between oil and water, and thereby increase the microscopic sweep in contacted zones. The total cumulative oil recovery after the surfactant injection was 83.55%, making this process more effective than the continuous surfactant flooding process, likely due to a pre-established low salinity environment.

6. A composite LSSP-injection study was conducted, where the effects of surfactant and polymer adsorption were examined, in addition to a sensitivity study on slug sizes. According to the simulations, the chemical adsorption reduced the oil recovery. Nevertheless, the EOR-chemicals were still effective in increasing oil recovery, indicating that the adsorption did not break down the slug size. The combined EOR-process yielded a higher oil recovery than the tertiary fluids alone. The reduction in surfactant and polymer slug size from 1/3 PV to 1/6 PV reduced the cumulative oil recovery by 1.27%. Due to the high implementation costs of surfactant and polymer flooding, the 1/6 slug size may be a more reasonable alternative.

Chapter 8

Recommendations for Further Work

This simulation study reveals a positive effect from the combination of low salinity waterflooding, surfactant flooding and polymer flooding. Nevertheless, there are some recommendations that may be implemented in further work on this topic:

1. Considering that the expenses of low salinity water injection, surfactant injection and polymer injection can be severe, a thorough economical analysis is necessitated, with an emphasis on the profits from the increased oil recovery by the EOR-processes versus the implementation expenditure.

2. Simulation studies conducted in this thesis revealed that the 1/3 PV surfactant and polymer slug size only generated 1.27% more oil than when the slug size was divided in half. It is recommended to perform more sensitivity studies on slug sizes, in order to evaluate whether the slug size can be reduced further and still stimulate oil recovery.

3. STARS is currently unable to correctly handle multiple relative permeability interpolation of more than two relative permeability sets. This indicates that only two components can be defined, which in this thesis are salt and surfactants. It is not possible to define more than two interpolation routines in the simulator simultaneously, and in the case of low salinity waterflooding process in combination with surfactants and polymers, a third set of polymer relative permeability curves cannot be defined. It is encouraged to conduct further research on this topic.

4. The viscosity of the microemulsion surfactant phase can affect the flow patterns and displacement of the fluids within the reservoir. Thus, a sensitivity study on the optimal microemulsion viscosity of the surfactant phase should be conducted. The viscosity of the following polymer slug should be in correspondence with the microemulsion viscosity, in order to enable a stable displacement of the microemulsion phase during LSSP-flooding.

Bibliography

1. *International Energy Outlook 2017*, in Analysis & Projections, U.S. Energy Information Administration, September, 2017

2. Muggeridge A., Cockin A., Webb K., Frampton H., Collins I., Moulds T., Salino P., *Recovery rates, enhanced oil recovery and technological limits*, Philosophical Transactions of the Royal Society A, 2014. **372**. doi:10.1098/rsta.2012.0320.

3. Dautel M., Pitcher .J, Bittear M., *Locating Bypassed Reserves in Geologically Complex Mature Fields Environments**, Search and Discovery Article #41022, 2012. Adapted from extended abstract prepared in conjunction with poster presentation at AAPG International Convention and Exhibition, Singapore, 16-19 September 2012.

4. Spildo K., Sun L., Djurhuus K., Skauge A., *A Strategy for Low Cost, Effective Surfactant Injection*, Journal of Petroleum Science and Engineering, 2014, **117**(5). doi: 10.1016/j.petrol.2014.03.006.

5. Shiran S. B., Skauge A., *Enhanced Oil Recovery (EOR) by Combined Low Salinity Water/Polymer Flooding*, Energy & Fuels, 2013. **27**(3): p. 1223-1235. doi: 10.1021/ef301538e.

6. Pettersen Ø., Skauge A., *Simulation of Complex Composite EOR Processes at Lab and Field Scale*, in SPE Europec featured at 78th EAGE Conference and Exhibition. 2016, Society of Petroleum Engineers: Vienna, Austria. doi:10.2118/180098-MS.

.

7. *Short-Term Energy Outlook*, in Analysis & Projections, U.S. Energy Information Administration, February, 2018.

8. Stosur G. J., Hite J. R., Carnahan N. F., Miller, K., *The Alphabet Soup of IOR, EOR and AOR: Effective Communication Requires a Definition of Terms*, in *SPE* International Improved Oil Recovery Conference in Asia Pacific. 2003, Society of Petroleum Engineers: Kuala Lumpur, Malaysia. doi:10.2118/84908-MS.

9. Teigland R., Kleppe J., *EOR Survey in the North Sea*, in SPE/DOE Symposium on Improved Oil Recovery. 2006, Society of Petroleum Engineers: Tulsa, Oklahoma, USA. doi:10.2118/99546-MS.

10. Abdalla A., Sun R., Guiyun T., Huang A., Wang M., *Low Salinity as New Technique of Enhanced Oil Recovery*, International Journal of Chemical Engineering and Applications, 2017. **8**. doi: 10.18178/ijcea.2017.8.2.641.

11. Strand S., Puntervold T., Austad T., *Water based EOR from clastic oil reservoirs by wettability alteration: A review of chemical aspects*, Journal of Petroleum Science and Engineering, 2016. **146**: p. 1079-1091. doi: 10.1016/j.petrol.2016.08.012.

12. Alotaibi M.B., Azmy R., Nasr-El-Din H.A,, *A Comprehensive EOR Study Using Low Salinity Water in Sandstone Reservoirs*, in SPE Improved Oil Recovery Symposium. 2010, Society of Petroleum Engineers: Tulsa, Oklahoma, USA. doi:10.2118/129976-MS.

13. Austad T., Rezaeidoust A., Puntervold T,, *Chemical Mechanism of Low Salinity Water Flooding in Sandstone Reservoirs*, in SPE Improved Oil Recovery Symposium. 2010, Society of Petroleum Engineers: Tulsa, Oklahoma, USA. doi:10.2118/129767-MS.

14. Alagic, E, Skauge A., *Combined Low Salinity Brine Injection and Surfactant Flooding in Mixed−Wet Sandstone Cores*, Energy & Fuels, 2010. **24**(6): p. 3551-3559. doi: 10.1021/ef1000908.

15. Lien J.R., Jakobsen M., Skauge A., *PTEK100 - Introduksjon til petroleums- og prosessteknologi.* Universitetet i Bergen, 2007. 99 p.

16. Lien J., *PTEK211 - Grunnleggende Reservoarfysikk (Kjerneanalyse og logging).* Institutt for fysikk og teknologi, Universitetet i Bergen, 2004. 176 p.

17. Satter A., Iqbal G., Buchwalter J., *Rock Characteristics, Significance in Petroleum Reservoirs, and Applications* in Practical Enhanced Reservoir Engineering: Assisted with Simulation Software. 2007, Tulsa, Oklahoma: PennWell Corporation. p. 17-30.

18. Giles, M.R. and R.B. de Boer, *Secondary porosity: creation of enhanced porosities in the subsurface from the dissolution of carbonate cements as a result of cooling formation waters*, Marine and Petroleum Geology, 1989. **6**(3): p. 261-269. doi: 10.1016/0264-8172(89)90005-6.

19. Reaves M., *Porosity, Cement and Packing*, Department of Civil and Geological Engineering, University of Saskatchewan, Canada.

20. Nelson S., *Sediment and Sedimentary Rocks*, Physical Geology, Tulane University, United States, 2018.

21. Hu, X., Hu, S., Jin, F., Huang, S., *Physical Properties of Reservoir Rocks*, in Physics of Petroleum Reservoirs, Springer-Verlag Berlin Heidelberg, 2017. p. 7-164. doi: 10.1007/978-3-662-55026-7.

22. Anderson W.G., *Wettability Literature Survey Part 5: The Effects of Wettability on Relative Permeability.* 1987. doi:10.2118/16323-PA.

23. Kronberg B., Holmberg K., Lindman B., *Surface and Interfacial Tension*, Surface Chemistry of Surfactants and Polymers. John Wiley & Sons, Ltd., 2014. p. 232-251. doi: 10.1002/9781118695968.

24. Alagic E., Spildo, K., Skauge, A., Solbakken, J., *Effect of crude oil ageing on low salinity and low salinity surfactant flooding*, Journal of Petroleum Science and Engineering, 2011. **78**(2): p. 220-227. doi: 10.1016/j.petrol.2011.06.021.

25. Tiab D., Donaldson E.C., *Capillary Pressure,* Petrophysics, 4th Edition: Theory and Practice of Measuring Reservoir Rock and Fluid Transport Properties. 2015: Gulf Professional Publishing. p. 313-359.

26. Anderson W.G., *Wettability Literature Survey- Part 4: Effects of Wettability on Capillary Pressure.* 1987. doi:10.2118/15271-PA.

27. Viswanath D.S., Ghosh T., Prasad D.H.L., Dutt N.V.K., Rani K.Y., *Theories of Viscosity*, Viscosity of Liquids: Theory, Estimation, Experiment, and Data, Springer Netherlands, 2007. p. 109-133. doi: 10.1007/978-1-4020-5482-2.

28. Yoon S.H., *Rheological property of biological mixed liquor*, Membrane Bioreactor Processes: Processes and Applications, CRC Press, 2016. 433 p.

29. Sorbie K., *Polymer-Improved Oil Recovery*, Glasgow: Blackie CRC Press, 1991. 359 p.

30. Mireault R., Dean L., *Reservoir Engineering for Geologists*, Canadian Society of Petroleum Geologists, CPGS Reservoir Magazine, 2008.

31. Glasbergen G., Wever D., Keijzer E., Farajzadeh R., *Injectivity Loss in Polymer Floods: Causes, Preventions and Mitigations*, in SPE Kuwait Oil and Gas Show and Conference, 2015, Society of Petroleum Engineers: Mishref, Kuwait. doi:10.2118/175383-MS.

32. Miller R.G., Sorrell S.R., *The future of oil supply*, Philosophical Transactions of the Royal Society A, 2013. **372**. doi: 10.1098/rsta.2013.0179.

33. Donaldson E.C., *Enhanced Oil Recovery: Fundamentals and analysis.* Old SPE Journal, 1985. **23**: p. 311-326.

34. Lien J., *PTEK212 - Reservoarteknikk I.* Institutt for fysikk og teknologi, Universitetet i Bergen, 2014. 173 p.

35. Habermann B., *The Efficiency of Miscible Displacement as a Function of Mobility Ratio*, Petroleum Transactions, AIME, 1960. **219,** p. 264-272. Paper presented at 35th Annual Fall Meeting of SPE, Oct. 2-5, 1960 in Denver, and at the California Regional Fall Meeting of SPE, Oct. 20-21, 1960 in Pasadena, California.

36. Skauge A., *PTEK313 - Reservoarteknikk II.* Universitetet i Bergen, 2009. 217 p.

37. Mohamed A.M.A., Abdullah A.M., Younan A.N., *Corrosion Behavior of Superhydrophobic Surfaces: A Review*, Arabian Journal of Chemistry, King Saud University, 2014. **43**. p. 749–765.

38. Abdallah W., *Fundamentals of Wettability*, Oilfield Review, Schlumberger, 2007. **19** (2).

39. Ahmed T., *Section 2.3: Wettability,* Working Guide to Reservoir Rock Properties and Fluid Flow. Fundamentals of Rock Properties, 2006, Gulf Prodessional Publishing. p 40.

40. Anderson, W.G., *Wettability Literature Survey-Part 6: The Effects of Wettability on Waterflooding.* 1987. doi:10.2118/16471-PA.

41. Skauge A., *Selected Topics in Petroleum Engineering*. Lecture Notes from PTEK312. University of Bergen.

42. Ruidiaz, E.M., Winter A., Trevisan O.V., *Oil recovery and wettability alteration in carbonates due to carbonate water injection*, Journal of Petroleum Exploration and Production Technology, 2018. **8**(1): p. 249-258. doi: 10.1007/s13202-017-0345.

43. Anderson, W., *Wettability Literature Survey- Part 2: Wettability Measurement.* 1986. doi:10.2118/13933-PA. **10**(1).

44. Roof J.G., *Snap-Off of Oil Droplets in Water-Wet Pores,* Society of Petroleum Engineers, 1970, doi:10.2118/2504-PA.

45. Raza S.H., Treiber L.E., Archer D.L, *Wettability of reservoir rocks and its evaluation.* Prod. Mon, 1968. **32**.

46. Morrow N.R., *Wettability and Its Effect on Oil Recovery,* 1990. **42**(12). doi:10.2118/21621-PA.

47. Jadhunandan P., *Effects of Brine Composition, Crude Oil, and Aging Conditions on Wettability and Oil Recovery*, New Mexico Institute of Mining & Technology, 1990.

48. Wardlaw N.C., Li Y., *The Influence of Wettability and Critical Pore-Throat Size Ratio on Snap-off*, Journal of Colloid and Interface Science, 1986. **109**(2), p. 461-472.

49. Wever D.A.Z., Picchioni F., Broekhuis A.A, *Polymers for enhanced oil recovery: A paradigm for structure–property relationship in aqueous solutio*, Progress in Polymer Science, 2011. **36**(11). p. 1558-1628.

50. Thomas S., *Enhanced Oil Recovery – An Overview*, Oil & Gas Science and Technology, IFP International Conference, 2007. **63**. p. 9-19. doi: 10.2516/ogst:2007060.

51. Lake L., *A Technical Survey of Micellar Polymer Flooding.* Presented at EOR, a symposium for the Independent Producer, Southern Methodis University, Dallas, Texas 1984.

52. Cullum D.C., *Surfactant types; classification, identification, separation*, Introduction to Surfactant Analysis, Springer Netherlands, 1994. p. 17-41. doi: 10.1007/978-94-011-1316-8.

53. Som I., Bhatia K., Yasir M., *Status of surfactants as penetration enhancers in transdermal drug delivery,* Journal of Pharmacy and BioAllied Sciences, 2012. **4**(1). doi: 10.4103/0975-7406.92724.

54. Zolotukhin A.B., Ursin J.R., *Introduction to Reservoir Engineering*, Høyskoleforlaget, Norwegian Academic Press, 2000. 407 p.

55. Lake, L.W., *Enhanced oil recovery*. 1989, Englewood Cliffs, N.J.: Prentice Hall. 550 p.

56. Ahsan T.R., Aveyard R., Binks B.P., *Winsor transitions and interfacial film compositions in systems containing sodium dodecylbenzene sulphonate and alkanols*, Colloids and Surfaces, 1991. **52**. p. 339-352.

57. Kumar A., Mandal A., *Synthesis and physiochemical characterization of zwitterionic surfactant for application in enhanced oil recovery*, Journal of Molecular Liquids, 2017. **243**. p. 61-71.

58. Koltzenburg S., Maskos M., Nuyken Oskar., *Introduction and Basic Consepts*, Polymer Chemistry, Springer-Verlag Berlin Heidelberg, 2017. p. 1-16. doi: 10.1007/978-3-662-49279-6.

59. Saldivar-Guerra E., Vivaldo-Lima E., *Introduction to Polymers and Polymer Types*, Handbook of Polymer Synthesis, Characterization, and Processing, Wiley, 2013. p. 3-40. doi: 1117316.

60. Zamani N., Bondino I., Kaufmann R., Skauge A., *Computation of polymer in-situ rheology using direct numerical simulation*, Journal of Petroleum Science and Engineering, 2017. **159**: p. 92-102. doi: 10.1016/j.petrol.2017.09.011.

61. Lund T., Bjørnestad E.Ø., Stavland A., Gjøvikli N.B., Fletcher A.J.P., Flew S.G., Lamb S.P., *Polymer retention and inaccessible pore volume in North Sea reservoir material*, Journal of Petroleum Science and Engineering, 1992. **7**(1). p. 25-32. doi: 10.1016/0920-4105(92)90005-L.

62. Dawson R., Lantz R.B., *Inaccessible Pore Volume in Polymer Flooding*, Society of Petroleum Engineers, 1972. **12**(5). doi:10.2118/3522-PA.

63. Cohen Y., Christ F.R., *Polymer Retention and Adsorption in the Flow of Polymer Solutions Through Porous Media*, Society of Petroleum Engineers, 1986. **1**(2). doi:10.2118/12942-PA.

64. Zhang Q., Zhou J., Zhai Y., Feng Q., Gao G., *Effect of salt solutions on chain structure of partially hydrolyzed polyacrylamide*, Journal of Central South University of Technology, 2008. **15**(1). p. 80-83. doi: 10.1007/s11771-008-0319-x.

65. Yun W., Kovscek A.R., *Microvisual investigation of polymer retention on the homogeneous pore network of a micromodel*, Journal of Petroleum Science and Engineering, 2015. **128**. p. 115-127. doi: 10.1016/j.petrol.2015.02.004.

66. Collins I.R., Couves J.W., Hodges M., McBride E.K., Pedersen C.S., Salino P.A., Webb K.J., Wicking C., Zeng H., *Effect of Low Salinity Waterflooding on the Chemistry of the*

Produced Crude Oil, in SPE Improved Oil Recovery Conference. 2018, Society of Petroleum Engineers: Tulsa, Oklahoma, USA. doi:10.2118/190191-MS.

67. Smith, K.W., *Brines as Flooding Liquids.* Paper presented at 7th Annual Technical Meeting, Min. Ind. Expt. Sta., Penn. State College, 1942.

68. Martin, J.C., *The Effects of Clay on the Displacement of Heavy Oil by Water.* Paper SPE 1411-G presented at Venezuelan Annual Meeting, 14-16 October, Caracas, Venezuela, 1957.

69. Bernard, G.G., *Effect of Floodwater Salinity on Recovery of Oil from Cores Containing Clays.* Paper SPE 1725, presented at SPE California Regional Meeting, 26-27 October, Los Angeles, California, USA, 1967.

70. Yildiz H.O., Morrow N.R., *Effect of brine composition on recovery of Moutray crude oil by waterflooding*, Journal of Petroleum Science and Engineering, 1996. **14**(3): p. 159-168. doi: 10.1016/0920-4105(95)00041-0.

71. Tang G-Q., Morrow N.R, *Influence of brine composition and fines migration on crude oil/brine/rock interactions and oil recovery*, Journal of Petroleum Science and Engineering, 1999. **24**(2). p. 99-111. doi: 10.1016/S0920-4105(99)00034-0.

72. Filoco P.R., Sharma M.M., *Effect of Brine Salinity and Crude Oil Properties on Relative Permeabilities and Residual Saturations*, in *SPE Annual Technical Conference and Exhibition*, Society of Petroleum Engineers, New Orleans, Louisiana, 1998.

73. Zhang Y., Morrow N.R., *Comparison of Secondary and Tertiary Recovery With Change in Injection Brine Composition for Crude-Oil/Sandstone Combinations*, in *SPE/DOE Symposium on Improved Oil Recovery*, Society of Petroleum Engineers, Tulsa, Oklahoma, 2006.

74. Webb K.J., Black C.J.J., Al-Ajeel H., *Low Salinity Oil Recovery - Log-Inject-Log*, in *SPE/DOE Symposium on Improved Oil Recovery*, Society of Petroleum Engineers, Tulsa, Oklahoma, 2004. doi:10.2118/89379-MS

75. Skrettingland K., Holt T., Tweheyo M.T., Skjevrak I., *Snorre Low-Salinity-Water Injection--Coreflooding Experiments and Single-Well Field Pilot*, Society of Petroleum Engineers, 2011. doi: 10.2118/129877-PA.

76. Donaldson E.C., Thomas R.D., *Microscopic Observations of Oil Displacement in Water-Wet and Oil-Wet Systems*, in Fall Meeting of the Society of Petroleum Engineers of AIME, Society of Petroleum Engineers, New Orleans, Louisiana, 1971. doi:10.2118/3555-MS.

77. Hilner E., Andersson M.P., Hassenkam T., Matthiesen J., Salino P.A., Stipp S.L.S., *The effect of ionic strength on oil adhesion in sandstone – the search for the low salinity mechanism*, Scientific Reports, 2015. **5**. doi:10.1038/srep09933.

78. Lager A., Webb K. J., Black C. J. J., Singleton M., Sorbie, K. S., *Low Salinity Oil Recovery - An Experimental Investigation1*, Society of Petrophysicists and Well-Log Analysts, 2008. **49**(1).

79. Pouryousefy E., Xie Q., Saeedi A., *Effect of multi-component ions exchange on low salinity EOR: Coupled geochemical simulation study*, Petroleum, 2016. **2**(3). p. 215-224. doi: 10.1016/j.petlm.2016.05.004.

80. Ligthelm D. J., Gronsveld J., Hofman J., Brussee N., Marcelis,F., van der Linde H., *Novel Waterflooding Strategy By Manipulation Of Injection Brine Composition*, in EUROPEC/EAGE Conference and Exhibition, 2009, Society of Petroleum Engineers: Amsterdam, The Netherlands. doi:10.2118/119835-MS.

81. Pashley, R., *Applied Colloid and Surface Chemistry*, John Wiley & Sons, Ltd, 2005.

82. Leite F., Bueno C., Da Roz A., Ziemath E., Oliveira O., *Theoretical models for surface forces and adhesion and their measurement using atomic force microscopy*, Int J Mol Sci, 2012. **13**(10). p. 12773-856. doi: 10.3390/ijms131012773.

83. Berg S., Cense A. W., Jansen E., Bakker, K., *Direct Experimental Evidence of Wettability Modification By Low Salinity*, Society of Petrophysicists and Well-Log Analysts, 2010. **51**(5).

84. Surkalo H., *Enhanced Alkaline Flooding*, Journal of Petroleum Technology, 1990. **42**(1). doi: 10.2118/19896-PA.

85. McGuire P. L., Chatham J. R., Paskvan F. K., Sommer D. M., Carini F. H., *Low Salinity Oil Recovery: An Exciting New EOR Opportunity for Alaska's North Slope*, in *SPE Western Regional Meeting*. 2005, Society of Petroleum Engineers: Irvine, California. doi:10.2118/93903-MS.

86. Tavassoli S., Kazemi Nia Korrani A., Pope, G.A., Sepehrnoori K., *Low-Salinity Surfactant Flooding—A Multimechanistic Enhanced-Oil-Recovery Method*, Society of Petroleum Engineers, 2016. **21**(03). doi:10.2118/173801-PA.

87. Mohammadi H., Jerauld G., *Mechanistic Modeling of the Benefit of Combining Polymer with Low Salinity Water for Enhanced Oil Recovery*, in SPE Improved Oil Recovery Symposium, Society of Petroleum Engineers, 2012, Tulsa, Oklahoma, USA. doi:10.2118/153161-MS.

88. Trushenski S.P., *Micellar flooding: sulfonate-polymer interaction*, Improved Oil Recovery by Surfactant and Polymer Flooding, Academic Press, 1977. p. 555-575.

89. Sheng J., *Surfactant-Polymer Flooding*, Modern Chemical Enhanced Oil Recovery: Theory and Practice, Elsevier Science & Technology, 2010. p.371-387.

90. Pope G.A., Schechter R.S., Tsaur K., Wang B., *The Effect of Several Polymers on the Phase Behavior of Micellar Fluids*, Society of Petroleum Engineers, 1982. **22**(6). doi:10.2118/8826-PA.

91. *CMG Computer Modelling Group LTD.* STARS: Thermal&Advanced Processes Simulator, 2018.

92. Skauge A., Ghorbani Z., Delshad M., *Simulation of Combined Low Salinity Brine and Surfactant Flooding* (sub ID: 9874), The EAGE IOR Symposium 12th-14th April 2011 in Cambridge, UK.

93. Skauge, A., *Modelling of Hybrid Waterflood EOR Processes*, EAGE 18th European Symposium on Improved Oil Recovery in Dresden, Germany, 16. April, 2015.

94. Khorsandi S., Qiao C., Johns R. T., *Displacement Efficiency for Low-Salinity Polymer Flooding Including Wettability Alteration*, Pennsylvania State University, Society of Petroleum Engineers, 2017: p. 417-430. **22**(2). doi:10.2118/179695-PA.

95. *STARS User Guide*. CMG Computer Modelling Group LTD., 2016.

96. Zhang Y., Xie X., Morrow N. R., *Waterflood Performance By Injection Of Brine With Different Salinity For Reservoir Cores*, in *SPE Annual Technical Conference and Exhibition*. 2007, Society of Petroleum Engineers: Anaheim, California, U.S.A. doi:10.2118/109849-MS.

97. Hussain F., Zeinijahromi A., Bedrikovetsky P., Badalyan A., Carageorgos T., Cinar Y., *An experimental study of improved oil recovery through fines-assisted waterflooding*, Journal of Petroleum Science and Engineering, 2013. **109**. p. 187-197. doi: 10.1016/j.petrol.2013.08.031.

Appendix: STARS Data File

The base case data file used as input in the numerical simulator STARS is presented in this part. This data file is the basis for all the simulations performed, with the appropriate changes of injection components and injection rate for each run.

```
**********************************************************************

'STARS test model'



INUNIT SI

** INPUT / OUTPUT CONTROL =========

WPRN GRID 0
OUTPRN GRID NONE
OUTPRN RES NONE

WSRF WELL 1
WSRF GRID TIME
OUTSRF WELL DOWNHOLE
OUTSRF WELL MASS MOLE COMPONENT ALL
OUTSRF WELL LAYER ALL
OUTSRF GRID PRES SO SW W CAPN LOGCAPN KRINTER
OUTSRF GRID PRES SO SW VISW
OUTSRF SPECIAL AVGVAR PRES
OUTSRF SPECIAL MOLEFRAC 'WI01' 'Salt'
OUTSRF SPECIAL MOLEFRAC 'OP01' 'Salt'
OUTSRF SPECIAL MOLEFRAC 'WI01' 'Surf'
OUTSRF SPECIAL MOLEFRAC 'OP01' 'Surf'
OUTSRF SPECIAL MOLEFRAC 'WI01' 'Poly'
OUTSRF SPECIAL MOLEFRAC 'OP01' 'Poly'



** GRID ============================

GRID CORNER 195 155 25
KDIR DOWN

include 'JS1_coord.grdecl'
include 'JS1_zcorn.grdecl'
include 'JS1_null.grdecl'
include 'JS1_PERMI.GRDECL'
include 'JS1_PERMJ.GRDECL'
include 'JS1_PERMK.GRDECL'
include 'JS1_POR.GRDECL'

END-GRID
```

```
** Rock compressibility
ROCKTYPE 1
CPOR  7.5E-7
PRPOR 19300

** FLUID DESCRIPTION ================

** Three-phase o-w-g, with live oil
** MODEL ncomp nfcomp nlcomp nwcomp
** ncomp: Total #comp
** nfcomp: #fluid comp (w,o,g)
** nlcomp: #liquid comp (w,o)
** nacomp: #aquous comp (w)


MODEL 6 6 6 4
COMPNAME 'Water' 'Salt' 'Surf' 'Poly' 'LiveOil' 'Gas'


** Table for K3 (gas/liquid)
GASLIQKV
** Table limits, p_lo p_hi T_lo T_hi
KVTABLIM 2500 42500 10 200
KVTABLE 'Gas'
2.630 1.846 1.581 1.446 1.363 1.307 1.265 1.232 1.206 1.184 1.165 1.148
      1.133 1.120 1.108 1.097 1.086
2.630 1.846 1.581 1.446 1.363 1.307 1.265 1.232 1.206 1.184 1.165 1.148
      1.133 1.120 1.108 1.097 1.086


** Molecular weights (estimates from typical values)
**   water  salt   surf   poly   oil   gas
CMM  0.018 0.05845 0.548  8.0  0.444 0.02144
** Critical pressure & temperature
PCRIT  0  0  0  0  0  0
TCRIT  0  0  0  0  0  0
** Mass density at ref. prs & temp



MASSDEN 1038.8 991 991 1000 846.3 401.0

** Liquid compressibility (1/kPa)
** Water    Salt      Surf     Poly   Oil      Gas
CP 4.15e-7  4.94e-7 4.94e-7  4.94e-7 1.66e-6  1.8e-6

** First coeff. of therm expansion coefficient
CT1  0.000184146 0 0 0 0.000184146 0.000184146

** Reference pressure ("MASSDEN" pres), temp., surface cond. press.
PRSR 100
TEMR 90
```

```
PSURF 101.1

**Specify gas oil separation at surface conditions
**SURFLASH SEGREGATED
**K_SURF 'LiveOil' 0
**K_SURF 'Gas'  130

** Viscosity table -- each table var. w. temp at given pressure
** Viscosity should be component values, which they're not so may need
** adjusting
**   temp   mu_w  mu_salt  mu_surf  mu_poly  mu_o    mu_g
VISCTABLE
      10    0.407 1.1    10.0     10000   1.25  0.304
     200    0.407 1.1    10.0     10000   1.25  0.304


** Nonlinear mixing rules: Found by requiring the resulting phase viscosity
** is linear between concentration end points.

** Nonlinear mixing rule for surfactant
** Mix-func defined such that with surfactant component viscosity 10 cP,
** effective water phase viscosity mu_wF increases linearly with surfactant
** concentration between 0.001 and 0.01,
** mu_wF(0) = 1.03 cP, mu_wF(0.001) = 1.05 cP, mu_wF(0.01) = 5.1 cP


VSMIXCOMP 'Surf'
VSMIXENDP 0 0.005
VSMIXFUNC 0 0.374795 0.541292 0.64970 0.730229 0.794326 0.847572 0.893115
0.932905 0.968233 1.0


** Nonlinear mixing rule for salt
** Mix-func defined such that with salt component viscosity 1.1 cP,
** effective water phase viscosity mu_wF increases linearly with salt
** concentration between 0.01 and 0.05,
** mu_wF(0) = 1.03 cP, mu_wF(0.01) = 1.05 cP, mu_wF(0.05) = 1.07 cP

VSMIXCOMP 'Salt'
VSMIXENDP 0 0.05
VSMIXFUNC 0 1.234026 1.782220 2.139157 2.404304 2.615343 2.790658 2.940610
3.071619 3.187938 3.292532



** Nonlinear mixing rule for polymer
** Mix-func defined such that with polymer component viscosity 10000 cP,
** effective water phase viscosity mu_wF increases linearly with polymer
** concentration,
** mu_wF(0) = 1.03 cP, mu_wF(0.007) = 10.3745

VSMIXCOMP 'Poly'
VSMIXENDP 0 0.00035
```

```
VSMIXFUNC 0 0.108855 0.159511 0.192885 0.217815 0.237722 0.254295 0.268493
0.280910 0.291946 0.301875

** ROCK FLUID SECTION ================
ROCKFLUID

**Surfactant curves:
RPT 1 STONE1 WATWET

INTCOMP 'Surf' WATER
**Set #1: Surf conc. 0

KRINTRP 1
**Nc = 6.25e-13
DTRAPW -12.20412


** Base HiSal no-surf curve, Corey exp: W: 1.5, O: 2
**    Sw          krw         kro        Pc
SWT
 SMOOTHEND QUAD
0.123       0           1           2.3536
0.12551     7.10E-07    0.99954     2.2065
0.13111     2.29E-06    0.99851     1.9123
0.13818     4.29E-06    0.9972      1.6181
0.14749     6.93E-06    0.99549     1.3239
0.15835     1.00E-05    0.99349     1.0791
0.16054     1.57E-05    0.9921      1.0297
0.16471     2.66E-05    0.98945     0.95615
0.1694      3.88E-05    0.98648     0.8826
0.1747      5.26E-05    0.98312     0.80905
0.18079     6.84E-05    0.97926     0.7355
0.18787     8.68E-05    0.97477     0.66195
0.1937      0.000102    0.97108     0.61066
0.19623     0.00012326  0.96794     0.5884
0.20633     0.00020811  0.95542     0.51485
0.21885     0.0003133   0.93991     0.4413
0.22905     0.000399    0.92727     0.39476
0.23497     0.00051204  0.91555     0.36775
0.2568      0.00092888  0.87236     0.2942
0.2644      0.001074    0.85732     0.27673
0.28879     0.0019627   0.79019     0.22065
0.29975     0.002362    0.76002     0.20563
0.3351      0.004577    0.64031     0.15719
0.34246     0.0053182   0.61309     0.1471
0.37045     0.008137    0.50958     0.12325
0.37698     0.0091456   0.48608     0.11768
0.4058      0.013597    0.38236     0.10092
0.42756     0.018581    0.3138      0.08826
0.44115     0.021694    0.27098     0.083549
0.4765      0.033396    0.18202     0.071293
0.51185     0.049967    0.11618     0.059038
0.51242     0.050339    0.11544     0.05884
```

```
0.5472      0.073031    0.070447    0.053498
0.58255     0.10461     0.040376    0.048068
0.6179      0.14711     0.021619    0.042639
0.65325     0.20311     0.010581    0.037209
0.6886      0.27494     0.004551    0.031779
0.70396     0.31345     0.0032661   0.02942
0.72395     0.36357     0.001594    0.027966
0.7593      0.46689     0.000383    0.025394
0.79465     0.57684     3.60E-05    0.022822
0.80512     0.60443     2.53E-05    0.02206
0.83        0.67        0           0.021122
1           1           0           0.01471


**Liquid-gas relperm (not used at RC, so simplified)
** SL   krg     krog
**SLT
**0.14    1.0     0.0
**0.81    0.0     0.9


** Curve #2: Max surf conc. curves
KRINTRP 2 COPY 1 1
** log(Nc) corresponding to concentration 0.005:
** Nc = 2.0e-9
DTRAPW -8.69897

** Base HiSal max-conc-surf curve, Corey exp: W: 1.1, O: 1.2
**    Sw          krw         kro        Pc
SWT
 SMOOTHEND QUAD
0.123       0           1           0
0.143811    0.023529    0.976471    0
0.164622    0.047058    0.952942    0
0.185433    0.070587    0.929413    0
0.206244    0.094116    0.905884    0
0.227055    0.117645    0.882355    0
0.247866    0.141174    0.858826    0
0.268677    0.164703    0.835297    0
0.289488    0.188232    0.811768    0
0.310299    0.211761    0.788239    0
0.33111     0.23529     0.76471     0
0.351921    0.258819    0.741181    0
0.372732    0.282348    0.717652    0
0.393543    0.305877    0.694123    0
0.414354    0.329406    0.670594    0
0.435165    0.352935    0.647065    0
0.455976    0.376464    0.623536    0
0.476787    0.399993    0.600007    0
0.497598    0.423522    0.576478    0
0.518409    0.447051    0.552949    0
0.53922     0.47058     0.52942     0
0.560031    0.494109    0.505891    0
```

```
0.580842    0.517638    0.482362    0
0.601653    0.541167    0.458833    0
0.622464    0.564696    0.435304    0
0.643275    0.588225    0.411775    0
0.664086    0.611754    0.388246    0
0.684897    0.635283    0.364717    0
0.705708    0.658812    0.341188    0
0.726519    0.682341    0.317659    0
0.74733     0.70587     0.29413     0
0.768141    0.729399    0.270601    0
0.788952    0.752928    0.247072    0
0.809763    0.776457    0.223543    0
0.830574    0.799986    0.200014    0
0.851385    0.823515    0.176485    0
0.872196    0.847325    0.152956    0
0.893007    0.871135    0.129427    0
0.913818    0.894945    0.105898    0
0.934629    0.918755    0.082369    0
0.95544     0.942565    0.05884     0
0.976251    0.966375    0.035311    0
0.997062    0.990185    0.011782    0
1     1     0     0


**Liquid-gas relperm (not used at RC, so simplified)
** SL   krg     krog
**SLT
**0.14    1.0     0.0
**0.95    0.0     0.9


IFTTABLE
** cift     sigift
 0.0        16
 0.001      0.01
 0.005      0.005

** Salinity curves

** ROCK FLUID TYPE 2: Salt
RPT 2 STONE1 WATWET

** Interpolation between losal and surfactant curves
RPT_INTRP
 COMP 'Salt' WATER
 LOWER_BOUND 0.0
 UPPER_BOUND 0.04
 UPPERB_RPT 1

INTCOMP 'Salt' WATER
** Curve #1: High Sal no surfactant curves

KRINTRP 1
```

```
DTRAPW 0.004   ** comp corresponding to krwA (Losal)


** Base LoSal no-surf curve, Corey exp: W: 1.2, O: 1.4
**    Sw          krw         kro        Pc
SWT
 SMOOTHEND QUAD
0.123       0           1           2.3536
0.12551     2.03127E-11 0.999977829 2.2065
0.13111     2.23045E-09 0.999764239 1.9123
0.13818     2.76386E-08 0.999154706 1.6181
0.14749     1.89613E-07 0.99773256  1.3239
0.15835     8.35522E-07 0.995108852 1.0791
0.16054     1.06585E-06 0.99444568  1.0297
0.16471     1.63382E-06 0.993052554 0.95615
0.1694      2.51868E-06 0.991275406 0.8826
0.1747      3.91123E-06 0.988989276 0.80905
0.18079     6.15923E-06 0.985983681 0.7355
0.18787     9.8789E-06  0.981957805 0.66195
0.1937      1.40566E-05 0.978194945 0.61066
0.19623     1.62391E-05 0.976431991 0.5884
0.20633     2.76355E-05 0.968580561 0.51485
0.21885     4.92906E-05 0.956956805 0.4413
0.22905     7.50194E-05 0.945855423 0.39476
0.23497     9.40791E-05 0.938713533 0.36775
0.2568      0.000198516 0.907765148 0.2942
0.2644      0.000250648 0.895245568 0.27673
0.28879     0.000493059 0.848920012 0.22065
0.29975     0.000648827 0.825108079 0.20563
0.3351      0.001431016 0.736830816 0.15719
0.34246     0.001662108 0.716535148 0.1471
0.37045     0.002829127 0.634964404 0.12325
0.37698     0.003178883 0.615202669 0.11768
0.4058      0.005167975 0.52666574  0.10092
0.42756     0.007263132 0.460351633 0.08826
0.44115     0.008894767 0.420071332 0.083549
0.4765      0.014617113 0.322314714 0.071293
0.51185     0.023150441 0.238124415 0.059038
0.51242     0.0233166   0.236892356 0.05884
0.5472      0.035573999 0.169470494 0.053498
0.58255     0.053290536 0.116067483 0.048068
0.6179      0.078076565 0.076228807 0.042639
0.65325     0.112095386 0.047656545 0.037209
0.6886      0.157822394 0.02798536  0.031779
0.70396     0.181992177 0.021659481 0.02942
0.72395     0.217804955 0.015076732 0.027966
0.7593      0.294164626 0.007132759 0.025394
0.79465     0.387788764 0.002703765 0.022822
0.80512     0.418706941 0.001891441 0.02206
0.88        0.67        0           0.021122
1           1           0           0.01471
```

```
**Liquid-gas relperm (not used at RC, so simplified)
** SL   krg     krog
 SLT SMOOTHEND QUAD
      0.123       0.801       0
      0.223       0.8         0
      0.25935     0.79922     0.006026
      0.2957      0.79656     0.026309
      0.33205     0.79137     0.063808
      0.3684      0.78287     0.12033
      0.40475     0.77004     0.19561
      0.4411      0.75165     0.28673
      0.47745     0.72626     0.38822
      0.5138      0.69226     0.49308
      0.55015     0.64808     0.59434
      0.5865      0.59252     0.68638
      0.62285     0.52524     0.76577
      0.6592      0.44745     0.8312
      0.69555     0.36236     0.88302
      0.7319      0.27524     0.92258
      0.76825     0.1927      0.95169
      0.8046      0.12116     0.97224
      0.84095     0.065335    0.98597
      0.8773      0.027244    0.99439
      0.91365     0.006279    0.99874
      0.95        0           1
      1           0           1


KRINTRP 2 COPY 2 1
DTRAPW 0.04    ** comp corresponding to krwB (High sal)

** Base HiSal no-surf curve, Corey exp: W: 1.5, O: 2
**    Sw          krw         kro        Pc
SWT
 SMOOTHEND QUAD
0.123       0           1           2.3536
0.12551     7.10E-07    0.99954     2.2065
0.13111     2.29E-06    0.99851     1.9123
0.13818     4.29E-06    0.9972      1.6181
0.14749     6.93E-06    0.99549     1.3239
0.15835     1.00E-05    0.99349     1.0791
0.16054     1.57E-05    0.9921      1.0297
0.16471     2.66E-05    0.98945     0.95615
0.1694      3.88E-05    0.98648     0.8826
0.1747      5.26E-05    0.98312     0.80905
0.18079     6.84E-05    0.97926     0.7355
0.18787     8.68E-05    0.97477     0.66195
0.1937      0.000102    0.97108     0.61066
0.19623     0.00012326  0.96794     0.5884
0.20633     0.00020811  0.95542     0.51485
0.21885     0.0003133   0.93991     0.4413
0.22905     0.000399    0.92727     0.39476
0.23497     0.00051204  0.91555     0.36775
```

```
0.2568      0.00092888  0.87236     0.2942
0.2644      0.001074    0.85732     0.27673
0.28879     0.0019627   0.79019     0.22065
0.29975     0.002362    0.76002     0.20563
0.3351      0.004577    0.64031     0.15719
0.34246     0.0053182   0.61309     0.1471
0.37045     0.008137    0.50958     0.12325
0.37698     0.0091456   0.48608     0.11768
0.4058      0.013597    0.38236     0.10092
0.42756     0.018581    0.3138      0.08826
0.44115     0.021694    0.27098     0.083549
0.4765      0.033396    0.18202     0.071293
0.51185     0.049967    0.11618     0.059038
0.51242     0.050339    0.11544     0.05884
0.5472      0.073031    0.070447    0.053498
0.58255     0.10461     0.040376    0.048068
0.6179      0.14711     0.021619    0.042639
0.65325     0.20311     0.010581    0.037209
0.6886      0.27494     0.004551    0.031779
0.70396     0.31345     0.0032661   0.02942
0.72395     0.36357     0.001594    0.027966
0.7593      0.46689     0.000383    0.025394
0.79465     0.57684     3.60E-05    0.022822
0.80512     0.60443     2.53E-05    0.02206
0.83  0.67  1.0E-05      0.021122
1           1           0           0.01471
```

```
**Liquid-gas relperm
** SL   krg     krog
 SLT SMOOTHEND QUAD
      0.123       0.801       0
      0.223       0.8         0
      0.25935     0.79922     0.006026
      0.2957      0.79656     0.026309
      0.33205     0.79137     0.063808
      0.3684      0.78287     0.12033
      0.40475     0.77004     0.19561
      0.4411      0.75165     0.28673
      0.47745     0.72626     0.38822
      0.5138      0.69226     0.49308
      0.55015     0.64808     0.59434
      0.5865      0.59252     0.68638
      0.62285     0.52524     0.76577
      0.6592      0.44745     0.8312
      0.69555     0.36236     0.88302
      0.7319      0.27524     0.92258
      0.76825     0.1927      0.95169
      0.8046      0.12116     0.97224
      0.84095     0.065335    0.98597
      0.8773      0.027244    0.99439
      0.91365     0.006279    0.99874
```

```
      0.95        0           1
      1           0           1


KRTYPE CON 2


** Initialisation

INITIAL

VERTICAL DEPTH_AVE

REFDEPTH 1900
REFPRES 19300
DWOC 1940

** Specify Sw below OWC
** WOC_SW 1.0

** Initial mole fractions and bubble point
MFRAC_WAT 'Water'   CON 0.96
MFRAC_WAT 'Salt'    CON 0.04
MFRAC_WAT 'Surf'    CON 0.0
MFRAC_WAT 'Poly'   CON 0.0

** Adjusted to improve convergence

PBC 'Gas' CON 9500

** Spec of num. method parameters ====
NUMERICAL


DTMAX 0.25
MAXSTEPS 100000
ITERMAX 200
NORTH 150
NEWTONCYC 25
ISOTHERMAL


RUN
** Dynamic section ==================
** Start date
DATE 2000 1 1

** First time step
DTWELL 0.05


GROUP 'Default-Group' ATTACHTO 'FIELD'
```

```
WELL 'WI01' VERT   27 25 ATTACHTO 'Default-Group'
WELL 'OP01' VERT 160 120 ATTACHTO 'Default-Group'


INJECTOR 'WI01'
**           Water Salt Surf Poly Oil Gas
INCOMP WATER 0.96  0.04  0.0  0.0  0.0  0.0
OPERATE MAX STW 7500
OPERATE MAX BHP 42500 CONT

**      Dir wrad  geom_fac wfrac skin
GEOMETRY K  0.09525  0.249     1.0   0.0

PERF GEOA 'WI01'
** i  j  k     FF  status  connection
   27  25  16:17    1.0  OPEN    FLOW-FROM  'SURFACE'

PRODUCER 'OP01'
OPERATE MAX STO 7500
OPERATE MAX STL 10000 CONT
OPERATE MIN BHP 15000 CONT

GEOMETRY K 0.09525  0.249 1.0 0.0

PERF GEOA 'OP01'
** i  j  k    FF  status  connection
 160   120   1:13   1.0 OPEN  FLOW-TO  'SURFACE'

GCONI 'Default-Group'
VREP WATER 1.0
GTARGET STW 7500

DATE 2000 2 25
DATE 2000 3 1

INJECTOR 'WI01'
INCOMP WATER 0.96 0.04  0.0  0.0  0.0  0.0
OPERATE MAX STW 7500
OPERATE MAX BHP 42500 CONT

DTWELL 0.05

DATE 2000 3 2
DTMAX 5

DATE 2001 1 1
DATE 2001 7 1
DATE 2002 1 1
DATE 2002 7 1

DATE 2003 1 1
DATE 2003 7 1
```

```
DATE 2004 1 1
DATE 2004 7 1

DATE 2005 1 1
DATE 2005 7 1
DATE 2006 1 1
DATE 2006 7 1

DATE 2007 1 1
DATE 2007 7 1
DATE 2008 1 1
DATE 2008 7 1

DATE 2009 1 1
DATE 2009 7 1
DATE 2010 1 1
DATE 2010 7 1

DATE 2011 1 1
DATE 2011 7 1
DATE 2012 1 1
DATE 2012 7 1

DATE 2013 1 1
DATE 2013 7 1
DATE 2014 1 1
DATE 2014 7 1

DATE 2015 1 1
DATE 2015 7 1
DATE 2016 1 1
DATE 2017 1 1

DATE 2018 1 1
DATE 2019 1 1
DATE 2020 1 1
DATE 2021 1 1

DATE 2022 1 1
DATE 2023 1 1
DATE 2024 1 1
DATE 2025 1 1

DATE 2026 1 1
DATE 2027 1 1
DATE 2028 1 1
DATE 2029 1 1
DATE 2030 1 1

STOP
```